UNIVERSIDADE DE LISBOA

INSTITUTO SUPERIOR TÉCNICO

BIOGEOCHEMISTRY OF PLATINUM GROUP ELEMENTS IN AQUATIC ECOSYSTEMS

Carlos Eduardo Salgueiro e Silva Monteiro

Supervisor: **Doctor Miguel José Martins Caetano**

Co-Supervisors: **Doctor Margarida Maria Portela Correia dos Santos Romão**

Doctor Antonio Cobelo-García

Thesis approved in public session to obtain the PhD Degree in Environmental Engineering

Jury final classification: Pass with Distinction

2020

UNIVERSIDADE DE LISBOA

INSTITUTO SUPERIOR TÉCNICO

BIOGEOCHEMISTRY OF PLATINUM GROUP ELEMENTS IN AQUATIC ECOSYSTEMS

Carlos Eduardo Salgueiro e Silva Monteiro

Supervisor: Doctor Miguel José Martins Caetano

Co-Supervisors: Doctor Margarida Maria Portela Correia dos Santos Romão

Doctor Antonio Cobelo-García

Thesis approved in public session to obtain the PhD Degree in Environmental Engineering

Jury final classification: Pass with Distinction

Chairperson:
Doctor Maria Teresa Nogueira Leal da Silva Duarte, Instituto Superior Técnico, Universidade de Lisboa.

Members of the Committee:
Doctor Margarida Maria Portela Correia dos Santos Romão, Instituto Superior Técnico, Universidade de Lisboa.
Doctor Maria Joana Castelo-Branco de Assis Teixeira Neiva Correia, Instituto Superior Técnico, Universidade de Lisboa.
Doctor Alexandra Maria Francisco Cravo, Faculdade de Ciências e Tecnologia, Universidade do Algarve.
Doctor Mário Jorge dos Santos Gustavo Mil-Homens, Instituto Português do Mar e da Atmosfera.

Funding Institution: Fundação para a Ciência e Tecnologia
Ministério da Ciência, Tecnologia e Ensino Superior
SFRH/BD/111087/2015

2020

Título: Biogeoquímica dos elementos do grupo da Platina em ecossistemas aquáticos

Nome: Carlos Eduardo Salgueiro e Silva Monteiro

Doutoramento em Engenharia do Ambiente

Orientador: Doutor Miguel José Martins Caetano

Co-orientadores: Doutora Margarida Maria Portela Correia dos Santos Romão

Doutor Antonio Cobelo-García

Resumo

Os elementos do grupo da Platina (PGE), onde a platina (Pt) e o ródio (Rh) se incluem, são elementos tecnologicamente críticos de preocupação ambiental emergente com uma grande variedade de aplicações e crescente necessidade global. Consequentemente, as concentrações de Pt e Rh aumentaram em vários compartimentos ambientais, incluindo os ecossistemas aquáticos. Esta tese apresenta dados recentemente adquiridos no estuário do Rio Tejo. Este sistema é adequado ao estudo da Pt e Rh devido a pressões antropogénicas ativas e históricas, assim como a sua conexão com o mar. Assim, esta tese relata novas visões sobre a ocorrência e transporte de Pt e Rh das áreas urbanas para o estuário, bem como as suas implicações geoquímicas num estuário muito hidrodinâmico. A voltametria de redissolução catódica com adsorção (AdCSV) foi otimizada para a determinação simultânea de Pt e Rh num único varrimento, aproveitando a transformação do sinal usando a segunda derivada. Este passo melhora os picos mal definidos, habitualmente encontrados em concentrações ultra-traço, como as de Pt e Rh em matrizes ambientais.

A distribuição espacial de Pt e Rh foi avaliada nos sedimentos superficiais (n = 72). As concentrações variaram entre 0.18–5.1 ng Pt g^{-1} e 0.019–1.5 ng Rh g^{-1}. Os níveis de referência (base) estimados para o estuário foram 0.55 ng Pt g^{-1} e 0.27 ng Rh g^{-1}. Os níveis de Pt e Rh próximos dos emissários das estações de tratamento de águas residuais (ETAR) e locais de descarga pluvial foram semelhantes aos níveis de referência. As concentrações mais elevadas no estuário foram encontradas junto às áreas industriais e ponte Vasco da Gama, apontando como fontes de Pt e Rh os catalisadores quer industriais quer dos automóveis, respetivamente. Tendo como foco a transferência de Pt e Rh da área urbana para o estuário e as suas alterações químicas, foi investigada a especiação de ambos os elementos usando uma abordagem com múltiplos métodos. O pó de estrada (<63 µm) recolhido numa faixa com tráfego intenso foi exaustivamente caracterizado e incubado durante 7 dias em água sintética da chuva e do mar.

As espécies verdadeiramente dissolvidas medidas por voltametria (AdCSV) corresponderam a 0.01% e 0.1% do total de Pt e Rh no pó de estrada e as concentrações foram relativamente constantes ao longo do tempo. Nos lixiviados (<0.45 µm), as concentrações verdadeiramente dissolvidas de Pt e Rh foram aproximadamente 10 e 40%, respetivamente, do total de espécies medidas por espectrometria de massa atómica (ICP-MS). Estes resultados sugerem a presença de partículas coloidais ou (nano)partículas insolúveis. Foram ainda observadas variações temporais para o total de espécies de Pt <0.45 µm, por oposição ao Rh.

As concentrações e a partição de Pt e Rh foram também investigadas na coluna de água do estuário do Tejo. A determinação simultânea de Rh particulado e dissolvido na coluna de água de um estuário é reportada pela primeira vez. Amostras de água foram colhidas à entrada (VFX – Vila Franca de Xira) e na embocadura (ALC – Alcântara) do estuário durante ciclos semidiurnos de maré, em maré morta (MM) e em maré viva (MV). Adicionalmente, no ciclo MM em VFX, o ICP-MS foi usado também para determinar Pt na fração dissolvida (<0.45 µm). Ambos os elementos seguiram o regime hidrodinâmico, apresentando geralmente as concentrações mais elevadas durante a baixa-mar. As concentrações de Pt_P (1.0–25.6 ng g^{-1}) e Pt_D (0.1–11.7 ng L^{-1}) foram maiores que as de Rh_P (0.1–5.1 ng g^{-1}) e Rh_D (0.03–0.12 ng L^{-1}), respetivamente, e ambas as frações de Pt foram maiores em ALC do que em VFX, espelhando diferentes entradas antropogénicas para o estuário do Tejo. A principal fonte de Pt e Rh teve como origem os catalisadores dos automóveis. No entanto, na estação de ALC foi encontrada uma fonte adicional de Pt presumivelmente derivada de compostos à base de Pt usados em quimioterapia. O comportamento da Pt pareceu ser não-conservativo devido às quantidades emitidas serem maiores do que as de Rh. Os coeficientes de distribuição (K_D) calculados para a Pt e Rh foram aproximadamente de 10^4 e mostraram ser independentes do gradiente de salinidade. Na campanha de VFX em MM, a análise de especiação mostrou que as formas verdadeiramente dissolvidas representaram 39±9 % da Pt total na coluna de água, enquanto o total de espécies de Pt que passaram o filtro foram maiores, 65±14 %. Como também encontrado para Pt_D em ALC, estes resultados sugerem que as formas dissolvidas controlam a especiação de Pt na coluna de água. Contrariamente, as formas particuladas de Rh representaram a principal porção deste elemento na coluna de água uma vez que o Rh dissolvido foi frequentemente inferior ao limite de deteção.

Adicionalmente, a recirculação destes metais dentro do estuário e a potencial troca com a zona costeira adjacente foram avaliadas na estação a jusante usando um modelo hidrodinâmico do estuário do Rio Tejo (MOHID). Tanto a Pt quanto o Rh apresentaram de uma

forma geral as concentrações mais elevadas na vazante em oposição à enchente. Além disso, o modelo Lagrangiano da dispersão de partículas também apontou para a ocorrência de recirculação dentro do estuário e que a exportação para o Oceano Atlântico pode ocorrer 2 dias após a emissão. Por fim, os resultados obtidos mostram que os estuários são uma via importante para a introdução de PGE de origem urbana na região costeira, transferindo-os para o oceano com implicações na circulação regional e/ou global.

Palavras-chave

Platina e Ródio, Voltametria, Distribuição espacial, Análise de especiação, Estuário do Tejo.

Title: Biogeochemistry of platinum group elements in aquatic ecosystems

Abstract

Platinum-group elements (PGE), in which platinum (Pt) and rhodium (Rh) are included, are technology-critical elements of environmental emerging concern with a large variety of applications and increasing global demand. Consequentially, Pt and Rh concentrations have increased in several environmental compartments, including aquatic ecosystems. This thesis presents data acquired recently in the Tagus River-estuary system. This system is adequate to study Pt and Rh due to active and historical anthropogenic pressures and its connection to the sea. Thus, the thesis provides new insights on the occurrence and transport from urban areas to the estuary, and geochemical implications as well in a highly hydrodynamic estuary. A voltammetric procedure was optimized for the simultaneous determination of Pt and Rh in a single scan, taking advantage of signal transformation using the second derivative. This procedure improves ill-defined peaks usually found at ultra-trace concentrations, such as those of Pt and Rh found in environmental matrices.

The spatial distribution of Pt and Rh was assessed in surface sediments (n=72). Concentrations ranged between 0.18–5.1 ng Pt g^{-1} and 0.019–1.5 ng Rh g^{-1}. Estimated reference (background) levels in the estuary were 0.55 ng Pt g^{-1} and 0.27 ng Rh g^{-1}. Levels of Pt and Rh close to wastewater treatment plants (WWTP) outfalls and pluvial discharge sites were similar to the reference levels. The higher concentrations were found in the vicinity of industrial areas and the Vasco da Gama bridge, pointing out the source of Pt and Rh in industrial catalysts and automotive catalytic converters (ACC), respectively. Focusing on Pt and Rh transfer from the urban area into the estuary and their chemical alterations, a speciation analysis study of both elements was evaluated using a multi-method approach. Road dust collected (<63 µm) in a high traffic lane was thoroughly characterized and incubated during 7 days in synthetic rainwater and seawater. Truly dissolved species measured by adsorptive cathodic stripping voltammetry (AdCSV) corresponded to 0.01% and 0.1% of total Pt and Rh, respectively, in the road dust and concentrations were relatively constant over time. In the leachates (0.45 µm), truly dissolved concentrations of Pt and Rh were approximately 10 and 40 %, respectively, of total filter-passing species measured by inductively coupled plasma mass spectrometry (ICP-MS). This suggests the presence of colloidal- or insoluble (nano)particles. Furthermore, temporal variations were observed for total filter-passing Pt species, as opposed to Rh.

The concentrations and partition of Pt and Rh were assessed in the water column of Tagus estuary. The simultaneous determination of particulate and dissolved Rh in the estuarine water column is reported for the first time. Samples were collected at the entrance (VFX – Vila Franca de Xira) and mouth (ALC – Alcântara) of the estuary during semi-diurnal tidal cycles over neap (NT) and spring tide (ST). Additionally, in VFX NT cycle, ICP-MS was used to determine Pt in the dissolved fraction (<0.45 µm). Both Pt and Rh followed the hydrodynamic regime, in general presenting higher concentrations during low tide. Concentrations of Pt_P (1.0–25.6 ng g^{-1}) and Pt_D (0.1–11.7 ng L^{-1}) were higher than Rh_P (0.1–5.1 ng g^{-1}) and Rh_D (0.03–0.12 ng L^{-1}), respectively, and both fractions of Pt were higher at ALC than in VFX, mirroring different anthropogenic inputs to the Tagus estuary. The main source of Pt and Rh was the ACC but, at ALC station, Pt also had origin in Pt-based compounds. The behavior of Pt appeared to be non-conservative due to the higher inputs than Rh. Distribution coefficients (K_D) around 10^4 were calculated for Pt and Rh and were independent of the salinity gradient. In VFX NT survey, speciation analysis showed that truly dissolved forms represented 39±9 % of total Pt in the water column, while total filter-passing species were higher, 65±14 %. As also found for Pt_D in ALC, these results suggest that dissolved forms control Pt speciation in the water column. Contrarily, particulate forms represented the main proportion of bulk Rh in the water column since dissolved Rh was often below the LOD.

Additionally, metals recirculation within the estuary and the potential exchange to the Atlantic Ocean were also assessed at the downstream station using a hydrodynamic model of Tagus River estuary (MOHID). Both Pt and Rh presented in general higher concentrations associated with the ebb opposing to the flood. Moreover, the Lagrangian modelling of the particles' spread also pointed out that recirculation within the estuary takes place and the export towards the Atlantic Ocean can occur within 2 days after release. Ultimately, the obtained results show that estuaries are an important pathway to introduce PGE in the coastal region, transferring them towards the ocean with implications in regional and/or global circulation.

Keywords

Platinum and Rhodium, Voltammetry, Spatial distribution, Speciation analysis, Tagus estuary.

A toda a minha família, pelo enorme apoio.

To all my family, for the huge support.

"*Flutuar na vida como um barco à deriva é a tragédia de todos aqueles que deixaram de ser autênticos.*"

- Desconhecido

"*Floating in life like a drifting boat is the tragedy of all those who are no longer authentic*."

- Unknown

Acknowledgements

Since the beginning of my academic pathway, obtaining a PhD degree was a personal long-term goal. This goal was finally achieved, culminating in the elaboration of this thesis. A PhD journey may be a lonely road sometimes and with many difficulties but surely the existence of others along the road made this journey much more enjoyable and easier. Certainly, I would like to recognize my sincere appreciation to many of you. Although neither time nor space allow it, to all those who pushed me, accompanied me, supported me, helped me and 'put up with' me in the most difficult moments, my big THANK YOU!

Firstly, I would like to acknowledge my supervisors Doctor Miguel Caetano, Prof. Doctor Margarida Correia dos Santos and Doctor Antonio Cobelo-García for all mentorship and excellent scientific guidance, help and unlimited support throughout all these years, for sharing their knowledge and expertise, as well as their precious time and all scientific (and non-scientific) discussions. A special appreciation to Miguel for introducing me to this group of elements and to all for giving me the opportunity to work with you. Thank you very much!

Secondly, I also gratefully acknowledge the institutions that have participated in this work. To IPMA and CQE-IST for receiving me over the past years and allowing me to develop my work having the best conditions. In addition, to IIM-CSIC for receiving me although for short but important periods for this work.

I would also like to acknowledge the Portuguese Foundation for Science and Technology (FCT – Fundação para a Ciência e Tecnologia) for the grant funding of my PhD, SFRH/BD/111087/2015. I would also like to acknowledge the support of FCT projects UID/QUI/001002013 and CQE multiannual funding 2020 – 2023, as well as PTDC/QEQ-EPR/1249/2014 'Recovery versus environmental impacts of Rare Earth Elements derived from human activities' (REEuse).

Furthermore, to the COST Action TD1407 – "Network on Technology-Critical Elements (NOTICE) - from environmental processes to human health threats" whose funding I gratefully acknowledge. It has supported me by means of a short-term scientific mission and allowed me to attend international conferences, contributing to the increase of my professional network.

This work would not be possible without valuable collaborations and the contribution of several people. Therefore, I also acknowledge and I am grateful for the contributions of Prof. Doctor Manuel Francisco Pereira (CERENA-IST) for the help with XRD analysis; Prof. Doctor José Paulo Farinha and Bárbara Casteleiro (CQFM-IST) for the help with NTA analysis; Doctor Fátima Abrantes and her group (IPMA), Warley Soares, Cremilde Monteiro and Doctor Emília Salgueiro for the particle size distribution, as well as Mafalda Freitas for the CHNS analysis; Nuno Rosa (IPMA) for the ICP-MS analysis; Pedro Brito and Rute Cesário (IPMA) for the field work and ICP-MS analysis as well; Doctor Ana Isabel Rodrigues (IPMA) for the volatile compounds analysis; and Hilda de Pablo (MARETEC) for the major help with the hydrodynamic model.

I am also grateful to Doctor Marta Nogueira for the help in the field campaigns, for letting me use her lab when necessary, and for the many discussions, scientific and personal.

To all my colleagues, both at IPMA and at CQE-IST, whose companionship made this journey very pleasant and with the best environment to work, I express my gratitude. From IPMA, to Pedro B., Mário M.-H., Joana R., Clara L., Rui S., Rute G., Isabelina S., Cristina M., Cidália B., and many others who have joined me along the road in other 'battles'. To my colleagues at CQE-IST, João C., Rute C., Inês C., Cristina A., Zita M., Lígia C., Diogo F., Martin J., and all students that have worked in the lab over the past years. Thank you all!

I would also like to acknowledge the anonymous reviewers that have significantly contributed to the improvement of the manuscripts that resulted from this work.

Last but not the least, the final steps of this journey have been irregular and unpredictable due to COVID-19 pandemic as well as other health issues that threw me down a 'little' and for which family and friends were of major importance. For that reason, I would like to express my sincere thanks to all my friends, recognizing here my gratitude, for caring about me and for all the efforts to motivate me. Thank you all, whose all names I won't mention because I do not want to forget anyone. Only a few honorable mentions, in particular, to Miguel T. for always being there, as a pillar along the journey; to Martha, Mónica, Sara, Xico, Mena, Zé, Rute, Cláudia and Bruno… To my family, who has supported me unconditionally and supported the distance over the years, particularly in these last steps, perhaps the most difficult ones to walk along this journey. To my mom and dad, my sister, my brother, and all the other family members, whether blood or non-blood, I love you all. Closer or distant, you are always in my heart. Thank you all!!!

Table of Contents

List of Main Figures

List of Annex Figures

List of Main Tables

List of Annex Tables

Scope of the Work

The increase of technology-critical elements (TCE) in the environment, which include the platinum-group elements (PGE), is considered a hot topic for researchers because of their environmental emerging concern related with potential ecological impacts. The platinum-group elements, i.e. platinum (Pt), palladium (Pd), rhodium (Rh), iridium (Ir), osmium (Os), and ruthenium (Ru), have low abundance in the earth's continental crust (Peucker-Ehrenbrink and Jahn 2001) but their extraction and usage have increased over the last decades (Rauch and Peucker-Ehrenbrink 2015; Ravindra et al. 2004). Applications of PGE are varied, but half of the anthropogenic emissions are attributed to the deterioration of automobile catalysts (Dubiella-Jackowska et al. 2007; Pawlak et al. 2014; Ravindra et al. 2004; Rauch and Peucker-Ehrenbrink 2015; Whiteley and Murray 2005; Wiseman and Zereini 2009; Zereini et al. 1997), releasing PGE mainly as fine particulate materials. However, other sources may contribute significantly to the bulk emissions of PGE to the environment (Rauch and Peucker-Ehrenbrink 2015). The release of PGE from industrial activities remain poorly documented, whose catalysts used in their manufacturing processes include those metals. Furthermore, the inventory of Pt emissions derived from Pt-based chemotherapeutic drugs needs more investigation. Thus, point sources are often localized in urban and industrial regions. Spreading occurs through the atmosphere on airborne particles (Wiseman and Zereini 2009) or the hydrological cycle, being found in all environmental compartments (rainwater, groundwater, surface waters, seawater, sediments, biota, etc.) (e.g. Zereini and Wiseman 2015). Main PGE-enriched materials are road dust, soils, terrestrial vegetation and organisms (Pawlak et al. 2014; Ravindra et al. 2004).

In aquatic systems, PGE undergo various oxidation states and molecular forms. The most common oxidation states are Rh as +3, whereas Pt and Pd can occur in either +2 or +4 valence states in aqueous solutions (Colombo et al. 2008; Hartley 1991). It has been suggested that Pt(IV) is the most abundant species in seawater, whereas Pt(II) is in freshwater (Cobelo-García et al. 2013). The divalent state largely predominates over the tetravalent state at 25ºC, except under extremely oxidizing conditions (Hartley 1991), where oxidation takes place and solubility increases in the presence of organic compounds (OM).

Platinum remains the most studied element amongst its group, but more recently researchers have been paying attention to the other PGE, in particular Rh. It has been reported that Pd may pose greater environmental risk than the other PGE due to its larger solubility (Fortin et al. 2011; Wiseman and Zereini 2009). Recently, Almécija et al. (2015) provided new insights on the geochemical reactivity and range of dispersion of Pt and Os. Overall, there is a lack of scientific information related to the distribution, transport and fate of PGE, as well as their biogeochemical processes in sediments and waters. Speciation analysis studies under environmentally relevant conditions also remain very limited. In addition, information concerning the driving processes that influence PGE mobility and partition are vital to understanding the extension of environmental contamination. The effects of rainwater and seawater, either the major ions composition or organic compounds, in the various PGE forms are still unclear. Integrative modelling tools could support the estimation of mass balance between compartments but those are still missing. Platinum group elements in environmental matrices are usually found at the ultra-trace level. Therefore, to have suitable methods for their determination is of major importance. In general, most of the commonly used techniques quantify the total concentration of elements. However, sensitive and selective methods are still needed, in particular those for speciation studies under relevant environmental conditions that demand sufficient selectivity and low limits of detection.

The European Commission predicted a significant increase in the demand and supply of these technology-materials until the end of 2020 (European Commission 2014). Certainly, the search for these elements will continue to rise in the upcoming decades, with subsequent increase of PGE levels in the environment. Still, it lacks an accurate environmental risk assessment concerning the Water Framework Directive (WFD; 2000/60/EC) and Marine Strategy Framework Directive. Concurrently, the Environment Canada report (Fortin et al. 2011) has identified major knowledge gaps related with analytical techniques (Dubiella-Jackowska et al. 2007; Fortin et al. 2011) and the lack of thermodynamic, bioaccumulation and toxicity data (Fortin et al. 2011). Thus, investigation on these elements is needed to evaluate the environmental transformations and impacts in coastal and transitional areas, such as estuaries.

References

Almécija, C., Sharma, M., Cobelo-García, A., Santos-Echeandía, J., & Caetano, M. (2015). Osmium and platinum decoupling in the environment: Evidences in intertidal sediments (Tagus Estuary, SW Europe). *Environmental Science and Technology*, *49*(11), 6545–6553. doi:10.1021/acs.est.5b00591

Cobelo-García, A., López-Sánchez, D. E., Almécija, C., & Santos-Echeandía, J. (2013). Behavior of platinum during estuarine mixing (Pontevedra Ria, NW Iberian Peninsula). *Marine Chemistry*, *150*, 11–18. doi:10.1016/j.marchem.2013.01.005

Colombo, C., Oates, C. J., Monhemius, a. J., & Plant, J. a. (2008). Complexation of platinum, palladium and rhodium with inorganic ligands in the environment. *Geochemistry: Exploration, Environment, Analysis*, *8*(1), 91–101. doi:10.1144/1467-7873/07-151

Dubiella-Jackowska, A., Polkowska, Z., & Namieśnik, J. (2007). Platinum group elements: A challenge for environmental analytics. *Polish Journal of Environmental Studies*, *16*(3), 329–345.

European Commission. (2014). *Report on critical raw materials for the EU, Report of the Ad hoc Working Group on defining critical raw materials*. Brussels. http://ec.europa.eu/enterprise/policies/raw-materials/files/docs/crm-report-on-critical-raw-materials_en.pdf.

Fortin, C., Wang, F., & Pitre, D. (2011). *Critical Review of Platinum Group Elements (Pd, Pt, Rh) in Aquatic Ecosystems - Research Report No R-1269*.

Hartley, F. (1991). *Chemistry of the Platinum Group Metals: Recent Developments*. (Frank Hartley, Ed.). Amsterdam: Elsevier.

Pawlak, J., Lodyga-Chruścińska, E., & Chrustowicz, J. (2014). Fate of platinum metals in the environment. *Journal of Trace Elements in Medicine and Biology*, *28*(3), 247–254. doi:10.1016/j.jtemb.2014.03.005

Peucker-Ehrenbrink, B., & Jahn, B. (2001). Rhenium-osmium isotope systematics and platinum group element concentrations: Loess and the upper continental crust. *Geochemistry, Geophysics, Geosystems*, *2*(10), n/a-n/a. doi:10.1029/2001GC000172

Rauch, S., & Peucker-Ehrenbrink, B. (2015). Sources of platinum group elements in the environment. In *Platinum metals in the environment* (pp. 3–17). Springer.

Ravindra, K., Bencs, L., & Van Grieken, R. (2004). Platinum group elements in the environment and their health risk. *The Science of the total environment*, *318*(1–3), 1–43. doi:10.1016/S0048-9697(03)00372-3

Whiteley, J. D., & Murray, F. (2005). Autocatalyst-derived platinum, palladium and rhodium (PGE) in infiltration basin and wetland sediments receiving urban runoff. *Science of the Total Environment*, *341*(1–3), 199–209. doi:10.1016/j.scitotenv.2004.09.030

Wiseman, C. L. S., & Zereini, F. (2009). Airborne particulate matter, platinum group elements and human health: a review of recent evidence. *The Science of the total environment*, *407*(8), 2493–2500. doi:10.1016/j.scitotenv.2008.12.057

Wood, S. A., & Van Middlesworth, J. (2004). The influence of acetate and oxalate as simple organic ligands on the behavior of palladium in surface environments. *Canadian Mineralogist*, *42*(2), 411–4213. doi:10.2113/gscanmin.42.2.411

Zereini, F., Skerstupp, B., Alt, F., Helmers, E., & Urban, H. (1997). Geochemical behaviour of platinum-group elements (PGE) in particulate emissions by automobile exhaust catalysts: Experimental results and environmental investigations. *Science of the Total Environment*, *206*(2–3), 137–146. doi:10.1016/S0048-9697(97)00219-2

Zereini, F., & Wiseman, C. L. S. (2015). *Platinum Metals in the Environment*. (F. Zereini & C. L. S. Wiseman, Eds.). Berlin, Heidelberg: Springer Berlin Heidelberg. doi:10.1007/978-3-662-44559-4

Outline of the Thesis

This thesis discusses the platinum-group elements Pt and Rh in aquatic ecosystems, with particular emphasis on the Tagus estuary and its surrounding urban and coastal areas. Different environmental compartments were assessed, such as sediments, road dust, SPM and waters. Related topics such as analytical methodologies, occurrence and behaviour, cycling and modelling in the estuarine environment were addressed separately, overviewing the work in the context of the actual state of the art. The thesis is outlined in distinct chapters, as follows:

Chapter 1 – *Literature review*

This chapter addresses a general review of the state of the art literature about PGE. It is introduced by a historical overview, followed by a general characterization of PGE properties. Their natural and anthropogenic sources are discriminated and various technology-based applications are described. In addition, the analytical techniques used in the determination of PGE and the present challenges are also overviewed. Finally, the presence, distribution, behaviour and cycling of PGE in the different environmental compartments is concisely reviewed, focusing in the aquatic ecosystems.

Chapter 2 – *Objectives*

This section summarizes the general hypothesis raised and the list of main goals defined to be answered in the present work.

Chapter 3 – *Study area*

The study area of this work, the Tagus estuary and its involving region, is described in this chapter. It overviews the morphological features, pollution vulnerability and main physicochemical characteristics, necessary to interpret PGE behaviour in a hydrodynamic system. A historical up to date context of the region is given for urban and industrial sprawl over the past years. The lessons learned over the past decades from various fields of research are integrated to introduce the PGE study in the estuary.

Chapter 4 – *Improved voltammetric method for simultaneous determination of Pt and Rh using second derivative signal transformation – application to environmental samples*

This chapter reports the optimization of the voltammetric method used for simultaneous determination of Pt and Rh in environmental samples. It introduces the

chemicals, apparatus and laboratory analysis of both metals. Data processing takes account of a signal transformation of the voltammograms using the second derivative. The optimized conditions include the electrolyte composition, equilibration time, deposition potential and time, limits of detection, and assessment of major interferences as well. Finally, the method was applied to certified reference material and environmental samples.

Chapter 5 – *Platinum and rhodium in Tagus estuary, SW Europe: sources and spatial distribution*

This chapter evaluates the spatial distribution of Pt and Rh in superficial sediments of the Tagus estuary and discriminates their main anthropogenic sources. In addition, it establishes baseline concentrations of both metals in the estuary. The reference levels are discussed against ancillary parameters. The pathway from the urban area towards the estuary is assessed through waste- and pluvial discharge sites. The anthropogenic signature of automotive catalytic converters is also discussed. Point sources of Pt and Rh with origin in industrial catalysts were confirmed.

Chapter 6 – *Speciation analysis of Pt and Rh in road dust leachates*

This chapter explores the behaviour of Pt and Rh in road dust leachates under relevant environmental conditions. Firstly, road dust was thoroughly characterized by several analytical techniques. Secondly, aliquots were incubated in artificial rain- and seawater up to 7 days and leachates retrieved. The speciation analysis of Pt and Rh was then evaluated through the combination of different analytical techniques, such as adsorptive cathodic stripping voltammetry, inductively coupled plasma–mass spectrometry and nanoparticle tracking analysis, as well as discussed based on physicochemical properties of the samples.

Chapter 7 – *Drivers of Pt and Rh variability in the water column of a hydrodynamic estuary: effects of contrasting environments*

This chapter discusses the occurrence and behaviour of both metals in two contrasting water columns of the Tagus estuary, during semi-diurnal tidal cycles. The effects of neap and spring tides are evaluated in the upper estuary, at the mouth of Tagus River, and in the lower estuary, at the discharge site of a treated wastewater effluent near the Atlantic Ocean. The behaviour of particulate and dissolved fractions of Pt and Rh are discussed based on physicochemical characteristics of the water and hydrodynamic

forcing. The potential metals transport towards the adjacent coastal area is also investigated, which also includes a numerical simulation approach.

Chapter 8 – *General discussion*

The overall discussion of the major findings in this thesis based on the abovementioned chapters is addressed. In the perspective of evaluating PGE cycling across the Tagus estuary, Pt and Rh data were integrated in a conceptual model of circulation and biogeochemistry at a regional scale.

Chapter 9 – *Conclusions and future perspectives*

This chapter summarizes the conclusions draw from the main results in the thesis. In addition, it presents future perspectives to further increase the current knowledge of PGE in aquatic systems and fulfil current existing gaps.

References are presented at the end of each chapter and supporting information of the chapters are presented in the end of the document.

Several chapters of this thesis were outlined based on a research article format and intended to be presented as standalone publications. Chapter 1 was adapted from a published book chapter and chapters 4 to 6 were published as original research articles. Chapter 7 is ready for submission in a peer-reviewed journal. Thus, parts of the present manuscript may show some repetition throughout the thesis.

I. LITERATURE REVIEW

***adapted from the chapter published*: P. Brito, R. Cesário and C. E. Monteiro, 2020. Least-known metals with potential impacts in the marine environment. *in* Coastal and Deep Ocean Pollution (pp. 215–247), CRC Press. DOI: 10.1201/9780203704271-10 (Book ISBN: 978-1-13-856939-3)**

1.1. Historical Perspective

Civilization has partially evolved based on metals and their mining activities. According to the International Union of Pure and Applied Chemistry (IUPAC 2005), platinum-group elements (PGE) are a group of rare and noble transitional elements that include ruthenium, rhodium and palladium (Ru, Rh and Pd; atomic numbers 44-46, respectively), as well as osmium, iridium and platinum (Os, Ir and Pt; atomic numbers 76-78, respectively).

The first known use of PGE goes back thousands of years to the Egyptian's period, in jewellery. Despite being a metal of antiquity, Pt was discovered in the 16th century, followed by Pd, Rh, Os and Ir in the 18th century approximately when Pt was brought to Europe (Hartley, 1991). Ruthenium was the last element to be found and isolated, in the 19th century (Griffith 2008; Hartley 1991). Since then, PGE were introduced in the modern days with increasingly and varied applications after the Industrial Revolution, especially over the past decades. The advance of modern technologies led to the search and exploitation of new mineral resources, with materials expected to be more resistant, durable and light, and to develop new forms of 'green' energy as well. However, this development has not always been accompanied by adequate studies of environmental impacts, which in general are confined to mining and ore processing activities. The exploitation and use of platinum group elements (PGE) have increased significantly in the last decades, whereas information on their biogeochemical cycles and impacts remains scarce.

1.2. Characterization and General Properties

The PGE are located in groups 8 to 10 in the periodic table, with the 'triad' Ru-Rh-Pd in the V period and Os-Ir-Pt in the VI period (Griffith, 2008; IUPAC, 2005). The PGE are highly siderophile, with a strong affinity to Fe, and chalcophile as well, having high affinity to S, opposing to the low affinity to O. The similar characteristics amongst PGE make these elements unique. Owing to their particular physical and chemical properties, the most remarkable features of PGE are the excellent catalytic properties and the high resistance to temperature and corrosion. Despite also having a strong tendency to form a variety of complexes, their kinetics is usually very slow except Pd. The chemical

similarities of the abovementioned 'triads' were initially observed in 1829 by Johann Dobereiner. In 1853, John Hall Gladstone identified the relation between both triads, in which the atomic weights of Pt-Ir-Os were roughly twice those of Rh-Ru-Pd (Griffith 2008). The PGE are also included in the densest elements of the periodic table: Pt, Os and Ir have ≈22 g cm^{-3}, being denser than Au (19 g cm^{-3}), while Pd, Rh and Ru are lighter than those, ≈12.5 g cm^{-3}, but in the same order of Hg and Pb. Yet, Pt and Pd are soft and ductile, which in turn are easier to work with and often used in metal alloys or with the addition of other metals. Opposing to that, Rh and Ir are more difficult to work with, but valuable either alone and in alloys. The hardest and brittle metals are Ru and Os, almost unworkable in the metallic state and with poor oxidation states. However, these are valuable as additions to other metals (Johnson Matthey 2016).

The PGE and some other elements included, namely Rare Earth Elements (REE), Ga, Ge, In, Nb, Ta, Te and Tl, are considered technology-critical elements (TCE) due to their current importance in energy and other technology-based industries, for which the global demand continues to increase (Cobelo-García et al. 2015). As such, and because of their increasing concentrations in different environmental compartments, many of those elements are considered anthropogenic contaminants of emerging environmental concern. This is particularly important in transitional environments such as estuaries, because of the strategic location of land-based industries with easy access to worldwide transportation. Significant changes in their concentrations and their natural cycle in the Earth's surface are due to extensive mining and usage. Consequentially, these are likely to cause disturbances on their biogeochemical cycles and potentially may pose hazardousness to biota and humans in the future.

1.3. Natural Sources

Platinum group elements occur at very low concentrations in the earth's upper continental crust (UCC). Global average concentrations of PGE are 0.4 ng g^{-1} for Pt and Pd; 0.1 ng g^{-1} for Ru; 0.06 ng g^{-1} for Rh; and 0.05 ng g^{-1} for Ir and Os (Peucker-Ehrenbrink and Jahn 2001; Ravindra et al. 2004). The highest PGE concentrations are estimated to be found in the earth's core, up to 5000 ng g^{-1} (Lorand et al. 2008), as a result of primordial material accretion, or even trapped in the upper layers during the lithosphere formation (Pilchin and Eppelbaum 2017).

The main natural sources of PGE (Figure I-1) include terrestrial emissions of volcanic origin and weathering of local parent rock caused by rain and watercourses, whereas hydrothermal crusts and vents, and Fe-Mn nodules as well may represent the major natural contribution of these metals to the deep-sea environment. As elemental metals or in the form of alloys, PGE may be present also in alluvial deposits, usually with iridium (e.g. platiniridium), and as well in nickel or copper deposits, arsenides (e.g. sperrylite, $PtAs_2$), sulphides (e.g. cooperate, (Pt, Pd, Ni)S), tellurides (e.g. PtBiTe) and antimonides (e.g. PdSb) (Fortin et al. 2011; Pilchin and Eppelbaum 2017). Pyrite minerals are known to contain PGE and they naturally occur in a variety of natural environments. In addition, cosmic dust may also contribute to both terrestrial and aquatic environments with small amounts of PGE (Almécija et al. 2017).

The exploitation of critical elements in the world, such as PGE, is limited to a low number of sites. In fact, the European Union is highly dependent on the imports of those materials, particularly from China and South Africa, since it does not have any economically viable mining areas for the exploitation of TCE (Cobelo-García et al. 2015). The different PGE ores are distributed along the world in singular geological settings that allowed the formation of those unique deposits, such as the Bushveld Igneous Complex

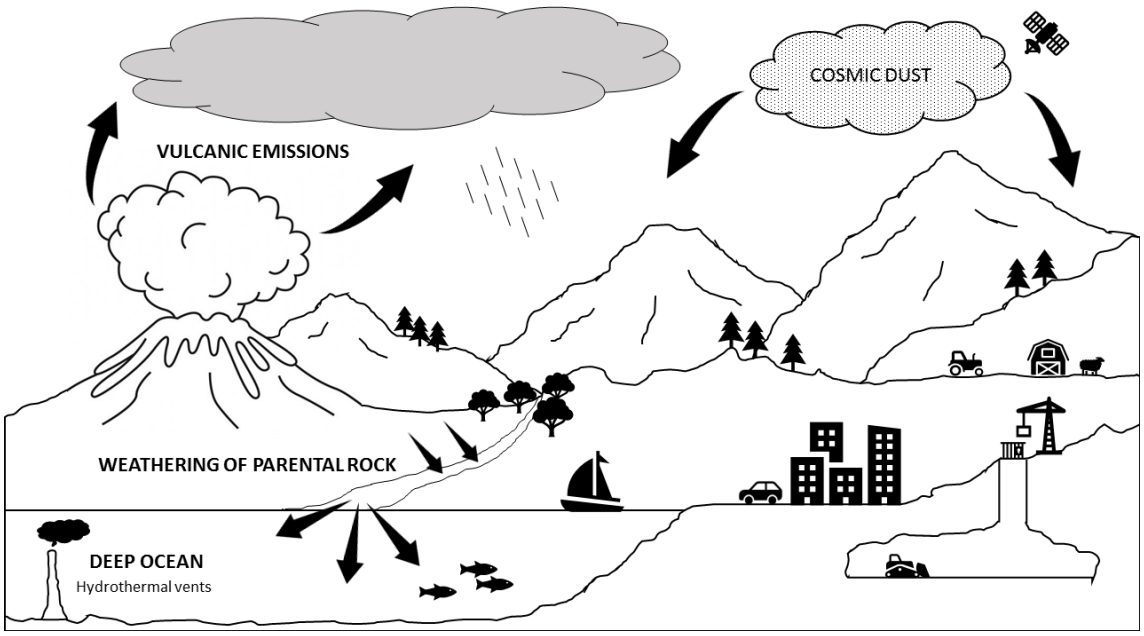

Figure I-1 – Natural sources of PGE (from Brito et al. 2020).

(South Africa), Noril'sk (Russia), Stillwater Complex (Montana, US) or Great Dyke (Zimbabwe) (Holwell and Mcdonald, 2010). The largest ore, the Bushveld Igneous Complex, contains about 75, 54, and 82 % of Pt, Pd, and Rh world resources, respectively; it is estimated that its mineral reserve is large enough to supply the anthropogenic demand for decades (Cawthorn 2010; Glaister and Mudd 2010).

1.4. Anthropogenic Sources and Uses

Regardless of the natural occurrence of mantle plumes entailed in the Earth's UCC that contain PGE, the supply of these elements has almost doubled over the last decade to more than 500 tons per year. Likewise, it is expected to increase in the upcoming years. Accordingly, mining activities for the extraction of PGE, which are often associated with other metals of economic interest, are transforming those regions in risky anthropogenic sources to the environment (Figure I-2). Consequently, PGE can result in by-products from the smelt and extraction of other metals that are intimately linked to localized higher levels of contamination than those from natural abundance. Thus, one of the main anthropogenic sources of PGE derives from the mining, extraction and purification activities of these and other metals.

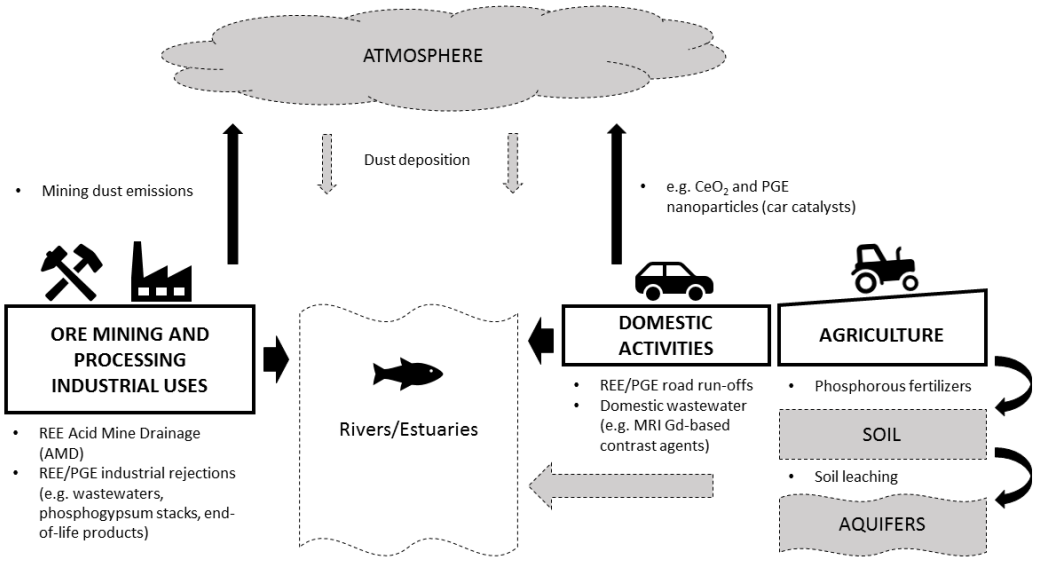

Figure I-2 – Main anthropogenic sources of PGE and other TCE (from Brito et al. 2020).

The increasing variety of PGE applications are as well transverse to several sector-based industries of economic interest. Platinum, Rh and Pd are usually the most used among the PGE and therefore are amongst the most expensive materials. Despite some particular applications, the other PGE are usually present in metal alloys or as by-pass products. The use of PGE in investment markets is a growing sector. Coins and metal bars produced from Pt and Pd are used in exchange-trading markets as investment funds in stock exchanges and bank accounts. The jewellery sector has also grown in the use of PGE over the past decades, in particular reaching around 30% of Pt global demand. In the modern days, decorative and ornamental objects such as earrings, necklaces and rings are among the most usual objects. In addition, watches also include Pt in their machinery.

The industrial/technological sectors have, however, the widest range of PGE applications. In electronics, PGE are used in the production of microchips, circuits, hard disks and sensors, liquid crystal displayers (LCD) and fibreglass production. Platinum is used as a coating in motor engine blades of airplanes and rockets, whereas Rh is used on lighthouse reflectors and lamps. In the medical field, sensors and health devices such as pacemakers and defibrillators also include Pt in their machinery. Dental applications are also known for Pt and Pd, such as crowns and bridgeworks. Moreover, the catalytic properties of PGE also have a long history in the industrial production of nitric and sulphuric acids, cortisone, ammonia and fertilizers. Summarizing, the large diversity of PGE applications potentially leads to an increase in their emissions into the environment. This occurs either through direct point sources, resulting from industrial effluents discharge, or indirect emissions because of their increased use and production of waste residues by the society.

In addition, the ability of Pt to inhibit the division of living cell turned this metal attractive in the production of Pt-based anticancer drugs, such as cisplatin, carboplatin and oxaliplatin. Worldwide use of Pt-based compounds attempts to treat various human malignancies, such as head, cervical, neck, ovarian and testicular cancers, and non-small cell lung cancer, including many other solid tumours (Qi et al. 2019). Platinum is the only metal still used to efficiently treat this disease. Currently, four new Pt-derivative formulas have regulatory approval in oriental nations, such as Japan, Korea and China (Oun et al. 2018), and new Pt-based complexes are being explored by the pharmaceutical industry (e.g. Ndagi et al. 2017). Cancer is a global health problem of modern times and often considered the ‘pathology of the century’ (Falzone et al. 2018). Its pervasive incidence

reinforces the need to find a cure since it represents the second leading cause of death around the world. In the past couple of decades, the number of incidences has increased more than 30 %, despite the advances in the diagnostic, medical and interventional fields (Falzone et al. 2018). This is directly linked to the growing population and an increase in the average age of life. Some projections point out that the number of incidences will continue to rise in the next decades and thus it is most likely that the use of Pt-based drugs will accompany this trend. Regardless, the efficacy of anti-cancer drug therapies includes large quantities of metal administration (200 – 500 mg Pt L^{-1}). Consequently, hospital and domestic sewage drained from urban areas raise environmental concerns related to wastewaters contaminated specifically by Pt. Thus, medical uses of Pt represent an important source of this metal (Laschka and Nachtwey 1997), which may cause impacts to aquatic organisms due to its rising dissolved concentrations.

The automobile industry is the most demanding sector for PGE, accounting for 50 % of Pt, 75 % of Pd and 80 % of Rh (Johnson Matthey 2016). Despite their use in other components of the automobiles, such as fuel cells and spark plugs in combustion engines, the manufacturing of automotive catalytic converters (ACC) accounts *per se* for approximately 50 % of PGE global demand. Catalytic converters were introduced in order to reduce the emissions of other pollutants such as nitrous and carbon oxides, unburned hydrocarbons and other pollutants, including particulate matter (Ravindra et al. 2004). Particles released from ACC, due to mechanical degradation and abrasion result in widespread distribution of PGE. This is particularly important near high traffic roads (Schäfer and Puchelt 1998), which in turn are mobilized and transported reaching the aquatic systems (Zereini and Wiseman 2015) or even distant unspoiled regions (e.g. Barbante et al. 2001).

1.5. Analytical Methodologies

Platinum group elements in environmental matrices are usually found at ultra-trace levels. Therefore, to have suitable methods for their determination is of major importance. In general, most of the commonly used techniques quantify the total concentration of elements. However, sensitive and selective methods are still needed, in particular those for speciation studies under relevant environmental conditions that demand sufficient selectivity and low limits of detection. Moreover, considering monitoring purposes, those

techniques should be inexpensive and easy to work with. Various analytical tools have been developed, in particular concerning multi-elemental capacity, although with some disadvantages and analytical limitations. In particular, spectrophotometric methods and atomic absorption spectrometry (AAS) were tentatively applied, yet also with some analytical drawbacks. Adsorptive cathodic stripping voltammetry (AdCSV) has been one of the techniques used in PGE determination, with great improvements in recent years. Moreover, the use of inductively coupled plasma mass spectrometry (ICP-MS) has been extensively used for PGE quantification in environmental matrices (e.g. Labarraque et al. 2015).

Among the PGE studies, the utmost attention has been given to Pt. More recently, Pd and Rh in environmental samples have been reckoned with. Yet, emphasis has been given in urban and roadside solid samples, where they are usually concentrated. Thus, data on its total dissolved concentrations are still very limited. The improvement of analytical techniques over the past few decades, such as electrothermal atomic absorption spectrometry (ET-AAS) and ICP-MS, allowed the individual and simultaneous determination of those elements in different environmental matrices (Zereini and Wiseman 2015). Despite the high sensitivity of ICP-MS for PGE analysis, the need of matrix separation due to spectral interferences from other elements has some disadvantages (Labarraque et al. 2015). Overall, this is a quite expensive technique and time-consuming as well, often needing a preconcentration step of the sample. Voltammetric techniques provide a simple and sensitive way to determine Pt and Rh at ultra-trace levels. Unfortunately, the same is not feasible for Pd because the limits of detection are high to its determination in environmental samples. Moreover, voltammetric techniques are in general less expensive and, after optimization, they appear to be suitable for routine analysis (e.g. Locatelli 2007; Monteiro et al. 2017). Electroanalytical procedures reported for PGE analysis are mainly based on the adsorptive process on a mercury electrode. Alternatives envisaging a similar analytical performance to the Hg electrode have been investigated (e.g. Pérez-Ràfols et al. 2017; Silwana et al. 2014). However, the reported detection and quantification limits remain insufficiently low to allow the quantification of PGE in pristine environments (Peucker-Ehrenbrink and Jahn 2001). More recently, the voltammetric signal transformation using the second derivative has proven to increase the accuracy of Pt and particularly Rh determinations at the ultra-

trace levels (Almécija et al. 2016; Cobelo-García et al. 2014; Monteiro et al. 2017), paving the way for the other PGE.

The solubility and bioavailability of PGE, as of any other substance, is generally determined by its speciation. Several variables, such as pH, ionic strength (salinity), organic matter or the presence of other anions and cations, are determinant on their chemical forms. These variables may be responsible for the differences in PGE speciation occurring in salt water, mainly as chloride complexes, while in freshwater those metals are essentially complexed with hydroxide anions and humic substances. The most relevant oxidation states for the three main PGE are Pt(II) and Pt(IV), Pd(II) and Rh(III), which depend on salinity and redox conditions. According to Cobelo-García (2013) and Cobelo-García et al. (2014), inorganic speciation is dominated by aquo-hydroxo, aquo-chloro and mixed aquo-hydroxo-chloro complexes. Furthermore, there is evidence of Pt and Rh interaction with organic matter, which may be key in speciation and thus in the mobility and distribution of PGE in aquatic ecosystems (Bowles et al. 1994; Cobelo-García 2013). Nevertheless, there is a general lack of knowledge about PGE speciation, particularly in aquatic environments. This goal, parallel to the evolution of analytical techniques, led to outcomes more rapidly in the case of some elements rather than others. Studies were devoted to Pt, whereas other PGE were more difficult to be evaluated. This is associated either due to low concentrations in different environmental compartments, such as Rh, or due to faster reaction kinetics and higher mobility in the environment, namely with Pd. More recently, some works have suggested that Pt emitted from ACC contained in road dust is present in the metallic state. Folens et al. (2018) used single-particle ICP-MS (spICP-MS) to determine metallic Pt nanoparticles in road dust. However, the soluble fraction of Pt could not be observed. In a recent study, the combination of ICP-MS and AdCSV allowed performing a speciation analysis of Pt and Rh in road dust leachates, discriminating a truly dissolved fraction of both metals under relevant environmental conditions (Monteiro et al. 2020).

Despite the limitations of some analytical techniques at first, the scientific community was able to quantify PGE in several matrices. However, efforts are still needed to improve the current knowledge of their behaviour in the environment. Regarding their speciation, this is particularly important since the total concentration of an element does not reflect its potential toxicity for an organism. Moreover, which PGE forms may cause adverse effects needs further investigation. Higher concentrations of

PGE in environmental matrices are expected and thus those potential toxic species need to be accurately differentiated.

1.6. Platinum-Group Elements Cycling in the Environment

The mobility and transport of PGE across different environmental compartments have been a matter of debate over the past decades, owing to the increase of their concentrations particularly in urban areas. The PGE emitted as solutes (e.g. Pt-based drugs used in chemotherapy) or as fine-grained size particles, nanoparticles (e.g. PGE emitted from ACC), may undergo chemical changes during their transport from the source to the aquatic systems. However, studies with the scope of understanding their behaviour in those compartments are still needed. Despite the limited information available in the literature, it is expected that PGE may undergo the same chemical transformations as most of transient metals. As with other metals, PGE are prone to be affected by changes in master environmental variables. It is hypothesised that PGE may form different species depending, firstly, on the ionic strength of the involving media such as the changes caused by the transition from fresh- to seawater, or on pH variations, namely from slightly acidic rainwater to alkaline seawater. Secondly, the nature of the particles, whichever on the atmospheric, terrestrial or aquatic compartments, may play a major role on processes as adsorption, scavenging and retention of metals. With this regard, particles composition may vary according to the elemental and organic matter composition, which may further affect PGE partitioning.

Besides the essential chemical characterization of environmental samples, there is the necessity of understanding the physical mechanisms that can act as driving forces on regional and worldwide transport of PGE. Physical drivers, such as wind and rain events, may force the transfer of PGE between compartments, affecting their distribution and ultimately transferring them from urban areas to the nearby aquatic systems. Along their path, chemical changes occur and PGE may become bioavailable. As a result, PGE concentration in sediments and aquatic vegetation often largely exceeds the natural background levels contrasting with lower levels in waters (Zereini and Wiseman 2015). In this section is presented a brief overview on the occurrence and cycling of PGE in the different environmental compartments.

1.6.1. Atmosphere

Anthropogenic activities have largely affected the natural biogeochemical cycle of PGE and the atmosphere may well be considered the compartment in which contamination is globally disseminated. Despite activities such as mining and biomass burning contribute to the increase of PGE levels in the atmosphere, their main anthropogenic source has been essentially attributed to automotive catalytic converters (ACC). Emissions of PGE from ACC vary according to the type of engine (diesel or petrol), the age of the catalyst and the velocity during vehicle operation. The particles resulting from thermal degradation and mechanical abrasion from ACC during vehicle operation can be directly emitted into the atmosphere, through the exhaust fumes containing PGE as fine particulate material usually in the form of micro- or nanoparticles. On the other hand, it is consensual amongst scientists that PGE in those particles tend to accumulate and concentrate in the pavement, as road dust and in the near roadside soils. The concentrations of PGE deriving from ACC in urbanized areas worldwide are comprehensively described in the literature (e.g. Wiseman et al. 2016; Zereini and Wiseman 2015). Nevertheless, road dust emission and its resuspension continue to draw attention for the possible environmental and human health hazardousness in highly populated cities around the world (e.g. Bocca et al. 2006; Diong et al. 2016; Rauch et al. 2005; Rinkovec et al. 2018; Zereini et al. 2012, 2004). Amato et al. (2014) showed that road dust emissions can increase up to 35 % PM_{10} (airborne particulate matter, PM, with aerodynamic diameter below 10 μm) at impacted stations by traffic and even in urban background sites, as well as up to 22 % at industrial and rural sites. Airborne PM of smaller dimensions is easily dispersed by the wind action, mostly depending on its intensity, which is thought to be the main mechanism responsible for regional- to long-range transport of PGE (Barbante et al. 2001; Zereini et al. 2012). Ultimately, those particles carrying PGE return towards the earth's surface by either wet or dry atmospheric deposition on land or sea. Although limited data is available on PGE concentrations in rainwater, some results point out that those concentrations are usually very low, often beneath 1 ng L^{-1} (Eriksson 2001; Mashio et al. 2016). Mashio et al. (2016) did not find a clear relationship between Pt and the amount of precipitation. However, these authors observed a trend for higher Pt concentrations with decreasing pH in rainwater.

Some studies point out the presence of PGE in remote and pristine environments. In the Arctic, Barbante et al. (2001) presented the first millennial time series for PGE in

ice cores from Greenland, in which three different periods were ascribed. The first period regards the past natural occurrence of PGE in ancient ice, which revealed extremely low levels of PGE. Most likely, those derived from cosmic dust and other natural sources. A second period revealed that the atmosphere in the northern hemisphere was already contaminated with PGE, just before the introduction of ACC in the United States of America during the mid-1970s. The origin of PGE contamination by that period could be attributed also to the large expansion of several industries, including mining and smelters of metals, chemical and petroleum, or iron and steel manufacturing, and some natural emissions from forest wildfires and volcanic aerosols as well. Finally, a third period showed a markedly increase on PGE concentrations towards the recent ice layers, soon after the introduction of catalytic converters in vehicles. Similarly, the 50-year record in the Antarctic ice reported by Soyol-Erdene et al. (2011) also suggests that increase of PGE concentrations in the recent years, most likely due to the large-scale atmospheric circulation and wet deposition of the growing anthropogenic emissions since the 1980s.

1.6.2. Water Column

Although PGE are not key trace elements included in the priority pollutants list to monitor in water quality programs from the European Union and the United States of America, there is rising interest about their concentrations and distribution in waters. These include groundwater, rain, riverine, estuarine, coastal and oceanic waters. Despite potential environmental effects or fate of PGE remaining unclear, the interest arises from their increased use and consequential emissions that extend to aquatic ecosystems.

Waste- and pluvial waters can be regarded as the main pathway of PGE mobility and transfer from urban areas to nearby aquatic systems. One of the PGE sources to waste- and pluvial waters derives from the particulate matter deposited on the roadside, which includes ACC emissions accumulated over time that are washed by rainwater during storm events. An additional Pt source to wastewaters is the excreting products from chemotherapeutic patients. Platinum enters the municipal sewage systems either in the hospital or in domestic effluents, for which wastewater treatment plants (WWTP) lack suitable treatment processes of those active compounds. Monteiro et al. (2017) reported dissolved concentrations of Pt and Rh in waters from the inflow and outflow of a WWTP. These samples reflected the anthropogenic loading, with Pt levels intensified after the

first rain, as previously reported in Europe (Laschka and Nachtwey 1997; Vyas et al. 2014). To the best knowledge of the authors, dissolved Rh concentrations in wastewaters were reported for the first time, having concentrations one order of magnitude lower than Pt.

The concentration of Pt in riverine waters ranges in general up to 15 ng L^{-1} (Cobelo-García et al. 2014, 2013; Soyol-Erdene and Huh 2012). Data on the other PGE remain scarce, despite all the efforts to understand PGE biogeochemical implications in aquatic ecosystems. As examples, dissolved Pt concentrations ranged from 0.04 to 0.12 ng L^{-1} in Lérez Estuary, Spain (Cobelo-García et al. 2013), and from 0.07 to 0.16 ng L^{-1} in Gironde Estuary, France (Cobelo-García et al. 2014). Higher concentrations were reported in Tokyo Bay, Japan, between 0.98 and 6.83 ng L^{-1} (Obata et al. 2006) and in Tagus Estuary, Portugal, ranging up to 11.7 ng L^{-1} (Monteiro et al. *in prep*). In addition, the industries located on the margins of rivers and estuaries are considered one major and important anthropogenic source of PGE. Many industrial processes use PGE as catalysts that also degrade over time and release soluble compounds directly to surface waters. In estuarine systems, Pt concentrations were reported to be higher than in open ocean seawater. Concentrations of Pt in seawater-end members exceed those of typical coastal and oceanic waters (Cobelo-García et al. 2014, 2013; López-Sánchez et al. 2019; Mashio et al. 2017, 2016), suggesting inputs of this element within the estuaries. Monteiro et al. (*in prep*) reported that major inputs of Pt and Rh to the Tagus Estuary occurred through a WWTP outfall compared to the riverine discharge. Furthermore, Cobelo-García et al. (2013) observed a non-conservative behaviour of Pt during estuarine mixing, due to redox transformations along a salinity gradient.

The distribution and geochemical behaviour of PGE in oceanic waters have been studied sparingly since the early 1980s. Mainly focusing on Pt, studies in seawater have depicted different types of vertical profiles for different regions of the ocean. The recycled type profile in the eastern North Pacific Ocean was reported by Hodge et al. (1986), with concentrations varying between 0.09 and 0.22 ng Pt L^{-1}. The scavenged type was reported for the Indian Ocean by van den Berg and Jacinto (1988), with concentrations between 0.033 and 0.31 ng Pt L^{-1}. Colodner et al. (1993) reported the conservative profile of Pt in the Atlantic, with concentrations ranging from 0.04 to 0.1 ng Pt L^{-1}. More recently, and within the same range of dissolved Pt, Suzuki et al. (2014) and Fischer et al. (2018) observed for the North Pacific Ocean a similar conservative behaviour. However, López-

Sanchéz et al. (2019) reported for the Atlantic Ocean a dissimilar and more complex behaviour of Pt, whose concentrations found were similar to the latter authors. The authors observed a surface enrichment in the western Atlantic at high latitudes as opposed to the conservative mixing below 1000 m depth (López-Sanchéz et al. 2019). Regarding the other PGE, Rh has the second-highest concentrations in seawater and displays a nutrient-type depth profile in the Pacific Ocean (Bertine et al. 1993). Metals with nutrient-type or mixed profiles in the ocean are often associated with biological functions (Bruland et al. 2014), however, such functions are unknown for the PGE.

As with the dissolved phase, data on PGE particulate concentrations in the water column, usually associated with suspended particulate matter (SPM), continues to be scarce. The few published studies reporting Pt concentrations in estuarine SPM are those of Cobelo-García et al. (2013) for the Lérez River Estuary, NW Iberian Peninsula, and Cobelo-García et al. (2014) for the Gironde Estuary, SW France. Concentrations of particulate Pt were relatively low and close to sediments background levels. More recently, Abdou et al. (2020) also observed that phytoplankton reflected the Pt levels in contrasting sites from the Atlantic and Mediterranean sea. Monteiro et al. (*in prep*) reported for the Tagus Estuary concentrations of particulate Pt one order of magnitude higher in SPM than those found in superficial sediments (Monteiro et al. 2019). The distribution coefficients (K_D) computed for Pt were lower in the Gironde Estuary than those in the Lérez River Estuary, as well as a dissimilar behaviour along the salinity gradient was found for both settings. As for the Tagus Estuary, Monteiro et al. (*in prep*) did not found a decreasing pattern along the salinity gradient as well. These discrepancies may result from different hydrodynamic regimes in the two systems and turbidity as well. Moreover, different local anthropogenic pressures may affect soluble/insoluble Pt species also (Cobelo-García et al. 2014), as well as Pt partitioning may be controlled by primary producers (Abdou et al. 2020).

1.6.3. Sediments

Terrestrial and aquatic sediments have been the most studied environmental compartments for PGE over the past decades. The increase of PGE concentrations in urban environments has been well documented (Birke et al. 2017; Mihaljevič et al. 2013; Rauch et al. 2006; Rauch and Peucker-Ehrenbrink 2015; Ruchter and Sures 2015;

Wiseman et al. 2016, 2013; Zereini et al. 2007, 2004). Although, research has focused mainly on Pt emissions, and particularly on its distribution comprising areas under rural, urban and industrial pressures (e.g. Zereini and Wiseman 2015). It is noteworthy that studies dealing with spatially-resolved distribution of PGE in worldwide aquatic environments are quite limited (Cobelo-García et al. 2013, 2011; Monteiro et al. 2019; Terashima et al. 1993; Wei and Morrison 1994; Zhong et al. 2012). For Rh, such studies are even scarcer (Essumang et al. 2008; Monteiro et al. 2019). Catalytic converters from vehicles are considered perhaps the most widespread source of anthropogenic PGE in the environment. Yet, other sources cannot be disregarded (Rauch and Peucker-Ehrenbrink 2015) and data from spatial distribution in sediments are important to effectively assess local sources to the aquatic systems (Monteiro et al. 2019; Zhong et al. 2012). Medicinal uses of Pt and industrial PGE emissions remain poorly documented and need further investigation on the extent of their contamination (Rauch and Peucker-Ehrenbrink 2015).

Wei and Morrison (1994) reported size-fractioned Pt concentrations in road dust and urban river sediments from Goteborg region, Sweden, that receive pluvial runoff and sewage discharges. Despite Pt concentrations found in sediments reflecting those of the road dust, and depicting their source on ACC, the authors did not find a particular spatial pattern of Pt distribution. Recently, Zhong et al. (2012) assessed the background levels and distribution of Pt and Pd in superficial sediments, as their possible sources as well, in Pearl River Estuary, China. The author's findings revealed relatively low concentrations of both elements, on average 1.1 ng Pt g^{-1} and 3.6 ng Pd g^{-1}. However, some localized high concentrations of Pd (38 ng g^{-1}) in sediments reflected other sources, such as the ones deriving from industrial processes that may have contributed to the increase of PGE levels in that estuary. More recently, Monteiro et al. (2019) have reported for the Tagus estuary, Portugal, several areas impacted by Pt and Rh having origin on different sources. Concentrations of Pt and Rh in the industrial areas were in general below 5 ng Pt g^{-1}, having a similar range to those found in China, a country with large industrial activities (Zhong et al. 2012). Source emissions from ACC showed to be associated to the urban drainage and a bridge, where a high traffic impacted highway crosses the estuary. Yet, the concentrations found in the Tagus saltmarsh near the bridge were 40 ng Pt g^{-1} (Almécija et al. 2016). Moreover, the Pt signal derived from hospital and domestic effluents could not be discriminated due to dilution from the drainage system and/or additional Rh sources, such as those from ACC (Monteiro et al. 2019).

When shifting from coastal to the open marine environment data becomes scarcer, which demonstrates today's lack of knowledge on the behaviour of PGE in those environments. Earlier reports on Pt concentrations in ocean sediments point to a range up to 22 ng g^{-1} (Hodge et al. 1986). However, Terashima et al. (1993) found Pt and Pd concentrations in sediments off the Japan coast close to their crustal abundance (0.4 ng g^{-1}), and both elements showed to have similar patterns of distribution. The authors concluded that Pt and Pd might be supplied to the deeper sediments through rivers and seawater. At the continental shelf, Mashio et al. (2017) suggested that Pt in sediments could potentially have source in the coastal waters, reporting the increase of dissolved Pt concentrations with increasing depth. As with dissolved species, Pt and Pd can be reduced to elemental metal species under O_2 minimum zones, co-precipitating with other sediment particles such as manganese oxides (Halbach et al. 1989; Terashima et al. 1993). Nevertheless, geochemical processes at the sediment-water interface may govern the balance of PGE between compartments, changing them to more or less bioavailable species to the biota (Sures et al. 2002).

1.6.4. Biota

The biosphere is ultimately the environmental compartment in which scientists deposit their major concern, due to hazardousness potential of these elements to humans and other terrestrial and aquatic organisms. The free aqueous metal ions are usually regarded as the most (or only) reactive species with respect to toxicity effects towards marine organisms. One must keep in mind that different forms of a metal may be assimilated through contaminated food (Mulholland and Turner 2011). Because PGE are non-essential metals, i.e. there is no evidence of any biological function involving PGE, it is assumed that they are subjected to net accumulation rather than biologic regulation. In the past, research on the PGE effects in biota has been focused greatly in Pt disregarding the other PGE. However, environmental and health concerns have raised recently, considering Pd faster reactivity than Pt or Rh, because of the shift to use Pd instead of Pt in ACC and industrial catalysts. Nevertheless, those concentrations will likely continue to rise in the future, mostly owed to the growing use of PGE in several industries and ACC. The interest in aquatic organisms as potential biomonitors of PGE contamination contributed to several studies, in which other questions such as possible

bioaccumulation and biomagnification in the food web were also addressed. While in urban areas the monitoring of PGE may use trees (Bonanno and Pavone 2015) or mosses (Ayrault et al. 2006), in aquatic systems the attention was drawn to plants, macroinvertebrates and fish species from transitional areas (e.g. Moldovan et al. 2001; Mulholland and Turner 2011; Ruchter and Sures 2015; Sures and Zimmermann 2007; Zimmermann et al. 2004). Recently, Ruchter and Sures (2015) showed the accumulation of Pt by the clam *Corbicula sp.* in the field, however, Pt concentrations remained relatively low. In addition, Neira et al. (2015) observed a temporal variation of Pt concentrations in mussels *Mytilus galloprovincialis* over two decades of anthropogenic emissions mainly related with ACC and linked with the increasing concentrations in the environment. Abdou et al. (2016) reported the same trend using a historical series of wild oysters, which showed a bioconcentration factor of ~10^3 for a similar range of concentrations in the sediments (1–7 ng Pt g^{-1}). Though, chronic exposure of organisms to the PGE in their natural environment still needs to be reckoned, particularly in the case of Pd. In addition, the different metal forms should be considered in the evaluation of toxicity effects, considering either truly dissolved species and/or colloidal forms, the latter also including PGE nanoparticles.

1.7. Future Perspectives

Despite the advances with respect to the knowledge of PGE levels in aquatic ecosystems over the past decades, many questions continue to be posed. These maintain the urgent need to elucidate the mobility, speciation and bioavailability of PGE in estuaries and the adjoining coastal areas. With respect to these issues, the improvement of the available analytical techniques, and their combination, is necessary to assess accurate information. The different forms of PGE, e.g. as metallic nanoparticles, still need to be assessed for their potential toxicity to the biota. In addition, considering the most likely increase of those metals in the aquatic environment, the estimation of regional and/or global PGE fluxes needs to be re-evaluated. Consequently, there is also the need to develop new and integrative modelling tools, which will allow computing global fluxes, as well as the prediction of "worst-case scenario" impacts on regions vulnerable to anthropogenic activities. Ideally, this should include the main environmental compartments, i.e. the atmosphere, land, aquatic (water and sediments) and biota. The

health issues raised by the increasing demand and uses of those technology-critical elements still needs further elucidation. In particular, to respond to this need, surveying biota species used for human consumption that may be continuously exposed to PGE contamination is also needed. Thus, impacted estuaries and coastal areas subjected to continuously PGE inputs should be monitored. Field studies are an urgent necessity, considering that at the Earth's surface the fluxes of PGE have been, and will continue to be, altered mainly by anthropogenic emissions.

References

Abdou, M., Gil-Díaz, T., Schäfer, J., Catrouillet, C., Bossy, C., Dutruch, L., Blanc, G., Cobelo-García, A., Massa, F., Castellano, M., Magi, E., Povero, P., Tercier-Waeber, M. Lou, 2020. Short-term variations of platinum concentrations in contrasting coastal environments: The role of primary producers. Mar. Chem. 222, 103782. doi:10.1016/j.marchem.2020.103782

Abdou, M., Schäfer, J., Cobelo-García, A., Neira, P., Petit, J.C.J., Auger, D., Chiffoleau, J.-F., Blanc, G., 2016. Past and present platinum contamination of a major European fluvial–estuarine system: Insights from river sediments and estuarine oysters. Mar. Chem. 185, 104–110. doi:https://doi.org/10.1016/j.marchem.2016.01.006

Almécija, C., Cobelo-García, A., Santos-Echeandía, J., 2016. Improvement of the ultra-trace voltammetric determination of Rh in environmental samples using signal transformation. Talanta 146, 737–743. doi:10.1016/j.talanta.2015.06.032

Almécija, C., Cobelo-García, A., Wepener, V., Prego, R., 2017. Platinum group elements in stream sediments of mining zones: The Hex River (Bushveld Igneous Complex, South Africa). J. African Earth Sci. 129, 934–943. doi:https://doi.org/10.1016/j.jafrearsci.2017.02.002

Amato, F., Alastuey, A., de la Rosa, J., Gonzalez Castanedo, Y., de la Campa, A.M., Pandolfi, M., Lozano, A., Contreras González, J., Querol, X., 2014. Trends of road dust emissions contributions on ambient air particulate levels at rural, urban and industrial sites in southern Spain. Atmos. Chem. Phys. 14, 3533–3544. doi:10.5194/acp-14-3533-2014

Ayrault, S., Li, C., Gaudry, A., 2006. Biomonitoring of Pt and Pd with mosses, in: Palladium Emissions in the Environment. Springer, pp. 525–536.

Barbante, C., Veysseyre, A., Ferrari, C., Van De Velde, K., Morel, C., Capodaglio, G., Cescon, P., Scarponi, G., Boutron, C., 2001. Greenland snow evidence of large scale atmospheric contamination for platinum, palladium, and rhodium. Environ. Sci. Technol. 35, 835–839. doi:10.1021/es000146y

Bertine, K.K., Koide, M., Goldberg, E.D., 1993. Aspects of rhodium marine chemistry. Mar. Chem. 42, 199–210. doi:https://doi.org/10.1016/0304-4203(93)90012-D

Birke, M., Rauch, U., Stummeyer, J., Lorenz, H., Keilert, B., 2017. A review of platinum

group element (PGE) geochemistry and a study of the changes of PGE contents in the topsoil of Berlin, Germany, between 1992 and 2013. J. Geochemical Explor. doi:https://doi.org/10.1016/j.gexplo.2017.09.005

Bocca, B., Caimi, S., Smichowski, P., Gómez, D., Caroli, S., 2006. Monitoring Pt and Rh in urban aerosols from Buenos Aires, Argentina. Sci. Total Environ. 358, 255–264. doi:https://doi.org/10.1016/j.scitotenv.2005.04.010

Bonanno, G., Pavone, P., 2015. Leaves of Phragmites australis as potential atmospheric biomonitors of Platinum Group Elements. Ecotoxicol. Environ. Saf. 114, 31–37. doi:https://doi.org/10.1016/j.ecoenv.2015.01.005

Bowles, J.F.W., Gize, A.P., Cowden, A., 1994. The mobility of the platinum-group elements in the soils of the Freetown Peninsula, Sierra Leone. Can. Mineral. 32, 957 LP – 967.

Bruland, K.W., Middag, R., Lohan, M.C., 2014. 8.2 - Controls of Trace Metals in Seawater, in: Holland, H.D., Turekian, K.K.B.T.-T. on G. (Second E. (Eds.), . Elsevier, Oxford, pp. 19–51. doi:https://doi.org/10.1016/B978-0-08-095975-7.00602-1

Cawthorn, R.G., 2010. The Platinum Group Element Deposits of the Bushveld Complex in South Africa. Platin. Met. Rev. 54, 205–215. doi:10.1595/147106710X520222

Cobelo-García, A., 2013. Kinetic effects on the interactions of Rh(III) with humic acids as determined using size-exclusion chromatography (SEC). Environ. Sci. Pollut. Res. Int. 20, 2330–2339. doi:10.1007/s11356-012-1113-8

Cobelo-García, A., Filella, M., Croot, P., Frazzoli, C., Du Laing, G., Ospina-Alvarez, N., Rauch, S., Salaun, P., Schäfer, J., Zimmermann, S., 2015. COST action TD1407: network on technology-critical elements (NOTICE)—from environmental processes to human health threats. Environ. Sci. Pollut. Res. 22, 15188–15194. doi:10.1007/s11356-015-5221-0

Cobelo-García, A., López-Sánchez, D.E., Almécija, C., Santos-Echeandía, J., 2013. Behavior of platinum during estuarine mixing (Pontevedra Ria, NW Iberian Peninsula). Mar. Chem. 150, 11–18. doi:10.1016/j.marchem.2013.01.005

Cobelo-García, A., López-Sánchez, D.E., Schäfer, J., Petit, J.C.J., Blanc, G., Turner, A., 2014. Behavior and fluxes of Pt in the macrotidal Gironde Estuary (SW France). Mar. Chem. 167, 93–101. doi:10.1016/j.marchem.2014.07.006

Cobelo-García, A., Neira, P., Mil-Homens, M., Caetano, M., 2011. Evaluation of the contamination of platinum in estuarine and coastal sediments (Tagus Estuary and Prodelta, Portugal). Mar. Pollut. Bull. 62, 646–650. doi:10.1016/j.marpolbul.2010.12.018

Colombo, C., Oates, C.J., Monhemius, a. J., Plant, J. a., 2008. Complexation of platinum, palladium and rhodium with inorganic ligands in the environment. Geochemistry Explor. Environ. Anal. 8, 91–101. doi:10.1144/1467-7873/07-151

Diong, H.T., Das, R., Khezri, B., Srivastava, B., Wang, X., Sikdar, P.K., Webster, R.D., 2016. Anthropogenic platinum group element (Pt, Pd, Rh) concentrations in PM10 and PM2.5 from Kolkata, India. Springerplus 5, 1242. doi:10.1186/s40064-016-2854-5

Eriksson, J., 2001. Concentrations of 61 trace elements in sewage sludge, farmyard manure, mineral fertiliser, precipitation and in oil and crops. Stockholm.

Essumang, D. K., Dodoo, D. K., & Adokoh, C. K. (2008). The impact of vehicular fallout on the Pra estuary of Ghana (a case study of the impact of platinum group metals (PGMs) on the marine ecosystem). *Environmental Monitoring and Assessment*, *145*(1), 283–294. doi:10.1007/s10661-007-0037-0

Falzone, L., Salomone, S., Libra, M., 2018. Evolution of cancer pharmacological treatments at the turn of the third millennium. Front. Pharmacol. doi:10.3389/fphar.2018.01300

Fortin, C., Wang, F., Pitre, D., 2011. Critical Review of Platinum Group Elements (Pd, Pt, Rh) in Aquatic Ecosystems - Research Report No R-1269.

Glaister, B.J., Mudd, G.M., 2010. The environmental costs of platinum-PGM mining and sustainability: Is the glass half-full or half-empty? Miner. Eng. doi:10.1016/j.mineng.2009.12.007

Griffith, W.P., 2008. The periodic table and the platinum group metals. Platin. Met. Rev. 52, 114–119. doi:10.1595/147106708X297486

Halbach, P., Kriete, C., Prause, B., Puteanus, D., 1989. Mechanisms to explain the platinum concentration in ferromanganese seamount crusts. Chem. Geol. 76, 95–106. doi:https://doi.org/10.1016/0009-2541(89)90130-7

Hartley, F.R. (Ed.), 1991. Chemistry of the Platinum Group Metals, Volume 11, 1st editio. ed. Elsevier Science.

Hodge, V., Stallard, M., Koide, M., Goldberg, E.D., 1986. Determination of platinum and iridium in marine waters, sediments, and organisms. Anal. Chem. 58, 616–620. doi:10.1021/ac00294a029

Holwell, D.A., Mcdonald, I., 2010. A review of the behaviour of platinum group elements within natural magmatic sulfide ore systems. Platin. Met. Rev. 54, 26–36. doi:10.1595/147106709X480913

IUPAC, 2005. Nomenclature of Inorganic Chemistry – IUPAC Recommendations 2005. Chem. Int. -- Newsmag. IUPAC 27. doi:10.1515/ci.2005.27.6.25

Johnson Matthey, 2016. Platinum Group Metals Market Report - November.

Labarraque, G., Oster, C., Fisicaro, P., Meyer, C., Vogl, J., Noordmann, J., Rienitz, O., Riccobono, F., Donet, S., 2015. Reference measurement procedures for the quantification of platinum-group elements (PGEs) from automotive exhaust emissions. Int. J. Environ. Anal. Chem. 95, 777–789. doi:10.1080/03067319.2015.1058931

Laschka, D., Nachtwey, M., 1997. Platinum in municipal sewage treatment plants. Chemosphere 34, 1803–1812. doi:http://dx.doi.org/10.1016/S0045-6535(97)00036-2

Locatelli, C., 2007. Voltammetric Analysis of Trace Levels of Platinum Group Metals – Principles and Applications. Electroanalysis 19, 2167–2175. doi:10.1002/elan.200704026

López-Sánchez, D.E., Cobelo-García, A., Rijkenberg, M.J.A., Gerringa, L.J.A., de Baar,

H.J.W., 2019. New insights on the dissolved platinum behavior in the Atlantic Ocean. Chem. Geol. 511, 204–211. doi:https://doi.org/10.1016/j.chemgeo.2019.01.003

Lorand, J.P., Luguet, A., Alard, O., 2008. Platinum-group elements: A new set of key tracers for the Earth's interior. Elements 4, 247–252. doi:10.2113/GSELEMENTS.4.4.247

Mashio, A.S., Obata, H., Gamo, T., 2017. Dissolved Platinum Concentrations in Coastal Seawater: Boso to Sanriku Areas, Japan. Arch. Environ. Contam. Toxicol. 73, 240–246. doi:10.1007/s00244-017-0373-1

Mashio, A.S., Obata, H., Tazoe, H., Tsutsumi, M., Ferrer i Santos, A., Gamo, T., 2016. Dissolved platinum in rainwater, river water and seawater around Tokyo Bay and Otsuchi Bay in Japan. Estuar. Coast. Shelf Sci. 180, 160–167. doi:10.1016/j.ecss.2016.07.002

Mihaljevič, M., Galušková, I., Strnad, L., Majer, V., 2013. Distribution of platinum group elements in urban soils, comparison of historically different large cities Prague and Ostrava, Czech Republic. J. Geochemical Explor. 124, 212–217. doi:https://doi.org/10.1016/j.gexplo.2012.10.008

Moldovan, M., Rauch, S., Gómez, M., Antonia Palacios, M., Morrison, G.M., 2001. Bioaccumulation of palladium, platinum and rhodium from urban particulates and sediments by the freshwater isopod Asellus aquaticus. Water Res. 35, 4175–4183. doi:https://doi.org/10.1016/S0043-1354(01)00136-1

Monteiro, C. E.; Cobelo, A.; Correia dos Santos, M.; Caetano, M., n.d. Drivers of Pt and Rh variability in the water column of a hydrodynamic estuary: effects of contrasting environments. *in prep*.

Monteiro, C.E., Cobelo-García, A., Caetano, M., Santos, M.M.C. dos, 2017. Improved voltammetric method for simultaneous determination of Pt and Rh using second derivative signal transformation – application to environmental samples. Talanta. doi:10.1016/j.talanta.2017.06.067

Monteiro, C.E., Correia dos Santos, M., Cobelo-García, A., Brito, P., Caetano, M., 2019. Platinum and rhodium in Tagus estuary, SW Europe: sources and spatial distribution. Environ. Monit. Assess. 191, 579. doi:10.1007/s10661-019-7738-z

Mulholland, R., Turner, A., 2011. Accumulation of platinum group elements by the marine gastropod Littorina littorea. Environ. Pollut. 159, 977–982. doi:https://doi.org/10.1016/j.envpol.2010.12.009

Ndagi, U., Mhlongo, N., Soliman, M.E., 2017. Metal complexes in cancer therapy - an update from drug design perspective. Drug Des. Devel. Ther. 11, 599–616. doi:10.2147/DDDT.S119488

Neira, P., Cobelo-García, A., Besada, V., Santos-Echeandía, J., Bellas, J., 2015. Evidence of increased anthropogenic emissions of platinum: Time-series analysis of mussels (1991–2011) of an urban beach. Sci. Total Environ. 514, 366–370. doi:https://doi.org/10.1016/j.scitotenv.2015.02.016

Obata, H., Yoshida, T., Ogawa, H., 2006. Determination of picomolar levels of platinum in estuarine waters: A comparison of cathodic stripping voltammetry and isotope

dilution-inductively coupled plasma mass spectrometry. Anal. Chim. Acta 580, 32–38. doi:https://doi.org/10.1016/j.aca.2006.07.044

Oun, R., Moussa, Y.E., Wheate, N.J., 2018. The side effects of platinum-based chemotherapy drugs: a review for chemists. Dalt. Trans. 47, 6645–6653. doi:10.1039/C8DT00838H

Pérez-Ràfols, C., Trechera, P., Serrano, N., Díaz-Cruz, J.M., Ariño, C., Esteban, M., 2017. Determination of Pd(II) using an antimony film coated on a screen-printed electrode by adsorptive stripping voltammetry. Talanta 167, 1–7. doi:http://dx.doi.org/10.1016/j.talanta.2017.01.084

Peucker-Ehrenbrink, B., Jahn, B., 2001. Rhenium-osmium isotope systematics and platinum group element concentrations: Loess and the upper continental crust. Geochemistry, Geophys. Geosystems 2, n/a-n/a. doi:10.1029/2001GC000172

Pilchin, A., Eppelbaum, L., 2017. Concentration of Platinum Group Elements during the Early Earth Evolution: A Review*. Nat. Resour. 08, 172–233. doi:10.4236/nr.2017.83012

Qi, L., Luo, Q., Zhang, Y., Jia, F., Zhao, Y., Wang, F., 2019. Advances in Toxicological Research of the Anticancer Drug Cisplatin. Chem. Res. Toxicol. 32, 1469–1486. doi:10.1021/acs.chemrestox.9b00204

Rauch, S., Hemond, H.F., Barbante, C., Owari, M., Morrison, G.M., Peucker-Ehrenbrink, B., Wass, U., 2005. Importance of automobile exhaust catalyst emissions for the deposition of platinum, palladium, and rhodium in the northern hemisphere. Environ. Sci. Technol. 39, 8156–8162.

Rauch, S., Peucker-Ehrenbrink, B., 2015. Sources of platinum group elements in the environment, in: Platinum Metals in the Environment. Springer, pp. 3–17.

Rauch, S., Peucker-Ehrenbrink, B., Molina, L.T., Molina, M.J., Ramos, R., Hemond, H.F., 2006. Platinum Group Elements in Airborne Particles in Mexico City. Environ. Sci. Technol. 40, 7554–7560. doi:10.1021/es061470h

Ravindra, K., Bencs, L., Van Grieken, R., 2004. Platinum group elements in the environment and their health risk. Sci. Total Environ. 318, 1–43. doi:10.1016/S0048-9697(03)00372-3

Rinkovec, J., Pehnec, G., Godec, R., Davila, S., Bešlić, I., 2018. Spatial and temporal distribution of platinum, palladium and rhodium in Zagreb air. Sci. Total Environ. 636, 456–463. doi:https://doi.org/10.1016/j.scitotenv.2018.04.295

Ruchter, N., Sures, B., 2015. Distribution of platinum and other traffic related metals in sediments and clams (Corbicula sp.). Water Res. 70, 313–324. doi:http://dx.doi.org/10.1016/j.watres.2014.12.011

Schäfer, J., Puchelt, H., 1998. Platinum-Group-Metals (PGM) emitted from automobile catalytic converters and their distribution in roadside soils. J. Geochemical Explor. 64, 307–314. doi:http://dx.doi.org/10.1016/S0375-6742(98)00040-5

Silwana, B., van der Horst, C., Iwuoha, E., Somerset, V., 2014. Screen-printed carbon electrodes modified with a bismuth film for stripping voltammetric analysis of platinum group metals in environmental samples. Electrochim. Acta 128, 119–127. doi:http://dx.doi.org/10.1016/j.electacta.2013.11.045

Soyol-Erdene, T.-O., Huh, Y., 2012. Dissolved platinum in major rivers of East Asia: Implications for the oceanic budget. Geochemistry, Geophys. Geosystems 13, n/a-n/a. doi:10.1029/2012GC004102

Soyol-Erdene, T.-O., Huh, Y., Hong, S., Hur, S. Do, 2011. A 50-Year Record of Platinum, Iridium, and Rhodium in Antarctic Snow: Volcanic and Anthropogenic Sources. Environ. Sci. Technol. 45, 5929–5935. doi:10.1021/es2005732

Sures, B., Thielen, F., Zimmermann, S., 2002. Untersuchungen zur Bioverfügbarkeit Kfz-emittierter Platingruppenelemente (PGE) für die aquatische Fauna unter besonderer Berücksichtigung von PalladiumInvestigations on the bioavailability of traffic-related platinum group elements (PGE) to the aquatic fauna with special consideration being given to palladium. Umweltwissenschaften und Schadstoff-forsch. 14, 30–36. doi:10.1007/bf03038656

Sures, B., Zimmermann, S., 2007. Impact of humic substances on the aqueous solubility, uptake and bioaccumulation of platinum, palladium and rhodium in exposure studies with Dreissena polymorpha. Environ. Pollut. 146, 444–451. doi:10.1016/j.envpol.2006.07.004

Terashima, S., Katayama, H., Itoh, S., 1993. Geochemical behavior of Pt and Pd in coastal marine sediments, southeastern margin of the Japan Sea. Appl. Geochemistry 8, 265–271. doi:https://doi.org/10.1016/0883-2927(93)90041-E

van den Berg, C.M.G., Jacinto, G.S., 1988. The determination of platinum in sea water by adsorptive cathodic stripping voltammetry. Anal. Chim. Acta 211, 129–139. doi:http://dx.doi.org/10.1016/S0003-2670(00)83675-2

Wei, C., Morrison, G.M., 1994. Platinum in road dusts and urban river sediments. Sci. Total Environ. 146–147, 169–174. doi:https://doi.org/10.1016/0048-9697(94)90234-8

Wiseman, C.L.S., Hassan Pour, Z., Zereini, F., 2016. Platinum group element and cerium concentrations in roadside environments in Toronto, Canada. Chemosphere 145, 61–67. doi:https://doi.org/10.1016/j.chemosphere.2015.11.056

Wiseman, C.L.S., Zereini, F., Püttmann, W., 2013. Traffic-related trace element fate and uptake by plants cultivated in roadside soils in Toronto, Canada. Sci. Total Environ. 442, 86–95. doi:https://doi.org/10.1016/j.scitotenv.2012.10.051

Wood, S. a., Van Middlesworth, J., 2004. The influence of acetate and oxalate as simple organic ligands on the behavior of palladium in surface environments. Can. Mineral. 42, 411–4213. doi:10.2113/gscanmin.42.2.411

Zereini, F., Alsenz, H., Wiseman, C.L.S., Püttmann, W., Reimer, E., Schleyer, R., Bieber, E., Wallasch, M., 2012. Platinum group elements (Pt, Pd, Rh) in airborne particulate matter in rural vs. urban areas of Germany: concentrations and spatial patterns of distribution. Sci. Total Environ. 416, 261–268. doi:10.1016/j.scitotenv.2011.11.070

Zereini, F., Alt, F., Messerschmidt, J., von Bohlen, A., Liebl, K., Püttmann, W., 2004. Concentration and Distribution of Platinum Group Elements (Pt, Pd, Rh) in Airborne Particulate Matter in Frankfurt am Main, Germany. Environ. Sci. Technol. 38, 1686–1692. doi:10.1021/es030127z

Zereini, F., Wiseman, C., Püttmann, W., 2007. Changes in Palladium, Platinum, and

Rhodium Concentrations, and Their Spatial Distribution in Soils Along a Major Highway in Germany from 1994 to 2004. Environ. Sci. Technol. 41, 451–456. doi:10.1021/es061453s

Zereini, F., Wiseman, C.L.S., 2015. Platinum Metals in the Environment, Environmental Science and Engineering. Springer Berlin Heidelberg, Berlin, Heidelberg. doi:10.1007/978-3-662-44559-4

Zhong, L., Yan, W., Li, J., Tu, X., Liu, B., Xia, Z., 2012. Pt and Pd in sediments from the Pearl River Estuary, South China: background levels, distribution, and source. Environ. Sci. Pollut. Res. 19, 1305–1314. doi:10.1007/s11356-011-0653-7

Zimmermann, S., Baumann, U., Taraschewski, H., Sures, B., 2004. Accumulation and distribution of platinum and rhodium in the European eel Anguilla anguilla following aqueous exposure to metal salts. Environ. Pollut. 127, 195–202. doi:https://doi.org/10.1016/j.envpol.2003.08.006

II. OBJECTIVES

This thesis aims to improve the understanding of Pt and Rh cycle in transitional ecosystems. The Tagus estuary was chosen considering its particular features that make it a natural setting for the study of these elements and the limited knowledge on the levels and extension of PGE contamination. Other sources to the estuary than the ACC remain unclear, namely the anthropogenic pressure that results from heavily industrialised areas, with legacy in historical and present-day activities, and the concomitant Pt contamination due to medicinal applications. Furthermore, biogeochemical processes involving PGE in sediments and waters remain poorly understood. In particular, there is a knowledge gap regarding Pt and Rh in the water column of the Tagus estuary. One of the main goals of this research was to study the biogeochemical processes involving Pt and Rh in the chain sediment-water, which ultimately may have effects on the biota. To date, technical and analytical limitations still need to be overcome, whose speciation analysis of those elements is strongly dependent. Moreover, the physical features of aquatic ecosystems and chemical behavior of PGE need to be integrated into one tool that allows monitoring of the good environmental status and to foresee potentially impacted areas.

To achieve the proposed goals several questions were risen:

A. Can the current available methods be improved for the accurate determination of ultra-trace PGE in environmental samples?

B. What are the main sources of PGE to the Tagus estuary and their contamination levels in the several compartments?

C. What are the driven parameters that influence the cycle of PGE in waters and sediments?

D. To what extent do environmental drivers affect different forms of PGE?

E. What is the role of estuarine hydrodynamic in the export/import of PGE to the adjacent coastal area?

In order to answer these questions, specific objectives were delineated:

1. To improve the simultaneous analysis of Pt and Rh by AdCSV in a single scan using a second derivative signal transformation (Question A);

2. To improve the accuracy of Rh determination in environmental samples, with emphasis in water samples (Question A);

3. To quantify Pt and Rh concentrations in the Tagus estuary compartments and surrounding urban environment: waste-, river- and estuarine waters, suspended particulate matter (SPM), road dust and sediments (Question B);
4. To assess the influence of anthropogenic sources loading into the estuary through the analysis of superficial sediments (Question B);
5. To define baseline patterns for future monitoring studies envisaging unknown Pt and Rh emissions to this aquatic system (Question B);
6. To evaluate Pt and Rh physicochemical behaviour in the water column of Tagus estuary (Question C);
7. To study Pt and Rh desorption from road dust to water in different ionic strengths, pH and organic matter conditions (Question C);
8. To evaluate the pathways and mobility of Pt and Rh during urban-estuarine transport (Questions C and D);
9. To study Pt and Rh speciation analysis in road dust leachates using a combination of analytical methods (Question D);
10. To assess partition of Pt and Rh in the estuarine water column (Question D);
11. To evaluate Pt and Rh exchanges between different environmental compartments of the Tagus estuary under different hydrodynamic regimes (Questions D and E);
12. To simulate the distribution and fate of PGE using numerical tools and to foresee potential impacted areas (Question E);

III. STUDY AREA

Estuaries are very important in the interchange of mass between the land and the ocean. The Tagus estuary (Figure III-1) is one of the largest estuaries in SW Europe dominated by tidal oscillations. It has an area of *ca.* 320 km^2, which approximately 40 % are intertidal areas comprising small islands, sand banks, and intertidal mudflats. A narrow single channel marks the northward entrance of the Tagus River that opens to the shallow bay through a set of smaller channels. The inner bay has approximately 25 km long and 15 km wide, and the bathymetry ranges between 0 and 7 meters depth. This part has a complex bottom topography with channels that funnel towards a long, narrow and deep inlet. This inlet reaches up to 47 m depth and 2 km wide and connects the Tagus estuary to the Atlantic Ocean (Vale and Sundby 1987; Fortunato et al. 1999; Freire et al. 2007; Taborda et al. 2009; Vaz et al. 2011).

The Tagus River is the longest river in the Iberian Peninsula and the main source of freshwater to the estuary (in average 350 m^3 s^{-1}). Freshwater runoff from the Tagus shows high inter-annual variation according to the season, with river discharges between 50 and 2000 m^3 s^{-1}. Other small tributaries exist but only represent a minor contribution

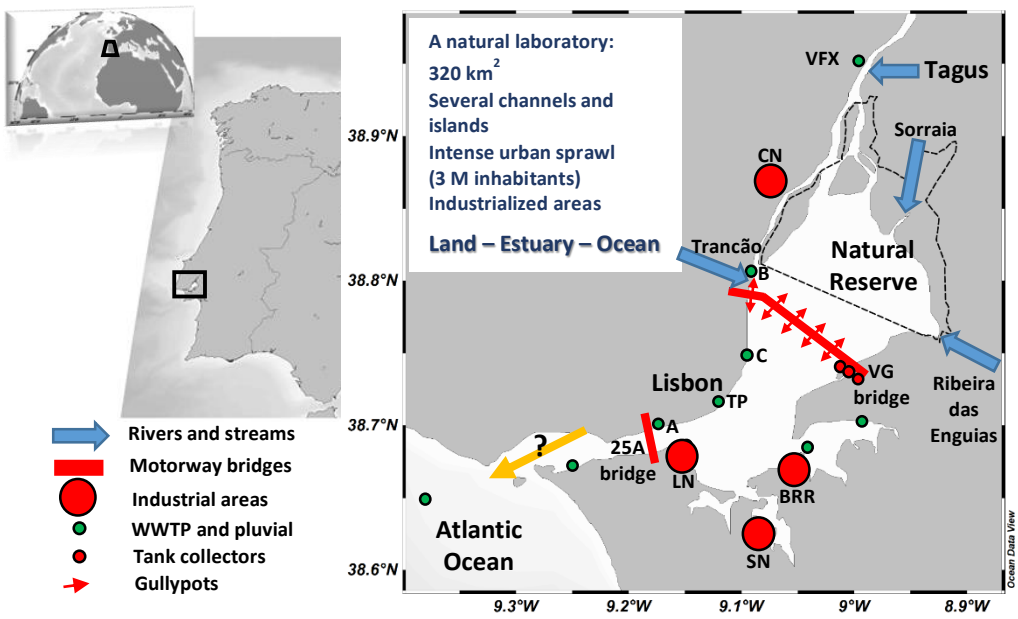

Figure III-1 – Representation of the study area location, the Tagus estuary, SW Europe, with depicted watercourses and main anthropogenic features: motorway bridges (25 de Abril (25A) and Vasco da Gama (VG); red lines); industrialized areas (CN, LN, SN and BRR; red circles); waste- (Alcântara (A), Beirolas (B) and Chelas (C)), and pluvial- (Terreiro do Paço (TP)) waters discharge sites (green circles); Natural reserve delimitation (dotted line).

of freshwater (in average <35 $m^3 s^{-1}$). Although the salinity within the estuary depends on the entrance of freshwater, the water circulation in Tagus estuary is mainly tidally driven, which controls the mixing processes. Considering that the tidal prism inside the estuary is 640×10^6 m^3, the river flow is only relevant to the non-linear mixing processes during high river flow events (de Pablo et al. 2019). Thus, the Tagus estuary is often considered mesotidal and vertically well-mixed (Vaz et al. 2011). However, partial stratification of the estuary can occur particularly under extreme conditions, such strong rainy events (Fortunato et al. 1997).

The tidal regime of the Tagus estuary is mainly semi-diurnal, ranging from 0.8 m (neap tide) to 4.0 m (spring tide), which may increase towards the estuary's interior due to resonance effects (Fortunato et al. 1997; Neves 2010). The tidal wave is asymmetric and progressive, causing delays up to two hours between Lisbon and Vila Franca de Xira (Neves 2010; Vale and Sundby 1987). Typically, ebbs are shorter than floods in the Tagus estuary (Fortunato et al. 1999; Guerreiro et al. 2015; Vaz and Dias 2014), which mirrors the stronger current velocities during ebbs (Vaz and Dias 2014). Tidal currents near the surface can be higher than 1.5 m s^{-1} during spring tides in the lower estuary inlet (Neves 2010). However, for this area of the estuary, different flow circulation patterns between ebb- and flooding conditions have been proposed based on numerical simulations (Fortunato et al. 1997). Residence times within the Tagus estuary vary according to location and in addition are influenced by the seasonal variability of Tagus river runoff, which can be between >20 days in the shallow bay and <10 days in the inlet channel (Braunschweig et al. 2003).

During spring tides, the immersed area may decrease from 320 km^2 at high tide to 130 km^2 at low tide (Silva et al. 2013), letting the tidal flats consecutively exposed to the atmosphere in between semi-diurnal cycles. Channels and pools formed in intertidal areas remain during part of the tidal cycle. There, resuspension of particulate matter from sediments over the tidal cycling can occur due to wind forcing, rising tide, and water exchange with the main channels (Alvera-Azcárate et al. 2003; Vale and Sundby 1987; Freire et al. 2007). Particle's settling occurs during the turnover of tides, depending on the current velocity and bathymetry (Vale and Sundby 1987). The particle resuspension-settling cycles in each semi-diurnal tide may play a key role on the transport and scavenging of Pt and Rh to the sediments.

The Tagus Estuary have been traditionally a region of several activities since the last century, whether industrial or agricultural, or linked to salt extraction and fisheries, amongst others. Consequently, it has been an important region for exportation of these products. Over decades, the increasing activities and population overloaded the Tagus margins with pollutants, being identified around 600 pollution sources associated to those anthropogenic pressures, as well as river runoff and atmospheric deposition (Dias and Marques 1999). As of those peak activities in the middle of the 20th century, researchers have devoted attention to the estuary in many aspects. The Tagus is well characterized with respect to the hydrodynamics (e.g. Vale and Sundby 1987; Fortunato et al. 1999; Vaz et al. 2011), trace elements (e.g. Vale et al. 2008; Santos-Echeandía et al. 2010; Caçador et al. 2012; Monteiro et al. 2016), persistent organic pollutants (e.g. Gil and Vale 1999; Mil-Homens et al. 2016), and nutrients (e.g. Cabeçadas 1999; Cabrita et al. 1999; Mateus and Neves 2008). For PGE, only data on Pt, Rh and Os were reported before in spot areas of the estuary and coastal sediments (Cobelo-García et al. 2011; Almécija et al. 2015, 2016a; 2016b), pointing to anthropogenic inputs.

The Tagus estuary (Figure III-1) has particular features that makes it a natural setting for the study of these elements. Intense urban sprawl reaches nearly 3 million of inhabitants around the estuary (Marques da Costa 2016) with several wastewater treatment plants (WWTP) and pluvial water drainage channels dispersed in the margins. Three of the main WWTP existing in the northern margin are located in Alcântara (A), Beirolas (B) and Chelas (C). From these, Alcântara receives wastewater and sewage from three municipalities where a dense urban area is settled and that accounts nearly 2 million people (Marques da Costa, 2016). At Terreiro do Paço (TP) is located one of the main channels for the pluvial runoff washed from the Lisbon area, which may represent another pathway for ACC emissions towards the estuary. Moreover, the Tagus estuary is crossed by two high traffic motorway bridges, Vasco da Gama (VG bridge) and 25 de Abril (25A bridge), where 175000 – 225000 vehicles pass every day (IMT 2016). The first was built in the mid-1990s and opened in 1998. Its extent reaches 18 km and crosses the middle estuary. The latter bridge is shorter than VG bridge, having an extension around 2 km.

The anthropogenic pressures also result from heavily industrialised areas, with historical and present-day activities. At the southern margin exists an active metallurgic complex (SN), an inactive shipyard (LN), and a chemical complex (BRR) with a large area decommissioned but with a few industries operating, namely in the production of

fertilizers that use Pt as a catalyst (e.g. Eastin 1991). Nearby, the decommissioned industrial area of BRR used to include a smelter and pyrite ore processing to extract metals of economic interest, such as Cu, Pb, Au and Ag (Vale et al. 2008). At the northern margin continues to operate a chemical industrial unit (CN) having a record of activities for nearly a century. This industry produces chemical products, such as nitric acid and hydrogen peroxide, that also use PGE as catalysts in their manufacturing processes (e.g. Lemaire et al. 2014; Paparatto et al. 2010).

All the characteristics described for the Tagus estuary make it a natural laboratory suitable for the study of Pt and Rh, for which research continues to be limited in this system (Cobelo-García et al. 2011; Almécija et al. 2015, 2016a; 2016b).

References

Almécija, C., Cobelo-García, A., & Santos-Echeandía, J. (2016a). Improvement of the ultra-trace voltammetric determination of Rh in environmental samples using signal transformation. *Talanta*, *146*, 737–743. doi:10.1016/j.talanta.2015.06.032

Almécija, C., Cobelo-García, A., Santos-Echeandía, J., & Caetano, M. (2016b). Platinum in salt marsh sediments: Behavior and plant uptake. *Marine Chemistry*, *185*, 91–103. doi:10.1016/j.marchem.2016.05.009

Almécija, C., Sharma, M., Cobelo-García, A., Santos-Echeandía, J., & Caetano, M. (2015). Osmium and platinum decoupling in the environment: Evidences in intertidal sediments (Tagus Estuary, SW Europe). *Environmental Science and Technology*, *49*(11), 6545–6553. doi:10.1021/acs.est.5b00591

Alvera-Azcárate, A., Ferreira, J. G., & Nunes, J. P. (2003). Modelling eutrophication in mesotidal and macrotidal estuaries. The role of intertidal seaweeds. *Estuarine, Coastal and Shelf Science*, *57*(4), 715–724. doi:10.1016/S0272-7714(02)00413-4

Braunschweig, F., Martins, F., Chambel, P., & Neves, R. (2003). A methodology to estimate renewal time scales in estuaries: the Tagus Estuary case. *Ocean Dynamics*, *53*(3), 137–145. doi:10.1007/s10236-003-0040-0

Cabeçadas, L. (1999). Phytoplankton production in the Tagus estuary (Portugal). *Oceanologica Acta*, *22*(2), 205–214. doi:https://doi.org/10.1016/S0399-1784(99)80046-2

Cabrita, M. T., Catarino, F., & Vale, C. (1999). The effect of tidal range on the flushing of ammonium from intertidal sediments of the Tagus estuary, Portugal. *Oceanologica Acta*, *22*(3), 291–302. doi:10.1016/S0399-1784(99)80053-X

Caçador, I., Costa, J. L., Duarte, B., Silva, G., Medeiros, J. P., Azeda, C., et al. (2012). Macroinvertebrates and fishes as biomonitors of heavy metal concentration in the Seixal Bay (Tagus estuary): Which species perform better? *Ecological Indicators*, *19*, 184–190. doi:https://doi.org/10.1016/j.ecolind.2011.09.007

Cobelo-García, A., Neira, P., Mil-Homens, M., & Caetano, M. (2011). Evaluation of the contamination of platinum in estuarine and coastal sediments (Tagus Estuary and Prodelta, Portugal). *Marine Pollution Bulletin*, *62*(3), 646–650. doi:10.1016/j.marpolbul.2010.12.018

de Pablo, H., Sobrinho, J., García, M., Campuzano, F., Juliano, M., & Neves, R. (2019). Validation of the 3D-MOHID hydrodynamic model for the Tagus coastal area. *Water (Switzerland)*, *11*(8). doi:10.3390/w11081713

Dias, M., & Marques, J. (1999). *Estuários. Estuário do Tejo: O seu valor e um pouco da sua história*. (I. da C. da N. Reserva Natural do Estuário do Tejo, Ed.). Reserva Natural do Estuário do Tejo, Instituto da Conservação da Natureza. Lisboa, Portugal.

Eastin, J. A. (1991, April 10). Manufacturing and using nitrogen fertilizer solutions on a farm. Google Patents.

Fortunato, A., Baptista, A. M., & Luettich, R. A. (1997). A three-dimensional model of tidal currents in the mouth of the Tagus estuary. *Continental Shelf Research*, *17*(14), 1689–1714. doi:https://doi.org/10.1016/S0278-4343(97)00047-2

Fortunato, A., Oliveira, A., & Baptista, A. M. (1999). On the effect of tidal flats on the hydrodynamics of the Tagus estuary. *Oceanologica Acta*, *22*(1), 31–44. doi:https://doi.org/10.1016/S0399-1784(99)80030-9

Freire, P., Taborda, R., & Silva, A. (2007). Sedimentary characterization of Tagus estuarine beaches (Portugal). *Journal of Soils and Sediments*, *7*(5), 296–302. doi:10.1065/jss2007.08.243

Gil, O., & Vale, C. (1999). DDT concentrations in surficial sediments of three estuarine systems in Portugal. *Aquatic Ecology*, *33*(3), 263–269. doi:10.1023/A:1009961901782

Guerreiro, M., Fortunato, A. B., Freire, P., Rilo, A., Taborda, R., Freitas, M. C., et al. (2015). Evolution of the hydrodynamics of the Tagus estuary (Portugal) in the 21st century. *Journal of Integrated Coastal Zone Management*, *15*(1), 65–80. doi:10.5894/rgci515

IMT. (2016). *Relatório de Tráfego na Rede Nacional de Autoestradas - 4º Trimestre*. Lisboa, Portugal.

Lemaire, A., Dournel, P., & Deschrijver, P. (2014, March 13). Process for the manufacture of hydrogen peroxide. Google Patents.

Marques da Costa, E. (2016). Sócio-Economia. In J. Rocha (Ed.), *Atlas Digital da Área Metropolitana de Lisboa*. Lisboa, Portugal: Centro de Estudos Geográficos.

Mateus, M., & Neves, R. (2008). Evaluating light and nutrient limitation in the Tagus estuary using a process-oriented ecological model. *Journal of Marine Engineering & Technology*, *7*(2), 43–54. doi:10.1080/20464177.2008.11020213

Mil-Homens, M., Vicente, M., Grimalt, J. O., Micaelo, C., & Abrantes, F. (2016). Reconstruction of organochlorine compound inputs in the Tagus Prodelta. *Science of The Total Environment*, *540*, 231–240. doi:https://doi.org/10.1016/j.scitotenv.2015.07.009

Monteiro, C. E., Cesário, R., O'Driscoll, N. J., Nogueira, M., Válega, M., Caetano, M.,

& Canário, J. (2016). Seasonal variation of methylmercury in sediment cores from the Tagus Estuary (Portugal). *Marine Pollution Bulletin*, *104*(1), 162–170. doi:https://doi.org/10.1016/j.marpolbul.2016.01.042

Neves, F. J. (2010). *Dynamics and hydrology of the Tagus estuary: results from in situ observations.* PhD Thesis, University of Lisbon, Portugal.

Paparatto, G., De, A. G., D'aloisio, R., & Buzzoni, R. (2010, September 28). Catalyst and its use in the synthesis of hydrogen peroxide. Google Patents.

Santos-Echeandía, J., Vale, C., Caetano, M., Pereira, P., & Prego, R. (2010). Effect of tidal flooding on metal distribution in pore waters of marsh sediments and its transport to water column (Tagus estuary, Portugal). *Marine environmental research*, *70*(5), 358–67. doi:10.1016/j.marenvres.2010.07.003

Silva, T. A., Freitas, M. C., Andrade, C., Taborda, R., Freire, P., Schmidt, S., & Antunes, C. (2013). Geomorphological response of the salt-marshes in the Tagus estuary to sea level rise. *Journal of Coastal Research*, *65*(65 (10065)), 582–587. doi:10.2112/si65-099.1

Taborda, R., Freire, P., Silva, A., Andrade, C., & Freitas, M. (2009). Origin and evolution of Tagus estuarine beaches. *Journal of Coastal Research*, *SI*(56), 213–217.

Vale, C., Canário, J., Caetano, M., Lavrado, J., & Brito, P. (2008). Estimation of the anthropogenic fraction of elements in surface sediments of the Tagus Estuary (Portugal). *Marine Pollution Bulletin*, *56*(7), 1364–1367. doi:https://doi.org/10.1016/j.marpolbul.2008.04.006

Vale, C., & Sundby, B. (1987). Suspended sediment fluctuations in the Tagus estuary on semi-diurnal and fortnightly time scales. *Estuarine, Coastal and Shelf Science*, *25*(5), 495–508. doi:http://dx.doi.org/10.1016/0272-7714(87)90110-7

Vaz, N., Mateus, M., & Dias, J. M. (2011). Semidiurnal and spring-neap variations in the Tagus estuary: Application of a process-oriented hydro-biogeochemical model. *Journal of Coastal Research*, *SI*(SPEC. ISSUE 64), 1619–1623.

Vaz, N., & Dias, J. M. (2014). Residual currents and transport pathways in the Tagus estuary, Portugal: the role of freshwater discharge and wind. *Journal of Coastal Research*, 610–615. doi:10.2112/SI70-103.1

IV. IMPROVED VOLTAMMETRIC METHOD FOR SIMULTANEOUS DETERMINATION OF PT AND RH USING SECOND DERIVATIVE SIGNAL TRANSFORMATION – APPLICATION TO ENVIRONMENTAL SAMPLES

***published*: C. E. Monteiro, A. Cobelo-García, M. Caetano and M. Correia dos Santos, 2017. Improved voltammetric method for simultaneous determination of Pt and Rh using second derivative signal transformation – application to environmental samples, *Talanta* 175, 1-8.**
DOI: https://doi.org/10.1016/j.talanta.2017.06.067

Graphical Abstract

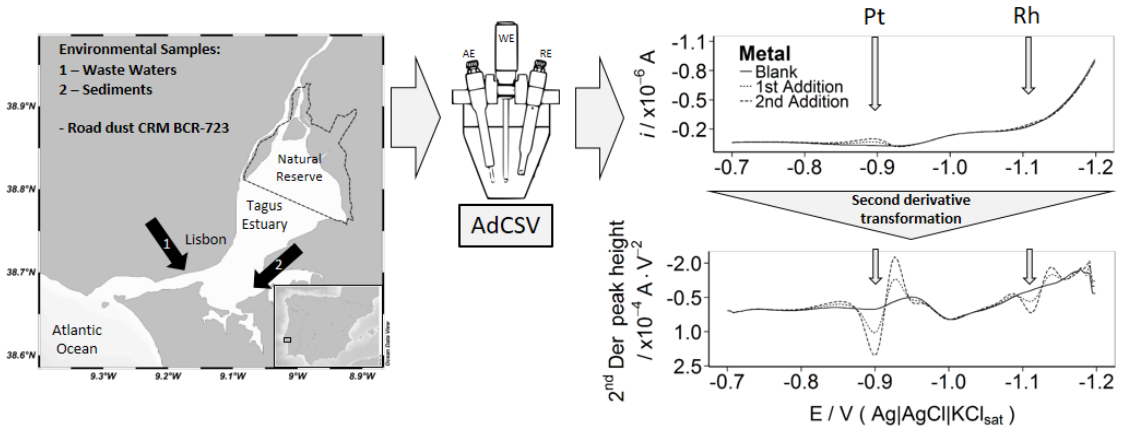

Abstract

The determination of Platinum-group elements (PGE) in relevant environmental matrices is a challenging task. Sensitive and accurate analytical procedures for simultaneous determination of Pt and Rh are still needed. In this study, we report for the first time on the use of second derivative signal transformation to the ultra-trace simultaneous determination of Pt and Rh by Adsorptive Cathodic Stripping Voltammetry (AdCSV). With that step, the ill-defined peaks typically observed in the original voltammograms are transformed into well-shaped peaks, resulting in accurate detection. The experimental conditions were investigated and optimised: a suitable electrolyte for both elements, with less reagents consumption (0.25 M H_2SO_4, 0.05 M HCl, 0.01 M FA and 0.5 mM HZ), deposition time (t_d) and deposition potential (E_d). For t_d = 120 s and E_d = –0.75 V, linear relationships r > 0.999 were obtained in the concentration range up to 5.8 ng L^{-1} (27 pM) for Pt and up to 3.4 ng L^{-1} (34 pM) for Rh. Limits of detection were 0.2 ng L^{-1} for Pt and 0.08 ng L^{-1} for Rh. Lower values can be achieved by increasing the deposition time. Limits of quantification, LOQ, calculated as 3 times LOD, were 0.5 ng L^{-1} for Pt and 0.2 ng L^{-1} for Rh. The sensitivity of Pt was affected by elevated Zn concentrations, whereas a minor effect was observed for Rh. However, Pt and Rh determinations were not influenced using the standard addition method. Precision as intermediate precision and expressed as relative standard deviation, based on Pt and Rh spiked solutions and digested road dust CRM BCR-723 was 17 % and 20 % for Pt and Rh, respectively. Recoveries of CRM were around 90 % for both elements. The method was successfully applied in the simultaneous determination of Pt and Rh in sediments from Tagus estuary and, for the first time, dissolved Rh was determined in water samples of a waste water treatment plant. Application of this technique in a multidisciplinary approach will be a relevant contribution to the current understanding of PGE cycle and fate in the environment.

Keywords

Platinum, Rhodium, Simultaneous determination, Adsorptive voltammetry, Second derivative, Environmental samples

4.1. Introduction

Platinum-group elements (PGE) constitute a group of rare and noble elements which includes platinum (Pt), palladium (Pd), rhodium (Rh), iridium (Ir), osmium (Os) and ruthenium (Ru). PGE are severely depleted in the earth's crust: 0.4 ng g^{-1} for Pt and Pd; 0.1 ng g^{-1} for Ru; 0.06 ng g^{-1} for Rh; and 0.05 ng g^{-1} for Ir and Os (Peucker-Ehrenbrink and Jahn 2001; Ravindra et al. 2004). Yet they have been increasingly explored and used over the past decades in several applications due to their physical and chemical properties (Rauch and Morrison 2008). The automobile industry is the main sector responsible for the PGE global demand, representing approximately 45 % Pt, 50 % Pd and 5 % Rh in 2016 (Johnson Matthey 2016). This is mostly due to the use of PGE in automobile catalytic converters to reduce the emissions of other pollutants, carbon monoxide, nitrogen oxides and hydrocarbon (Ravindra et al. 2004). As a result, anthropogenic emissions of PGE have grown significantly over the last decade (Zereini and Wiseman 2015). Particles released from catalytic converters due to abrasion or degradation result in widespread distribution of PGE, mainly near high traffic roads (Schäfer and Puchelt 1998). Thus, accumulation of PGE has been observed in sediments and vegetation, exceeding largely the natural background levels (Zereini and Wiseman 2015; Schäfer and Puchelt 1998). As to platinum and rhodium in aquatic systems, Pt(II), Pt(IV) and Rh(III) are the most important oxidation states, depending on salinity and redox conditions (Cobelo-García et al. 2014; Cobelo-García 2013). Inorganic speciation is dominated by aquo-hydroxo, aquo-chloro and mixed aquo-hydroxo-chloro complexes (Cobelo-García et al. 2014; Cobelo-García 2013). Furthermore, there is evidence of Pt and Rh interaction with organic matter, which may be a key parameter in speciation and distribution of PGE in aquatic ecosystems (Cobelo-García 2013; Bowles et al. 1994).

Platinum has received the utmost attention among the PGE studies. More recently, Rh in environmental samples has been reckoned, but only with emphasis on urban and roadside solid samples. Thus, data on its total dissolved concentrations still lacks (Zereini and Wiseman 2015), and Rh speciation studies are scarce (e.g. Cobelo-García 2013). The improvement of analytical techniques over the past few decades, such as electrothermal atomic absorption spectrometry (ET-AAS) and inductively coupled plasma mass spectrometry (ICP-MS), allowed the individual and simultaneous determination of those elements in different environmental matrices (Zereini and Wiseman 2015). Despite the high sensitivity of ICP-MS for PGE analysis it has some disadvantages, such as the need

of matrix separation due to polyatomic interferences from other elements (Labarraque et al. 2015). Overall, this is an expensive technique, as well as time-consuming, and susceptible of cross-contamination.

Voltammetric techniques provide a simple and sensitive way to directly determine Pt and Rh at ultra-trace levels. Additionally, it is less expensive and appears adequate for routine analysis (Zereini and Wiseman 2015; Locatelli 2007). Several electroanalytical procedures have been reported mostly based on adsorptive cathodic stripping voltammetry (AdCSV) on a mercury electrode. Although alternative electrodes have been investigated envisaging a similar analytical performance to mercury (Silwana et al. 2014); (Pérez-Ràfols et al. 2017), detection and quantification limits reported are insufficient to study the behavior of PGEs in unspoiled environments, particularly in the case of Rh.

Platinum-group elements can form highly stable complexes which can act as catalysts for hydrogen production after metal reduction on a mercury electrode (Heyrovský and Kůta 1966). In the case of Pt, the surface active complex mostly explored is that with formazone, produced *in situ* from the reaction of formaldehyde (FA) and hydrazine (HZ) (Locatelli 2007; van den Berg and Jacinto 1988; León et al. 1997; Cobelo-García et al. 2014). The surface active complex adsorbs on the mercury electrode and the catalytic-promoted hydrogen reduction occurs in acidic (e.g. H_2SO_4) conditions due to the formation of Pt(0) at the electrode surface, giving rise to a catalytic wave upon metal reduction. Furthermore, the catalytic behaviour of Pt(IV) is similar to Pt(II), since hydrazine can quantitatively reduce Pt(IV) to Pt(II) (Zhao and Freiser 1986). Alternative methods using other ligands were described, and found comparable with those employing formazone (Dalvi et al. 2008). In the case of Rh, catalytic waves in formaldehyde–HCl media have been reported and the nature of the surface active complexes may well be chloro-complexes and/or formaldehyde complexes (Cobelo-García 2013; Hong et al. 1994; Almécija et al. 2016).

The pioneer works of Zhao and Freiser (1986) and van den Berg and Jacinto (1988) established the ultra-trace individual determination of Pt, while Wang and Taha (1991) and Hong et al. (1994) have set up a methodology for Rh. Other works dealing with environmental samples followed, prevalently addressing Pt (Zereini and Wiseman 2015). Another challenge has been the simultaneous determination of Pt and Rh in real environmental samples and some applications were reported (Locatelli 2007; León et al. 1997). Various supporting electrolytes and different complexing agents have been used

and although in most works an optimised procedure is presented, in some cases the nature of the surface active complexes for rhodium remains elusive (Hong et al. 1994; Locatelli 2005).

In most of the works, voltammetric peak currents were used for quantification, which can have a drawback. One disadvantage is the intense background current or interfering peaks that affects the target signal, causing ill-defined peaks influencing the accuracy of measurements (Cobelo-García et al. 2014). At ultra-trace concentrations, Pt and in particular Rh peak currents may be almost imperceptible. An improvement was achieved on the individual determination of Pt and Rh using second derivative signal transformation, as reported by Cobelo-García et al. (2014) and Almécija et al. (2016), respectively. Low background interferences due to current noise or matrix elements were better discriminated, as well-defined peaks and low LOD were achieved using signal transformation.

We hypothesized that (1) the use of second derivative signal transformation improve the simultaneous analysis of Pt and Rh by AdCSV in a single scan. Simultaneous analysis of both elements will (2) reduce the cost of reagents used during the analytical procedure, being the method more environmentally friendly, and (3) reduce the time of analysis, making it appropriate for routine analysis. Therefore, in this study we report the optimised conditions (electrolyte composition and instrumental parameters) for the simultaneous analysis of Pt and Rh by AdCSV using the second derivative signal transformation in the voltammograms.

The suitability of the method to real environmental matrices is well demonstrated by its application to Pt and Rh determinations in sediments from Tagus estuary and water samples from an urban waste water treatment plant (WWTP).

4.2. Material and Methods

4.2.1. Material and Chemicals

Laboratory material was previously acid-cleaned with immersion in ~20 % nitric acid (HNO_3) and hydrochloric acid (HCl) baths for at least 48 hours. Afterwards, all material was rinsed with Milli-Q water (18.2 MΩ cm, 25 ºC) and let to dry in a clean room. All reagents used in analysis and samples digestion were of high-purity grade:

sulphuric acid (H_2SO_4) ≥ 95 % (*Trace*SELECT, Fluka), HNO_3 65 % and HCl 30 % (*Suprapur*, Merck), formaldehyde 13 M (FA 36.5 %, Riedel-de-Haen), hydrazine sulphate (HZ; p.a., Fluka), and hydrogen peroxide (H_2O_2) 30 % (p.a., ACS ISO, Emsure). Solutions of 0.53 M FA and 50 mM HZ were prepared in Milli-Q water and stored in perfluoroalkoxy (PFA) flasks. These solutions are stable for several weeks (Cobelo-García et al. 2014). Standard solutions 1000 mg L^{-1} (*Trace*CERT, Fluka) of Pt and Rh were used to prepare daily diluted standard solutions of 1.0 µg L^{-1} Pt in 1M HCl and 1.0 µg L^{-1} Rh in 0.1M HCl. The electrolyte final concentrations in the voltammetric cell were 0.25 M H_2SO_4, 0.05 M HCl, 0.01 M FA and 0.5 mM HZ.

4.2.2. Apparatus and Analysis

Voltammetric determinations were performed in an Autolab PGSTAT 128N (Metrohm) coupled to a polarographic stand model 663 VA (Metrohm). Parameters of the equipment and data acquisition were controlled with GPES v. 4.9 software (EchoChemie). All measurements were performed in triplicate under clean and acclimatised conditions (25 ± 2 ºC). The stand was equipped with a static mercury drop electrode (SDME) as working electrode, a Ag/AgCl as reference electrode, placed inside a salt bridge with saturated KCl (3 M) and a glassy carbon rod as counter electrode. Polytetrafluoroethylene (PTFE) vessels were used as voltammetric cells in all experiments.

For the voltammetric analysis, after purging with N_2 for 10 minutes prior to the measurements and homogenization using a rotating PTFE rod, at 3000 rpm, a new mercury drop was extruded. While stirring, a deposition potential E_d = –0.75 V was applied for the deposition time t_d = 120 s (or t_d= 300 s) (see section **4.3.2** ***Optimisation of the conditions***). Afterwards, 10 s of quiescence period was given. Then, a stripping scan was performed using differential pulse (DP) mode from –0.7 to –1.2 V, at a scan rate of 20 mV s^{-1} with modulation time of 0.04 s and amplitude of 25 mV, an interval time of 0.2 s and step potential of 4 mV. Total Pt and Rh were quantified using the standard addition method.

4.2.3. Procedure for Pt and Rh Digestion in Sediments and CRM

Sediments and certified reference material (CRM) were ashed in quartz crucibles at 800 ºC following the heating scheme of Nygren et al. (1990) to remove the organic matter that interferes with the voltammetric determination. The residue was transferred to PTFE vessels and digested using a mixture of concentrated acids (3 mL HCl and 1 mL HNO_3) at 195 ºC for 4 hours in a hot plate. After cooling, the caps were removed from the vessels and samples were allowed to evaporate the acids near dryness at 85 ºC. Samples were then re-dissolved in 1 mL of H_2SO_4 and the remaining HCl and HNO_3 were left to evaporate to a constant volume. The residue was transferred to polypropylene (PP) Digitubes (SCP Science) and diluted to 25 mL with 0.1 M HCl following the procedures previously described (Cobelo-García et al. 2014; Almécija et al. 2016).

4.2.4. Procedure for Pt and Rh Analysis in Waters

Water samples from an urban WWTP were collected and stored in acid-washed PP bottles (Nalgene). Samples were filtered using acid-cleaned 0.2 µm polycarbonate (PC) membranes (Millipore). Filtered samples were immediately acidified with concentrated HCl (Suprapur, Merck) to pH ≈ 1.0. Previously to the voltammetric analysis, the water samples were UV digested under a 125 W high-pressure mercury lamp (Osram) for 3 hours (Cobelo-García et al. 2013). This step removes the dissolved organic content, which causes interferences in the voltammetric determination. To assure rapid and complete degradation of organic matter, 1 µL of concentrated H_2O_2 per 1 mL of sample was added into the digestion quartz tube (Sodré et al. 2004).

4.2.5. Data Processing

Using the GPES v4.9 software the original voltammograms were processed as described by Cobelo-García et al. (2014) and Almécija et al. (2016). To the original voltammogram was applied a smoothing step by a factor of 2, according to the Savitsky-Golay (SG) algorithm, which removes noise signals that could be intensified after the double derivation step. Then, the second derivative signal transformation (2^{nd} Der) was obtained by applying twice the derivative transformation, expressed as:

$$\frac{dy}{dx} \approx 0.5\left(\frac{y(n)-y(n-1)}{x(n)-x(n-1)}\right) + 0.5\left(\frac{y(n+1)-y(n)}{x(n+1)-x(n)}\right) \quad (1)$$

where $y = I$ and $x = E$ corresponding to the current intensity (in A) and applied potential (in V), respectively, and n indicates the number of data points. This procedure removed very efficiently background interferences while keeping good peak-shaped transformed signals. After signal transformation, each metal peak height was measured based on peak–peak linear baseline, which has been proven to provide the most accurate results for Pt (Cobelo-García et al. 2014) and for Rh (Almécija et al. 2016).

Additionally, the necessary statistical analysis and graphical representations were performed with the open source language R and the available packages (R Core Team 2014).

4.2.6. Samples from the Tagus Estuary River and WWTP

To apply our optimised method we have chosen different environmental samples to monitor PGE levels. Superficial sediments were collected in the Tagus estuary nearby an industrial area in early June 2016. Additionally, water was collected in a WWTP of Lisbon (Portugal). Two water samples were collected (inflow and outflow of the WWTP) after a long dry period, just before raining, and soon after the first intense rainfall in early October 2016.

4.3. Results and Discussion

4.3.1. Second Derivative Transformation

Several parameters were investigated to optimise the procedure for simultaneous determination of Pt and Rh by means of AdCSV using the second derivative (2^{nd} Der) signal transformation (see section **4.3.2** ***Optimisation of the Conditions***). In addition to the electrolyte composition, working conditions like equilibration time, deposition potential and deposition time, were assessed and optimised. Possible interferences,

mainly from electrochemical signals close to the analytical signals of Pt and Rh, were also investigated.

Figure IV-1a shows the original voltammograms obtained in the optimised conditions of an aliquot of digested road dust CRM BCR-723 (100 uL of sample digest in 15 mL) corresponding to 3.0 ng L^{-1} Pt and 0.47 ng L^{-1} Rh, and two standard additions of 1.0 ng L^{-1} Pt and 0.33 ng L^{-1} Rh. Ill-defined peaks were observed for Pt, around –0.89 V, and especially for Rh where a broad shoulder is barely seen, at potentials close to –1.11 V, superimposed by the high background current. Signals like these are difficult to measure and thus often lack the necessary accuracy. The use of the 2nd Der transformation, showed in Figure IV-1b, provided well-defined peaks for both metals, which were easily measured and diminished the errors associated with this step.

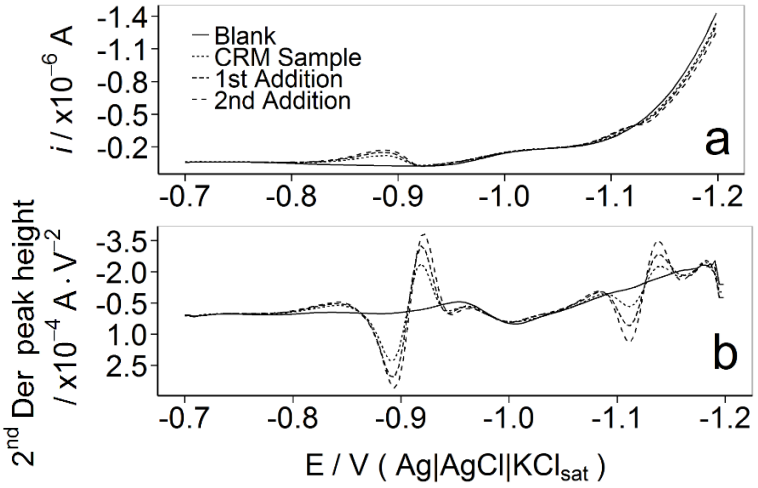

Figure IV-1 – (**a**) Original and (**b**) second derivative (2nd Der) voltammograms of road dust CRM BCR-723, obtained in the optimised conditions: 1) blank (solid line); 2) CRM sample BCR-723 (100 uL of sample digest in 15 mL) corresponding to 3.0 ng L^{-1} Pt and 0.47 ng L^{-1} Rh (small dotted line); 3) first standard addition (dotted line), 1.0 ng L^{-1} Pt and 0.33 ng L^{-1} Rh; and 4) second standard addition (long dotted line), 2.0 ng L^{-1} Pt and 0.67 ng L^{-1} Rh. t_d =120 s and E_d = –0.75 V. Electrolyte: 0.25 M H_2SO_4, 0.05 M HCl, 0.01 M FA and 0.5 mM HZ.

4.3.2. Optimisation of the Conditions

4.3.2.1. Electrolyte Composition

For Pt determination by AdCSV, previous studies have taken advantage of the well-established complex with formazone, produced *in situ* by the reaction of HZ with FA (van den Berg and Jacinto 1988; León et al. 1997; Cobelo-García et al. 2014; Locatelli 2005). Formazone was also referred as the ligand for Rh determination by AdCSV (Locatelli 2005). In HCl media and in the presence of FA, the Rh surface active complexes are supposed to be a mixture of complexes with FA and chloro-complexes (Hong et al. 1994; Almécija et al. 2016). In any case, high acid concentration is needed in the electrolyte to obtain a catalytic hydrogen current and H_2SO_4 and/or HCl have been used.

To achieve the optimum procedure, we explored the nature of the surface active complexes in hydrazine + formaldehyde and the acids media to be used for the simultaneous determination of Pt and Rh. The concentrations of 10 mM FA and 0.5 mM HZ followed our previous experience in the individual determination of Pt and Rh (Cobelo-García et al. 2014; Almécija et al. 2016). As to the effect of the acids, various mixtures of HCl and H_2SO_4 were prepared. Figure IV-2a shows the influence of H_2SO_4 concentration on 2.0 ng L^{-1} Pt and 0.67 ng L^{-1} Rh signals while keeping the HCl concentration constant (0.4 M (Almécija et al. 2016)). Sensitivity of Rh slightly decreased for H_2SO_4 concentrations higher than 0.25 M and Pt sensitivity above 0.4 M. A compromise for the H_2SO_4 concentration was 0.25 M. As to the influence of the HCl concentration on the voltammetric signals at constant H_2SO_4 concentration (0.5 M (Cobelo-García et al. 2014), Figure IV-2b shows that the sensitivity for both Rh and Pt is less dependent on the HCl concentration, in opposition to previous reports, e.g. León et al. (1997) and Locatelli (2005). The sensitivity obtained in the absence of HCl does not differ, within the experimental errors, from that in the presence of HCl up to 0.5 M HCl. Therefore, Rh chloro-complexes are not relevant surface active complexes in H_2SO_4, 0.01 M FA and 0.5 mM HZ medium and HCl can be removed from the electrolyte. Because HCl is present in some samples due to the conditions used for sample preparation, as previously described, a concentration of 0.05M HCl was set in the voltammetric cell in all experiments.

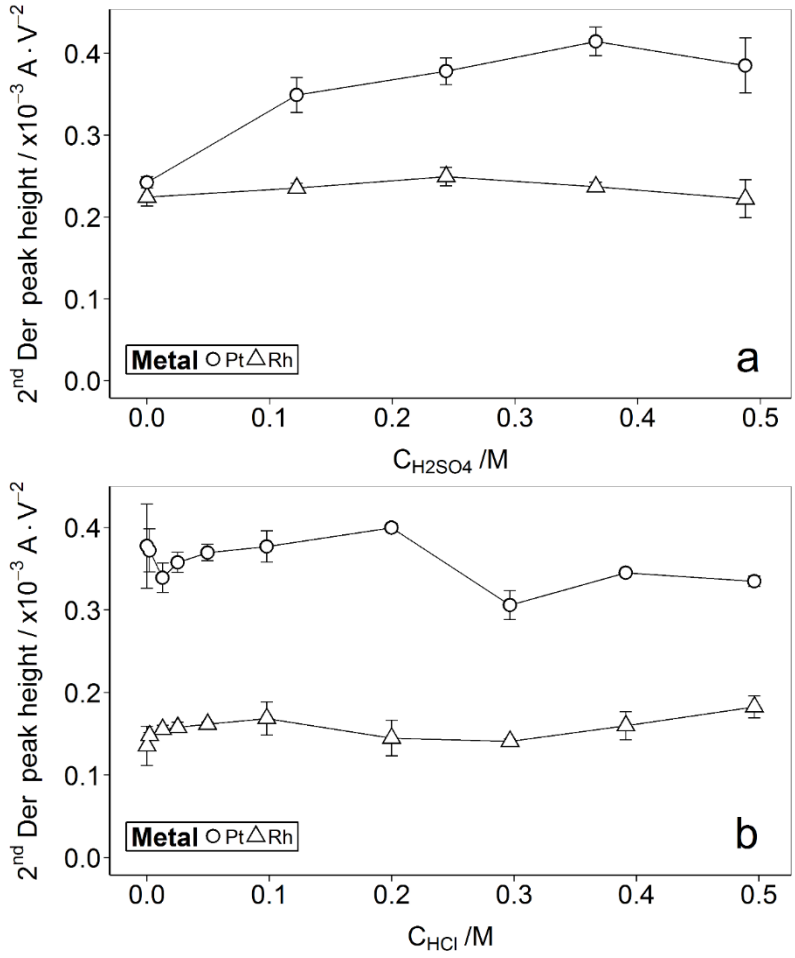

Figure IV-2 – Second derivative (2^{nd} Der) peak heights of 2.0 ng L^{-1} Pt (circles) and 0.67 ng L^{-1} Rh (triangles) with (**a**) variation of H_2SO_4 concentration in 0.4 M HCl and (**b**) variation of HCl concentration in 0.5 M H_2SO_4. Electrolyte: 0.01 M FA and 0.5 mM HZ; deposition times: t_d^1 = 120 s and t_d^2 = 60 s; deposition potentials: E_d^1 = –0.3 V and E_d^2 = –0.7 V.

The nature of Rh surface active complexes was assessed by adding formaldehyde followed by hydrazine to 0.25 M H_2SO_4 electrolyte and in the presence of 2.0 ng L^{-1} Pt and 0.67 ng L^{-1} Rh. The voltammetric signal of Rh was immediately observed after FA addition and its characteristics (intensity and potential) did not change upon HZ addition (S.I. Figure S.IV 1). Only in the presence of both FA and HZ, with formazone being produced *in situ*, was observed the Pt signal, while Rh characteristics kept stable within the experimental error. Accordingly, Pt adsorbs on the electrode surface as the Pt-formazone complex, as expected, while the surface active complex in the case of Rh is that with formaldehyde (S.I Figure S.IV 1).

4.3.2.2. Equilibration Time

After the addition of all reagents in the voltammetric cell, the effect of equilibration time on the signal of Pt and Rh was tested from 10 to 30 minutes while stirring. No detectable differences were found by varying the equilibration time prior to the analysis for Rh signal. The same occurred with Pt signal. Therefore an equilibration time of 10 minutes (coincident with the purging and stirring period) was used in all experiments.

4.3.2.3. Deposition Potential and Deposition Time

For the most convenient deposition potential for Pt and Rh determination, previous works referred E_d= –0.3 V and E_d= –0.7 V as more favourable for Pt (Cobelo-García et al. 2014) and Rh determination (Almécija et al. 2016), respectively. Consequently, in this work E_d was varied between 0 V and –1.1 V for a deposition time (t_d) of 120 s (Figure IV-3).

The sensitivity for Pt was almost constant between –0.1 and –0.85 V, decreasing abruptly at more negative potentials due to Pt reduction. Otherwise, the sensitivity for Rh tended to increase with the more negative potential. Therefore, –0.75 V was selected as a suitable deposition potential for the simultaneous determination of Pt and Rh. When the concentration of Pt is low compared to Rh, it is possible to use a more positive deposition

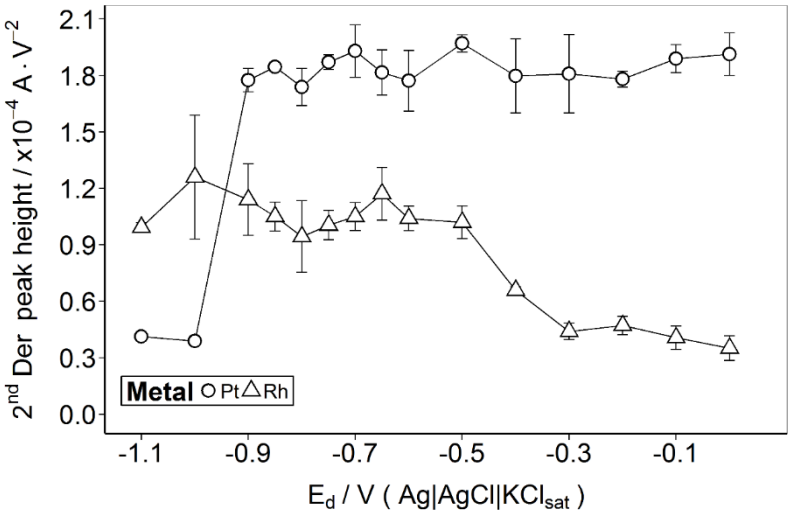

Figure IV-3 – Second derivative (2nd Der) peak heights of 1.0 ng L^{-1} Pt (circles) and 0.36 ng L^{-1} Rh (triangles) with variation of deposition potentials, E_d; t_d = 120 s. Electrolyte: 0.5 M H_2SO_4, 0.4 M HCl, 0.01 M FA and 0.5 mM HZ.

potential (e.g. –0.3 V; Cobelo-García et al. 2014) where the adsorption of the rhodium complex is less favourable. However, this is not found in most environmental matrices, where higher Pt concentrations than Rh are expected (up to 10-fold; Schindl and Leopold 2015). So, a pre-accumulation at the more favourable potential for Rh is desirable.

The influence of deposition time on the analytical signal, peak heights measured using the second derivative transformation, was also investigated for Pt and Rh solutions at two different levels of concentration (Figure IV-4): a) 2.0 and 4.0 ng L^{-1} Pt; and b) 0.66 and 1.3 ng L^{-1} Rh. Linear relationships with correlation coefficients > 0.999 were obtained for deposition times up to 300 s. Also in Figure IV-4 can be observed that saturation of the electrode surface does not occur in this range of concentrations either for Pt or Rh. The choice of the optimum t_d value will be dependent on the concentration of the analyte to be determined. Accumulation times of 120 s proved to be adequate for the determination of Pt and Rh in relevant environmental matrices, such as sediments and road dust CRM BCR-723. However, in water samples these metals tend to be present in lower concentrations. Thus, the deposition time should be increased in order to attain an accurate separation of Pt and Rh signals from background values.

The optimised conditions for the simultaneous determination of Pt and Rh using the second derivative are given in Table IV.1.

4.3.3. Interferences

Interferences in voltammograms can be due either to the presence of surface active compounds or interfering peaks. The effect of surface active compounds can be quite serious and that is why samples are previously treated, e.g. in order to destroy all organic matter. Other interferences could be due to the formation of other metal complexes with formazone. However, these complexes were reported as negligible for metal ions such as Fe and Cu (van den Berg and Jacinto 1988; León et al. 1997). Contrarily, the existence of elevated concentrations of Zn in samples may be problematic, because Zn can be reduced at a mercury electrode in the potential range between the Pt and Rh signals.

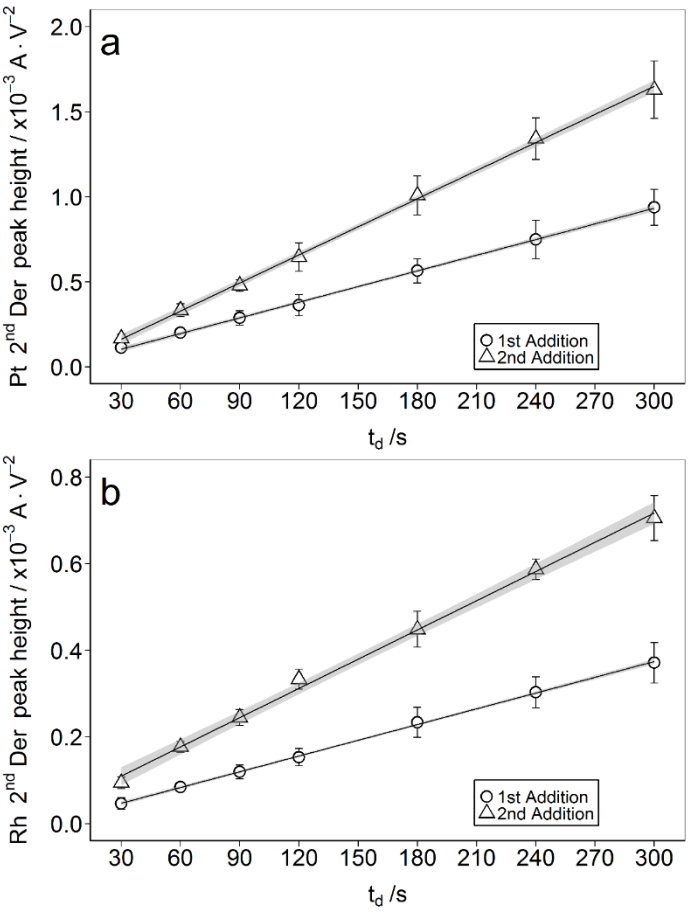

Figure IV-4 – Effect of deposition time, t_d, in second derivative (2^{nd} Der) peak heights, measured using optimised conditions: (**a**) Pt: 2.0 ng L^{-1}, 2^{nd} Der peak height = $1.2x10^{-5} + 3.1x10^{-6}\,t_d$ (circles) and 4.0 ng L^{-1}, 2^{nd} Der peak height = $-1.7x10^{-6} + 5.5x10^{-6}\,t_d$ (triangles) and **(b)** Rh: 0.66 ng L^{-1}, 2^{nd} Der peak height = $1.1x10^{-5} + 1.2x10^{-6}\,t_d$ (circles) and 1.3 ng L^{-1} Rh, 2^{nd} Der peak height = $4.2x10^{-5} + 2.2x10^{-6}\,t_d$ (triangles). E_d = –0.75 V. Electrolyte: 0.25 M H_2SO_4, 0.05 M HCl, 0.01 M FA and 0.5 mM HZ. The grey shaded area represents the 95 % confidence interval of the curve.

Consequently, we examined Zn interferences in the simultaneous determination of Pt and Rh in solutions containing 1.0 ng L^{-1} Pt and 0.33 ng L^{-1} Rh, while varying the Zn concentration (Figure IV-5). When compared to the Pt and Rh signals without Zn in solution (Figure IV-5a), the signal intensity of Rh was not immediately affected in the range of Zn concentrations analysed, while there was a decrease of the signal intensity for Pt at Zn concentrations higher than 0.7 mg L^{-1} (~11 µM) (Figure IV-5b). This decrease may not be immediately detected in the original voltammogram (Figure IV-5c). Instead, a broad shoulder between Pt and Rh stripping potentials appears with the increase of Zn concentration causing distortion, in particular to the Pt signal.

Table IV.1 – Optimised experimental conditions used for both Pt and Rh determination in different matrices.

Electrolyte		
H_2SO_4	0.25	M
HCl	0.05	M
FA	0.01	M
HZ	0.5	mM
Parameters		
Temperature	25 ± 2	ºC
Equilibration and Purging time	10	min
Deposition potential	–0.75	V
Deposition time	120	s
Quiescent time	10	s
Initial potential	–0.7	V
End potential	–1.2	V
Scan rate	20	mV s^{-1}
Modulation amplitude	25	mV
Modulation time	0.04	s
Interval time	0.2	s
Step potential	4	mV
Signal transformation	Smoothing SG 2 + 2nd derivative	

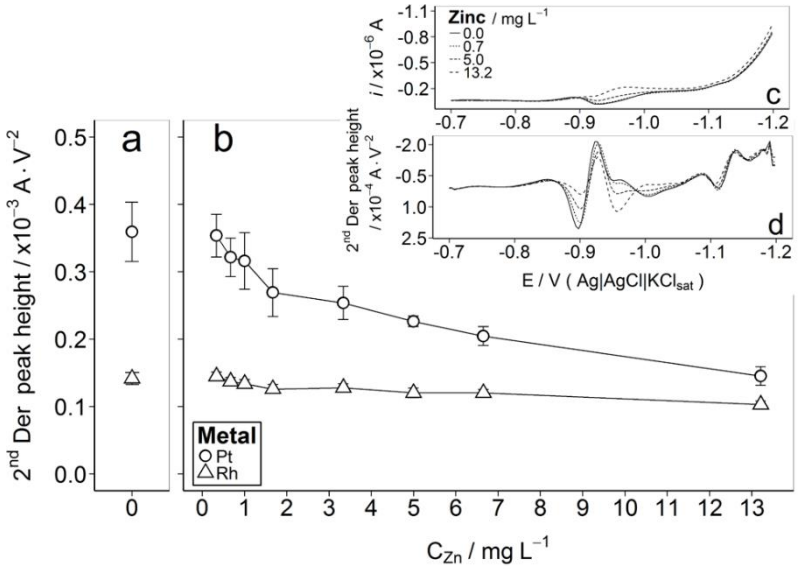

Figure IV-5 – Effect of Zn in peak heights of 1.0 ng L^{-1} Pt (circles) and 0.33 ng L^{-1} Rh (triangles) measured using the second derivative (2nd Der) transformation in optimised conditions: (**a**) without any Zn concentration (0 mg L^{-1}), and (**b**) Zn ranging up to 13 mg L^{-1}; (**c**) original and (**d**) second derivative transformation voltammograms. t_d =120 s and E_d = –0.75 V. Electrolyte: 0.25 M H_2SO_4, 0.05 M HCl, 0.01 M FA and 0.5 mM HZ.

The use of 2nd Der transformation improved the ill-defined peaks, evidencing how the Pt signal is more affected than that of Rh by the presence of Zn in solution (Figure IV-5d). Platinum and Rh determination by the standard addition method were not affected in the presence of at least 2 mg L^{-1} Zn, regardless of the decreasing sensitivity for Pt. This result is in line with those previously reported, having maximum tolerable of 2 – 3 mg L^{-1} (León et al. 1997) or 10 mg L^{-1} (Locatelli 2005). If it is considered the Zn concentrations found in salt marsh sediments colonized by vascular plants, which typically retain very high levels in their root tissues, it is possible to estimate a Zn concentration value in the voltammetric cell. Santos-Echeandía et al. (2010) found up to 6000 µg g^{-1} of Zn in the roots of salt marsh plants and 2500 µg g^{-1} of Zn in sediments of the Tagus estuary, in SW Europe. Considering the amount of sample used for acid digestion (0.2 g), their final volume (25 mL), the frequent aliquot used for Pt and Rh analysis (1 mL) and the volume in the voltammetric cell (15 mL), then the concentration of Zn will be 3.2 mg L^{-1} for the roots sample and 1.3 mg L^{-1} Zn for the sediment. In sediments, typical concentrations of Zn are lower than 700 µg g^{-1} (Caçador and Vale 2001; Caetano et al. 2008), and this does not represent concern. Additionally, Zn concentrations in waters are usually much lower (tens of µg L^{-1}) than those in sediments and should not constitute a problem. It is noteworthy the potential Zn contamination and interference when analysing Pt and Rh. Thus, depending on the degree of Zn contamination, this metal should be also monitored.

4.3.4. Characteristics of the Analytical Procedure

Very good linear calibration curves ($r > 0.999$) were obtained in the concentration range up to 5.2 ng L^{-1} Pt and 3.5 ng L^{-1} Rh in the optimised conditions (S.I. Figure S.IV 2). Limits of detection (LOD) were calculated as 3 times the standard deviation of the blank and also from $LOD = 3S_{x/y}/m$ ($S_{x/y}$ is the standard error of the calibration curve and m the slope of the calibration curve (Miller and Miller 2010). Similar values of LOD were obtained using both approaches, and only the latter is presented in Table IV.2. The average values of LOD were 0.2 ng L^{-1} for Pt and 0.08 ng L^{-1} for Rh ($n > 10$). Lower values can be achieved increasing the deposition time. Limits of quantification, LOQ, were calculated as 3 times LOD (Table IV.2) and were 0.5 ng L^{-1} for Pt and 0.2 ng L^{-1} for Rh ($n > 10$).

Table IV.2 – Analytical characteristics of the method for the simultaneous determination of Pt and Rh: LOD, limits of detection, LOQ, limits of quantification, RSD, relative standard deviation; experimental conditions: electrolyte 0.25 M H_2SO_4, 0.05 M HCl, 0.01 M FA and 0.5 mM HZ; t_d =120 s and E_d = –0.75 V.

	Platinum			**Rhodium**		
	ng g^{-1} *	ng L^{-1}	mol L^{-1}	ng g^{-1} *	ng L^{-1}	mol L^{-1}
LOD	0.02	0.20	0.8×10^{-12}	0.01	0.08	0.8×10^{-12}
LOQ	0.06	0.50	3×10^{-12}	0.03	0.20	2×10^{-12}
Sensitivity (average slope)						
(A V^{-2} / mol L^{-1})	$(2.9 \pm 0.5) \times 10^{7}$			$(2.5 \pm 0.6) \times 10^{7}$		
(A V^{-2} / ng L^{-1})	$(1.5 \pm 0.2) \times 10^{-4}$			$(2.4 \pm 0.6) \times 10^{-4}$		
RSD (%)	17			20		

*Calculated for a digestion using 0.2 g of solid sample in 25 mL.

The sensitivity of the method was assessed by the slope of calibration curves obtained for reagent blanks (n > 10), recovery solutions (n = 5) and CRM BCR-723 (n = 7), showed in Table IV.2.

Intermediate precision of voltammetric determinations with the optimised method, expressed as RSD, was calculated based on Pt and Rh spiked solutions (n = 5) and the digested CRM (road dust BCR-723, n = 7) comparing the results obtained on different days using the same instrument. Statistical analysis was performed to check the data for outliers. The values are shown in Table IV.2 and are similar to those previously reported in Pt and Rh determination (Almécija et al. 2016; Locatelli 2005).

4.3.5. Application of the Method to Estuarine Sediments and Water Samples

After the optimisation of the method for the simultaneous determination of Pt and Rh, it was applied to environmental samples: estuarine sediments (#A and #B) from the Tagus estuary, and water samples from an urban WWTP collected after a dry period and soon after the first heavy rains.

The accuracy of the determination was assessed using the CRM road dust BCR-723. The transformation of the original signal by using the 2nd Der clearly improved the ill-defined peaks originally observed, especially in the case of Rh. As depicted in Figure IV-1, the voltammograms for the road dust CRM BCR-723 showed well-defined peaks after the second derivative transformation, and in particular for Rh the accuracy of the measurements increased. Recoveries around 90 % for Pt and Rh were obtained in BCR-723 digested samples using the digestion procedure previously described for Pt (Cobelo-García et al. 2014). In addition, these results confirm that the procedure used for Pt extraction is also suitable for the extraction of Rh in solid matrices (Almécija et al. 2016). With the spiked solutions, recoveries were higher than 95 % for both elements (Table IV.3). In Figure IV-6 is now shown for sediment #B a complete set of standard additions using the 2nd derivative voltammograms (Figure IV-6a), and the corresponding calibration plot (Figure IV-6b) illustrating the powerfulness of the technique.

In the sediments from the Tagus estuary the concentrations of Pt and Rh in sample #A were 3.50 ± 0.03 ng g^{-1} and 0.14 ± 0.04 ng g^{-1}, respectively, while in sample #B the concentrations were 6.8 ± 0.9 ng g^{-1} of Pt and 0.53 ± 0.08 ng g^{-1} of Rh (Table IV.3). These values clearly highlight an enrichment of up to 10-fold of Pt and Rh in bed sediments when compared to Pt background concentration in Tagus estuary

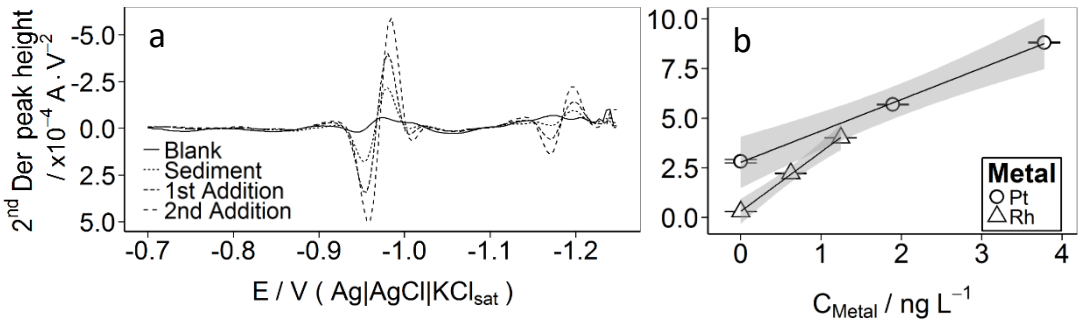

Figure IV-6 – (**a**) Second derivative (2nd Der) voltammograms of sediment sample #B, obtained in the optimised conditions: 1) blank (solid line); 2) sediment #B (500 uL of sample digest in 15 mL) corresponding to 1.6 ng L^{-1} Pt and 0.05 ng L^{-1} Rh (small dotted line); 3) first standard addition (dotted line), 1.9 ng L^{-1} Pt and 0.6 ng L^{-1} Rh; and 4) second standard addition (long dotted line), 3.8 ng L^{-1} Pt and 1.2 ng L^{-1} Rh. t_d =120 s and E_d = –0.75 V. Electrolyte: 0.25 M H_2SO_4, 0.05 M HCl, 0.01 M FA and 0.5 mM HZ. (**b**) Calibration curve plot of 2nd Der peak heights (n = 8) with two standard additions, respectively: Pt (circles), 2nd Der peak height = 5.4x10^{-5} + 6.0x10^{-6} C_{Pt} ng L^{-1}, r = 0.999; and Rh (triangles), 2nd Der peak height = 3.2x10^{-6} + 3.2x10^{-6} C_{Rh} ng L^{-1}, r = 0.999. The grey shaded area represents the 95 % confidence interval of the curve.

(Cobelo-García et al. 2011) and to natural crustal abundance of Rh (Peucker-Ehrenbrink and Jahn 2001). The high levels of Pt and Rh may have resulted from emissions of automotive catalytic converters since 1990s (Rauch and Peucker-Ehrenbrink 2015). Assessment of Pt and Rh sources to the different environmental matrices are frequently discussed in terms of Pt/Rh concentration ratios (Sutherland et al. 2015). The ratio calculated for the bed sediment #A was 25 and for #B was 13, which clearly evidences the anthropogenic pressure, and being #B within the range of values typically found for three-way catalytic converters (4 – 16; (Rauch and Peucker-Ehrenbrink 2015). The Pt/Rh ratio often shows high variability depending on the type of sample, on its preparation and/or analysis procedures. Therefore, it is difficult to compare data. However, it has been suggested that high variability of Pt/Rh in sediments is explained by different sources, namely industrial or hospital effluents where distinct signatures may be identified (Laschka and Nachtwey 1997), than by the changes in actual PGE ratio in the composition of automotive three-way catalytic converters (Ruchter et al. 2015), which nowadays are commonly used. Sediment #A was in the surroundings of an industrialised area, which could explain higher Pt/Rh than in #B. Furthermore, chemical processes may differently affect Pt and Rh causing higher ratio variability.

In the determination of Pt and Rh in WWTP water samples, a longer accumulation time was used: t_d = 300 s. It is noteworthy that increasing the deposition time allowed the clear separation of metal signal in the samples from the background wave (blanks) using the 2nd Der step. This was especially evident in the case of Rh. Lower LOD are also obtained, of 0.05 ng L^{-1} and 0.04 ng L^{-1} for Pt and Rh, respectively. Pt concentrations of 5.0 ± 0.7 ng L^{-1} to 16 ± 2 ng L^{-1} were determined in the outflow and inflow samples, respectively, collected after a period of dry weather. Samples collected soon after the first rains depicted higher Pt concentrations, of 10.4 ± 0.3 ng L^{-1} to 25 ± 2 ng L^{-1} in the outflow and inflow samples, respectively. In the case of Rh, the concentrations determined either in the inflow or outflow samples, collected before and soon after the rainfall, were similar within the experimental errors, averaging 0.21 ± 0.05 ng L^{-1} (Table IV.3). Dissolved Pt and Rh concentrations determined in WWTP samples also reflect the anthropogenic pressure, with Pt levels intensified after the first rains as previously reported in Europe (Laschka and Nachtwey 1997).

Table IV.3 – Determination of Pt and Rh (mean ± SD) in road dust CRM BCR-723 and environmental samples. Experimental conditions: electrolyte 0.25 M H_2SO_4, 0.05 M HCl, 0.01 M FA and 0.5 mM HZ; t_d =120 s and E_d = –0.75 V.

Recoveries (%)		**Platinum**	**Rhodium**	**Pt/Rh**
CRM BCR-723	(n = 7)	87 ± 12	90 ± 10	6
Spiked Solution	(n = 5)	100 ± 5	95 ± 9	
Samples				
Tagus Estuary Sediments (ng g^{-1})	(n = 4)			
	#A	3.50 ± 0.03	0.14 ± 0.04	25
	#B	6.8 ± 0.9	0.53 ± 0.08	13
Urban WWTP Waters* (ng L^{-1})	(n = 4)			
Before the rain				
	Inflow	16 ± 2	0.24 ± 0.08	67
	Outflow	5.0 ± 0.7	0.3± 0.1	18
Soon after the rain				
	Inflow	25 ± 2	0.17 ± 0.06	147
	Outflow	10.0 ± 0.3	0.19 ± 0.02	53

* Dissolved fraction (< 0.2 µm). Deposition time was increased for 300 s, LOD: Pt = 0.05 ng L^{-1} and Rh = 0.04 ng L^{-1}.

Published data on dissolved concentrations of Rh in environmental samples are scarce, either due to the type of sample analysed or the high LOD of the techniques used. To the best of our knowledge, these are the first values reported for a WWTP and one of the few published for waters (Schindl and Leopold 2015). Moreover, these results prove well the advantage of the low cost, sensitive and reliable voltammetric technique here optimised. The Pt/Rh ratio is usually applied to soils and sediments and was never reported for water samples, perhaps due to the absence of dissolved Rh values. In the water samples from the WWTP elevated ratios were found reaching 147 in the inflow water soon after the rain, although decreasing to 53 in the outflow water. Additional research is needed to evaluate the relationship between these values and the published ones for soils and sediments. Further research is ongoing to fully characterise PGE distribution within the Tagus estuary.

4.4. Final Remarks

A method for the simultaneous determination of Pt and Rh by Adsorptive Cathodic Stripping Voltammetry using second derivative of the voltammograms was optimised and successfully applied to relevant environmental samples. At ultra-trace concentrations ill-defined peaks are usually observed and the use of the second derivative transformation improves the Pt and in particular Rh signals. In addition, reagents consumption and time of analysis were also optimised in the analytical procedure. Less reagents were needed and the overall time of analysis reduced.

Comparable LOD were achieved as for the individual determination of Pt or Rh, being appropriate for environmental matrices. Intermediate precision of the method, expressed as RSD, was also within the acceptable values for determinations at ultra-trace levels. Recoveries were around 90% for both Pt and Rh using CRM BCR-723 and evidenced the accuracy of the procedure. The application to relevant environmental samples indicated that the method is suitable for the analytical quantification of Pt and Rh, reducing the costs and time by the simultaneous determination and making the method attractive for routine analysis. Longer deposition times can be used to accurately separate the metals signal from background voltammograms at lower concentrations. To the best of our knowledge, dissolved Rh concentrations in water samples of WWTP are reported for the first time.

The method here developed and validated offers the high resolution necessary to measure the low signals frequently observed in low contaminated environmental samples, therefore improve the accuracy of Pt and in particular Rh concentrations determined in pristine environments. Thus, application of this technique in a multidisciplinary approach may be a relevant contribute, giving rise to the current understanding of these elements cycle and fate in the environment.

References

Almécija, C., Cobelo-García, A., & Santos-Echeandía, J. (2016). Improvement of the ultra-trace voltammetric determination of Rh in environmental samples using signal transformation. *Talanta, 146,* 737–743. doi:10.1016/j.talanta.2015.06.032

Bowles, J. F. W., Gize, A. P., & Cowden, A. (1994). The mobility of the platinum-group elements in the soils of the Freetown Peninsula, Sierra Leone. *The Canadian*

Mineralogist, *32*(4), 957 LP – 967.

Caçador, I., & Vale, C. (2001). Salt marshes. *Metals in the Environment. Marcel Dekker, Hyderabad*, 95–115.

Caetano, M., Vale, C., Cesário, R., & Fonseca, N. (2008). Evidence for preferential depths of metal retention in roots of salt marsh plants. *The Science of the total environment*, *390*(2–3), 466–474. doi:10.1016/j.scitotenv.2007.10.015

Cobelo-García, A. (2013). Kinetic effects on the interactions of Rh(III) with humic acids as determined using size-exclusion chromatography (SEC). *Environmental Science and Pollution Research*, *20*(4), 2330–2339. doi:10.1007/s11356-012-1113-8

Cobelo-García, A., López-Sánchez, D. E., Almécija, C., & Santos-Echeandía, J. (2013). Behavior of platinum during estuarine mixing (Pontevedra Ria, NW Iberian Peninsula). *Marine Chemistry*, *150*, 11–18. doi:10.1016/j.marchem.2013.01.005

Cobelo-García, A., López-Sánchez, D. E., Schäfer, J., Petit, J. C. J., Blanc, G., & Turner, A. (2014). Behavior and fluxes of Pt in the macrotidal Gironde Estuary (SW France). *Marine Chemistry*, *167*, 93–101. doi:10.1016/j.marchem.2014.07.006

Cobelo-García, A., Neira, P., Mil-Homens, M., & Caetano, M. (2011). Evaluation of the contamination of platinum in estuarine and coastal sediments (Tagus Estuary and Prodelta, Portugal). *Marine Pollution Bulletin*, *62*(3), 646–650. doi:10.1016/j.marpolbul.2010.12.018

Cobelo-García, A., Santos-Echeandía, J., López-Sánchez, D. E., Almécija, C., & Omanović, D. (2014). Improving the Voltammetric Quantification of Ill-Defined Peaks Using Second Derivative Signal Transformation: Example of the Determination of Platinum in Water and Sediments. *Analytical Chemistry*, *86*(5), 2308–2313. doi:10.1021/ac403558y

Dalvi, A. A., Satpati, A. K., & Palrecha, M. M. (2008). Simultaneous determination of Pt and Rh by catalytic adsorptive stripping voltammetry, using hexamethylene tetramine (HMTA) as complexing agent. *Talanta*, *75*(5), 1382–1387. doi:10.1016/j.talanta.2008.01.053

Heyrovský, J., & Kůta, J. (1966). *Principles of Polarography*. Academic Press.

Hong, T.-K., Czae, M.-Z., Lee, C., Kwon, Y.-S., & Hong, M.-J. (1994). Determination of Ultratraces of Rhodium by Adsorptive Stripping Voltammetry of Formaldehyde Complex. *Bulletin of the Korean Chemical Society*, *15*(12), 1035–1037.

Johnson Matthey. (2016). *Platinum Group Metals Market Report - November*.

Labarraque, G., Oster, C., Fisicaro, P., Meyer, C., Vogl, J., Noordmann, J., et al. (2015). Reference measurement procedures for the quantification of platinum-group elements (PGEs) from automotive exhaust emissions. *International Journal of Environmental Analytical Chemistry*, *95*(9), 777–789. doi:10.1080/03067319.2015.1058931

Laschka, D., & Nachtwey, M. (1997). Platinum in municipal sewage treatment plants. *Chemosphere*, *34*(8), 1803–1812. doi:http://dx.doi.org/10.1016/S0045-6535(97)00036-2

León, C., Emons, H., Ostapczuk, P., & Hoppstock, K. (1997). Simultaneous ultratrace

determination of platinum and rhodium by cathodic stripping voltammetry. *Analytica Chimica Acta*, *356*(1), 99–104. doi:http://dx.doi.org/10.1016/S0003-2670(97)00520-5

Locatelli, C. (2005). Platinum, Rhodium, Palladium and Lead: Elements Linked to Vehicle Emissions. Their Simultaneous Voltammetric Determination in Superficial Water. *Electroanalysis*, *17*(2), 140–147. doi:10.1002/elan.200403082

Locatelli, C. (2007). Voltammetric Analysis of Trace Levels of Platinum Group Metals – Principles and Applications. *Electroanalysis*, *19*(21), 2167–2175. doi:10.1002/elan.200704026

Miller, J., & Miller, J. (2010). *Statistics and chemometrics for analytical chemistry* (6th ed.). Pearson Education Limited.

Nygren, O., Vaughan, G. T., Florence, T. M., Morrison, G. M., Warner, I. M., & Dale, L. S. (1990). Determination of platinum in blood by adsorptive voltammetry. *Analytical chemistry*, *62*(15), 1637–40. doi:10.1021/ac00214a020

Pérez-Ràfols, C., Trechera, P., Serrano, N., Díaz-Cruz, J. M., Ariño, C., & Esteban, M. (2017). Determination of Pd(II) using an antimony film coated on a screen-printed electrode by adsorptive stripping voltammetry. *Talanta*, *167*, 1–7. doi:http://dx.doi.org/10.1016/j.talanta.2017.01.084

Peucker-Ehrenbrink, B., & Jahn, B. (2001). Rhenium-osmium isotope systematics and platinum group element concentrations: Loess and the upper continental crust. *Geochemistry, Geophysics, Geosystems*, *2*(10), n/a-n/a. doi:10.1029/2001GC000172

R Core Team. (2014). A language and environment for statistical computing. R Foundation for Statistical Computing, Vienna, Austria. URL http://www.R-project.org/.

Rauch, S., & Morrison, G. M. (2008). Environmental Relevance of the Platinum-Group Elements. *Elements*, *4*(4), 259 LP – 263.

Rauch, S., & Peucker-Ehrenbrink, B. (2015). Sources of platinum group elements in the environment. In *Platinum metals in the environment* (pp. 3–17). Springer.

Ravindra, K., Bencs, L., & Van Grieken, R. (2004). Platinum group elements in the environment and their health risk. *The Science of the total environment*, *318*(1–3), 1–43. doi:10.1016/S0048-9697(03)00372-3

Ruchter, N., Zimmermann, S., & Sures, B. (2015). Field studies on PGE in aquatic ecosystems. In *Platinum Metals in the Environment* (pp. 351–360). Springer.

Santos-Echeandía, J., Vale, C., Caetano, M., Pereira, P., & Prego, R. (2010). Effect of tidal flooding on metal distribution in pore waters of marsh sediments and its transport to water column (Tagus estuary, Portugal). *Marine environmental research*, *70*(5), 358–67. doi:10.1016/j.marenvres.2010.07.003

Schäfer, J., & Puchelt, H. (1998). Platinum-Group-Metals (PGM) emitted from automobile catalytic converters and their distribution in roadside soils. *Journal of Geochemical Exploration*, *64*(1–3), 307–314. doi:http://dx.doi.org/10.1016/S0375-6742(98)00040-5

Schindl, R., & Leopold, K. (2015). Analysis of Platinum Group Elements in Environmental Samples: A Review. In F. Zereini & C. L. S. Wiseman (Eds.), *Platinum Metals in the Environment* (pp. 109–128). Berlin, Heidelberg: Springer Berlin Heidelberg. doi:10.1007/978-3-662-44559-4_8

Silwana, B., van der Horst, C., Iwuoha, E., & Somerset, V. (2014). Screen-printed carbon electrodes modified with a bismuth film for stripping voltammetric analysis of platinum group metals in environmental samples. *Electrochimica Acta*, *128*, 119–127. doi:http://dx.doi.org/10.1016/j.electacta.2013.11.045

Sodré, F. F., Peralta-Zamora, P. G., & Grassi, M. T. (2004). Digestão fotoquímica, assistida por microondas, de águas naturais: aplicação em estudos de partição e especiação do cobre . *Química Nova* . scielo .

Sutherland, R. A., Pearson, G. D., Ottley, C. J., & Ziegler, A. D. (2015). Platinum-Group Elements in Urban Fluvial Bed Sediments—Hawaii. In *Platinum Metals in the Environment* (pp. 163–186). Springer.

van den Berg, C. M. G., & Jacinto, G. S. (1988). The determination of platinum in sea water by adsorptive cathodic stripping voltammetry. *Analytica Chimica Acta*, *211*, 129–139. doi:http://dx.doi.org/10.1016/S0003-2670(00)83675-2

Wang, J., & Taha, Z. (1991). Trace measurements of rhodium by adsorptive stripping voltammetry. *Talanta*, *38*(5), 489–492. doi:http://dx.doi.org/10.1016/0039-9140(91)80168-Y

Zereini, F., & Wiseman, C. L. S. (2015). *Platinum Metals in the Environment*. (F. Zereini & C. L. S. Wiseman, Eds.). Berlin, Heidelberg: Springer Berlin Heidelberg. doi:10.1007/978-3-662-44559-4

Zhao, Z., & Freiser, H. (1986). Differential pulse polarographic determination of trace levels of platinum. *Analytical Chemistry*, *58*(7), 1498–1501. doi:10.1021/ac00298a050

V. PLATINUM AND RHODIUM IN TAGUS ESTUARY, SW EUROPE: SOURCES AND SPATIAL DISTRIBUTION

***published*: C. E. Monteiro, M. Correia dos Santos, A. Cobelo-García, P. Brito and M. Caetano, 2019. Platinum and Rhodium in Tagus Estuary, SW Europe: sources and spatial distribution, *Environmental Monitoring and Assessment* 191:579.**
DOI: 10.1007/s10661-019-7738-z

Graphical Abstract

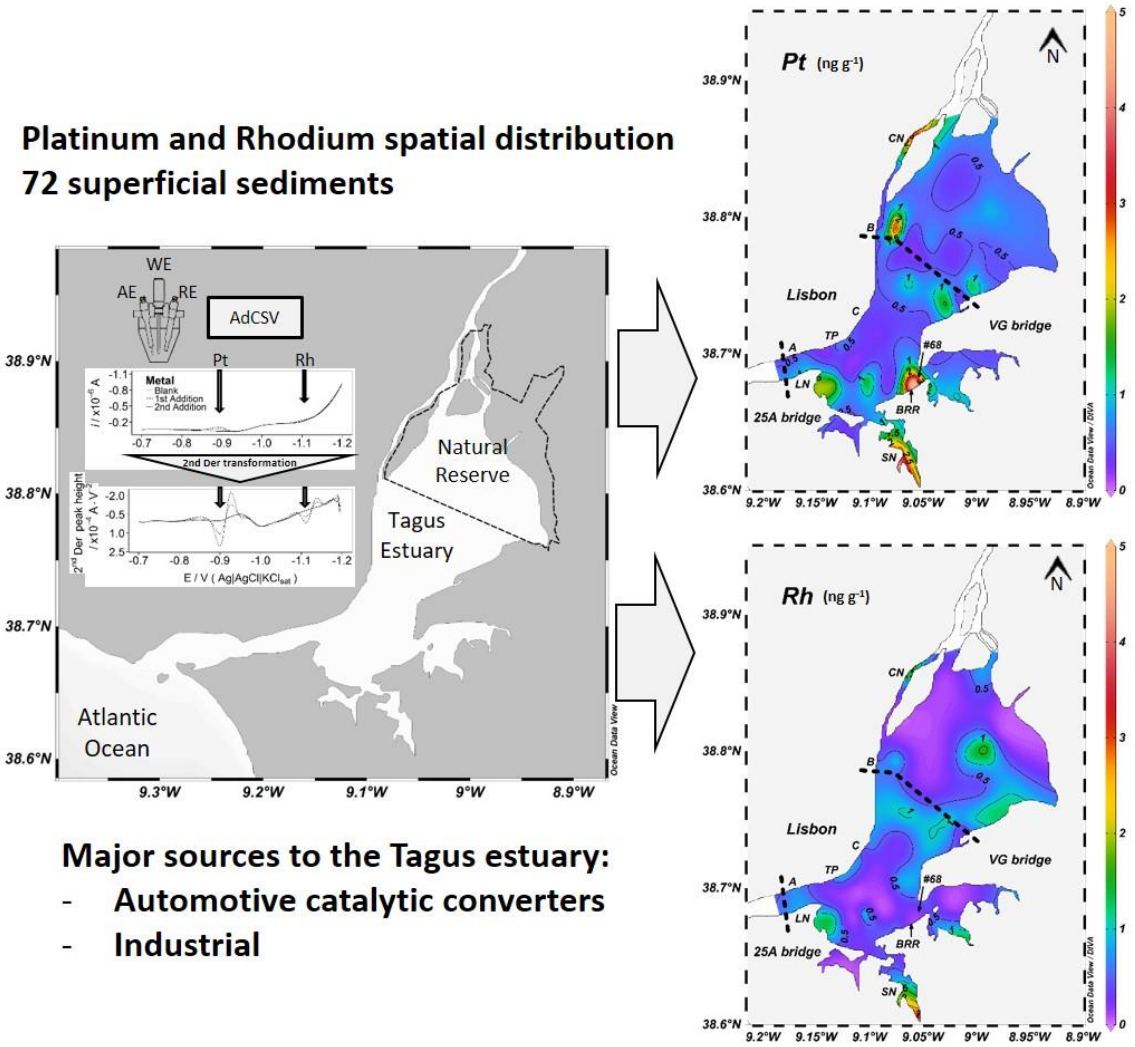

Abstract

The spatial distribution of Pt and Rh was assessed in Tagus estuary and their sources discussed. Both elements were analysed in superficial sediment samples (n = 72) by adsorptive cathodic stripping voltammetry. Concentrations varied within the following ranges: 0.18–5.1 ng Pt g^{-1} and 0.02–1.5 ng Rh g^{-1}. Four distinct areas were established: "reference"; waste- and pluvial water discharge; motorway bridges and industrialised areas. The calculated reference median concentrations were 0.55 ng Pt g^{-1} and 0.27 ng Rh g^{-1}. Linear relationships were found between Pt and Al, Fe and LOI, whereas Rh depicted scattered patterns. The highest concentrations were found nearby industrialised areas and a motorway bridge, corresponding to the enrichment of 10 and 6 times the background of Pt and Rh, respectively. The main sources of contamination to the Tagus estuary derived from historical and present industrial activities and from automotive catalytic converters. Large variations of Pt/Rh ratio (0.48–39) point to different sources, reactivity and dilution effects.

Keywords

Platinum group elements, Spatial distribution, Superficial sediments, Tagus estuary, Anthropogenic contamination

5.1. Introduction

Technology-critical elements (TCE) are contaminants of environmental concern due to increasing use in several technology-based sectors. Platinum-group elements (PGE) are part of the TCE and include platinum (Pt), palladium (Pd), rhodium (Rh), iridium (Ir), osmium (Os) and ruthenium (Ru). Their global demand continues to rise despite the ultra-trace concentrations found in the earth's upper continental crust (UCC) (Taylor and McLennan 1995; Peucker-Ehrenbrink and Jahn 2001; Ravindra et al. 2004).

Anthropogenic emissions of PGE have been largely attributed to the extensive use in automotive catalytic converters (ACC) (European Comission 1991; Kašpar et al. 2003). Platinum and Rh are included onto the ACC in the metallic or oxide forms. Due to degradation and mechanical abrasion during vehicle operation, they are released into the environment as fine grained particulate material (Ely et al. 2001; Moldovan et al. 2002; Ek et al. 2004; Rauch et al. 2002; Prichard and Fisher 2012; Zereini and Wiseman 2015). Regardless the emission rates of ng *per* kilometre *per* car (Ely et al. 2001), it has been observed the increase of Pt and Rh concentrations in road dust and roadside soils reaching up to 3 orders of magnitude of their crustal abundance (UCC: 0.5 ng Pt g^{-1} and 0.06 ng Rh g^{-1} (Taylor and McLennan 1995; Peucker-Ehrenbrink and Jahn 2001; Zereini and Wiseman 2015). The mass Pt/Rh ratio is often used to track different sources of Pt and Rh (Rauch and Peucker-Ehrenbrink 2015). In particular, the typical range for ACC emissions varies between 5 – 16 (Ely et al. 2001; Ravindra et al. 2004; Rauch and Peucker-Ehrenbrink 2015). Additionally, shifts in the ratio may point to inputs of industrial activities and hospital effluents to the environment (Laschka and Nachtwey 1997; Rauch and Peucker-Ehrenbrink 2015).

The increase of PGE concentrations in urban environments has been documented over the past years (Ek et al. 2004; Rauch et al. 2005, 2006; Zereini et al. 2004, 2007; Wiseman and Zereini 2009; Mihaljevič et al. 2013; Rauch and Peucker-Ehrenbrink 2015; Ruchter and Sures 2015; Wiseman et al. 2013, 2016; Birke et al. 2017). Studies dealing with spatially-resolved distribution provide useful information in the assessment of potential contamination sources to the aquatic systems. These studies in estuaries are mainly focused in Pt (Terashima et al. 1993; Wei and Morrison 1994; Cobelo-García et al. 2011, 2013; Zhong et al. 2012) and very scarce information exists for Rh (e.g. Essumang et al. 2008). Most of the works focused on Rh center their research only in

restricted areas or samples of estuarine systems (e.g. Essumang et al. 2008; Almécija et al. 2016a). Thus, the very limited research of Pt and Rh spatial distribution in river-estuarine systems exists to overcome the sinks and sources of these elements. We hypothesised that Pt and Rh contamination in Tagus estuary could be imprinted in superficial sediments because of the anthropogenic pressures and hydrodynamic of the estuary. Thus, we aimed (1) to quantify Pt and Rh concentrations in superficial sediments of the Tagus estuary; (2) to assess the influence of anthropogenic sources loading into the sediments; and (3) to define baseline patterns for future monitoring studies envisaging unknown PGE emissions to this aquatic system.

5.2. Material and Methods

5.2.1. Study Area

Estuaries are very important in the interchange of mass between the land and the ocean. The Tagus estuary (Figure V-1) is one of the largest in western Europe, with approximately 320 km^2 comprising small islands, sand banks, and intertidal mudflats that account for ~40% of the total area. The inner bay has approximately 25 km long and 15 km wide, and the bathymetry ranges between 0 and 7 meters depth. Downstream, a narrow channel reaching 47 m depth and 2 km wide connects the estuary to the Atlantic Ocean (Fortunato et al. 1999; Freire et al. 2007; Taborda et al. 2009; Vaz et al. 2011).

The freshwater input to the Tagus estuary depends on rain events and it has its origin mainly from the Tagus river (350 $m^3 s^{-1}$, average annual flow), as well as from other small tributaries (< 35 $m^3 s^{-1}$). The water circulation in Tagus estuary is mainly tidally driven, often considered mesotidal and vertically well-mixed (Vaz et al. 2011). Resuspension of particulate matter from sediments over the tidal cycling can occur due to wind forcing, rising tide, and water exchange with the main channels (Vale and Sundby 1987; Freire et al. 2007). Particle's settling occurs during the turnover of tides, depending on the current velocity and bathymetry. The particle resuspension-settling cycles in each semi-diurnal tide may play a key role on the scavenging of Pt and Rh to the sediments.

The Tagus estuary is well characterised with respect to the hydrodynamics (e.g. Vale and Sundby 1987; Fortunato et al. 1999; Vaz et al. 2011), trace elements

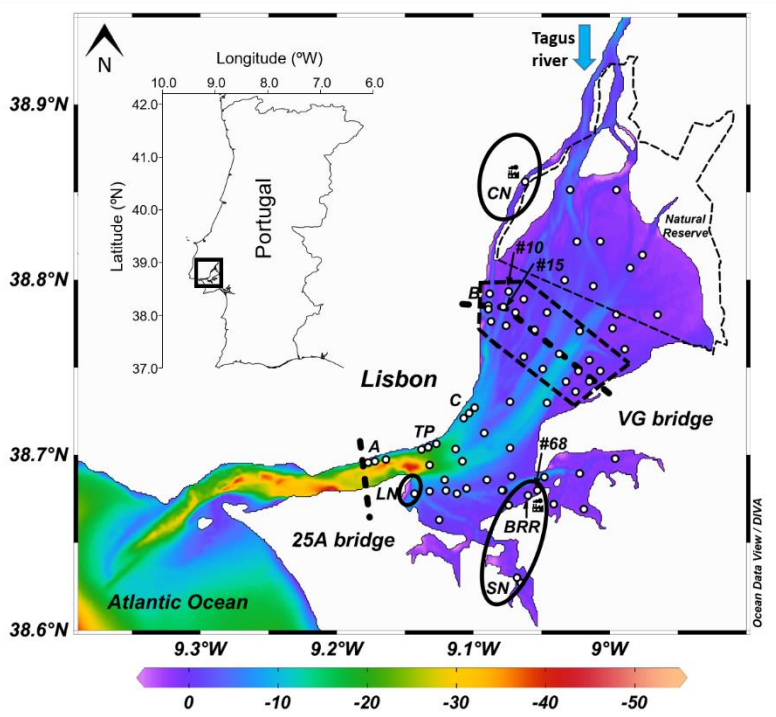

Figure V-1 – Map representation of the study area location, the Tagus estuary, SW Europe. Bathymetric data in meters (obtained from the Portuguese Hydrographic Institute; http://www.hidrografico.pt) with depicted stations where superficial sediments were collected (white dots); (**25A**) 25 de Abril bridge; (**VG**) Vasco da Gama bridge (area in dashed line); Industrialised areas (**CN**, **LN**, **SN** and **BRR**, in circles); WWTP: (**A**) Alcântara, (**B**) Beirolas and (**C**) Chelas; and pluvial waters discharge (**TP**) Terreiro do Paço. Most relevant stations and the Natural Reserve area of the estuary are also indicated.

(Vale et al. 2008; Santos-Echeandía et al. 2010; Caçador et al. 2012; Monteiro et al. 2016), persistent organic pollutants (Gil and Vale 1999; Mil-Homens et al. 2016), and nutrients (Cabeçadas 1999; Cabrita et al. 1999; Mateus and Neves 2008). For PGE, only data on Pt, Rh and Os were reported before in spot areas of the estuary and coastal sediments (Cobelo-García et al. 2011; Almécija et al. 2015, 2016a, 2016b), pointing to anthropogenic inputs. The Tagus estuary (Figure V-1) has particular features that makes it a natural setting for the study of these elements. The anthropogenic pressures result from heavily industrialised areas, with historical and present-day activities. At the southern margin exits a metallurgic complex (SN), a chemical complex (BRR) with a large area decommissioned, and an inactive shipyard (LN). At the northern margin operates a chemical industrial unit (CN) and the denser urban area is settled. Intense urban sprawl reaches 2.8 million of inhabitants around the estuary (Marques da Costa 2016) with several Waste Water Treatment Plants (WWTP) and pluvial water drainage channels dispersed in the margins. Three major WWTP exist in the northern margin: Alcântara

(A), Beirolas (B) and Chelas (C); and at Terreiro do Paço (TP) is located one of the main channels for the pluvial runoff. Moreover, the Tagus estuary is crossed by two high traffic motorway bridges, Vasco da Gama (VG bridge) and 25 de Abril (25A bridge), where 175000 – 225000 vehicles pass every day (IMT 2016).

5.2.2. Sediment Samples Collection and Preparation

Taking into account potential sources of Pt and Rh to the Tagus estuary, superficial sediment samples (< 5 cm depth) were collected in 72 stations on-board of a small vessel using a Van Veen grab sampler. A set of samples (n = 12) was collected in 2015 at the waste- and pluvial waters effluents (A, B, C and TP, in Figure V-1). In addition, two control samples were collected upstream (-U) and downstream (-D) of each effluent, spaced by approximately 0.5–1 km. Another set of superficial sediments (n = 60) was sampled in June 2016, following a spatial grid covering the immersed area of the estuary. Emphasis on VG bridge influence area was preferred since it was not feasible to collect samples nearby 25A bridge, due to the higher current velocity and coarser sediments (rocks, gravel and coarse sand) than in the rest of Tagus estuary (Figure V-1).

Sediment samples were dried in an oven at 40 ^{0}C. After homogenisation, aliquots were separated for grain size analysis and after sieving (< 2 mm) another portion was ground to a fine powder for further analyses.

5.2.3. Analytical Procedures

5.2.3.1. Material and Chemicals

All laboratory material used was acid-cleaned by successive immersion periods of 48 hours in ~20 % nitric acid (HNO_3) followed by ~20 % hydrochloric acid (HCl). Afterwards, the material was rinsed with Milli-Q water (18.2 MΩ.cm, 25 ºC) and let to dry in a clean room. All reagents used throughout the work were always of high-purity grade, either for samples digestion or analysis: hydrofluoric acid (HF) 40 %, HNO_3 65 % and HCl 30 % (*Suprapur*, Merck), sulphuric acid (H_2SO_4) ≥ 95 % (*Trace*SELECT, Fluka), hydrazine sulphate (HZ; p.a., Fluka) and formaldehyde 13 M (FA 36.5 %, Riedel-de-Haen). Diluted standards of 1.0 µg Pt L^{-1} and 1.0 µg Rh L^{-1} in 0.1 M HCl were weekly

prepared from standard solutions of Pt and Rh 1000 mg L^{-1} (*Trace*CERT, Fluka). Other solutions were prepared in Milli-Q (18.2 MΩ.cm) water and kept in perfluoroalkoxy flasks.

5.2.3.2. Grain Size and Loss on Ignition

Grain size analysis was carried out in sediments by dry sieving (Gaudêncio et al. 1991). According to Folk (1954), three classes of sediment grain sizes (%) were used to evaluate the contents of gravel (≥2 mm), sand (2 – 0.063 mm), and the finer fraction corresponding to silt and clay (< 0.063 mm). Organic matter was determined on the basis of Loss-on-Ignition (LOI, in %), estimated by the weight difference of dried samples at 105 ^{0}C and heated at 450 ^{0}C in a muffle furnace for 2 h (Craft et al. 1991). The temperature used in this procedure ensures that the sediment carbonate fraction was unchanged.

5.2.3.3. Major Elemental Composition

Major elemental composition of the sediments (total Al, Fe, Mn, Mg and Ca) was quantified in ≈0.1 g (dry weight, d.w.) aliquots after a two steps digestion. Complete dissolution was achieved using a mixture of 1 mL of *aqua regia* (a mixture of HCl:HNO_3; 3:1) and 3 mL of HF (40%), at 100 ^{0}C for 1 h in closed Teflon autoclaves (Loring and Rantala 1992). The resultant solution was evaporated to near dryness in Teflon vessels (DigiPrep HotBlock-SCP Science), re-dissolved with 1 mL of distilled HNO_3 and 5 mL of Milli-Q water, heated for 20 min at 75 ^{0}C and diluted in Milli-Q water to a final volume of 50 mL (Caetano et al. 2009). Inductively coupled plasma – mass spectrometry (ICP-MS) was used to determine major elemental composition of the sediments. The determinations were done in quadrupole ICP-MS from Thermo Elemental (X-Series), equipped with a concentric Meinhard nebulizer and a Peltier impact bead spray chamber, following the procedure previously reported Brito et al. (2018). Main experimental parameters were as follows: forward power 1400 W; peak jumping mode; 150 sweeps per replicate; dwell time of 10 ms; dead time of 30 ns.

5.2.3.4. Pt and Rh Determination

For the determination of Pt and Rh in the sediments the procedures of Nygren et al. (1990) and of Haus et al. (2009) were followed for samples digestion. Sediment samples of ≈0.2 g of each were heated in quartz crucibles up to 800 ºC in a muffle furnace. After cooling, samples were transferred to PFA pressurised digestion vessels (MarsXpress, CEM) and they were microwave-assisted digested in the presence of 4 ml of *aqua regia*. Afterwards, samples were evaporated to near dryness at 85 ºC in a hot plate, re-dissolved in 1 mL of H_2SO_4, and were left to evaporate the residual acids until constant volume. Finally the residue was transferred to polypropylene Digitubes (SCP Science) and diluted to 25 mL in 0.1 M HCl. Adsorptive Cathodic Stripping Voltammetry (AdCSV) was used for the determination of Pt and Rh, following the procedure optimised by Monteiro et al. (2017). Briefly, the voltammetric measurements were carried out in an acclimatized room at 25 ± 2 ºC. A potentiostat/galvanostat from ECO Chemie, Autolab PGSTAT 128N (Metrohm), was used as the source of the applied potential and as the measuring device, connected to the Metrohm Stand 663. A conventional three-electrode configuration was used: a Static Mercury Drop Electrode (SMDE) as the working electrode, an $Ag/AgCl/KCl_{(sat)}$ as the reference electrode (placed inside a salt bridge with 3 M KCl) and a carbon rod as auxiliary electrode. The whole system was controlled and data analyzed with the GPES v4.9 software (EchoChemie). The standard addition method was used to quantify Pt and Rh concentrations (Monteiro et al. 2017). All measurements were done at least in triplicate.

5.2.3.5. Quality Control of the Analytical Procedures

The quality control on major elements determination was assessed by running a multi-element solution in every 10 samples. Coefficients of variation for metal counts (n = 3) were < 2 %. Certified reference materials (CRM) MAG-1, G-2, and BHVO-1 (USGS), with different matrices, were used to control the analytical procedure. The results obtained did not differ significantly ($p > 0.05$) from the certified values. Procedural blanks always accounted for < 1 % of total concentrations in samples (Brito et al. 2018).

For Pt and Rh determinations, the accuracy was evaluated through the recoveries (%) in digested CRM road dust BCR-723 (EC-JRC-IRMM). Recoveries were 92 ± 11 %

for Pt and 85 ± 13 % for Rh (n > 10), which were within the certified ranges. Procedural blanks (n > 10) were analysed to evaluate potential cross contamination. The average limits of detection were 0.012 ± 0.005 ng Pt g^{-1} and 0.013 ± 0.005 ng Rh g^{-1} (n > 10). Further details are fully described in Monteiro et al. (2017).

5.2.4. Data Processing

All statistical analysis was performed using XLSTAT (Addinsoft). Normality of the data was assessed using the Shapiro–Wilk test. Since most of the variables did not present normal distribution, non–parametric Kruskal–Wallis (H) test was applied to assess the differences in median values, with post hoc test. In addition, Mann-Whitney (U) test was also applied to assess significant differences between groups. Grubbs test was used to check the data for outliers. In addition, Spearman rank correlations (r_S) were also computed to evaluate trend relationships (Miller and Miller 2010).

Images of the spatial distributions were generated using the Ocean Data View software (ODV; Schlitzer 2017) using Data Interpolating Variational Analysis (DIVA) method. This method takes into account topographic and dynamic constraints when generating grids based on a relative low number of observations (Troupin et al. 2012). However, boundary conditions were superimposed in ODV/DIVA by delimiting the area of interest of the Tagus estuary, with better resolution in the rough edges of the estuary in order to improve interpolations.

5.3. Results

5.3.1. Characterisation of Superficial Sediments

Sediment samples from Tagus estuary were characterised for grain-size, LOI and major elemental composition. Descriptive statistics of the data are summarised in Table V.1. The median value of the sand fraction (2 – 0.063 mm) was 41 % and in general lower than the fine-sized fraction (< 0.063 mm) that corresponds to silt and clay material (Table V.1). The contents of Al, Fe, and LOI ranged up to ~10 %, and the higher levels were associated with deposits of fine-grained material in the northern margin and mudflats of the upper and middle estuary.

Table V.1 – Descriptive statistics of the parameters used in the characterisation of the superficial sediments of Tagus estuary.

	Units	n	Min	1st Quartile	Median	Mean	3rd Quartile	Max
Al	%	72	2.0	4.8	6.0	6.2	7.7	9.8
Fe	%	72	0.50	1.6	2.5	2.6	3.6	7.0
Mn	%	70	0.010	0.023	0.030	0.033	0.041	0.71
Mg	%	70	0.16	0.49	0.80	0.76	1.0	1.4
Ca	%	70	0.01	0.49	1.2	1.7	2.5	7.1
Sand	%	57	2.4	15	41	42	64	98
Silt + Clay	%	57	2.1	34	59	57	85	98
LOI	%	72	0.51	2.2	3.9	3.9	5.4	8.8

Magnesium and Mn were below 1.4 and 0.71 %, respectively, with no clear distribution pattern within the estuary. Calcium ranged up to 7.1 % and the highest concentrations were found in samples containing fragments of bivalve shells.

5.3.2. Concentrations and Spatial Distribution of Pt and Rh

The concentrations of Pt and Rh in superficial sediments from the Tagus estuary varied between 0.18 – 5.1 ng Pt g^{-1} and 0.02 – 1.5 ng Rh g^{-1} (d.w.) (Figure V-2), being the median values 0.60 ng Pt g^{-1} and 0.54 ng Rh g^{-1} (Figure V-3a).

Based on the potential sources to the estuary and spatial distribution of both elements, four estuarine sections were outlined for further discussion (Figure V-3): (*i*) "*reference concentration"* of Pt and Rh that comprises the stations distant from potential sources; (*ii*) *waste- and pluvial waters discharge sites* in the northern margin; (*iii*) *motorway bridges*, in particular *VG bridge*; and (*iv*) *industrialised areas*, corresponding to sites BRR, SN, LN and CN. Differences on median values among groups were observed, being significantly different for Pt ($H(3, n=72) = 20.30$, $p<0.001$) and for Rh ($H(3, n=72) = 7.867$, $p<0.05$). When comparing paired– sections (Mann-Whitney (U) test), the industry section was significantly different from the other sections ($p<0.05$) (Figure V-3b) in the case of Pt. Although at VG bridge have been found higher values up to 6 times than in WWTP and reference sections, the broad interval of variation lead to no significant differences between sections ($p>0.05$).

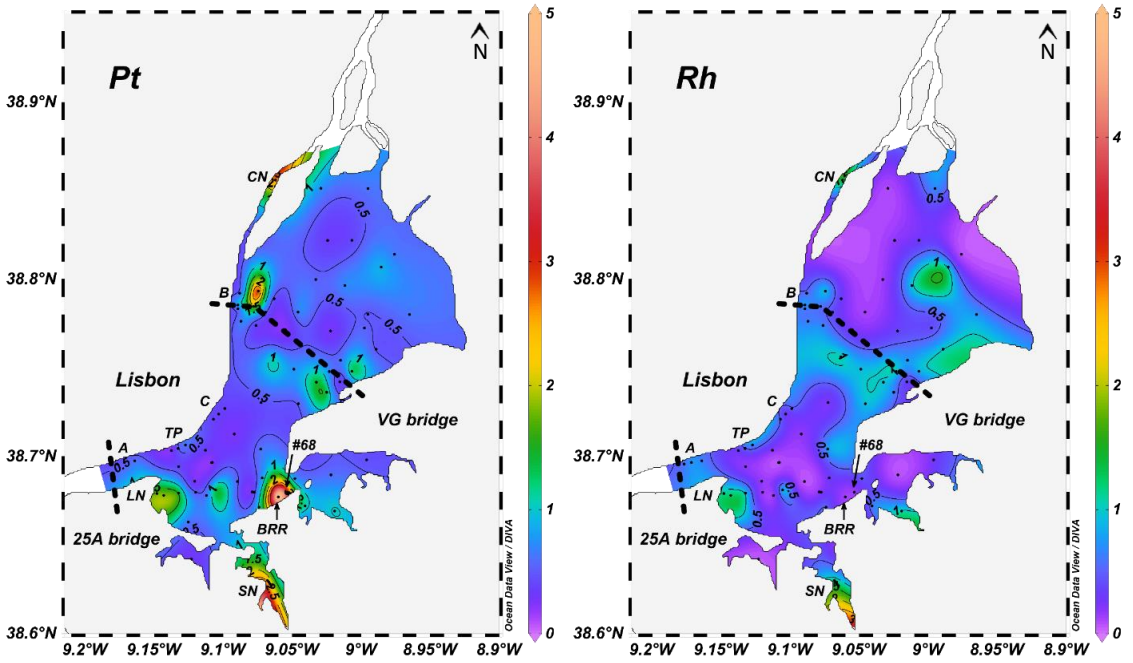

Figure V-2 – Spatial distribution of Pt and Rh concentrations, in ng g^{-1}, in superficial sediments of Tagus estuary.

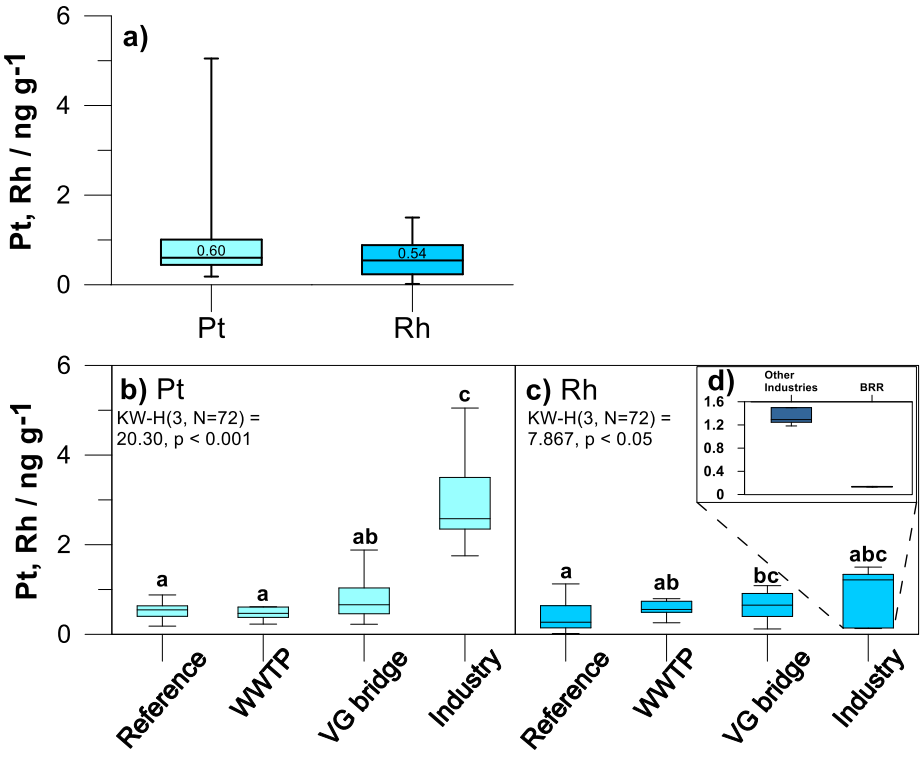

Figure V-3 – Boxplot of (**a**) median and total concentrations (ng g^{-1}) of Pt and Rh in superficial sediments of Tagus estuary; (**b**) Pt and (**c**) Rh concentrations depicted by section, respectively; (**d**) Rh concentrations depicted in industry section. Significant differences amongst groups were observed (Kruskal-Wallis (H) test; $p<0.05$) and are indicated by different letters (Mann-Whitney (U) test; $p<0.05$).

In the case of Rh, no significant differences were found between the reference, WWTP and industry sections ($p>0.05$) (Figure V-3c). Other statistical similarities found were those of WWTP section with VG bridge and industry sections ($p>0.05$) and between VG bridge and industry sections ($p>0.05$). However, the lack of statistical differences for Rh between industry and the other sections is largely dependent on the low concentrations found at BRR than in the other industrial sites (Figure V-3d). Nonetheless, their environmental significance should not be disregarded.

5.3.2.1. Reference Levels in Tagus Estuary

The lowest concentrations of Pt and Rh, up to the median values, were found mostly in the central areas of the estuary. Considering only the stations far from possible anthropogenic sources as reference stations, levels of Pt ranged from 0.18 – 1.5 ng g^{-1} (d.w.) with a median of 0.55 ng g^{-1}. For Rh concentrations varied within 0.02 – 1.3 ng g^{-1} (d.w.) with a median of 0.27 ng g^{-1}.

It was found in those stations a clear affinity of Pt for Al, Fe and LOI, with significant regressions (Figure V-4). When normalised, the spatial distribution of Pt/LOI and Pt/Fe (Figure V-5) resulted in a wider spread of Pt signature than that observed for Pt/Al. No significant correlations ($p>0.05$) were found between Rh concentrations and the content of Al, Fe and LOI (Figure V-4).

5.3.2.2. Waste- and Pluvial Waters Discharge

Relatively low concentrations of Pt and Rh were observed in the discharge sites of waste- and pluvial waters at the northern margin (A, B, C and TP, in Figure V-1). Concentrations of both metals were closer to the reference levels of the Tagus estuary, ranging from 0.23 – 1.0 ng Pt g^{-1} and 0.22 – 0.98 ng Rh g^{-1} (d.w.). However, when concentrations were normalized to Al or LOI, sediment levels from the discharge sites of Alcântara (A) and Beirolas (B) WWTP were higher than the values found in upstream and downstream control stations (A-U, B-U and A-D, B-D, respectively; Figure V-6). This trend was not found for WWTP of Chelas (C) and the pluvial waters discharge site at Terreiro do Paço (TP), presumably due to their low discharge into the estuary.

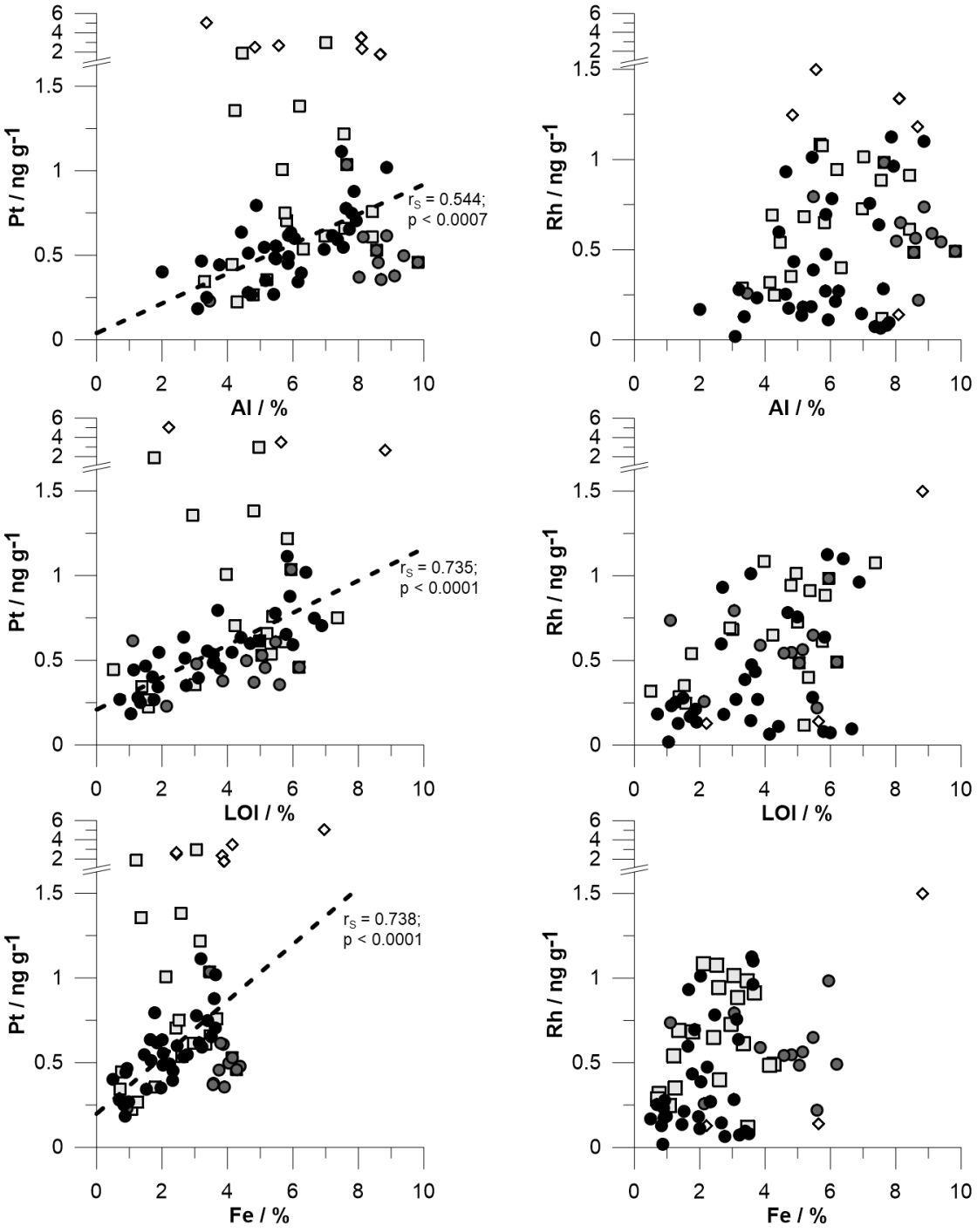

Figure V-4 – Bivariate plots between Pt and Rh with Al, LOI and Fe in superficial sediments of Tagus estuary. (●) reference stations in the estuary; (◉) waste- and pluvial waters discharges; (□) VG bridge; and (◇) industrialised areas. The dashed line represents the trends found in the background data and the Spearman correlations (r_S) found, respectively.

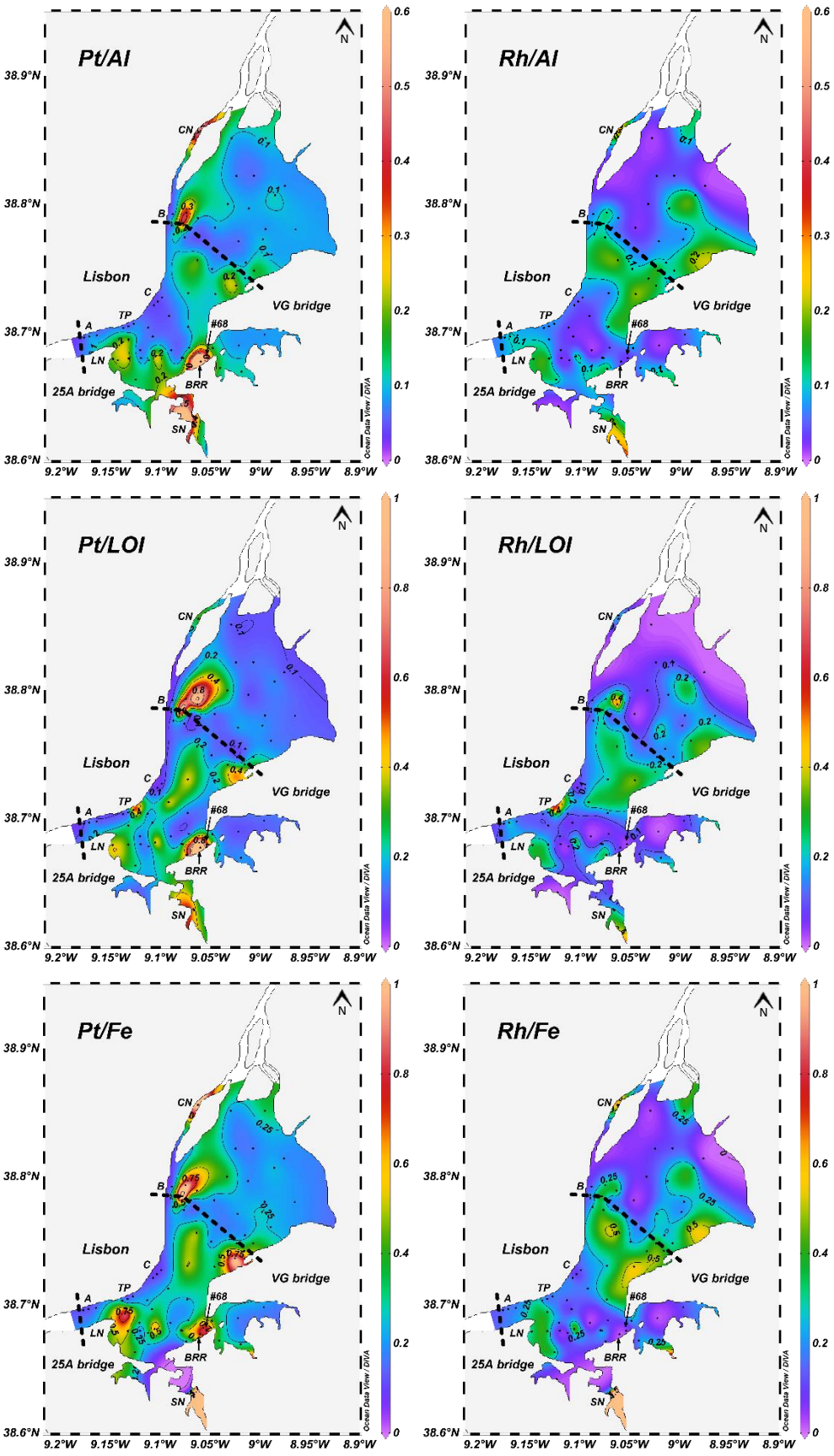

Figure V-5 – Spatial distributions of Pt and Rh with concentrations normalised to Al, LOI and Fe in superficial sediments of Tagus estuary.

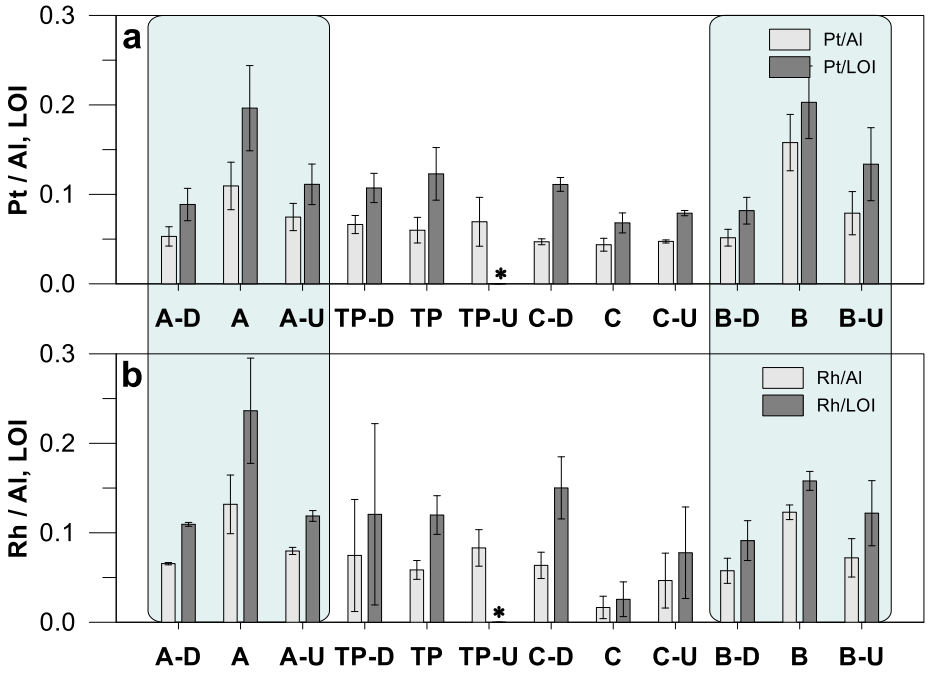

Figure V-6 – (**a**) Pt and (**b**) Rh concentrations normalised to Al and LOI from WWTP discharge sites (**A**) Alcântara, (**B**) Beirolas and (**C**) Chelas, and pluvial- waters discharge site (**TP**) Terreiro do Paço, and respective control stations in superficial sediments from Tagus estuary: Alcântara upstream (A-U) and downstream (A-D); Beirolas upstream (B-U) and downstream (B-D), Chelas upstream (C-U) and downstream (C-D), and Terreiro do Paço upstream (TP-U) and downstream (TP-D). (*) Data not presented due to an outlier value of LOI.

5.3.2.3. Anthropogenic Point Sources and Signature in Sediments

Concentrations of both elements increased downstream of the VG bridge and in both margins closer to the bridge ends, varying from 0.22 – 3.0 ng Pt g^{-1} and from 0.12 – 1.1 ng Rh g^{-1} (d.w.). Furthermore, the highest levels were found closer to the industrialised areas (Figure V-3 and S.I. Figure S.V 1). Platinum concentrations (d.w.) were 1.8 ng g^{-1} at LN, 2.5 ng g^{-1} at SN, 2.7 ng g^{-1} at CN and up to 3.5-5.1 ng g^{-1} at BRR sites. Regarding Rh levels, they varied between 1.2 and 1.5 ng g^{-1} at LN, SN and CN, but lower values were found at BBR, <0.01 – 0.13 ng g^{-1}.

In the Tagus estuary, Pt/Rh ranged within 2 orders of magnitude, between 0.48 and 39 (Figure V-7). The lowest Pt/Rh ratio corresponded to the reference signature, varying between 0.48 and 4.0 and with a median value of 1.6 (all reference stations). If it is only considered the innermost stations of the Tagus Natural Reserve area, where no direct anthropogenic activities exist, then the range of Pt/Rh decreases to a median value of 0.9.

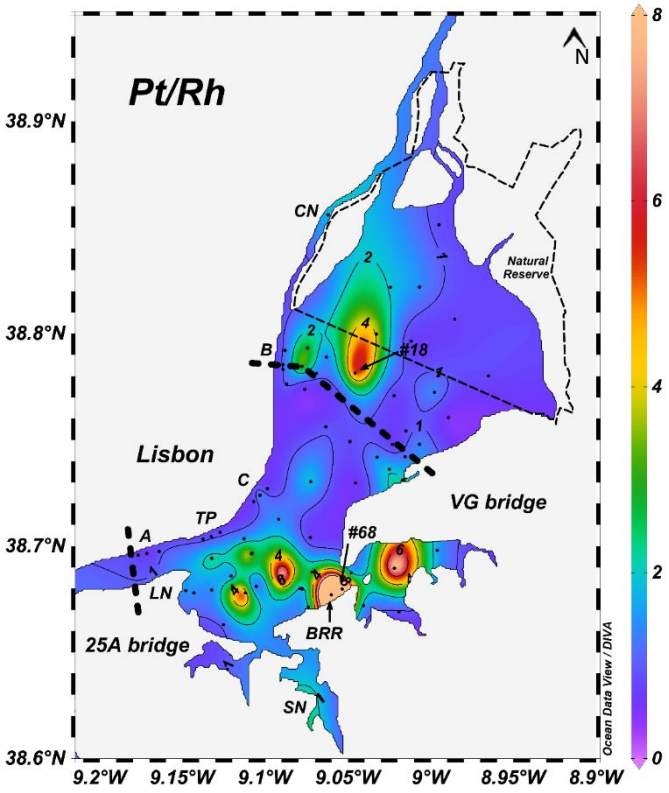

Figure V-7 – Signature of Pt and Rh in superficial sediments of Tagus estuary. The Pt/Rh range varied between 0.48 and 39, with the highest values found at BRR and #68 stations, 39 and 25 respectively.

Similar to that reference value, the signature of particles derived from the WWTP stations was low (0.6 – 1.6). In sediments closer to VG bridge, values were in general higher than the reference section (0.9), ranging from 0.5 to 5.6. Additionally, a road dust sample was collected in a dense traffic road, containing 551 ng Pt g^{-1} and 84 ng Rh g^{-1}, which corresponds to Pt/Rh of 6.6. The largest difference on Pt/Rh mass ratio (1.5 – 39) was observed in industrialised areas. At BRR it was found the highest Pt/Rh values (25 – 39), while in other industrial sites Pt/Rh values were low (1.5 – 2).

5.4. Discussion

The reference value of Pt concentration in Tagus estuary (0.55 ng g^{-1}) is similar to the concentration in the Upper Continental Crust (UCC, 0.5 ng Pt g^{-1}; Taylor and McLennan 1995; Peucker-Ehrenbrink and Jahn 2001; Ravindra et al. 2004). Furthermore, that value is comparable to the baseline concentration in shelf sediments of the Tagus in the sediment horizon corresponding to 1920, found by Cobelo-García et al. (2011). This

was not found for Rh since the estimated reference level in Tagus estuary sediments (0.27 ng g^{-1}) was 4 times higher than the value indicated for the UCC (0.06 ng Rh g^{-1}; Taylor and McLennan 1995) and also for the deepest layers of a salt marsh core, reported by Almécija et al. (2016a). The concentrations of Pt in Tagus estuary sediments (0.18 – 5.1 ng g^{-1}) are in the range of those reported by Zhong et al. (2012) for the Pearl River estuary, China, Wei and Morrison (1994) for three urban river sediments in Gothenburg, Sweden, and Prichard et al. (2008) in Humber estuary, UK. However, levels of this element in Tagus are lower than those found by Ruchter and Sures (2015) in the river Alb, Germany (up to 45 ng Pt g^{-1}) or by Sutherland et al. (2015) in the bed sediments of Nuuanu stream, Hawaii (5.8 – 40 ng Pt g^{-1}). The range of Rh concentrations determined in Tagus sediments (0.02 – 1.5 ng g^{-1}) is comparable to those reported by Sutherland et al. (2015) for in Hawaii (0.32 – 3.5 ng g^{-1}) or by Prichard et al. (2008) for the Humber estuary, UK (1 – 2 ng g^{-1}).

5.4.1. Variation of the Reference Levels in the Estuary

Low concentrations of Pt and Rh were observed in the central areas of the Tagus estuary, ranging from 0.18 – 1.5 ng Pt g^{-1} and 0.02 – 1.3 ng Rh g^{-1} (d.w.). In order to minimize the anthropogenic contributions of these elements (Dung et al. 2013), the variation of Pt and Rh in reference stations was assessed in sediments far from potential sources by evaluating the relationships with the ancillary parameters. Aluminium content is usually used due to the conservative behaviour and rare anthropogenic inputs, being a proxy for particle's nature in sediments (Loring and Rantala 1992; Matys Grygar and Popelka 2016). However, using Al-normalised metal concentrations is not straightforward and other parameters may be used, like Fe and organic matter (Matys Grygar and Popelka 2016). The affinity of Pt towards Al, Fe and LOI indicates that its distribution in sediments is governed by the sediment characteristics or by a group of several parameters, contrarily to Rh. A clear affinity of Pt to the fine-sized fraction (silt and clay) of the sediments was observed, but not for Rh. Thus, the transport of Pt and Rh within the estuary is likely to be differently affected by the nature of particulate material in association with the hydrodynamic regime of the estuary.

Different contribution of both margins on the sediment loadings is due to geologic features and intense, yet dissimilar, anthropogenic pressures (Taborda et al. 2009). The

reference levels of Pt and Rh in the Tagus estuary may derive from weathering of Neo-Cretaceous basalts and pyroclasts from the Lisbon Volcanic Complex (Prudêncio et al. 1993; Taborda et al. 2009). The higher contribution yielded by the southern margin sediments includes sandstones, sand, gravel, silt and clay from detrital Plio-Pleistocene that constitute the fluvial terraces, resulting mainly from erosion (Taborda et al. 2009). In addition, pyrite is the main group of minerals responsible for a background signature of PGE. However, the reference levels may be influenced by specific anthropogenic activities in the Tagus, such as different types of industry. The implementation of a chemical plant in the southern margin of the estuary that operated during the XX century (1909-1990s) included a pyrite-roasting unit and a smelter. During this period, the industry used pyrite from Lousal and Aljustrel mines, both part of the Iberian Pyrite Belt (Mil-Homens et al. 2013). This raw material was stored in large piles in the southern margin of the estuary and could cause the spread of particulate material containing PGE in a large area, including the estuary. Thus, the input of this geological material for such a long period could mask the background Pt and Rh values existing in the original minerals from the Tagus river basin.

5.4.2. Sources and Distribution of Pt and Rh

5.4.2.1. Waste- and Pluvial Waters Discharge Sites

The concentrations of Pt and Rh found in sediments closer to the WWTP outfalls were within the range of reference levels in Tagus estuary. However, the increased signal in stations A and B, after normalization to Al and/or LOI, reflects the drainage of a large urban area for a considerable period of time, from Lisbon, which mainly includes domestic and hospital effluents, and pluvial runoff. The presence of Pt-based anticancer drugs was recently reported in sewage and wastewaters (Vyas et al. 2014). These authors did not find evident relationships between the administered quantities of Pt and measured concentrations in drainage, reflecting the randomness of the excreted Pt. Furthermore, Monteiro et al. (2017) showed that an increase in dissolved Pt concentrations was detected in the effluents of the WWTP. During the water treatment along the WWTP, dissolved Pt concentrations reduced to half while dissolved Rh was kept invariable. Although low dissolved concentrations of Pt and Rh (ng L^{-1}) are introduced in the estuary through the WWTP, the input of high volume of water (3 – 100 m^3 s^{-1}) results in a detectable imprint

in sediments (ng g^{-1}). Furthermore, coupling other elements with Pt or Rh can be of major interest to track anthropogenic emissions of technology-critical elements. In fact, rare earth elements (REE) do support the transfer of urban contamination from different anthropogenic sources into the Tagus estuary. Brito et al. (2018) observed this signature for some of the REE at the same WWTP stations, e.g. Gd (S.I. Figure S.V 2) and Ce, which suggests the association of metals to the particulate load from urban effluents and runoff material. Despite having distinct point sources, their pathways into the estuary are in general the same. Along with Pt, Gd can be used to track anthropogenic contamination with source in medical applications (Ebrahimi and Barbieri 2019). In addition, Wiseman et al. (2016) used Ce coupled to Pt, Rh and Pd to evaluate ACC emissions in roadside soils from Toronto, Canada.

5.4.2.2. Motorway Bridges

Both Pt and Rh followed the same spatial distribution pattern with increasing levels downstream of VG bridge. Furthermore, a clear input was also found in the north margin at the bridge end. These results point that both elements have the same anthropogenic source, with these signatures of Pt and Rh most likely resulting from the abrasion and degradation of ACC. This particular spatial distribution may derive from the concrete structure of the VG bridge. The road dust material accumulates along the bridge during the dry season and then is flushed directly to the estuary during rain periods through a system of gully pots. The road dust enters the estuary at several points located along the bridge and is spread according to the tidal and hydrodynamic regime. The spreading of road dust enriched in Pt and Rh downstream the bridge results from the ebb and flushing semidiurnal cycles. The bridge is located approximately in the maximum turbidity zone of the estuary and major mixture of freshwater and seawater occurs towards the estuary mouth. In a previous study, Almécija et al. (2016b) found elevated concentrations of Pt (40 ng g^{-1}) in surface sediments from a system of channels and creeks in a salt marsh at the southern margin. In these ecosystems, particulate material including road dust is retained by halophyte plants and deposited in low hydrodynamic areas.

It should be pointed out that it was not feasible to collect samples in the surroundings of 25A bridge. Low sedimentation rate in the bridge area is due to the narrow connection to the sea, where higher depth (up to 47 m) and current velocity (up

to 2.0 m s^{-1}) are observed than in the rest of the estuary, and the nature of bottom substrate is mainly rock gravel. These characteristics coupled with the bridge structure do not favour a localised deposition site. This bridge has a gridded metallic deck that allows rainwater and road dust particles to pass through, without a channelled drainage system. It has a navigation clearance height of 70 m above the water level in comparison with the 14 m of VG bridge. Thus, 25A bridge it is more exposed to environmental conditions than VG bridge, such as strong winds. All these characteristics result in a wider spread of road dust. Therefore, it is hypothesised that no clear signatures of Pt and Rh from this source could be found in sediments.

The input of both elements through the motorway bridges can be estimated based on traffic and structural characteristics. It is noteworthy that regardless the higher traffic density in 25A bridge, three times higher (≈150 000 cars d^{-1}) than in VG bridge, Pt and Rh estimated emissions from ACC were lower. The estimated total emissions since the opening of VG bridge in 1998 ranged from 542 – 937 g of Pt and 130 – 262 g of Rh. Furthermore, if we calculate Pt emissions per year on VG bridge, we found that our lower value is ≈30 g Pt y^{-1} (542 g Pt /18.1 years), which is comparable to the ≈33 g Pt y^{-1} (450 g Pt /13.6 years) estimated by Almécija et al. (2015) using the same approach. This estimation may vary due to the different sedimentation rates found along the ~17 km of the VG bridge that crosses the larger section of the Tagus estuary. For the 25A bridge a lower interval of emissions was found, 171 – 312 g of Pt and 41 – 87 g of Rh (further details in S.I. Table S.V 1). Even with higher vehicle traffic on 25A bridge than in VG bridge, it is clear that their extension plays a major role in the estimated emissions of Pt and Rh from ACC.

5.4.2.3. Industrialised Areas

The levels of Pt and Rh at stations BRR, SN, LN, and CN (circles in Figure V-1) point to local anthropogenic sources. The concentrations correspond to an increase up to 10 (Pt) and 6 (Rh) times the reference levels estimated in the estuary.

The increase of Pt in BRR superficial sediments may suggest a recent point source, which could be explained by the current production of fertilizers or the historical slags in the area exposed to the atmospheric conditions. The chemical-industrial complex at BRR had a long history in the production of nitric and sulphuric acids, and fertilizers, which

may have used Pt as catalyst (e.g. Hatfield et al. 1987), with peak activity around the 1960s and early 1970s. The pyrite ore processing used to extract Cu, Pb, Au, and Ag, may have also contributed to that increase. The particulate material from the exposed piles of pyrite slag could be transported easily into the estuary through the air or drainage channels in the margin. However, Rh concentrations were very low. Metal contamination patterns from BRR industrial activities were previously reported for Hg (Canário et al. 2005), Cd, Pb, Ni and As (Vale et al. 2008), and more recently for the YREE, e.g. Y (Brito et al. 2018). Thus, BRR site may be a hotspot for PGE and further research is ongoing.

Part of the slag at BRR was transferred to another industrial complex and used as raw material in metallurgical industry. This unit located also in the southern margin of the Tagus (SN site) continues to operate producing steel and treating slag residues. At this unit, the increased Rh concentrations suggest that Rh was more mobilized to the aquatic environment compared to Pt.

Another anthropogenic source of both PGE was found at the LN site, currently a dismantled shipyard but fully operating in the 1960s and early 1970s. By that time, 30 % of the world tanker fleet was repaired in this shipyard that included a variety of iron and steel works, releasing large amounts of metallic residues. The former activity coupled with the remaining of such large and abandoned infrastructures could be responsible for the Pt and Rh input to the sediments. Considering the peak activity of the chemical-industrial complex at BRR and the shipyard at LN, Pt and Rh emitted to the Tagus estuary must have been larger than those estimated in this study. The industrial activity at BRR decreased after dismantling the acid production and pyrite processing units almost two decades ago. Thus, levels in superficial sediments suggest continuous input from the fertilizer unit currently operating and/or mobility of Pt within the sedimentary column.

In the northern margin, Pt and Rh concentrations found at the CN site are likely related to the chemical industry operating for more than half of a century. A chlor-alkali industry uses a catalytic hydrogenation process based on PGE non-supported or supported catalysts (e.g. on silica or alumina; Paparatto et al. 2010; Lemaire et al. 2014). The degradation of the catalyst releases Pt and Rh that may reach the estuary through the industrial effluent. The narrow estuary channel where this unit is located has lower current velocity and higher sedimentation rates, which favours the deposition of Pt and Rh in bottom sediments. Furthermore, the concentration of Rh found at CN site was the highest in the entire estuary, suggesting its use as a catalyst, as well as Pt. Moreover, relatively

high concentrations of some of the REE were also observed at this site (Brito et al. 2018). In addition to the previously reported contamination by Hg (Cesário et al. 2016), Pt, Rh and REE underpin the industrial point sources of contamination in Tagus estuary.

5.4.3. Signature of Pt and Rh in Sediments

Platinum and Rh sources are often assessed through the Pt/Rh mass ratio (e.g. Sutherland et al. 2015). This ratio variability relies on different sources, such as industrial or hospital effluents than on changes of ACC's composition (Ruchter et al. 2015). Biogeochemical processes in the water column or in bottom sediments may also affect Pt and Rh differently due to their different reactivity (Jarvis et al. 2001). Lower Pt/Rh values obtained on reference stations do not strictly represent a background because of the atmospheric input of material and tidal transport of particles from other estuarine areas. By shifting the concentration of one element, either Pt or Rh due to an additional source, this mass ratio can vary considerably. In WWTP section, the low values found may suggest that Pt signature derived from hospital and domestic effluents may be masked by dilution from the drainage system and/or additional Rh sources, such as those from ACC.

In sediments closer to VG bridge, Pt/Rh reflect mainly the ACC contribution. This section presented larger variations in the Pt/Rh ratio, having values within the typical range reported for ACC (Ely et al. 2001; Ravindra et al. 2004; Rauch and Peucker-Ehrenbrink 2015). Additionally, the road dust sample collected in a dense traffic road presented Pt/Rh mass ratio of 6.6. Thus, the variable Pt/Rh signature in sedimentary material closer to the VG bridge indicates that different dilution/concentration effects masking the real ACC signature may occur. At the estuary margins, around the VG bridge, a dilution effect exists due to the input of Pt and Rh from urban sources decreasing the signature. During the transport of road dust to the estuary, the partition of Pt or Rh may change and shift the ratio Pt/Rh. This suggests Pt and Rh in the Tagus estuary have a common source in ACC emissions from urban areas.

The highest Pt/Rh mass ratio observed in BRR sediments, compared to the other industrial sites (CN, SN and LN) that presented low values, is presumably related to the input of material with low Rh concentrations. This suggests that the industrial source at BRR has added to the estuary increased levels of Pt in comparison to Rh. At the other

sites, the industrial activities supplied both elements to the sediments, lowering the Pt/Rh ratio.

5.5. Conclusions

Platinum and Rh spatial distributions in superficial sediments of the Tagus estuary were assessed and reference levels are reported. Reference levels for Pt are close to the background, however Rh was ca. 5 times higher than its estimated crustal abundance. The main sources of these metals were confirmed, in particular those from cars and industries through their use as catalysts. Motorway bridges are a relevant via for the entrance of Pt and Rh into the estuary. The extent of this contribution relies on the structural characteristics and extension of the bridges. Even though, the Pt/Rh ratio found in sediments does not clearly reflect that typical of automotive catalytic converters. The highest contamination levels were found in industrialised areas, revealing the important contribution of industrial activities. The magnitude of those emissions remains unclear and needs further evaluation because they may be dominant. This work stands as reference information for future studies and highlights the importance of understanding Pt and Rh biogeochemistry in hydrodynamic estuaries, for which the lack of knowledge remains. Platinum and Rh concentrations will likely increase and medium-term monitoring of those elements is recommended.

References

Almécija, C., Cobelo-García, A., & Santos-Echeandía, J. (2016a). Improvement of the ultra-trace voltammetric determination of Rh in environmental samples using signal transformation. *Talanta*, *146*, 737–743. doi:10.1016/j.talanta.2015.06.032

Almécija, C., Cobelo-García, A., Santos-Echeandía, J., & Caetano, M. (2016b). Platinum in salt marsh sediments: Behavior and plant uptake. *Marine Chemistry*, *185*, 91–103. doi:10.1016/j.marchem.2016.05.009

Almécija, C., Sharma, M., Cobelo-García, A., Santos-Echeandía, J., & Caetano, M. (2015). Osmium and platinum decoupling in the environment: Evidences in intertidal sediments (Tagus Estuary, SW Europe). *Environmental Science and Technology*, *49*(11), 6545–6553. doi:10.1021/acs.est.5b00591

Alvera-Azcárate, a., Ferreira, J. G., & Nunes, J. P. (2003). Modelling eutrophication in mesotidal and macrotidal estuaries. The role of intertidal seaweeds. *Estuarine, Coastal and Shelf Science*, *57*(4), 715–724. doi:10.1016/S0272-7714(02)00413-4

Arpentinier, P., Koenig, J., & Vlaming, R. (1998, April 8). Nitric acid production. Google Patents.

Birke, M., Rauch, U., Stummeyer, J., Lorenz, H., & Keilert, B. (2017). A review of platinum group element (PGE) geochemistry and a study of the changes of PGE contents in the topsoil of Berlin, Germany, between 1992 and 2013. *Journal of Geochemical Exploration*. doi:https://doi.org/10.1016/j.gexplo.2017.09.005

Brito, P., Prego, R., Mil-Homens, M., Caçador, I., & Caetano, M. (2018). Sources and distribution of yttrium and rare earth elements in surface sediments from Tagus estuary, Portugal. *Science of The Total Environment*, *621*, 317–325. doi:https://doi.org/10.1016/j.scitotenv.2017.11.245

Cabeçadas, L. (1999). Phytoplankton production in the Tagus estuary (Portugal). *Oceanologica Acta*, *22*(2), 205–214. doi:https://doi.org/10.1016/S0399-1784(99)80046-2

Cabrita, M. T., Catarino, F., & Vale, C. (1999). The effect of tidal range on the flushing of ammonium from intertidal sediments of the Tagus estuary, Portugal. *Oceanologica Acta*, *22*(3), 291–302. doi:10.1016/S0399-1784(99)80053-X

Caçador, I., Costa, J. L., Duarte, B., Silva, G., Medeiros, J. P., Azeda, C., et al. (2012). Macroinvertebrates and fishes as biomonitors of heavy metal concentration in the Seixal Bay (Tagus estuary): Which species perform better? *Ecological Indicators*, *19*, 184–190. doi:https://doi.org/10.1016/j.ecolind.2011.09.007

Caetano, M., Prego, R., Vale, C., de Pablo, H., & Marmolejo-Rodríguez, J. (2009). Record of diagenesis of rare earth elements and other metals in a transitional sedimentary environment. *Marine Chemistry*, *116*(1), 36–46. doi:https://doi.org/10.1016/j.marchem.2009.09.003

Cobelo-García, A., López-Sánchez, D. E., Almécija, C., & Santos-Echeandía, J. (2013). Behavior of platinum during estuarine mixing (Pontevedra Ria, NW Iberian Peninsula). *Marine Chemistry*, *150*, 11–18. doi:10.1016/j.marchem.2013.01.005

Cobelo-García, A., Neira, P., Mil-Homens, M., & Caetano, M. (2011). Evaluation of the contamination of platinum in estuarine and coastal sediments (Tagus Estuary and Prodelta, Portugal). *Marine Pollution Bulletin*, *62*(3), 646–650. doi:10.1016/j.marpolbul.2010.12.018

Craft, C. B., Seneca, E. D., & Broome, S. W. (1991). Loss on ignition and kjeldahl digestion for estimating organic carbon and total nitrogen in estuarine marsh soils: Calibration with dry combustion. *Estuaries*, *14*(2), 175–179. doi:10.2307/1351691

Dare, S. A. S., Barnes, S.-J., Prichard, H. M., & Fisher, P. C. (2011). Chalcophile and platinum-group element (PGE) concentrations in the sulfide minerals from the McCreedy East deposit, Sudbury, Canada, and the origin of PGE in pyrite. *Mineralium Deposita*, *46*(4), 381–407. doi:10.1007/s00126-011-0336-9

Dung, T. T. T., Cappuyns, V., Swennen, R., & Phung, N. K. (2013). From geochemical background determination to pollution assessment of heavy metals in sediments and soils. *Reviews in Environmental Science and Bio/Technology*, *12*(4), 335–353. doi:10.1007/s11157-013-9315-1

Eastin, J. A. (1991, April 10). Manufacturing and using nitrogen fertilizer solutions on a

farm. Google Patents.

Ek, K. H., Morrison, G. M., & Rauch, S. (2004). Environmental routes for platinum group elements to biological materials--a review. *The Science of the total environment*, *334–335*, 21–38. doi:10.1016/j.scitotenv.2004.04.027

Ely, J. C., Neal, C. R., Kulpa, C. F., Schneegurt, M. A., Seidler, J. A., & Jain, J. C. (2001). Implications of Platinum-Group Element Accumulation along U.S. Roads from Catalytic-Converter Attrition. *Environmental Science & Technology*, *35*(19), 3816–3822. doi:10.1021/es001989s

Essumang, D. K., Dodoo, D. K., & Adokoh, C. K. (2008). The impact of vehicular fallout on the Pra estuary of Ghana (a case study of the impact of platinum group metals (PGMs) on the marine ecosystem). *Environmental Monitoring and Assessment*, *145*(1), 283–294. doi:10.1007/s10661-007-0037-0

European Commission. (1991). Council Directive 91/542/EEC of 1 October 1991 amending Directive 88/77/EEC on the approximation of the laws of the Member States relating to the measures to be taken against the emission of gaseous pollutants from diesel engines for use in vehicles. http://eur-lex.europa.eu/eli/dir/1991/542/oj. Accessed 22 January 2018

Folk, R. L. (1954). The Distinction between Grain Size and Mineral Composition in Sedimentary-Rock Nomenclature. *The Journal of Geology*, *62*(4), 344–359. doi:10.1086/626171

Fortunato, A., Oliveira, A., & Baptista, A. M. (1999). On the effect of tidal flats on the hydrodynamics of the Tagus estuary. *Oceanologica Acta*, *22*(1), 31–44. doi:https://doi.org/10.1016/S0399-1784(99)80030-9

Freire, P., Taborda, R., & Silva, A. (2007). Sedimentary characterization of Tagus estuarine beaches (Portugal). *Journal of Soils and Sediments*, *7*(5), 296–302. doi:10.1065/jss2007.08.243

Gaudêncio, M. J., Guerra, M. T., & Glémarec, M. (1991). Recherches biosédimentaires sur la zone maritime de l'estuaire du Tage, Portugal: données préliminaire. In M. Elliott & J.-P. Ducrotoy (Eds.), *Estuaries and Coasts: Spatial and Temporal Intercomparisons. ECSA 19 Symposium, Caen,* (pp. 11–16).

Gil, O., & Vale, C. (1999). DDT concentrations in surficial sediments of three estuarine systems in Portugal. *Aquatic Ecology*, *33*(3), 263–269. doi:10.1023/A:1009961901782

Hatfield, W. R., Beshty, B. S., Lee, H. C., Heck, R. M., & Hsiung, T. M. (1987, November 11). Method for recovering platinum in a nitric acid plant. Google Patents.

Haus, N., Eybe, T., Zimmermann, S., & Sures, B. (2009). Is microwave digestion using TFM vessels a suitable preparation method for Pt determination in biological samples by adsorptive cathodic stripping voltammetry? *Analytica chimica acta*, *635*(1), 53–57. doi:10.1016/j.aca.2008.12.043

IMT. (2016). *Relatório de Tráfego na Rede Nacional de Autoestradas - 4º Trimestre*. Lisboa, Portugal.

Jarvis, K. E., Parry, S. J., & Piper, J. M. (2001). Temporal and Spatial Studies of Autocatalyst-Derived Platinum, Rhodium, and Palladium and Selected Vehicle-

Derived Trace Elements in the Environment. *Environmental Science & Technology*, *35*(6), 1031–1036. doi:10.1021/es0001512

Kašpar, J., Fornasiero, P., & Hickey, N. (2003). Automotive catalytic converters: current status and some perspectives. *Catalysis Today*, *77*(4), 419–449. doi:https://doi.org/10.1016/S0920-5861(02)00384-X

Laschka, D., & Nachtwey, M. (1997). Platinum in municipal sewage treatment plants. *Chemosphere*, *34*(8), 1803–1812. doi:http://dx.doi.org/10.1016/S0045-6535(97)00036-2

Lemaire, A., Dournel, P., & Deschrijver, P. (2014, March 13). Process for the manufacture of hydrogen peroxide. Google Patents.

Loring, D. H., & Rantala, R. T. T. (1992). Manual for the geochemical analyses of marine sediments and suspended particulate matter. *Earth-Science Reviews*, *32*(4), 235–283. doi:https://doi.org/10.1016/0012-8252(92)90001-A

Marques da Costa, E. (2016). Sócio-Economia. In J. Rocha (Ed.), *Atlas Digital da Área Metropolitana de Lisboa*. Lisboa, Portugal: Centro de Estudos Geográficos.

Mateus, M., & Neves, R. (2008). Evaluating light and nutrient limitation in the Tagus estuary using a process-oriented ecological model. *Journal of Marine Engineering & Technology*, *7*(2), 43–54. doi:10.1080/20464177.2008.11020213

Matys Grygar, T., & Popelka, J. (2016). Revisiting geochemical methods of distinguishing natural concentrations and pollution by risk elements in fluvial sediments. *Journal of Geochemical Exploration*, *170*, 39–57. doi:http://dx.doi.org/10.1016/j.gexplo.2016.08.003

Mihaljevič, M., Galušková, I., Strnad, L., & Majer, V. (2013). Distribution of platinum group elements in urban soils, comparison of historically different large cities Prague and Ostrava, Czech Republic. *Journal of Geochemical Exploration*, *124*, 212–217. doi:https://doi.org/10.1016/j.gexplo.2012.10.008

Mil-Homens, M., Caetano, M., Costa, A. M., Lebreiro, S., Richter, T., de Stigter, H., et al. (2013). Temporal evolution of lead isotope ratios in sediments of the Central Portuguese Margin: A fingerprint of human activities. *Marine Pollution Bulletin*, *74*(1), 274–284. doi:https://doi.org/10.1016/j.marpolbul.2013.06.044

Mil-Homens, M., Vale, C., Raimundo, J., Pereira, P., Brito, P., & Caetano, M. (2014). Major factors influencing the elemental composition of surface estuarine sediments: the case of 15 estuaries in Portugal. *Marine pollution bulletin*, *84*(1–2), 135–46. doi:10.1016/j.marpolbul.2014.05.026

Mil-Homens, M., Vicente, M., Grimalt, J. O., Micaelo, C., & Abrantes, F. (2016). Reconstruction of organochlorine compound inputs in the Tagus Prodelta. *Science of The Total Environment*, *540*, 231–240. doi:https://doi.org/10.1016/j.scitotenv.2015.07.009

Miller, J., & Miller, J. (2010). *Statistics and chemometrics for analytical chemistry* (6th ed.). Pearson Education Limited.

Moldovan, M., Palacios, M. A., Gómez, M. M., Morrison, G., Rauch, S., McLeod, C., et al. (2002). Environmental risk of particulate and soluble platinum group elements released from gasoline and diesel engine catalytic converters. *Science of The Total*

Environment, *296*(1), 199–208. doi:https://doi.org/10.1016/S0048-9697(02)00087-6

Monteiro, C. E., Cesário, R., O'Driscoll, N. J., Nogueira, M., Válega, M., Caetano, M., & Canário, J. (2016). Seasonal variation of methylmercury in sediment cores from the Tagus Estuary (Portugal). *Marine Pollution Bulletin*, *104*(1), 162–170. doi:https://doi.org/10.1016/j.marpolbul.2016.01.042

Monteiro, C. E., Cobelo-García, A., Caetano, M., & Correia dos Santos, M. M. (2017). Improved voltammetric method for simultaneous determination of Pt and Rh using second derivative signal transformation – application to environmental samples. *Talanta*, *175*, 1–8. doi:10.1016/j.talanta.2017.06.067

Nygren, O., Vaughan, G. T., Florence, T. M., Morrison, G. M., Warner, I. M., & Dale, L. S. (1990). Determination of platinum in blood by adsorptive voltammetry. *Analytical chemistry*, *62*(15), 1637–40. doi:10.1021/ac00214a020

Paparatto, G., De, A. G., D'aloisio, R., & Buzzoni, R. (2010, September 28). Catalyst and its use in the synthesis of hydrogen peroxide. Google Patents.

Peucker-Ehrenbrink, B., & Jahn, B. (2001). Rhenium-osmium isotope systematics and platinum group element concentrations: Loess and the upper continental crust. *Geochemistry, Geophysics, Geosystems*, *2*(10), n/a-n/a. doi:10.1029/2001GC000172

Prichard, H. M., & Fisher, P. C. (2012). Identification of Platinum and Palladium Particles Emitted from Vehicles and Dispersed into the Surface Environment. *Environmental Science & Technology*, *46*(6), 3149–3154. doi:10.1021/es203666h

Prichard, H. M., Jackson, M. T., & Sampson, J. (2008). Dispersal and accumulation of Pt, Pd and Rh derived from a roundabout in Sheffield (UK): From stream to tidal estuary. *Science of The Total Environment*, *401*(1), 90–99. doi:https://doi.org/10.1016/j.scitotenv.2008.03.037

Prudêncio, M. I., Braga, M. A. S., & Gouveia, M. A. (1993). REE mobilization, fractionation and precipitation during weathering of basalts. *Chemical Geology*, *107*(3), 251–254. doi:https://doi.org/10.1016/0009-2541(93)90185-L

Rauch, S., Hemond, H. F., Barbante, C., Owari, M., Morrison, G. M., Peucker-Ehrenbrink, B., & Wass, U. (2005). Importance of automobile exhaust catalyst emissions for the deposition of platinum, palladium, and rhodium in the northern hemisphere. *Environmental science & technology*, *39*(21), 8156–8162.

Rauch, S., Morrison, G. M., & Moldovan, M. (2002). Scanning laser ablation-ICP-MS tracking of platinum group elements in urban particles. *Science of The Total Environment*, *286*(1), 243–251. doi:https://doi.org/10.1016/S0048-9697(01)00988-3

Rauch, S., & Peucker-Ehrenbrink, B. (2015). Sources of Platinum Group Elements in the Environment BT - Platinum Metals in the Environment. In F. Zereini & C. L. S. Wiseman (Eds.), (pp. 3–17). Berlin, Heidelberg: Springer Berlin Heidelberg. doi:10.1007/978-3-662-44559-4_1

Rauch, S., Peucker-Ehrenbrink, B., Molina, L. T., Molina, M. J., Ramos, R., & Hemond, H. F. (2006). Platinum Group Elements in Airborne Particles in Mexico City.

Environmental Science & Technology, *40*(24), 7554–7560. doi:10.1021/es061470h

Ravindra, K., Bencs, L., & Van Grieken, R. (2004). Platinum group elements in the environment and their health risk. *The Science of the total environment*, *318*(1–3), 1–43. doi:10.1016/S0048-9697(03)00372-3

Ruchter, N., & Sures, B. (2015). Distribution of platinum and other traffic related metals in sediments and clams (Corbicula sp.). *Water Research*, *70*, 313–324. doi:http://dx.doi.org/10.1016/j.watres.2014.12.011

Ruchter, N., Zimmermann, S., & Sures, B. (2015). Field studies on PGE in aquatic ecosystems. In *Platinum Metals in the Environment* (pp. 351–360). Springer.

Santos-Echeandía, J., Vale, C., Caetano, M., Pereira, P., & Prego, R. (2010). Effect of tidal flooding on metal distribution in pore waters of marsh sediments and its transport to water column (Tagus estuary, Portugal). *Marine environmental research*, *70*(5), 358–67. doi:10.1016/j.marenvres.2010.07.003

Schlitzer, R. (2017). Ocean Data View, odv.awi.de.

Sutherland, R. A., Pearson, G. D., Ottley, C. J., & Ziegler, A. D. (2015). Platinum-Group Elements in Urban Fluvial Bed Sediments—Hawaii. In *Platinum Metals in the Environment* (pp. 163–186). Springer.

Taborda, R., Freire, P., Silva, A., Andrade, C., & Freitas, M. (2009). Origin and evolution of Tagus estuarine beaches. *Journal of Coastal Research*, *SI*(56), 213–217.

Taylor, S. R., & McLennan, S. M. (1995). The geochemical evolution of the continental crust. *Reviews of Geophysics*, *33*(2), 241–265. doi:10.1029/95RG00262

Terashima, S., Katayama, H., & Itoh, S. (1993). Geochemical behavior of Pt and Pd in coastal marine sediments, southeastern margin of the Japan Sea. *Applied Geochemistry*, *8*(3), 265–271. doi:https://doi.org/10.1016/0883-2927(93)90041-E

Troupin, C., Barth, A., Sirjacobs, D., Ouberdous, M., Brankart, J.-M., Brasseur, P., et al. (2012). Generation of analysis and consistent error fields using the Data Interpolating Variational Analysis (DIVA). *Ocean Modelling*, *52–53*(Supplement C), 90–101. doi:https://doi.org/10.1016/j.ocemod.2012.05.002

Vale, C., Canário, J., Caetano, M., Lavrado, J., & Brito, P. (2008). Estimation of the anthropogenic fraction of elements in surface sediments of the Tagus Estuary (Portugal). *Marine Pollution Bulletin*, *56*(7), 1364–1367. doi:https://doi.org/10.1016/j.marpolbul.2008.04.006

Vale, C., & Sundby, B. (1987). Suspended sediment fluctuations in the Tagus estuary on semi-diurnal and fortnightly time scales. *Estuarine, Coastal and Shelf Science*, *25*(5), 495–508. doi:http://dx.doi.org/10.1016/0272-7714(87)90110-7

Vaz, N., & Dias, J. M. (2014). Residual currents and transport pathways in the Tagus estuary, Portugal: the role of freshwater discharge and wind. *Journal of Coastal Research*, 610–615. doi:10.2112/SI70-103.1

Vaz, N., Mateus, M., & Dias, J. M. (2011). Semidiurnal and spring-neap variations in the Tagus Estuary : Application of a process-oriented hydro-biogeochemical model. *Journal of Coastal Research*, *SI*(64), 1619–1623.

Vyas, N., Turner, A., & Sewell, G. (2014). Platinum-based anticancer drugs in waste

waters of a major UK hospital and predicted concentrations in recipient surface waters. *Science of The Total Environment*, *493*, 324–329. doi:https://doi.org/10.1016/j.scitotenv.2014.05.127

Wei, C., & Morrison, G. M. (1994). Platinum in road dusts and urban river sediments. *Science of The Total Environment*, *146–147*(Supplement C), 169–174. doi:https://doi.org/10.1016/0048-9697(94)90234-8

Wiseman, C. L. S., Hassan Pour, Z., & Zereini, F. (2016). Platinum group element and cerium concentrations in roadside environments in Toronto, Canada. *Chemosphere*, *145*, 61–67. doi:https://doi.org/10.1016/j.chemosphere.2015.11.056

Wiseman, C. L. S., & Zereini, F. (2009). Airborne particulate matter, platinum group elements and human health: a review of recent evidence. *The Science of the total environment*, *407*(8), 2493–2500. doi:10.1016/j.scitotenv.2008.12.057

Wiseman, C. L. S., Zereini, F., & Püttmann, W. (2013). Traffic-related trace element fate and uptake by plants cultivated in roadside soils in Toronto, Canada. *Science of The Total Environment*, *442*, 86–95. doi:https://doi.org/10.1016/j.scitotenv.2012.10.051

Zereini, F., Alt, F., Messerschmidt, J., von Bohlen, A., Liebl, K., & Püttmann, W. (2004). Concentration and Distribution of Platinum Group Elements (Pt, Pd, Rh) in Airborne Particulate Matter in Frankfurt am Main, Germany. *Environmental Science & Technology*, *38*(6), 1686–1692. doi:10.1021/es030127z

Zereini, F., & Wiseman, C. L. S. (2015). *Platinum Metals in the Environment*. (F. Zereini & C. L. S. Wiseman, Eds.). Berlin, Heidelberg: Springer Berlin Heidelberg. doi:10.1007/978-3-662-44559-4

Zereini, F., Wiseman, C., & Püttmann, W. (2007). Changes in Palladium, Platinum, and Rhodium Concentrations, and Their Spatial Distribution in Soils Along a Major Highway in Germany from 1994 to 2004. *Environmental Science & Technology*, *41*(2), 451–456. doi:10.1021/es061453s

Zhong, L., Yan, W., Li, J., Tu, X., Liu, B., & Xia, Z. (2012). Pt and Pd in sediments from the Pearl River Estuary, South China: background levels, distribution, and source. *Environmental Science and Pollution Research*, *19*(4), 1305–1314. doi:10.1007/s11356-011-0653-7

VI. SPECIATION ANALYSIS OF PT AND RH IN URBAN ROAD DUST LEACHATES

***published*: C. E. Monteiro, A. Cobelo-García, M. Caetano and M. Correia dos Santos, 2020. Speciation analysis of Pt and Rh in urban road dust leachates. *Science of The Total Environment, 722*, 137954.**
DOI:https://doi.org/10.1016/j.scitotenv.2020.137954

Graphical Abstract

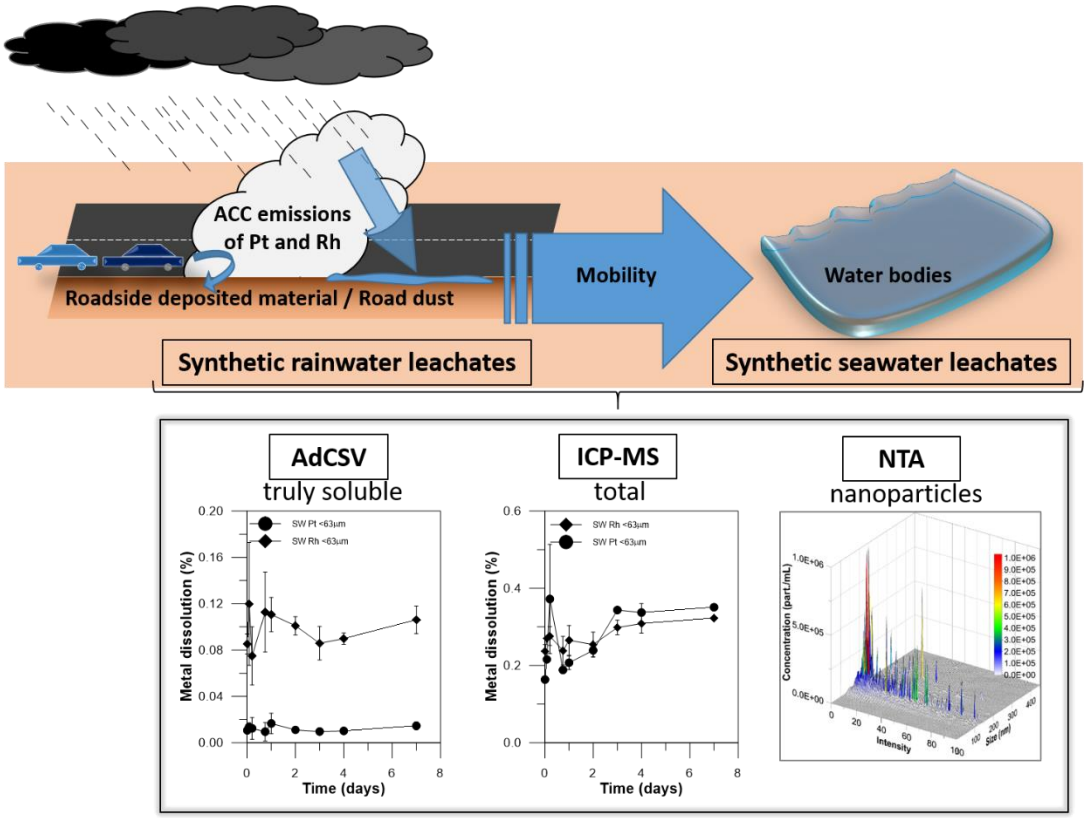

Abstract

Road dust is a major reservoir of anthropogenic Pt and Rh. However, information about how these elements are released to the aquatic systems under environmentally relevant conditions is scarce. In this work, an innovative combination of analytical strategies is used to provide insight into the speciation analysis of those elements. A composite sample of road dust thoroughly characterized was incubated over 7 days in synthetic rainwater and seawater. In the filtered (<0.45 µm) solutions, truly dissolved Pt and Rh concentrations were measured by adsorptive cathodic stripping voltammetry, while total concentrations were determined by inductively coupled plasma mass spectrometry. Truly dissolved species corresponded to a small fraction of total Pt and Rh in the road dust; accordingly, values of 0.01% and 0.1% were obtained in both media for Pt and Rh, respectively, which remained constant over time. The concentration of total filter-passing species predominates for both elements by a factor of 10 and 2-3 for Pt and Rh, respectively, evidencing that particulate species coexist with truly dissolved forms. Temporal variations were observed for Pt, as opposed to Rh. These findings contribute to the gap in knowledge regarding Pt and Rh mobility in aquatic systems.

Keywords

Platinum group elements, AdCSV, ICP-MS, Truly dissolved species, (Nano)Particulate species

6.1. Introduction

Platinum-group elements (PGE) occur naturally in the environment, with concentrations amongst the lowest found in the Earth's crust (Peucker-Ehrenbrink and Jahn 2001; Taylor and McLennan 1995). Nevertheless, it is well-recognized that concentrations of Pt and Rh in several environmental compartments have steadily increased over the past decades due to anthropogenic inputs (Zereini and Wiseman 2015). Their rise has been mainly attributed to the generalized use of Pt and Rh in automotive catalytic converters (ACC). Other potential sources exist but have been less characterized, namely those from industrial activities, and domestic and hospital effluents (Sebastien Rauch and Peucker-Ehrenbrink 2015), as well as new Pt uses will emerge in cancer chemotherapy (Sarkar 2017). More recently, it has become popular the addition of Pt as nanoparticles to various consumer products, such as foods and cosmetics (Fröhlich and Roblegg 2012). Recent investigations evidence that the introduction of Pt and Rh in the environment may have consequences for biota (Sures et al. 2015), and this will depend on the organism but also the PGE speciation.

Modern manufacturing processes produce ACC wash coats covered with PGE particles of 0.3 μm down to nanoparticle sizes (Prichard and Fisher 2012). Platinum and Rh are released from the ACC because of deterioration and mechanical abrasion. Once that occurs, particles end up accumulating on the roadside environment. Thus, road dust is a complex mixture of natural (mineral and organic material) and anthropogenic particles. While the former is due mainly to vegetation remains and weathering of the surrounding soils, the latter will depend on the type of asphalt pavement and circulating vehicles (Ermolin et al. 2017). Road dust and roadside soils are therefore a major anthropogenic reservoir of PGE (Zereini and Wiseman 2015) and their spreading in the environment can easily occur due to atmospheric transport and rain events (Liu et al. 2015).

The forms in which PGE are emitted from ACC are not yet completely elucidated. Some studies indicate that they are released mainly as particulate material (Ek et al. 2004; Ely et al. 2001; Prichard and Fisher 2012; Sébastien Rauch et al. 2002), but a soluble fraction has also been measured (Moldovan et al. 2002). The solubility of Pt and Rh can vary depending on engine type, the age of the ACC, and also upon the individual element chemistry (Ash et al. 2014). Once in the environment, Pt and Rh solubility can be

modulated by pH and commonly occurring complexing agents (Dahlheimer et al. 2007; Zimmermann et al. 2003). Consequently, it is foreseen that Pt and Rh from road dust will end up in aquatic systems in both truly dissolved (soluble species) and particulate forms, namely colloidal (with sizes from 1 to 1000 nm; Wilkinson et al. 2006). However, limited knowledge exists about the physicochemical characteristics of Pt an Rh in those systems (Cobelo-García et al. 2013; Folens et al. 2018; Jarvis et al. 2001). Speciation analysis schemes in aquatic environments discriminate between particulate and dissolved fractions, i.e. those passing through a 0.45 µm filter (Burden et al. 2002). The latter fraction also includes particulate species such as colloids, in addition to nanoparticles (<100 nm; Auffan et al. 2009), whose mobility and bioavailability may be different from truly dissolved species (Guo and Santschi 2006).

Although a panoply of data exists on concentrations of Pt and Rh in road dust samples (Zereini and Wiseman 2015), information about which forms and how these elements are released to the aquatic systems under environmentally relevant conditions is scarce (Folens et al. 2018; Jarvis et al. 2001). Nowadays, inductively coupled plasma-mass spectrometry (ICP-MS) is a powerful tool for the determination of Pt and Rh, giving a measurement of the total concentration of the elements (Perry et al. 1995). However, it does not discriminate truly dissolved and particulate Pt and Rh species. In one study, the solubility of Pt and Rh from road dust, with a ratio Pt/Rh close to 7.1, was investigated in deionized water and synthetic rainwater at pH 3, over 15 hours (Jarvis et al. 2001). The obtained leachates were analyzed for Pt and Rh by ICP-MS. For both PGE significant temporal variation was not observed. In another recent work (Folens et al. 2018), Pt nanoparticles were identified in road dust leachates using single-particle (sp)ICP-MS. Extraction was done in natural stormwater runoff at pH=7.4 using a sonicator for 30 minutes at 40 ˚C. Extractions efficiency varied between 0.2±0.2 % and 18±26 % depending on the road dust used. Platinum nanoparticles with average sizes of 9-21 nm were detected in all road dust leachates. Those authors also used ICP-MS and no soluble Pt was identified based on the comparison between the results of both techniques.

Adsorptive cathodic stripping voltammetry (AdCSV) enables the determination of truly dissolved Pt in aquatic systems, like estuaries (Cobelo-García et al. 2013) and the ocean (López-Sánchez et al. 2019). Only recently dissolved Rh concentrations in water samples were reported (Monteiro et al. 2017). In this work, we innovate by combining analytical methods to provide a better insight into the speciation analysis of Pt and Rh.

To achieve our goal, a composite sample of road dust was thoroughly characterized and used in leaching batch experiments with synthetic rainwater and seawater over 7 days. The objectives were to evaluate Pt and Rh speciation analysis in filtered leachates, through the determination of truly dissolved species of Pt and Rh by AdCSV and total filter-passing (<0.45 µm) species by ICP-MS. Ultimately, this study aims to contribute to the gap in knowledge regarding Pt and Rh mobility in aquatic systems.

6.2. Materials and Methods

All reagents used were of analytical grade and solutions were prepared with ultrapure water from a Milli-Q (Millipore) purification system (conductivity of 18.2 MΩ.cm, 25 ˚C). All laboratory material was previously acid-cleaned by immersion in ~20% nitric acid (HNO_3) and hydrochloric acid (HCl) baths for 48 h each.

6.2.1. Road Dust Sampling

Road dust samples (n=25) deposited in a section of 30 meters of a high-traffic road (Lisbon, Portugal: 38.733028 N; 9.223730 W) were collected on a single day during the summer of 2017. The deposited material was swept along the road's central barrier between the lanes, using an acid-washed plastic brush and stored into plastic zip bags. After drying at 40 ˚C in an oven, one composite sample was obtained by mixing thoroughly all sampled road dust.

6.2.2. Road Dust Characterization

The composite sample (~25 kg) was firstly dry-sieved through 2- and 0.85 mm mesh sieves to reduce the amount of coarser material. Subsequently, it was sieved to obtain the 850-63 µm and <63 µm fractions. After sieving, about 0.5 kg of fine particulate material (<63 µm) was collected and thoroughly homogenized before its use. Unless otherwise specified, road dust characterization and all subsequent experiments were done with the <63 µm fraction, hereafter referred to as road dust. The water content (%H_2O) at 105 ˚C and loss on ignition (LOI, in %) at 450 and 550 ˚C were calculated by the

difference of weights. Particle size distribution was measured using a laser diffraction particle size analyzer (Coulter LS13 320), after organic matter removal with hydrogen peroxide and sample dispersion in 0.033 M sodium hexametaphosphate. The mineralogical composition was determined by X-ray diffraction (XRD) using an X-Ray diffractometer (Panalytical X'PERT PRO model) equipped with a CuKα radiation source (35 mA and 40 kV). High Score Plus program was used for the analysis and the interpretation of diffractograms was supported by the PDF4 database.

As to elemental characterization, total carbon (C), hydrogen (H), nitrogen (N) and sulphur (S) were determined using a TruSpec CHNS micro analyser (LECO). The instrument is a dry combustion type with infrared detection for CHS and thermal conductivity detection for N. As to Pt and Rh, both elements were determined after acid-digestion in *aqua regia* by AdCSV, as previously described in Monteiro et al. (2017). The quantification of Pt and Rh was done using the standard addition method. All experiments were performed at least in duplicate and the certified reference material (CRM) BCR-723 was used throughout the procedures. The determination of other elements (Al, Fe, Pb, Cd, Cr and Zn) was done after acid-digestion (*aqua regia* + HF; Loring and Rantala 1992) by ICP-MS (Thermo Scientific X-SERIES 2), with a Peltier impact bead spray chamber and a concentric Meinhard nebulizer (Brito et al. 2018).

6.2.3. Road Dust Leaching Experiments

Leaching batch experiments were performed exposing road dust aliquots in synthetic rainwater and seawater and incubated at different times. The synthetic media were prepared according to the literature described for rainwater (Bielmyer et al. 2012) and seawater (Kester et al. 1967) (S.I. Table S.VI 1). The pH of synthetic rainwater was adjusted to 4.0±0.2 using 0.1 M HCl, while the seawater solution was aerated for 2 h until constant pH at 8.2±0.2.

Road dust aliquots of 10 g were weighed and transferred to 50 mL polypropylene tubes, to which 20 mL of synthetic rainwater or seawater were added. The initial pH was measured and then the mixtures were horizontally shaken at 250±10 rpm at room temperature (25±2 ^{0}C) for the time of interest. Solutions were collected after 0.01, 0.08, 0.2, 1, 2, 3, 4 and 7 days of exposure and filtered through polyethersulfone 0.45 µm filters (Sartorius), hereafter just called leachates. The final pH was also measured. Then,

leachates were acidified with HCl and kept refrigerated until further analysis. Dissolved organic carbon (DOC) was evaluated in rainwater and diluted 1:10 seawater leachates retrieved after 1 day of exposure. Determinations were done by wet chemical oxidation with persulfate method with an OI Analytical TOC Analyzer. All experiments were done in duplicate using freshly prepared solutions and blanks were processed following the same procedure.

6.2.4. Determination of Truly Dissolved Pt and Rh in the Leachates

The truly dissolved fraction of Pt and Rh was determined by AdCSV following the procedure optimized previously (Monteiro et al. 2017). Briefly, voltammetric determinations were performed in an Autolab PGSTAT 12 (Metrohm) connected to the VA stand model 663 (Metrohm). A static mercury drop electrode (SDME) was used as a working electrode, together with an Ag/AgCl reference electrode, placed inside a salt bridge with 3 M KCl, and a glassy carbon rod as the counter electrode. The GPES v4.9 software (EchoChemie) was used for experimental parameters and data acquisition control. To test the efficient of DOC breakdown in the leachates, which severely interferes with the voltammetric determination, a road dust leachate was UV-irradiated between 1 and 6 h before the analysis. The voltammetric signals remained unchanged after 2 h, and subsequently, all samples were UV-digested for 3 h in quartz tubes sealed with Teflon caps. To facilitate organic content destruction hydrogen peroxide was added in small amounts. All measurements were performed in triplicate under clean and acclimatised conditions (25±2 ^{0}C). Blanks were analyzed throughout the procedure and no cross-contamination was observed. Intermediate precision, expressed as RSD based on Pt and Rh acid-digested road dust CRM BCR-723 (n = 3), was 15% and 17% for Pt and Rh, respectively. Recoveries of CRM were higher than 90% for both elements.

6.2.5. Determination of Total Pt and Rh in the Leachates

The determination of total Pt and Rh in the leachates was undertaken using ICP-MS (Agilent 7900). Interferences of Hf ($^{179}Hf^{16}O^{+}$) on ^{195}Pt and Cu ($^{63}Cu^{40}Ar^{+}$), Pb ($^{206}Pb^{2+}$), Sr ($^{87}Sr^{16}O^{+}$), Rb ($^{87}Rb^{16}O^{+}$) and Zn ($^{67}Zn^{36}Ar^{+}$) on ^{103}Rh were monitored and

mathematically corrected for each sample using interference ratios derived from single-metal solutions. It was observed that the Hf interference on Pt signal was negligible (<0.1 %). However, interferences were significant for Rh, mainly from $^{87}Sr^{16}O^{+}$ (24±13 %, on average, of the ^{103}Rh signal) and $^{63}Cu^{40}Ar^{+}$ (7±4 %), whereas the interferences arising from $^{206}Pb^{2+}$, $^{87}Rb^{16}O^{+}$ and $^{67}Zn^{36}Ar^{+}$ were negligible (<0.1 %). Blanks derived from control incubations were <1 % of the concentrations obtained for the samples. In any case, the results presented were blank-corrected. The relative standard deviation of repeated measurements was in general <10 %.

6.2.6. Characterization of (Nano)Particles in the Leachates

Nanoparticle Tracking Analysis (NTA) was used to determine the concentration of the (nano)particles and their size distributions in the road dust leachates, after 1 day of incubation in both synthetic media. A Malvern Panalytical NanoSight NTA instrument was used. Two independent experiments were done for each medium and five replicate measurements with a duration of 60 s each were performed following injection of the fresh sample. The results are presented as the mean of each experiment. These were collected in a histogram for better statistical significance and representation. The analysis of blank solutions did not show the presence of any particles, therefore particles observed in the experiments derived only from the road dust leachates.

6.3. Results and Discussion

6.3.1. Road Dust Physicochemical Characteristics

The physicochemical characteristics of the road dust, fraction <63 µm, are summarized in Table VI.1, which also includes the values obtained for the tunnel dust CRM BCR-723 (European Comission 2002; Zischka et al. 2002). The CRM was used in parallel with the real road dust to assess the accuracy of the procedures and to evidence the different compositions that can be found amongst road dusts.

Particles from the road dust had a median grain size of 44.4 µm (S.I. Figure S.VI 1) while those of BCR-723 were 14.6 µm. The water and organic matter contents in

Table VI.1 – Physicochemical characterization of the road dust sample and certified reference material BCR-723.

	Road Dust	**BCR-723**	
	obtained	*obtained*	*certified*
Parameters			
Median grain size (µm)	44.4[#]		14.6
Water content (%)	1.27±0.02	5.4±0.1	
LOI - 450 ˚C (%)	6.04±0.01	19.28±0.01	
LOI - 550 ˚C (%)	6.66±0.01	22.28±0.01	23 to 25*
Elemental analysis			
Total C (%)	7.69±0.03	14.127±0.009	13.8±0.2
Total H (%)	0.45±0.06	1.69±0.01	1.66
Total N (%)	0.03±0.02	0.111±0.002	0.180
Total S (%)	1.1±0.1	4.51±0.09	2 to 5*
Total metal concentration (dry weight basis)[a]			
Al (%)	4.5±0.2	3.88±0.05	3.8±0.2
Fe (%)	9.0±0.6	3.47±0.05	3.3±0.2
Pb (µg g^{-1})	132±1	863±15	866±16
Cd (µg g^{-1})	0.6±0.1	2.4±0.2	2.5±0.4
Cr (µg g^{-1})	399±15	420±55	440±18
Zn (mg g^{-1})	0.8±0.1	1.4±0.2	1.7±0.1
PGEs total metal concentration (dry weight basis)[b]			
Pt (ng g^{-1})	294±15	80±6	81.3±2.5
Rh (ng g^{-1})	44±7	11.3±0.8	12.8±1.3

[#] Particle size distribution in S.I. Figure S.VI 1. * Estimations or reference values reported in literature (European Comission, 2002; Zischka et al., 2002). [a] Total concentrations measured by ICP-MS. [b] Total concentrations measured by AdCSV.

the road dust were lower than BCR-723, as can be concluded by the loss on ignition and the total carbon values. Some differences also existed in terms of the total content of hydrogen, nitrogen and sulphur that reflect the different composition of the matrices. A selected compilation of major, minor and trace elements shows that Fe predominated in the road dust reaching more than twice that of the CRM, while the Al content was similar in both materials.

In terms of priority pollutants, Pb and Cd in the road dust were lower than in BCR-723. As to Cr, an element of increasing concern, the concentration was comparable in both materials. The concentrations of Zn found in road dust were lower than in BCR-723. Besides, Zn was also determined to discard possible interferences in the determination of Pt and Rh by AdCSV (Monteiro et al. 2017). Regarding total concentrations in the collected road dust, 294 ng Pt g^{-1} and 44 ng Rh g^{-1} were found. These values were higher than those found in BCR-723, 81.3 ng Pt g^{-1} and 12.8 ng Rh g^{-1} (European Comission 2002; Zischka et al. 2002), but within the range of concentrations reported for other road dusts throughout the world (e.g. Chellam and Bozlaker 2015; Leśniewska et al. 2004; Lyubomirova and Djingova 2015; Mathur et al. 2010).

In Figure VI-1 can be seen XRD diffractograms of the road dust sample and the CRM BCR-273. Both matrices revealed to have in common quartz and calcite, which are minerals directly related to the existent materials in the roadways, like concrete with limestone and sand mortars. The presence of augite and anorthite minerals in road dust indicates that some of those materials may be of basic magmatic nature (gabbro or basalt), which are commonly used in Portugal. The higher content of Fe in road dust can be explained by the presence of augite, a ferromagnesian mineral. Illite was also identified, which is clay material found in most soils. In the case of CRM, gypsum was the main component identified that is directly related to tunnel walls. Noteworthy, the presence of an amphibole (mineral fibers – clinochrysotile), albeit in small quantity, may be associated with special coating products. There were also some clay materials (chlorite – clinochlore), which may be associated with airborne dust or building materials.

In summary, the road dust analyzed shared some of its characteristics with BCR-723 and other road dusts worldwide collected (Gunawardana et al. 2012), but it has its features. The differences found are due to local or regional circumstances, such as climacteric and moisture conditions that influence the organic matter content; the type of

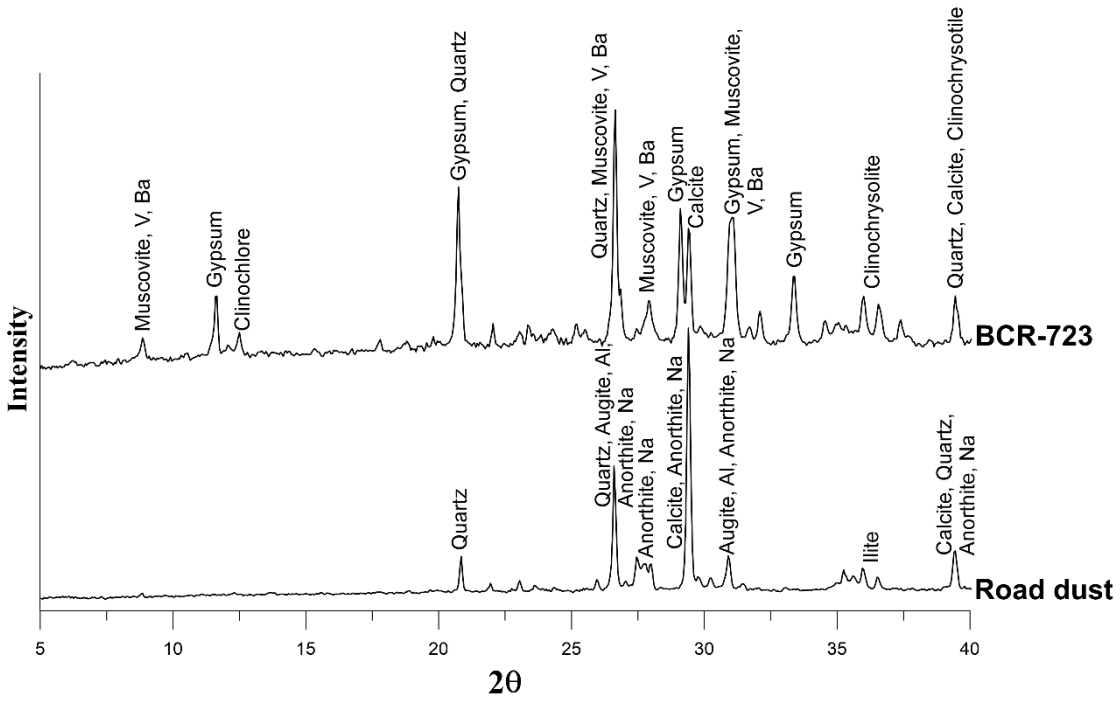

Figure VI-1 - X-ray diffractograms (XRD) of the collected sample of road dust and the tunnel dust certified reference material BCR-723.

soil and surface properties of the pavements that affect the road dust mineralogical composition. Furthermore, other factors such as the number and type of vehicles, and their speed, will determine the metal concentrations in the road dust, namely the PGE levels.

6.3.2. Temporal Dissolution of Pt and Rh in the Leaching Experiments

In the design of the leaching experiments, several aspects were taken into account. In the case of a rainy event, it is expected to occur changes in road dust composition and morphology, once the road dust will be exposed to rainwater with varying pH during the first minutes to several hours of rainfall. Also, depending on the intensity and duration of precipitation, road dust will end up in gully guts and other receptacles, being in close contact with rainwater for several days. Ultimately, road dust will be transported to nearby aquatic systems. Augmented concentrations of PGE found in aquatic sediments (Abdou et al. 2016; Cobelo-García et al. 2014; Essumang et al. 2008; Monteiro et al. 2019; Zhong et al. 2012) indicate that road dust particles reach transitional systems through sewage

outfalls or runoff. Particles are then mixed into freshwater or seawater, where interactions will depend on the ionic strength (Cobelo-García et al. 2014), water residence time and particle's settling velocity, among other factors. For instance, in Tagus estuary (Portugal) residence times vary between 7 and 23 days, depending on the influx of freshwater discharged by the river (Braunschweig et al. 2003).

Thus, to mimic environmentally relevant conditions, the dissolution of Pt and Rh was evaluated under two different media, mildly acidic synthetic rainwater and seawater, up to 7 days of exposure.

6.3.2.1. Truly Dissolved Pt and Rh in the Leachates

In Figure VI-2 is shown Pt and Rh temporal dissolution from road dust, expressed as %, measured in the leachates with AdCSV as truly dissolved forms. Preliminary experiments in synthetic rainwater were performed using two grain size ranges of particles, 63-850 µm and <63µm (Figure VI-2a). However, due to larger heterogeneity and dilution of Pt and Rh concentration in the coarser fraction (mainly sand), subsequent experiments in synthetic seawater were performed just using the fine-grained road dust (<63 µm; Figure VI-2b). Furthermore, particles <63 µm can be considered environmentally more relevant, in light of the increased mobility of PGE and easier transport along the watercourses from urban areas to the aquatic systems.

For both metals, dissolution was two to three times higher in the experiments with fine-grained road dust compared to the coarser fraction (Figure VI-2a). The dissolution was also different between the two metals, being Rh more soluble by a factor of ~10 (Figure VI-2a and b) in both fractions and both media. However, the dissolution of Pt and Rh was relatively constant over the surveyed period, within the experimental errors and seemed to be independent of the medium. Taking into account all the values determined with road dust over the 7 days, in the <63 µm fraction, the percentages of dissolution for Pt were 0.011±0.002 % and 0.012±0.003 % for rainwater and seawater, respectively, while for Rh corresponded to 0.09±0.01 % and 0.10±0.02 %, as summarized in Table VI.2.

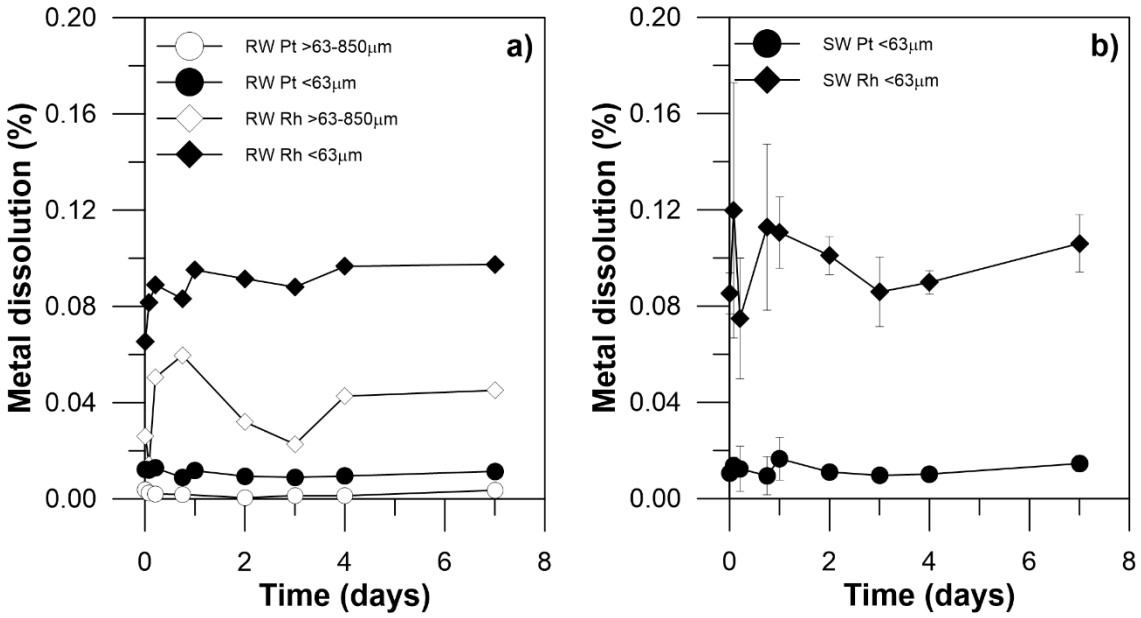

Figure VI-2 - Temporal dissolution (%) of Pt (circles) and Rh (diamonds) from road dust sample measured by AdCSV in **a)** synthetic rainwater (RW) and **b)** synthetic seawater (SW).

The amount of Pt and Rh dissolved in rainwater was higher in the experiment using the fraction <63 µm than in the 63-850 µm. This is due to an enrichment factor of total Pt and Rh concentrations in the fine-grained fraction, as found by Leśniewska et al. (2004). Road dust particle's size varies in a wide range, from nanometers to millimeters. Yet, the size of most particles contained in the exhaust gases of vehicles range between 50 and 1000 nm (Ermolin et al. 2017), which explains the higher values found in the fine-grained fraction. The sample with coarser particles (63-850 µm) had a less homogeneous composition, which was reflected in the standard deviation of the dissolution values, 0.002±0.001 % and 0.04±0.02 % for Pt and Rh, respectively. Consequently, all other leaching experiments were done only with <63µm fraction.

The obtained results show that the percentage of truly dissolved Pt and Rh was a small portion of the total content in the road dust, with a minor dependence of the medium. In previous studies, pH was found to have an impact on Pt dissolution (Jarvis et al. 2001). In our experiments, pH measured in all leachates was fairly constant and close to 8. Even in the experiments with synthetic rainwater, the pH raised from 4 to ≈8 in the first 15 minutes and remained unchanged thereafter (S.I. Figure S.VI 2). As well evidenced in the XRD analysis, calcite ($CaCO_3$) is a major mineral component of the road dust. Therefore, the pH variation is most likely related to the high buffering capacity of

calcite present in the road dust and its solubilization (Rieuwerts et al. 1998). Moreover, dissolved percentages of Pt and Rh were not dependent on inorganic anions like Cl^- in the medium. This finding corroborates previous observations on the effects of Cl^- on Pt dissolution (Šebek et al. 2011).

The lack of significant changes in the percentage of dissolution over the sampling period (Figure VI-2) suggests that no oxidation of metallic Pt and Rh took place. Thus, the truly dissolved species in solution resulted from the sparingly compounds already in the oxidized forms that are present in the road dust particles. The original road dust Pt/Rh mass ratio equals 6.5 while in the leachates the ratio of the truly dissolved portion is 0.8, either in synthetic rainwater or in seawater, evidencing higher oxidized species of Rh than Pt.

6.3.2.2. Total Pt and Rh in the Leachates

The temporal dissolution of Pt and Rh, expressed as %, measured in the leachates by ICP-MS as total concentration, is shown in Figure VI-3a and b, in synthetic rainwater and seawater respectively. Higher percentages of dissolution were determined for both metals when ICP-MS was used in comparison to those measured by AdCSV. In the case of Pt, the values were up to one order of magnitude higher, while for Rh they were about 2-3 times (Table VI.2). These results confirm that particulate Pt and Rh, i.e. colloidal species and/or (nano)particles, are measured by ICP-MS besides the truly dissolved forms. Moreover, they also show that particulate forms of Pt predominate over the soluble species in road dust leachates, while the difference is less noticeable for Rh.

In synthetic rainwater (Figure VI-3a) the percentage of dissolution was higher for Rh than Pt, following the trend observed in the experiments by AdCSV (Figure VI-2a). In seawater, similar values were obtained for both metals (Figure VI-3b), within the experimental error, dissimilar to what was observed when using AdCSV (Fig. 2b). Unlike the truly dissolved fraction, the total concentration of Pt measured by ICP-MS in the extracts showed that Pt appears to depend upon the time of contact. In rainwater, the dissolution of Pt diminished over time (Figure VI-3a) from 0.17 to 0.03 %. In seawater conditions, Pt concentration increased during the first three days, varying between 0.16 up to 0.34 %, and then concentrations seemed to be relatively constant (Figure VI-3b). Consequently, on day 1 the dissolution of Pt in seawater was about twice that found in

rainwater and on day 7 was ten times more (Table VI.2). This tendency was not found in the case of Rh. A thorough analysis of the data shows, within the experimental errors, that Rh dissolution was constant over time. Accordingly, during the experimental period, average values were 0.24±0.03 % and 0.28±0.03 % for synthetic rainwater and seawater, respectively (Figure VI-3 and Table VI.2). Those values also show that for Rh no differences in the percentage of dissolution measured by ICP-MS were found in synthetic rainwater and seawater.

Table VI.2 - Percentage of dissolution (average ± standard deviation) of Pt and Rh in road dust leachates, using the fraction with grain size <63 µm, from synthetic rainwater and seawater, measured during 7 days by AdCSV and ICP-MS.

Element	**Pt**		**Rh**	
Matrix	***Rainwater***	***Seawater***	***Rainwater***	***Seawater***
% AdCSV	0.011±0.002	0.012±0.003	0.09±0.01	0.10±0.02
% ICP-MS	0.12±0.01*	0.21±0.01*	0.24±0.03	0.28±0.03
	0.030±0.003**	0.35±0.01**		

*Values at day 1; **Values at day 7.

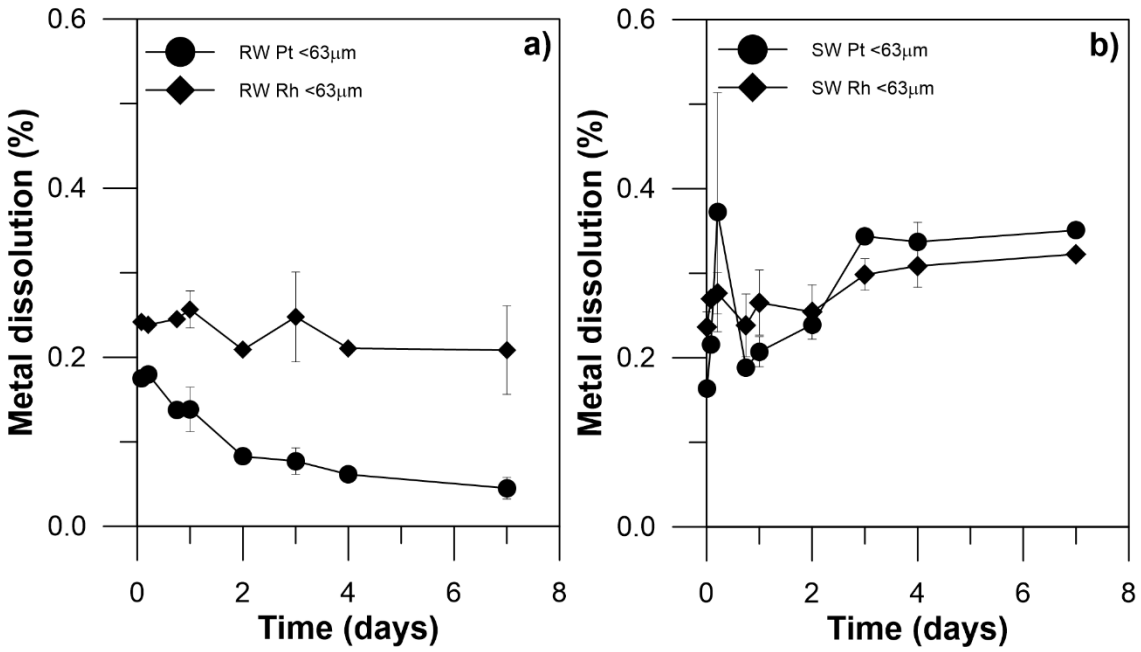

Figure VI-3 - Temporal dissolution (%) of Pt (circles) and Rh (diamonds) from road dust measured by ICP-MS in **a)** synthetic rainwater (RW) and **b)** synthetic seawater (SW).

As it is well known, metals tend to sorb on the particle's surface, and their fate ultimately will be controlled by colloids aggregation/disaggregation (Wilkinson et al. 2006). In the leachates, both organic and inorganic colloids, such as Fe oxides, Al and Si may be present. The existence of inorganic colloids is supported by the mineralogical analysis of the road dust (Figure VI-1). In the case of Pt in rainwater conditions after the initial dissolution, an increased fraction was retained by filtration over time, while in seawater conditions the opposite occurred at least during the first days. The behaviour observed for Pt cannot be rationalized in terms of the ionic strength differences. More frequently, the higher ionic strength of seawater compared to freshwater will tend to cause aggregation, due to an effective reduction of Coulombic repulsion of charged particles (Domingos et al. 2009). However, stereochemical effects imposed by adsorption to organic molecules may prevent aggregation. Actually, DOC in the leachates retrieved after day 1 was 53 and 101 mg L^{-1} in rainwater and seawater, respectively. The nature of DOC is not known but the results suggest that hydrophilic compounds in saline solution were more easily extracted (Provenzano et al. 2010; Rennert et al. 2007). The organic compounds, in higher concentration in seawater leachates, were able to participate in the stabilization of (nano)particles bearing Pt, favoring colloidal dispersion, since truly dissolved Pt concentrations remained constant over time (Figure VI-2a). In synthetic rainwater, the formation of inorganic aggregates appeared to be favoured over time and thus the decrease observed in Pt dissolution measured by ICP-MS. In the case of Rh, due to its higher solubility, the impact of particulate matter and/or particulate Rh forms on the percentage of dissolution was lower than for Pt.

Even though it is well recognized that road dust is both a sink and source of PGE to other environmental compartments, only a few studies addressed Pt and/or Rh solubility from road dust using field-collected samples and under environmentally relevant conditions (Jarvis et al. 2001, Folens et al. 2018). Despite the absence of additional information about the physical and chemical characteristics of the field-collected road dust, the values reported by Jarvis et al. (2001) are similar to those found in this work for Pt and Rh measured by ICP-MS (Table VI.2). Furthermore, the results obtained in our work show that truly dissolved Pt measured by AdCSV differs by one order of magnitude from ICP-MS quantification. Therefore, when ICP-MS and spICP-MS were used by Folens et al. (2018), truly dissolved species were probably difficult to be differentiated within the experimental errors.

6.3.3. Characteristics of (Nano)Particles in the Leachates

Despite the uncertainties regarding the nature of the (nano)particles bearing Pt and Rh and/or Pt and Rh nanoparticles in the leachates, the results discussed demonstrate that (nano)particles do exist in solution with a higher concentration in seawater extracts. Consequently, nanoparticle tracking analysis (NTA) was used to investigate the (nano)particles in the leachates and to estimate their concentrations on day 1. The leachates had to be diluted by a factor of 1:5 and 1:10 for rainwater and seawater, respectively. In Figure VI-4 is shown the average particle's concentrations (part.mL^{-1}) as a function of size (nm) and intensity of the light scattering (absence of units, a.u.) in the road dust leachates.

Only particles larger than 40 nm were identified in both media due to technical limitations (Jones-Lepp et al. 2011). In the case of rainwater, the distribution of sizes was bimodal with average sizes of 130 and 240 nm. In seawater, it was also found two populations of (nano)particles with average sizes of 100 and 175 nm, but the latter size showed to have lower light scattering intensities. From the different intensities observed, (nano)particles of different nature are present in the extracts, mainly in the case of rainwater. Those associated with the highest intensities are most likely to be of metallic nature, although in a lower concentration. It should be noted that more (nano)particles were found in the seawater leachates, with an average concentration of $(6\pm2)\times10^9$ part.mL^{-1}, while in rainwater the average concentration was $(1.4\pm0.4)\times10^9$ part.mL^{-1}. The nature of the (nano)particles cannot be determined by NTA. Nevertheless, the higher proportion of (nano)particles in seawater leachates may be explained by the presence of carbonate mineral, as well as other metal bearing (nano)particles stabilized by the organic compounds present in the leachates.

Although the NTA analysis could not be performed in leachates other than day 1, the obtained results fully support the conclusions drawn from AdCSV and ICP-MS data presented. NTA experiments constitute an additional and independent evidence that (nano)particles were present in both leachates, and with a higher concentration in seawater. Interestingly, road dust particles were recently studied by static light scattering analysis and scanning electron microscopy (Ermolin et al. 2017). The authors concluded

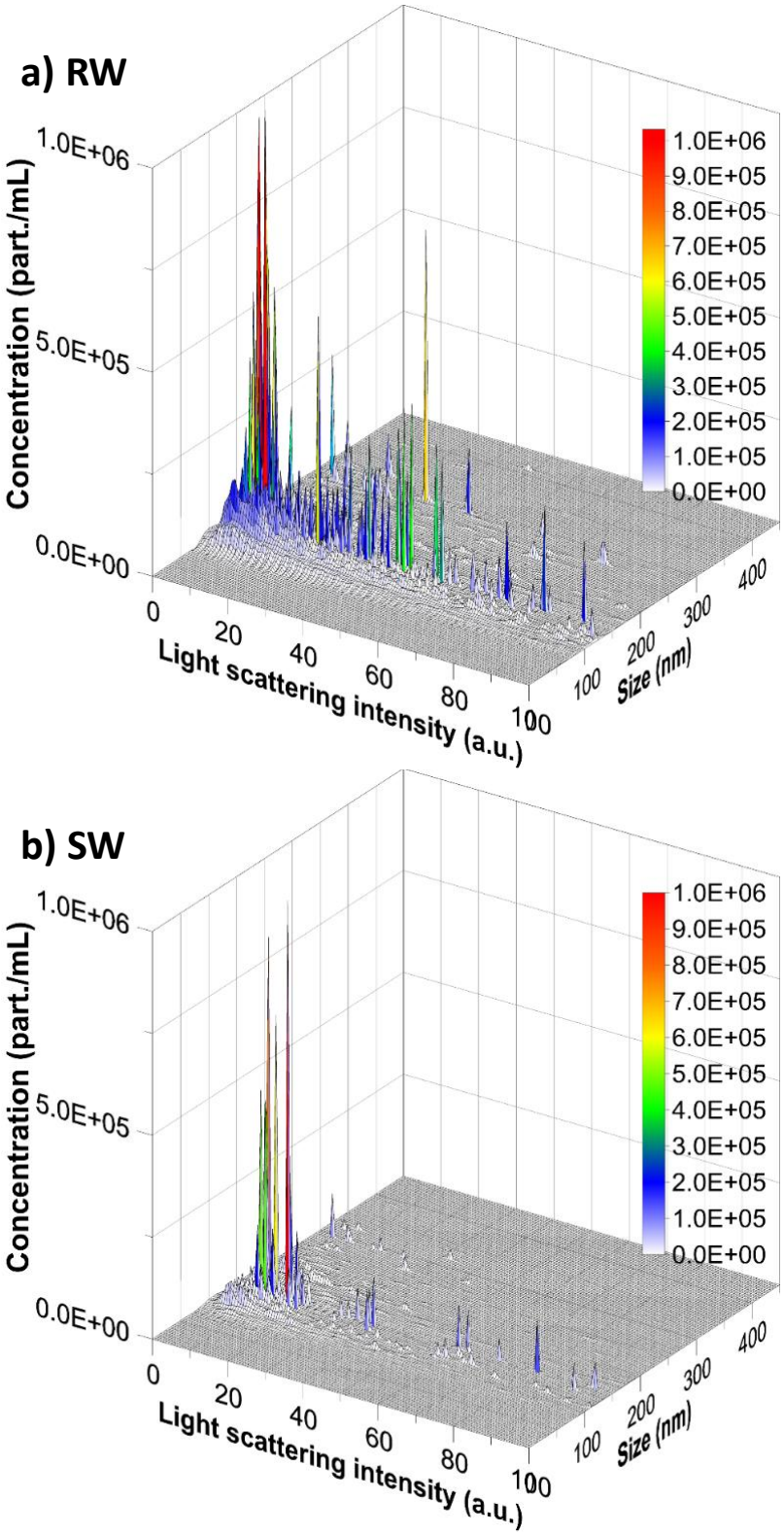

Figure VI-4 – Distribution of (nano)particles by size (nm), light scattering intensity (a.u.) and concentration (part. mL^{-1}) determined by NTA in **a)** rainwater leachates (RW, dilution 1:5) and **b)** seawater leachates (SW, dilution 1:10). Plots present the average of five replicate analysis.

that the average size of most of the particles (96 wt %) was close to 100 nm and particles having an average size of approximately 260 nm were also present in a small amount (4 wt %). Moreover, Pt was only determined in the nanoparticle's portion of one road dust, most likely due to insufficient concentration and sensitivity of the instrumental method of analysis (Ermolin et al. 2017).

6.4. Conclusions

The results here reported shed further light on Pt and Rh speciation analysis and their potential mobility in aquatic systems. An innovative combination of complementary analytical strategies distinguished different forms of Pt and Rh in urban road dust leachates (filtered <0.45 µm solutions). Truly dissolved species measured together with (nano)particles using ICP-MS can be discriminated employing AdCSV, which only determines the truly dissolved fraction. Non-dissolved species of Pt predominated over the dissolved forms, whereas for Rh truly dissolved species were an important fraction of the total content released by ACC.

While truly dissolved Pt and Rh remained constant during the experimental period, the (nano)particulate fraction in the leachates varied depending on the medium. This was more evident for Pt, for which longer exposure times in seawater led to an increase of total Pt concentration as opposed to the lower concentrations observed in rainwater. Such variations are most likely to reflect the behavior of (nano)particles in a complex environment rather than the effects of pH or ionic strength *per se*. The use of NTA confirmed the existence of (nano)particles in the leachates, in agreement with ICP-MS results that showed a higher proportion of Pt (nano)particles in seawater leachates.

The combination of AdCSV and ICP-MS for speciation analysis can be extended to other elements, namely to the other PGE, as long as an enough sensitive voltammetric procedure exits for their determination at relevant environmental concentrations. Palladium is also an important active component in ACC having relatively high mobility. However, the lack of Pd suitable voltammetric analytical determination hampered so far a speciation analysis in aquatic media such as demonstrated for Pt and Rh in this work.

References

Abdou, M., Schäfer, J., Cobelo-García, A., Neira, P., Petit, J. C. J., Auger, D., et al. (2016). Past and present platinum contamination of a major European fluvial–estuarine system: Insights from river sediments and estuarine oysters. *Marine Chemistry*, *185*, 104–110. doi:https://doi.org/10.1016/j.marchem.2016.01.006

Ash, P. W., Boyd, D. A., Hyde, T. I., Keating, J. L., Randlshofer, G., Rothenbacher, K., et al. (2014). Local Structure and Speciation of Platinum in Fresh and Road-Aged North American Sourced Vehicle Emissions Catalysts: An X-ray Absorption Spectroscopic Study. *Environmental Science & Technology*, *48*(7), 3658–3665. doi:10.1021/es404974e

Auffan, M., Rose, J., Bottero, J.-Y., Lowry, G. V, Jolivet, J.-P., & Wiesner, M. R. (2009). Towards a definition of inorganic nanoparticles from an environmental, health and safety perspective. *Nature Nanotechnology*, *4*(10), 634–641. doi:10.1038/nnano.2009.242

Bielmyer, G. K., Arnold, W. R., Tomasso, J. R., Isely, J. J., & Klaine, S. J. (2012). Effects of roof and rainwater characteristics on copper concentrations in roof runoff. *Environmental Monitoring and Assessment*, *184*(5), 2797–2804. doi:10.1007/s10661-011-2152-1

Braunschweig, F., Martins, F., Chambel, P., & Neves, R. (2003). A methodology to estimate renewal time scales in estuaries: the Tagus Estuary case. *Ocean Dynamics*, *53*(3), 137–145. doi:10.1007/s10236-003-0040-0

Brito, P., Prego, R., Mil-Homens, M., Caçador, I., & Caetano, M. (2018). Sources and distribution of yttrium and rare earth elements in surface sediments from Tagus estuary, Portugal. *Science of The Total Environment*, *621*, 317–325. doi:https://doi.org/10.1016/j.scitotenv.2017.11.245

Burden, F. R., Foerstner, U., McKelvie, I. D., & Guenther, A. (2002). *Environmental Monitoring Handbook*. New York: McGraw-Hill Education. doi:ISBN: 9780071351768

Chellam, S., & Bozlaker, A. (2015). Characterization of PGEs and Other Elements in Road Dusts and Airborne Particles in Houston, Texas BT - Platinum Metals in the Environment. In F. Zereini & C. L. S. Wiseman (Eds.), (pp. 199–242). Berlin, Heidelberg: Springer Berlin Heidelberg. doi:10.1007/978-3-662-44559-4_14

Cobelo-García, A., López-Sánchez, D. E., Almécija, C., & Santos-Echeandía, J. (2013). Behavior of platinum during estuarine mixing (Pontevedra Ria, NW Iberian Peninsula). *Marine Chemistry*, *150*, 11–18. doi:10.1016/j.marchem.2013.01.005

Cobelo-García, A., López-Sánchez, D. E., Schäfer, J., Petit, J. C. J., Blanc, G., & Turner, A. (2014). Behavior and fluxes of Pt in the macrotidal Gironde Estuary (SW France). *Marine Chemistry*, *167*, 93–101. doi:10.1016/j.marchem.2014.07.006

Dahlheimer, S. R., Neal, C. R., & Fein, J. B. (2007). Potential Mobilization of Platinum-Group Elements by Siderophores in Surface Environments. *Environmental Science & Technology*, *41*(3), 870–875. doi:10.1021/es0614666

Domingos, R. F., Baalousha, M. A., Ju-Nam, Y., Reid, M. M., Tufenkji, N., Lead, J. R., et al. (2009). Characterizing Manufactured Nanoparticles in the Environment:

Multimethod Determination of Particle Sizes. *Environmental Science & Technology*, *43*(19), 7277–7284. doi:10.1021/es900249m

Ek, K. H., Morrison, G. M., & Rauch, S. (2004). Environmental routes for platinum group elements to biological materials--a review. *The Science of the total environment*, *334–335*, 21–38. doi:10.1016/j.scitotenv.2004.04.027

Ely, J. C., Neal, C. R., Kulpa, C. F., Schneegurt, M. A., Seidler, J. A., & Jain, J. C. (2001). Implications of Platinum-Group Element Accumulation along U.S. Roads from Catalytic-Converter Attrition. *Environmental Science & Technology*, *35*(19), 3816–3822. doi:10.1021/es001989s

Ermolin, M. S., Fedotov, P. S., Ivaneev, A. I., Karandashev, V. K., Fedyunina, N. N., & Eskina, V. V. (2017). Isolation and quantitative analysis of road dust nanoparticles. *Journal of Analytical Chemistry*, *72*(5), 520–532. doi:10.1134/S1061934817050057

Essumang, D. K., Dodoo, D. K., & Adokoh, C. K. (2008). The impact of vehicular fallout on the Pra estuary of Ghana (a case study of the impact of platinum group metals (PGMs) on the marine ecosystem). *Environmental Monitoring and Assessment*, *145*(1), 283–294. doi:10.1007/s10661-007-0037-0

European Comission. (2002). *EUR 20307 - The certification of the contents (mass fractions) of Palladium, Platinum and Rhodium in road dust, BCR-723. Office for Official Publications of the European Comission*. Luxembourg.

Folens, K., Van Acker, T., Bolea-Fernandez, E., Cornelis, G., Vanhaecke, F., Du Laing, G., & Rauch, S. (2018). Identification of platinum nanoparticles in road dust leachate by single particle inductively coupled plasma-mass spectrometry. *Science of The Total Environment*, *615*, 849–856. doi:https://doi.org/10.1016/j.scitotenv.2017.09.285

Fröhlich, E., & Roblegg, E. (2012). Models for oral uptake of nanoparticles in consumer products. *Toxicology*, *291*(1), 10–17. doi:https://doi.org/10.1016/j.tox.2011.11.004

Gunawardana, C., Goonetilleke, A., Egodawatta, P., Dawes, L., & Kokot, S. (2012). Source characterisation of road dust based on chemical and mineralogical composition. *Chemosphere*, *87*(2), 163–170. doi:https://doi.org/10.1016/j.chemosphere.2011.12.012

Guo, L., & Santschi, P. H. (2006, December 15). Ultrafiltration and its Applications to Sampling and Characterisation of Aquatic Colloids. *Environmental Colloids and Particles*. doi:doi:10.1002/9780470024539.ch4

Jarvis, K. E., Parry, S. J., & Piper, J. M. (2001). Temporal and Spatial Studies of Autocatalyst-Derived Platinum, Rhodium, and Palladium and Selected Vehicle-Derived Trace Elements in the Environment. *Environmental Science & Technology*, *35*(6), 1031–1036. doi:10.1021/es0001512

Jones-Lepp, T., Rogers, K., & Snell, K. (2011). *Laser detection of nanoparticles in the environment. APM 31*. U.S. Environmental Protection Agency, Washington, DC, EPA/600/R-11/097,.

Kester, D. R., Duedall, I. W., Connors, D. N., & Pytkowicz, R. M. (1967). Preparation of Artificial Seawater. *Limnology and Oceanography*, *12*(1), 176–179. doi:10.4319/lo.1967.12.1.0176

Leśniewska, B. A., Godlewska-Żyłkiewicz, B., Bocca, B., Caimi, S., Caroli, S., & Hulanicki, A. (2004). Platinum, palladium and rhodium content in road dust, tunnel dust and common grass in Białystok area (Poland): a pilot study. *Science of The Total Environment*, *321*(1), 93–104. doi:https://doi.org/10.1016/j.scitotenv.2003.07.004

Liu, Y., Tian, F., Liu, C., & Zhang, L. (2015). Platinum group elements in the precipitation of the dry region of Xinjiang and factors affecting their deposition to land: the case of Changii City, China. *Atmospheric Pollution Research*, *6*(2), 178–183. doi:https://doi.org/10.5094/APR.2015.021

López-Sánchez, D. E., Cobelo-García, A., Rijkenberg, M. J. A., Gerringa, L. J. A., & de Baar, H. J. W. (2019). New insights on the dissolved platinum behavior in the Atlantic Ocean. *Chemical Geology*, *511*, 204–211. doi:https://doi.org/10.1016/j.chemgeo.2019.01.003

Loring, D. H., & Rantala, R. T. T. (1992). Manual for the geochemical analyses of marine sediments and suspended particulate matter. *Earth-Science Reviews*, *32*(4), 235–283. doi:https://doi.org/10.1016/0012-8252(92)90001-A

Lyubomirova, V., & Djingova, R. (2015). Accumulation and Distribution of Pt and Pd in Roadside Dust, Soil and Vegetation in Bulgaria BT - Platinum Metals in the Environment. In F. Zereini & C. L. S. Wiseman (Eds.), (pp. 243–255). Berlin, Heidelberg: Springer Berlin Heidelberg. doi:10.1007/978-3-662-44559-4_15

Mathur, R., Balaram, V., Satyanarayanan, M., Sawant, S. S., & Ramesh, S. L. (2011). Anthropogenic platinum, palladium and rhodium concentrations in road dusts from Hyderabad city, India. *Environmental Earth Sciences*, *62*(5), 1085–1098. doi:10.1007/s12665-010-0597-0

Moldovan, M., Palacios, M. A., Gómez, M. M., Morrison, G., Rauch, S., McLeod, C., et al. (2002). Environmental risk of particulate and soluble platinum group elements released from gasoline and diesel engine catalytic converters. *Science of The Total Environment*, *296*(1), 199–208. doi:https://doi.org/10.1016/S0048-9697(02)00087-6

Monteiro, C. E., Cobelo-García, A., Caetano, M., & Santos, M. M. C. dos. (2017). Improved voltammetric method for simultaneous determination of Pt and Rh using second derivative signal transformation – application to environmental samples. *Talanta*. doi:10.1016/j.talanta.2017.06.067

Monteiro, C. E., Correia dos Santos, M., Cobelo-García, A., Brito, P., & Caetano, M. (2019). Platinum and rhodium in Tagus estuary, SW Europe: sources and spatial distribution. *Environmental Monitoring and Assessment*, *191*(9), 579. doi:10.1007/s10661-019-7738-z

Perry, B. J., Barefoot, R. R., & Van Loon, J. C. (1995). Inductively coupled plasma mass spectrometry for the determination of platinum group elements and gold. *TrAC Trends in Analytical Chemistry*, *14*(8), 388–397. doi:https://doi.org/10.1016/0165-9936(95)90917-C

Peucker-Ehrenbrink, B., & Jahn, B. (2001). Rhenium-osmium isotope systematics and platinum group element concentrations: Loess and the upper continental crust. *Geochemistry, Geophysics, Geosystems*, *2*(10), n/a-n/a.

doi:10.1029/2001GC000172

Prichard, H. M., & Fisher, P. C. (2012). Identification of Platinum and Palladium Particles Emitted from Vehicles and Dispersed into the Surface Environment. *Environmental Science & Technology*, *46*(6), 3149–3154. doi:10.1021/es203666h

Provenzano, M. R., Caricasole, P., Brunetti, G., & Senesi, N. (2010). Dissolved Organic Matter Extracted With Water and a Saline Solution From Different Soil Profiles. *Soil Science*, *175*(6).

Rauch, S., Morrison, G. M., & Moldovan, M. (2002). Scanning laser ablation-ICP-MS tracking of platinum group elements in urban particles. *Science of The Total Environment*, *286*(1), 243–251. doi:https://doi.org/10.1016/S0048-9697(01)00988-3

Rauch, S., & Peucker-Ehrenbrink, B. (2015). Sources of platinum group elements in the environment. In *Platinum metals in the environment* (pp. 3–17). Springer.

Rennert, T., Gockel, K. F., & Mansfeldt, T. (2007). Extraction of water-soluble organic matter from mineral horizons of forest soils. *Journal of Plant Nutrition and Soil Science*, *170*(4), 514–521. doi:10.1002/jpln.200625099

Rieuwerts, J. S., Thornton, I., Farago, M. E., & Ashmore, M. R. (1998). Factors influencing metal bioavailability in soils: Preliminary investigations for the development of a critical loads approach for metals. *Chemical Speciation and Bioavailability*, *10*(2), 61–75. doi:10.3184/095422998782775835

Sarkar, A. (2017). Novel platinum compounds and nanoparticles as anticancer agents. *Pharmaceutical Patent Analyst*, *7*(1), 33–46. doi:10.4155/ppa-2017-0036

Šebek, O., Mihaljevič, M., Strnad, L., Ettler, V., Ježek, J., Štědrý, R., et al. (2011). Dissolution kinetics of Pd and Pt from automobile catalysts by naturally occurring complexing agents. *Journal of Hazardous Materials*, *198*, 331–339. doi:https://doi.org/10.1016/j.jhazmat.2011.10.051

Sures, B., Ruchter, N., & Zimmermann, S. (2015). Biological Effects of PGE on Aquatic Organisms BT - Platinum Metals in the Environment. In F. Zereini & C. L. S. Wiseman (Eds.), (pp. 383–399). Berlin, Heidelberg: Springer Berlin Heidelberg. doi:10.1007/978-3-662-44559-4_24

Taylor, S. R., & McLennan, S. M. (1995). The geochemical evolution of the continental crust. *Reviews of Geophysics*, *33*(2), 241–265. doi:10.1029/95RG00262

Wilkinson, K. J., Lead, J. R., & Eds. (2006). *Environmental Colloids and Particles: Behaviour, Separation and Characterisation, Volume 10*. *Environmental Colloids and Particles: Behaviour, Separation and Characterisation* (1st ed.). Chichester, UK: John Wiley & Sons, Ltd. doi:ISBN: 9780470024539

Zereini, F., & Wiseman, C. L. S. (2015). *Platinum Metals in the Environment*. (F. Zereini & C. L. S. Wiseman, Eds.). Berlin, Heidelberg: Springer Berlin Heidelberg. doi:10.1007/978-3-662-44559-4

Zhong, L., Yan, W., Li, J., Tu, X., Liu, B., & Xia, Z. (2012). Pt and Pd in sediments from the Pearl River Estuary, South China: background levels, distribution, and source. *Environmental Science and Pollution Research*, *19*(4), 1305–1314. doi:10.1007/s11356-011-0653-7

Zimmermann, S., Menzel, C. M., Stüben, D., Taraschewski, H., & Sures, B. (2003). Lipid solubility of the platinum group metals Pt, Pd and Rh in dependence on the presence of complexing agents. *Environmental Pollution*, *124*(1), 1–5. doi:https://doi.org/10.1016/S0269-7491(02)00428-1

Zischka, M., Schramel, P., Muntau, H., Rehnert, A., Gomez Gomez, M., Stojanik, B., et al. (2002). A new certified reference material for the quality control of palladium, platinum and rhodium in road dust, BCR-723. *TrAC Trends in Analytical Chemistry*, *21*(12), 851–868. doi:https://doi.org/10.1016/S0165-9936(02)01207-4

VII. DRIVERS OF PT AND RH VARIABILITY IN THE WATER COLUMN OF A HYDRODYNAMIC ESTUARY: EFFECTS OF CONTRASTING ENVIRONMENTS

in preparation: **C. E. Monteiro, A. Cobelo-García, M. Correia dos Santos and M. Caetano. Drivers of Pt and Rh variability in the water column of a hydrodynamic estuary: effects of contrasting environments.**

Graphical Abstract

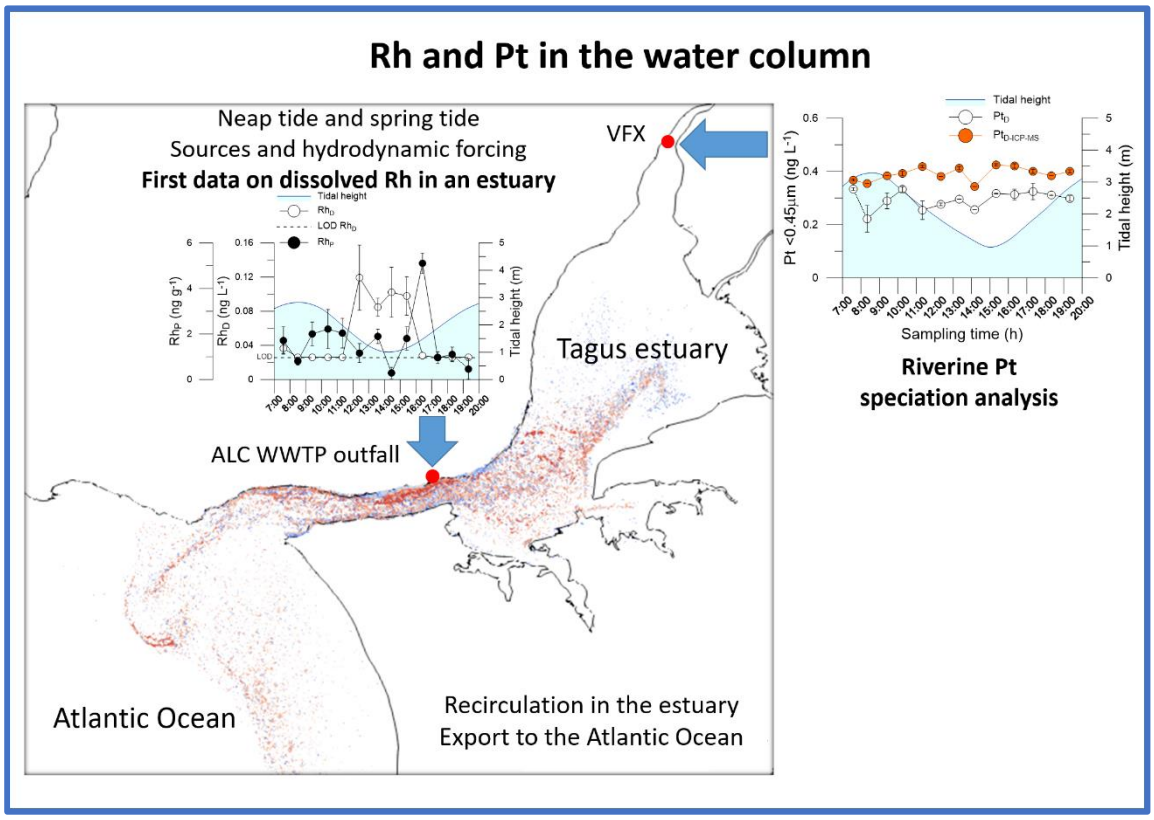

Abstract

Particulate and dissolved platinum (Pt_P and Pt_D, respectively) and rhodium (Rh_P and Rh_D, respectively) were determined in the water column of Tagus estuary in two stations (≈35 km apart): the upstream riverine end-member (VFX) and at the vicinity of an outfall from a wastewater treatment plant (ALC) near the estuary mouth. Samples were collected during neap tide (NT) and spring tide (ST) over a semi-diurnal cycle and analyzed for both elements using adsorptive cathodic stripping voltammetry. Additionally, in VFX NT cycle, Pt in the dissolved fraction (<0.45 µm) was determined by inductively coupled plasma-mass spectrometry ($Pt_{D\text{-}ICP\text{-}MS}$). Temperature, conductivity, pH, and dissolved oxygen were measured *in situ* and suspended particulate matter was also quantified. The simultaneous determination of Rh_P and Rh_D in the water column of a hydrodynamic estuary is reported for the first time.

Both Pt and Rh followed the hydrodynamic regime, in general presenting higher concentrations during low tide. Concentrations of Pt_P (1.0–25.6 ng g^{-1}) and Pt_D (0.1–11.7 ng L^{-1}) were higher than Rh_P (0.1–5.1 ng g^{-1}) and Rh_D (0.03–0.12 ng L^{-1}), respectively, and both fractions of Pt were higher at ALC than in VFX. Higher Rh_P concentrations were also determined in ALC but the dissolved fractions were similar in both stations. These results mirrored the different anthropogenic inputs to the Tagus estuary, attributed to automotive catalytic converters. An additional source of Pt with origin in Pt-based compounds was found at ALC station. Platinum appeared to have non-conservative behaviour due to the higher inputs than Rh. Distribution coefficients (K_D) of about 10^4 were computed for Pt and Rh and were independent of the salinity gradient.

In VFX NT survey, total Pt concentrations in the water column, ^{T}Pt (ng L^{-1}), were computed as the sum of Pt_P expressed in ng L^{-1} and $Pt_{D\text{-}ICP\text{-}MS}$. Speciation analysis showed that truly dissolved forms represented 39±9 % of ^{T}Pt in the water column, while total filter-passing species were higher, 65±14 %. The higher concentrations also found for Pt_D in ALC as compared to VFX suggest that speciation in the water column is controlled by the dissolved forms. For Rh, particulate forms represented an important proportion of the bulk value in the water column (>65 %).

Potential exchanges of Pt and Rh were also observed at the downstream station, presenting higher metal concentrations associated with the ebb opposing to the flood. The modelled Lagrangian spread of particles also pointed out that recirculation within the

estuary takes place and the export towards the Atlantic Ocean can occur within 2 days. Ultimately, the obtained results showed that estuaries are an important pathway to introduce PGE in the coastal region, transferring them towards the ocean.

Keywords

Platinum; Rhodium; Estuary water column; Particle-water interactions; Speciation analysis; Hydrodynamic spread

7.1. Introduction

Platinum-group elements (PGE) such as Pt and Rh have steadily increased in the environment over the past years despite their low abundance in Earth's crust (<0.5 ng g^{-1}; Peucker-Ehrenbrink and Jahn 2001; Taylor and McLennan 1995). Their concentrations in the environment derive from natural weathering and leaching of parent rocks containing PGE or from anthropogenic sources. The main anthropogenic sources of Pt and Rh originate in industrial catalysts and in the exhaust fumes of automotive catalytic converters (ACC) that release Pt and Rh into the environment. Moreover, Pt has also medicinal uses, namely in anticancer drugs owing to its ability to easily destroy cells (Ek et al. 2004; Pawlak et al. 2014; Ravindra et al. 2004). The rising use of Pt and Rh led to an increase of their concentrations in different environmental compartments. Anthropogenic emissions released in urban environments have impacts in aquatic systems (e.g. Ek et al. 2004; Monteiro et al. 2019), which consequentially reflect their mobility and transport from the continental urban areas to the nearby aquatic systems. In general, concentrations of Pt and Rh in estuaries (Cobelo-García et al. 2011, 2013, 2014; Monteiro et al. 2019) have been reported to be higher than in coastal areas (Abdou et al. 2020; Mashio et al. 2017; Obata et al. 2006) or the open ocean (Colodner 1991; López-Sánchez et al. 2019). Relatively high signatures of Pt have been found in several matrices, namely in sediments (Cobelo-García et al. 2013, 2014; Monteiro et al. 2019; Zhong et al. 2012) and suspended particulate matter (SPM; Abdou et al. 2020; Cobelo-García et al. 2013, 2014). The same has been found for Rh in sediments (Almécija et al. 2016; Essumang et al. 2008; Monteiro et al. 2019). Dissolved Pt has also been reported in the water column (Cobelo-García et al. 2013, 2014; López-Sánchez et al. 2019; Mashio et al. 2016; Obata et al. 2006; Suzuki et al. 2014), however, literature remains very limited about dissolved Rh concentrations in the aquatic environment (Bertine et al. 1993) and in wastewaters as well (Monteiro et al. 2017). Therefore, their occurrence, distribution, mobility and partitioning in the water column, as well as their fate and potential hazardousness to biota in estuarine and marine environments, remain dimly elucidated.

Limited information exists about the speciation of Pt and particularly Rh in aquatic media. Regarding the dissolved forms, it has been suggested that Pt(II) predominates in freshwaters, as $Pt(OH)_2$, while Pt(IV) dominates in seawater as $PtCl_5(OH)^{2-}$ (Cobelo-García et al. 2013, 2014; Mashio et al. 2017). As to Rh, its inorganic speciation appears to be dominated by aquo-hydroxo, aquo-chloro and mixed aquo-hydroxo-chloro

complexes (Bertine et al. 1996; Cobelo-García et al. 2008), with affinity to the organic matter (Turner et al. 2006). Simultaneously, there is a need for suitable techniques, adequately sensitive and selective to deal with the ultra-trace concentrations and their species, necessary to understand Pt and Rh speciation. Speciation analysis schemes discriminate between particulate and dissolved fractions in aquatic environments (Burden et al. 2002). A problem may arise from the different cut-off used in the separation of both fractions, i.e. there is not consensual use on the filter' mesh during water sampling. Either 0.2 μm filters (e.g. Cobelo-García et al. 2013, 2014) or 0.45 μm filters (e.g. Mashio et al. 2016) are currently used, which enhances the difficulty of comparing data sets. The operationally dissolved fraction *per se* (<0.45 μm) includes species such as colloids, with sizes varying from 1 to 1000 nm (Wilkinson and Lead 2006), and nanoparticles as well (<100 nm; Auffan et al. 2009), whose mobility and bioavailability may be different from truly dissolved species (Guo and Santschi 2006; Monteiro et al. 2020). Recently, speciation analysis has been performed in urban matrices such as road dusts (Folens et al. 2018) and their leachates under environmentally relevant conditions (Monteiro et al. 2020). The discrimination of soluble/insoluble species in real samples is a challenging task but can be overcome by combining different analytical techniques (Monteiro et al. 2020). Yet, further investigation is needed to increase the understanding on biogeochemical processes of Pt and Rh forms in waters.

Estuaries have improved their water quality in the past years due to regulatory demands. However, many potentially hazardous chemicals continue to be found in watercourses. Regarding Pt and Rh, environmental concerns arise due to the occurrence of different forms emitted into the environment, either soluble or (nano)particulate. Additionally, the estuarine hydrodynamic effects on the spread and environmental fate of Pt and Rh is poorly documented. Thus, this chapter aimed (1) to evaluate Pt and Rh physicochemical interactions and behaviour in the water column of a hydrodynamic estuary considering a salinity gradient. For that reason, and anticipating the forthcoming increase of Pt and Rh concentrations in water bodies, it also aimed (2) to quantify dissolved and particulate Pt and Rh in (a) the freshwater end-member of Tagus estuary and (b) in the receptor medium of a wastewater treatment plant (WWTP) effluent in the lower Tagus estuary (high salinity). In addition, (3) potential exchanges of Pt and Rh between the estuary and the Atlantic Ocean were also investigated. Consequently, dissolved (<0.45 μm) and particulate (>0.45 μm) Pt and Rh concentrations were evaluated

in the water column of two distinct locations of the Tagus estuary over semi-diurnal tidal cycles, at neap and spring tides, and potential exchanges with the adjacent coastal area were assessed.

7.2. Material and Methods

7.2.1. Description of the Study Area and Sampling Stations

The Tagus estuary is one of the largest estuaries in SW Europe dominated by tidal oscillations, having an area of *ca.* 320 km^2, which about 40 % are intertidal areas comprising mudflats and islands (Fortunato et al. 1999; Guerreiro et al. 2015; Vale and Sundby 1987). Succinctly, a narrow single-channel marks the northward entrance of the Tagus River that opens to the shallow bay through a set of smaller channels. The bay has a complex bottom topography with channels that funnel towards a long, narrow and deep inlet, connecting the Tagus estuary to the Atlantic Ocean (Figure VII-1) (Vale and Sundby 1987). The Tagus River is the longest river in the Iberian Peninsula and the main source of freshwater to the estuary, on average 350 $m^3 s^{-1}$. Freshwater runoff from the Tagus shows high inter-annual variation according to the season, with river discharges between 50 and 2000 $m^3 s^{-1}$. Other small tributaries exist but only represent a minor contribution of freshwater, on average <50 $m^3 s^{-1}$ (Fortunato et al. 1999; Guerreiro et al. 2015; Vale and Sundby 1987). Salinity variations in the estuary depend on the input of freshwater, thus, the main drive controlling the mixing process is the tide. Considering that the tidal prism inside the Tagus estuary is 640×10^6 m^3, the river flow is only relevant to the non-linear mixing during high river flow events (de Pablo et al. 2019). The tidal regime of the Tagus estuary is mainly semi-diurnal, ranging from 0.8 m (neap tide) to 4.0 m (spring tide), which may increase towards the estuary's interior due to resonance effects (Fortunato et al. 1997; Neves 2010). The tidal wave is asymmetric and progressive, causing delays up to two hours between the estuary mouth (Lisbon) and upstream locations (Vila Franca de Xira) (Neves 2010; Vale and Sundby 1987). Typically, ebbs are shorter than floods (Fortunato et al. 1999; Guerreiro et al. 2015; Vaz and Dias 2014), which mirrors the stronger current velocities during ebbs (Vaz and Dias 2014). Currents near the surface can be higher than 1.5 m s^{-1} during spring tides in the lower estuary inlet (Neves 2010). However, for this area of the estuary, different flow circulation patterns between ebb- and flooding conditions have been proposed based on numerical

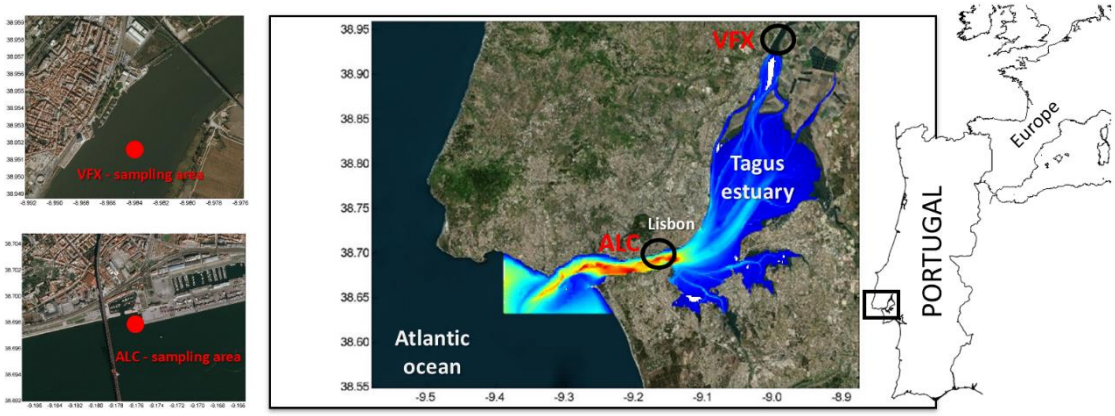

Figure VII-1 – Location of the sampling stations in the Tagus estuary, SW Europe. Imagery produced using MIRONE© software (Luis 2007) and bathymetric data obtained from the Portuguese Hydrographic Institute (http://www.hidrografico.pt).

simulations (Fortunato et al. 1997), which may act as potential barriers on the exchanges between the estuary and the ocean. Residence times within the Tagus estuary vary according to location and are influenced by the seasonal variability of the river runoff, ranging between <10 days in the inlet channel and >20 days in the shallow bay (Braunschweig et al. 2003).

Several anthropogenic pressures affect both margins of the Tagus estuary. Industries and dense population sprawl (*ca*. 3 M, Marques da Costa 2016) are the main contributors of Pt and Rh to the estuary. While industrial activities in the Tagus margins are confined to specific areas, the relevant urban sources of Pt and Rh for the two areas investigated in this study are the emissions from ACC and Pt-based anticancer drugs. The influence of the first source was documented previously in Monteiro et al. (2019), while the latter remains poorly understood.

The two sampling areas are ~35 km distant one from another and present different characteristics (Figure VII-1). The upstream sampling station (VFX; 38º57'4.49" N; 8º59'5.48" W; Figure VII-1) is located near the entrance of the estuary. This region is less populated, served by a low dimension WWTP and is crossed by a bridge. Freshwater is the main source of water in this site but an increase in salinity is observed due to tidal influence mainly during the high tides of spring tides. In opposition, the downstream sampling station (ALC; 38º41'53.9" N; 9º10'33.5" W; Figure VII-1) is located at the vicinity of a WWTP outfall, closer to the estuary mouth and therefore near the Atlantic

Ocean. Thus, estuarine waters in this station present higher salinity. This WWTP is one of the largest in Portugal and receives waste- and drainage waters from three municipalities in the Lisbon region that serves near 1 M persons (Marques da Costa 2016). The drainage includes domestic and hospital effluents that may contain Pt-based compounds used in cancer treatments and pluvial runoff that may have Pt and Rh from ACC, washed from roadside deposits. In addition, a high traffic impacted bridge crosses the inlet, where *ca*. 150,000 vehicles pass every day (IMT 2016).

7.2.2. Field Campaigns, Sampling and *In Situ* Measurements

Two surveys were carried out at each sampling station, during neap tide (NT, 31st of May and 1st June, 2017) and spring tide (ST, 7th and 8th of September, 2017). The campaigns covered semi-diurnal tidal cycles (12.5 h). Collection of water samples was done on-board of a semi-rigid vessel on an hourly basis. At VFX station two depths were considered in the water collection. The surface sample was collected at ~0.5 m depth and the bottom sample was collected ~0.5 m above the riverbed. Due to shallowness of the water column at ALC station (<3 m) over the tidal cycling, water was sampled only at an intermediate depth. Collection of water samples was performed using a 5 L horizontal Niskin bottle and stored in acid-washed 2.5 L PP bottles until filtration. Additional parameters, namely temperature (ºC), conductivity (mS cm^{-1}), pH, dissolved oxygen (DO) concentration (mg L^{-1}) and saturation (%DO), were measured *in situ* using a portable multi-parametric probe (YSI 600 QS) coupled to previously calibrated electrodes.

7.2.3. Analytical Procedures

All laboratory procedures were executed in acclimatized conditions using previously acid-cleaned material by immersion in ~20% both nitric acid (HNO_3) and hydrochloric acid (HCl) baths, for 48 h each. The necessary reagents for sample's digestion and analysis were of high-purity grade. All solutions were prepared with ultra-pure water from a Milli-Q (Millipore) purification system (conductivity of 18.2 MΩ.cm).

Water samples were filtered within the same day of collection using acid-washed filtration kits coupled to kitasato flasks under low-pressure vacuum. Beforehand weighted polycarbonate membrane filters (0.45 µm; Whatman Nuclepore) were used in the separation of particulate and dissolved phases.

As to the particulate fraction of the metals (Pt_P and Rh_P) and suspended particulate matter (SPM, mg L^{-1}), triplicate samples were obtained and kept in the freezer until analysis. Then, filters were dried in an oven at 40 ºC until constant weight. The SPM was calculated by the difference of dry weight (dw) and corrected for the filtered volume. Then, the filters were acid-digested for the Pt_P and Rh_P determinations. Succinctly, after combustion by means of a temperature ramp-up to 800 ºC in a muffle furnace (Nygren et al. 1990), samples were transferred to PFA flasks and digested in 4 mL *aqua regia* for 4 h at 195 ºC in a hot plate. After evaporating the acids, residues were re-dissolved in 1 mL H_2SO_4 until constant volume and diluted to 25 mL in 0.1 M HCl.

For the dissolved Pt and Rh concentrations (Pt_D and Rh_D, respectively), filtrates were immediately acidified with HCl 30 % to pH <2 and preserved cold in the dark. Prior to the analysis of Pt_D and Rh_D, filtered samples were UV-digested in quartz tubes, adding small volumes of H_2O_2 to facilitate the organic matter mineralization and then irradiated for 3 h (Cobelo-García et al. 2013; Monteiro et al. 2020). All procedure was done in triplicate, at least.

The determination of Pt and Rh was carried out in an acclimatized room at 25 ± 2 ºC by adsorptive cathodic stripping voltammetry (AdCSV) following the procedure optimized in Monteiro et al. (2017). Briefly, a potentiostat/galvanostat from ECO Chemie, Autolab PGSTAT 128N (Metrohm), was used for the voltammetric measurements connected to the Metrohm Stand 663. A Static Mercury Drop Electrode (SMDE) was used as the working electrode, an $Ag/AgCl/KCl_{(sat)}$ as the reference electrode (placed inside a salt bridge with 3 M KCl) and a carbon rod was the auxiliary electrode. The GPES v4.9 software (EchoChemie) was used to control the entire system and to analyse data. All measurements were done at least in triplicate using the standard addition method (Monteiro et al. 2017).

The samples of VFX corresponding to the neap tide cycle, filtered <0.45 µm and acidified, were also analysed by inductively coupled plasma–mass spectrometry (ICP-MS, Agilent 7900 equipment) for total concentrations of Pt and Rh in the filtrates

($Pt_{D\text{-}ICP\text{-}MS}$ and $Rh_{D\text{-}ICP\text{-}MS}$). Interferences of Hf ($^{179}Hf^{16}O^{+}$) on ^{195}Pt and Cu ($^{63}Cu^{40}Ar^{+}$), Pb ($^{206}Pb^{2+}$), Sr ($^{87}Sr^{16}O^{+}$), Rb ($^{87}Rb^{16}O^{+}$) and Zn ($^{67}Zn^{36}Ar^{+}$) on ^{103}Rh were monitored and mathematically corrected for each sample using interference ratios derived from single-metal solutions. It was observed that the Hf interference on Pt signal was negligible (<0.1 %). The relative standard deviation of repeated measurements for Pt was in general <10 %. However, interferences were significant for Rh and thus $Rh_{D\text{-}ICP\text{-}MS}$ could not be determined.

Dissolved organic carbon (DOC, mg C L^{-1}) was also determined in VFX samples (<0.45 μm) of the neap tide cycle. Determinations were done by wet chemical oxidation with persulfate method using an OI Analytical TOC Analyzer.

7.2.4. Quality Control of the Analytical Procedures

Blanks and certified reference material (CRM BCR-723) were used to control the quality of all analytical procedures. In addition, due to lack of CRM for Pt and Rh in waters, the accuracy of the analysis was checked by means of spiked samples (membrane filters and sampled waters) using known nominal concentrations of Pt and Rh. Briefly, mean recoveries were in general higher than 90 % and RSD below 15 %. The limits of detection (LOD) of AdCSV analysis obtained for the water samples using a deposition time of 300 s were 0.06 ng Pt L^{-1} and 0.03 ng Rh L^{-1}. For the total concentrations in the acid-digested solids, using deposition time of 120 s, LOD were 0.2 ng Pt L^{-1} and 0.1 ng Rh L^{-1}. No cross-contamination was observed. Furthermore, the LOD determined for Pt and Rh in the ICP-MS analysis was 0.05 ng L^{-1}.

7.2.5. Tidal Conditions and Current Velocity Data Acquisition

Tidal heights (m) and current velocities (m s^{-1}) at each station were obtained from the hydrodynamic model MOHID (Neves 1983). The three-dimensional (3D)-MOHID Water model was previously fully calibrated and validated for the Tagus estuary region of freshwater influence (de Pablo et al. 2019). Data measured *in situ* was used to calibrate the model for the days of field campaigns. The tidal heights were obtained from the tidal gauge located in the Tagus estuary (Lisbon harbour – LTG; 38.71ºN and –9.13ºW), provided by the Portuguese Hydrographic Institute. The current velocities were acquired

after forcing the model for the periods of interest and the components of current velocities were retrieved at each sampling site on an hourly basis.

7.2.6. Modelling of Pt and Rh Dispersion

An innovative Lagrangian-based approach was coupled to MOHID Water model and employed to trace estuarine and coastal dispersion of particles, which better maintains the physical meaning in tracking and identification of particle' locations through its trajectories (Suh 2006). With this method, each particle was considered as a passive tracer and statistical properties of trajectories may be assigned by the flow characteristics (Monti and Leuzzi 2010). In general, Lagrangian particle dispersion models use a number of pollutant particles that are released at the source location. Then, these passively follow the flow by integrating the particle's position vector in space and time using a velocity field obtained from the hydrodynamic model (Hegarty et al. 2013). Accordingly, the physical drivers acting on the distribution of Pt and Rh at ALC station during neap tide and spring tide were evaluated. This station was chosen due to the proximity to the Atlantic Ocean and potentially higher loadings of Pt and Rh to the estuary than the upstream station VFX. The model was forced over 3 weeks, which included the dates of the surveys, and assumed the continuous release of 20 spherical particles on an hourly basis. An additional assumption was the WWTP outflow in dry weather conditions, discharging ~1.8×10^5 m^3 d^{-1} of wastewater (www.aguasdotejoatlantico.adp.pt).

7.2.7. Statistical Analysis

Water variables and metals concentration were evaluated statistically using the software Statistica (v.12). Data were checked for outliers using Grubbs test and for normality using the Kolmogorov-Smirnov & Lilliefors tests. Since one or more variables failed to pass the latter (non-normal distribution) and because of the small sample size in each tidal cycle (n=13), subsequent analysis was carried out using non-parametric statistics. Differences in median values of the variables, between stations and tidal cycles (complete neap and spring tides), were assessed using Kruskal-Wallis (*H*) test, with post hoc test. Furthermore, at VFX station the same test was used to evaluate differences between surface and bottom layers of the water column. Spearman correlations (R_S) were

used for paired-wise multiple comparisons of variables. The minimum level of confidence used was 95 %. Principal component analysis (PCA) was applied to evaluate and discriminate which group of variables (principal components) explained the highest variance of the results. Additionally, PCA was also used to aid the interpretation of the relationships between variables (Miller and Miller 2010) on both tidal cycles and locations.

7.3. Results

7.3.1. Upstream Site: Vila Franca de Xira (VFX)

7.3.1.1. Physicochemical Characterization and Hydrographic Context

The physicochemical water properties of the surface and bottom layers of the water column at VFX site during the semi-diurnal tidal cycles, at neap tide (NT) and spring tide (ST), respectively, are presented in Figure VII-2. For both depths, temperature ranged from 22.2 to 24.3 ºC in NT and from 22.8 to 24.5 ºC in ST. The highest temperature values were observed during low tides, following an opposite trend to the other parameters. Conductivity varied from 0.4 to 4.7 mS cm^{-1} in NT and from 2.3 to 28.6 mS cm^{-1} in ST, with the highest values found in high tide and the lowest in low tide. The variations observed in the pH reflected as well the semi-diurnal tidal oscillation, in particular over ST cycle. The pH variation in both cycles was between 7.7 and 8.2 in general. An exceptional lower value (7.1) was found at the bottom layer during ST. The concentration of DO varied from 7.1 and 8.9 mg L^{-1} in NT and 7.7 and 8.8 mg L^{-1} in ST, reflecting also the tidal influence. This variability, in terms of %DO was between 86 to 110 % in both cycles, indicating that the waters were in general oxygenated. Concentrations of SPM ranged between 30 and 93 mg L^{-1} in NT and between 16 and 71 mg L^{-1} in ST. Three samples were excluded in the bottom layer during NT because bed resuspension was evident (outliers). Variations of SPM concentrations were more evident in NT compared to ST cycle. A slight increase in SPM was observed during the low tide period for both cycles and a few maximum values observed during high tide. The concentration of DOC (S.I. Figure S.VII 1) determined in NT ranged in a narrow interval between 3.0 and 4.0 mg C L^{-1} in both depths.

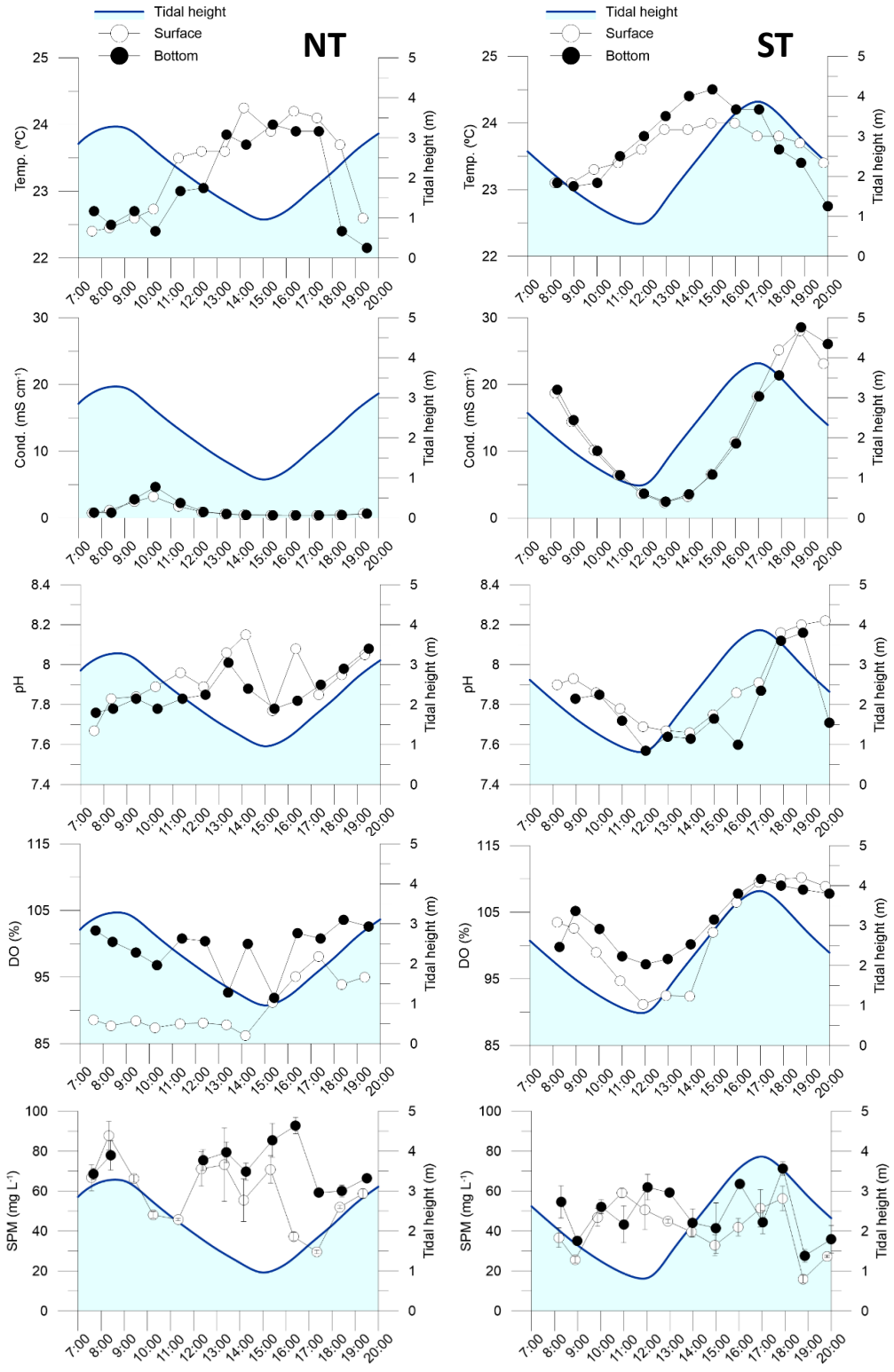

Figure VII-2 – Characteristics of the water at VFX station during neap tide (NT) and spring tide (ST) surveys: temperature (ºC), conductivity (mS cm^{-1}), pH, dissolved oxygen (expressed in percentage of saturation, DO%) and suspended particulate matter (SPM, mean±SD mg L^{-1}). Tidal height – blue line; surface – white circles; bottom – black circles.

In general, the variations observed in the water properties reflected the tidal semi-diurnal (high and low tides) and the fortnightly (NT and ST) oscillations, i.e. there was a trend in the parameters to increase during the flood and to decrease in the ebb tides. Minor variations observed between both depths reflected the mixture of the water column. Despite the tidal influence, no significant changes ($p>0.05$) were found between the two depths on each of the tidal cycles.

7.3.1.2. Variability of Pt and Rh Concentrations Over the Tidal Cycles

The concentrations of particulate Pt (Pt_P) and Rh (Rh_P) in surface and bottom layers of the water column, for both tidal cycles at VFX station, are shown in Figure VII-3. Concentrations of Pt_P varied between 1.0 and 11.3 ng Pt g^{-1} in NT and between 2.7 and 11.3 ng Pt g^{-1} in ST. Similarly, concentrations of Rh_P varied within one order of magnitude, between 0.1 and 2.0 ng Rh g^{-1} in NT and between 0.2 and 1.8 ng Rh g^{-1} in ST.

In both surveys, Pt_P concentrations were higher than Rh_P. The erratic variation for both Pt_P and Rh_P in the NT cycle was not observed in ST, where maximum concentrations were measured between 18:00 and 19:00 following the increase exhibited in conductivity and pH.

Dissolved metal concentrations measured by AdCSV, Pt_D and Rh_D , in surface and bottom layers of the water column for both tidal cycles at VFX station, are presented in Figure VII-4. Concentrations of Pt_D varied between 0.18 and 0.43 ng Pt L^{-1} in NT and between 0.12 and 0.73 ng Pt L^{-1} in ST. While in NT Pt_D was relatively constant, two increments were observed in ST cycle, at 12:00 and 16:00. The first peak was coincident with low tide while the second one occurred during the flood. As to Rh_D in NT, concentrations were below 0.03 ng Rh L^{-1} (LOD). The exception was observed in the bottom water, 0.05 ng Rh L^{-1}, between 9:00 and 10:00, which was closer to high tide. Contrastingly, Rh_D in ST increased almost one order of magnitude, between the LOD and 0.19 ng Rh L^{-1}. Increments of Rh_D were also found in the low tide, at 12:00, and during the flood period with the maximum value at 16:00, similarly to Pt.

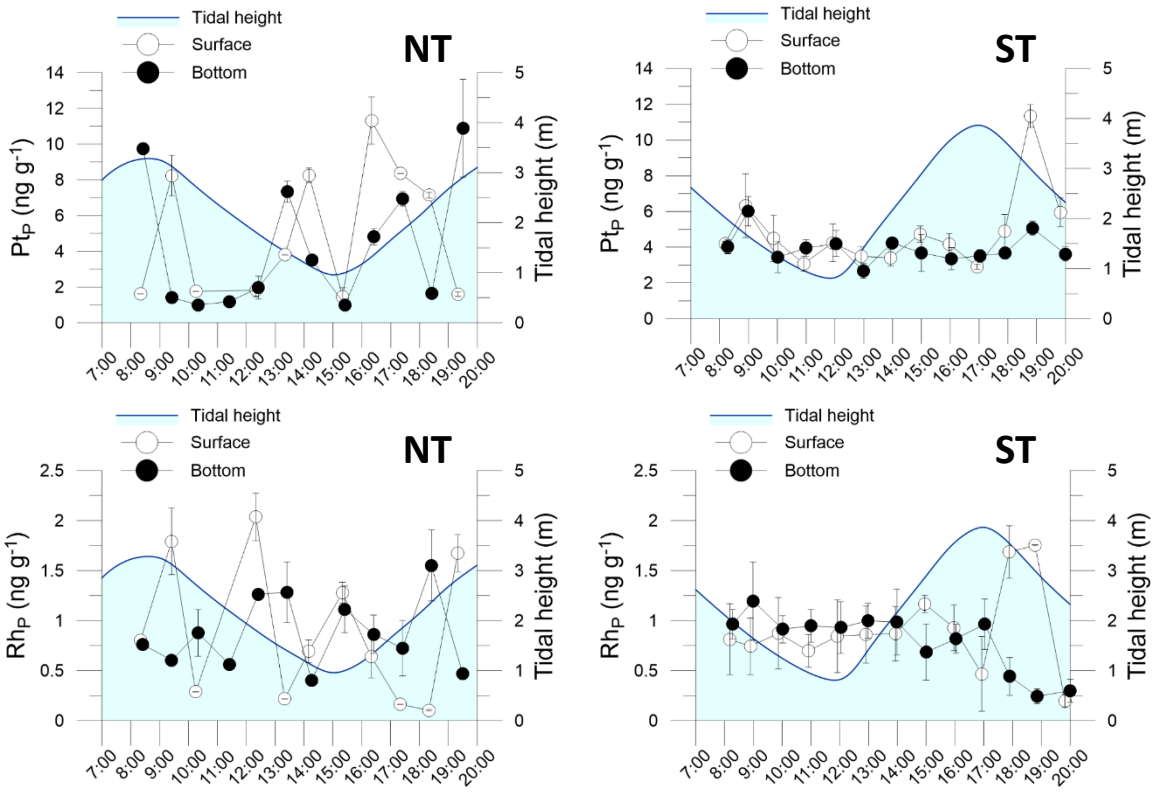

Figure VII-3 – Mean±SD particulate platinum (Pt_P) and rhodium (Rh_P) in the water column at VFX station during neap tide (NT) and spring tide (ST) surveys. Tidal height – blue line; surface – white circles; bottom – black circles.

In addition to the measurements of dissolved concentrations by AdCSV, the total concentrations of Pt in the filtrates (<0.45 μm) were also determined by ICP-MS ($Pt_{D\text{-}ICP\text{-}MS}$) in the samples with low conductivity (in average 1 mS cm^{-1}), i.e. in the NT cycle of VFX. Rhodium in the same samples could not be measured by ICP-MS due to the very low concentrations and the large polyatomic interferences to its determination (Cu, Pb, Sr, Rb). In Figure VII-5, Pt measured in the filtrates by AdCSV and ICP-MS is shown. Concentrations of $Pt_{D\text{-}ICP\text{-}MS}$ ranged from 0.34 to 0.42 ng Pt L^{-1} in surface and from 0.33 to 0.58 ng Pt L^{-1} in the bottom. For both depths, $Pt_{D\text{-}ICP\text{-}MS}$ was higher than Pt_D. Both $Pt_{D\text{-}ICP\text{-}MS}$ and Pt_D presented similar variation patterns along the tidal cycle.

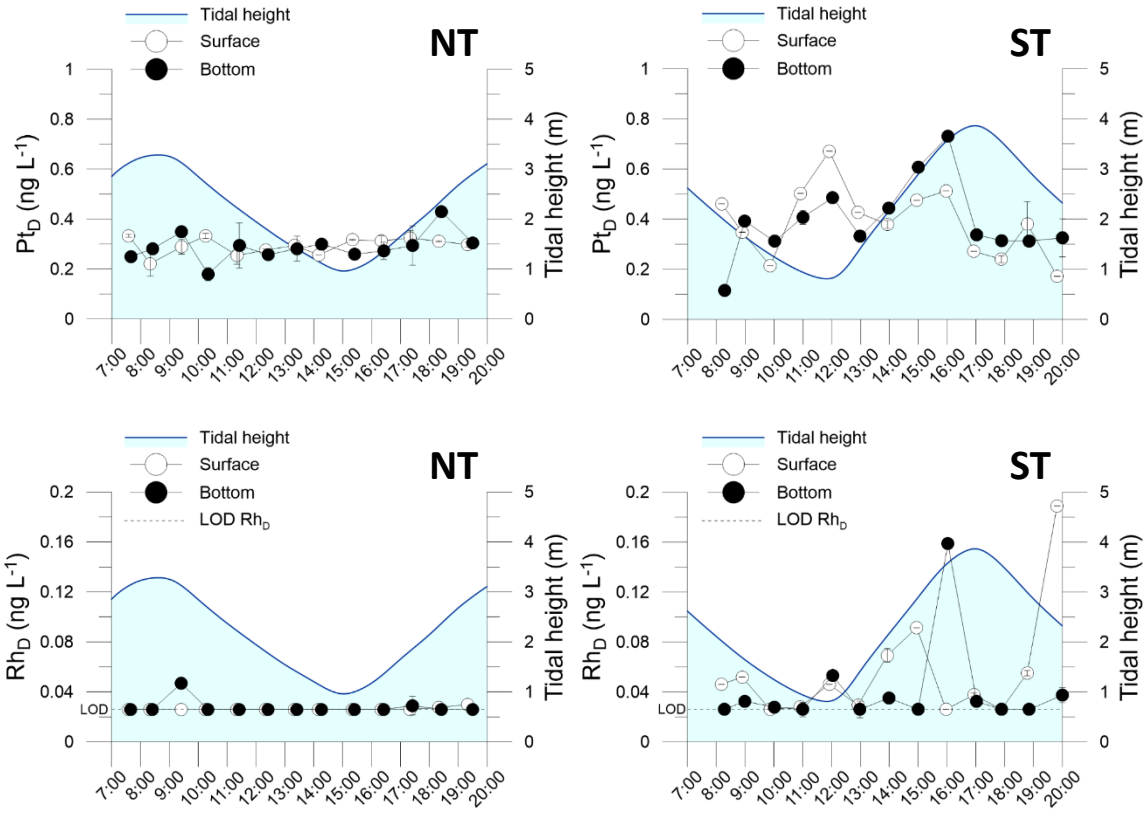

Figure VII-4 – Mean±SD dissolved platinum (Pt_D) and rhodium (Rh_D) in the water column at VFX station during neap tide (NT) and spring tide (ST) surveys. Tidal height – blue line; surface – white circles; bottom – black circles. Limit of detection for Rh_D is represented by the dotted line.

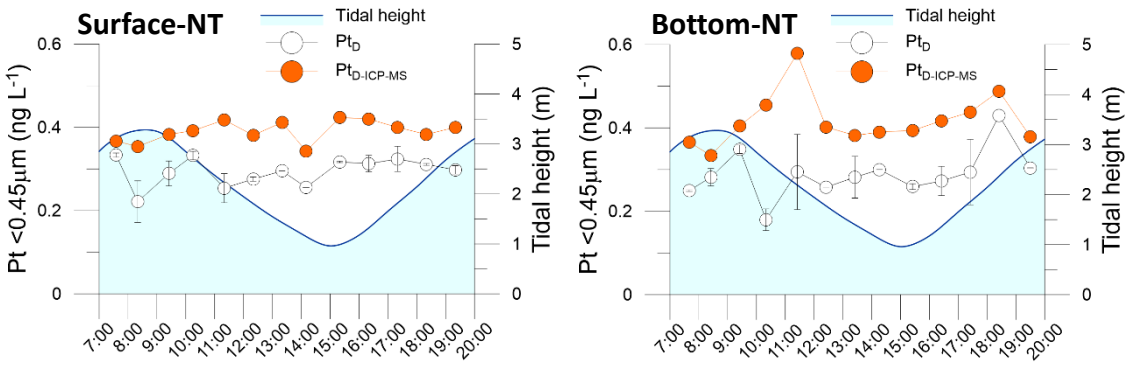

Figure VII-5 – Mean±SD Pt concentrations in the filtrates (<0.45 µm) measured by AdCSV (Pt_D) and ICP-MS ($Pt_{D\text{-}ICP\text{-}MS}$) in the water column at VFX station during neap tide (NT).

In spite of no significant differences ($p>0.05$) found on the water properties between depths for both NT and ST cycles, metals and their relationships with the water properties in the different cycles were evaluated combining both depths. The tables of correlation for NT and ST are presented in the supporting information (Table S.VII 1 and Table S.VII *2*, respectively), and unless stated along with R_S, all samples were considered (n=26).

For NT survey no significant correlations ($p>0.05$) were found for Pt and Rh with the water parameters analysed, except for Pt_P with SPM (R_S=-0.544; $p<0.05$). In the ST survey, correlations were observed for Pt_P with conductivity (R_S=0.412; $p<0.05$), pH (R_S=0.448; $p<0.05$) and SPM (R_S=-0.614; $p<0.001$). As to Pt_D, negative correlations were also observed with conductivity (R_S=-0.510; $p<0.01$) and pH (R_S=-0.404; $p<0.05$), whereas Pt_D correlated positively with temperature (R_S=0.437; $p<0.05$). Moreover, no significant correlations ($p>0.05$) were found for Rh.

7.3.1.3. PCA and Relationships Between Metals and Estuarine Water

Principle Component Analysis (PCA) was carried out to understand the main factors that explain variability and relationships between Pt and Rh data, for both NT and ST cycles, and with the water parameters temperature, conductivity, pH, DO and SPM (Figure VII-6). The Rh_D data was not included in the analysis since in the NT survey nearly all concentrations were below LOD. Two principal components (PC) were extracted and both explained half of the variance, 50.9 %. The first component, PC1, explained 35.9 % variability of the data and best described the tidal mixing at this location. Both tidal cycles were separated in the analysis. In addition, a separation between low and high tides was found, distinctly in ST. Parameters associated to the characteristics of estuarine waters had more influence in the high tide as opposed to low tide in ST campaign. Compared to NT cycle, higher variability of conductivity was observed during ST cycle. With PC2, the variance of data was affected by 15.0 %. The parameters that best described this component were temperature and Pt_D, which co-varied closely, as also expressed by the associated correlation found. None of the extracted components seemed to have a major relation with the Pt_P and Rh_P fractions, as observed by the low dimension of their vectors, yet significant correlations were found for Pt_P.

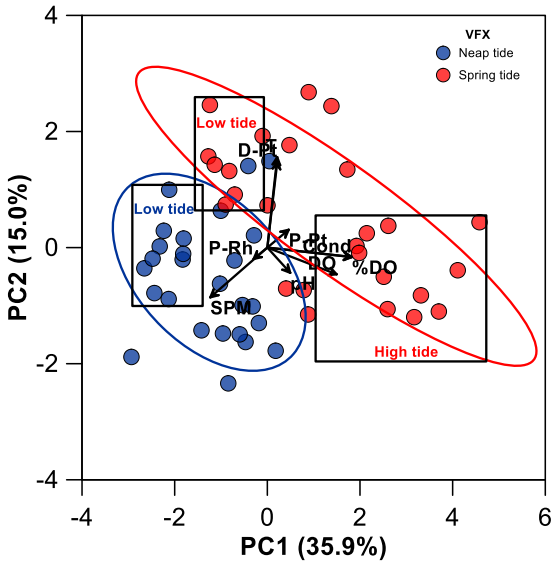

Figure VII-6 – Principal component analysis of VFX data (particulate Pt – P-Pt; dissolved Pt – D-Pt; particulate Rh – P-Rh; temperature – T; conductivity – Cond; pH, dissolved oxygen – DO and %DO; and suspended particulate matter – SPM) obtained during neap tide (NT) and spring tide (ST) surveys. Black boxes correspond to ebbing and flooding periods.

7.3.2. Downstream Site: Alcântara (ALC)

7.3.2.1. Environmental and Hydrographic Context

The physicochemical water properties of the intermediate depth sampled at ALC site during neap tide (NT) and spring tide (ST) are presented in Figure VII-7. In general, data analysis of the sampled temporal series showed good agreement between the measured variables and tidal oscillation in each cycle. Considering the water samples at this location were collected at the discharge site of a WWTP treated effluent, the minor variations observed on some of the variables were due to the input of freshwater from the effluent. Temperature ranged from 19.4 to 25.7 ºC in NT and from 18.3 to 23.0 ºC in ST. The highest temperature values were observed during low tide, in general exhibiting an opposite pattern compared to the other parameters. A maximum value was found during the flood in NT, at ~16:00. Conductivity varied from 24.9 to 53.9 mS cm^{-1} in NT and from 18.2 to 50.8 mS cm^{-1} in ST, following closely the tidal dynamics with the highest values found in high tides (e.g. around 17:00 in ST) and the lowest in low tides (e.g. around 16:00 in NT). The pH variation in both cycles was between 7.4 and 8.2.

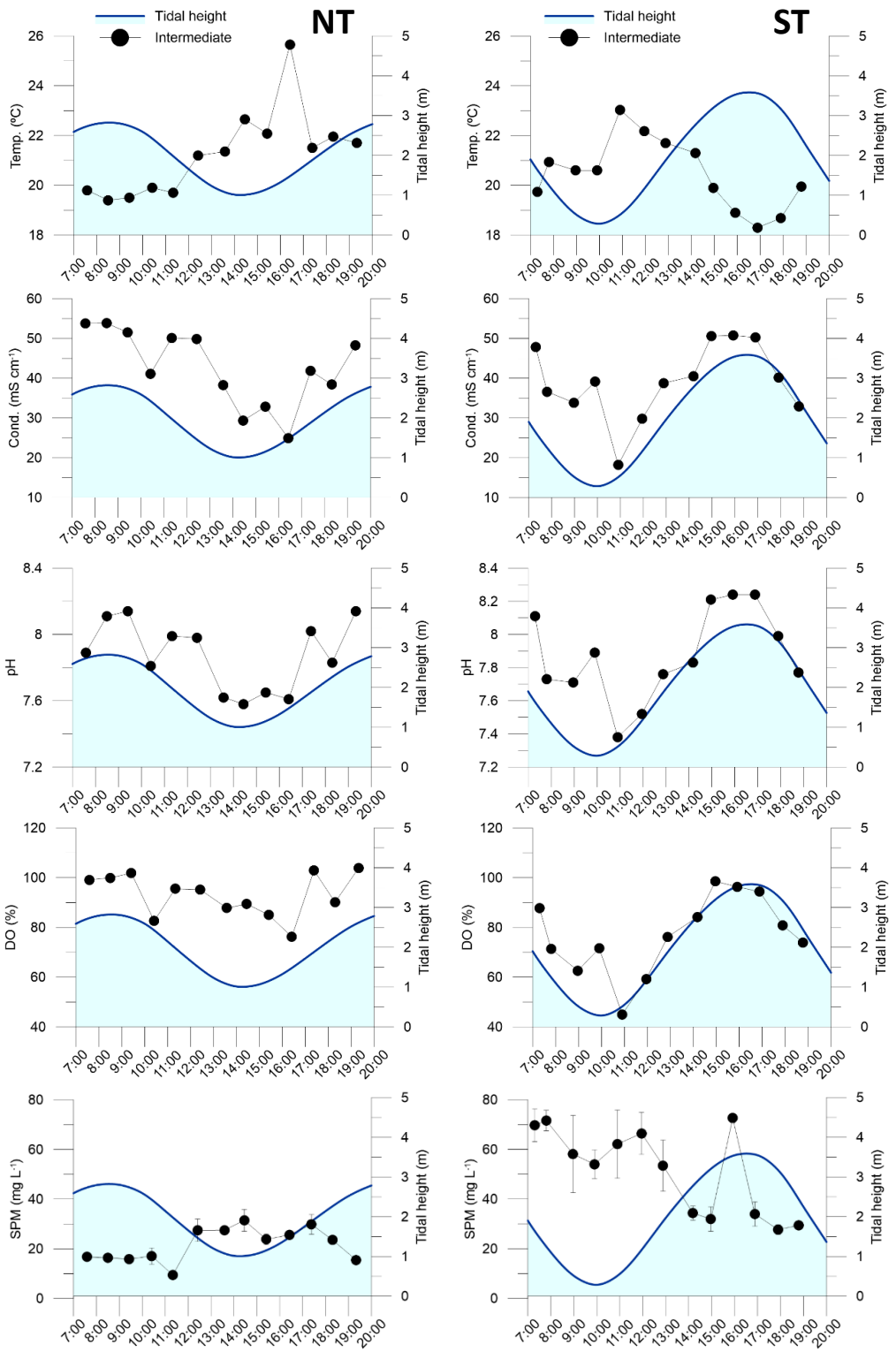

Figure VII-7 – Characteristics of the water at ALC station during neap tide (NT) and spring tide (ST) surveys: temperature (ºC), conductivity (mS cm^{-1}), pH, dissolved oxygen (expressed in percentage of saturation, %DO) and suspended particulate matter (SPM, mean±SD mg L^{-1}). Tidal height – blue line; intermediate depth (<3 m) – black circles.

The variations observed in pH parallels the semi-diurnal tidal oscillation, in particular over ST cycle. The concentration of DO varied from 5.8 and 8.1 mg L^{-1} in NT and 3.7 and 7.9 mg L^{-1} in ST, also mimicking the tidal effect. Consequently, %DO ranged between 76 to 104 % in both cycles, pointing to lower dissolved oxygen in those waters as compared to VFX. The content of SPM over the NT cycle was considerably lower than in ST. Concentrations of SPM ranged between 10 and 31 mg L^{-1} in NT and between 28 and 73 mg L^{-1} in ST. In both tidal cycles, SPM presented an inverse relation with the tidal variations, consisting in SPM increase at low tides.

7.3.2.2. Variability of Pt and Rh Concentrations Over the Tidal Cycles

The concentrations of particulate (Pt_P and Rh_P) and dissolved (Pt_D and Rh_D) metals in the water column for both tidal cycles at ALC station are shown in Figure VII-8. Concentrations of Pt_P varied from 2.0 to 25.6 ng Pt g^{-1} in NT and from 4.2 to 22.1 ng Pt g^{-1} in ST. As found for Pt_P concentrations, values in the dissolved fraction ranged within an order of magnitude, between 0.2 and 5.3 ng Pt L^{-1} in NT, and between 0.2 and 11.7 ng Pt L^{-1} in ST. Both particulate and dissolved fractions of Pt presented a similar variation pattern, with the highest concentrations at low tides. In addition, a relative increase of both Pt_P and Pt_D concentrations also occurred at ~10:00 and ~18:00 during the NT survey. The same increase on both periods of the day was also observed in ST, however, those coincided with the tidal height (low and high tide, respectively).

Concentrations of Rh_P varied from 0.3 to 5.1 ng Rh g^{-1} in NT and from 0.2 to 4.3 ng Rh g^{-1} in ST. Small peak concentrations of Rh_P were observed in the NT survey around 10:00 and a maximum at ~16:00. For the same periods of the day, at 9:00 and 17:00, increments were similarly found in the ST survey. As to Rh_D concentrations in both cycles, these ranged from LOD to 0.12 ng Rh L^{-1}. The variation pattern displayed by Rh_P did not appear to follow the tidal dynamics, as opposed to Rh_D that in general presented the highest concentrations in low tides of NT and ST.

The main relationships found between Pt, Rh and the water parameters at ALC are shown in Figure VII-9. The corresponding correlations for NT and ST are presented in the supporting information (Table S.VII 3 and Table S.VII 4, respectively), and unless

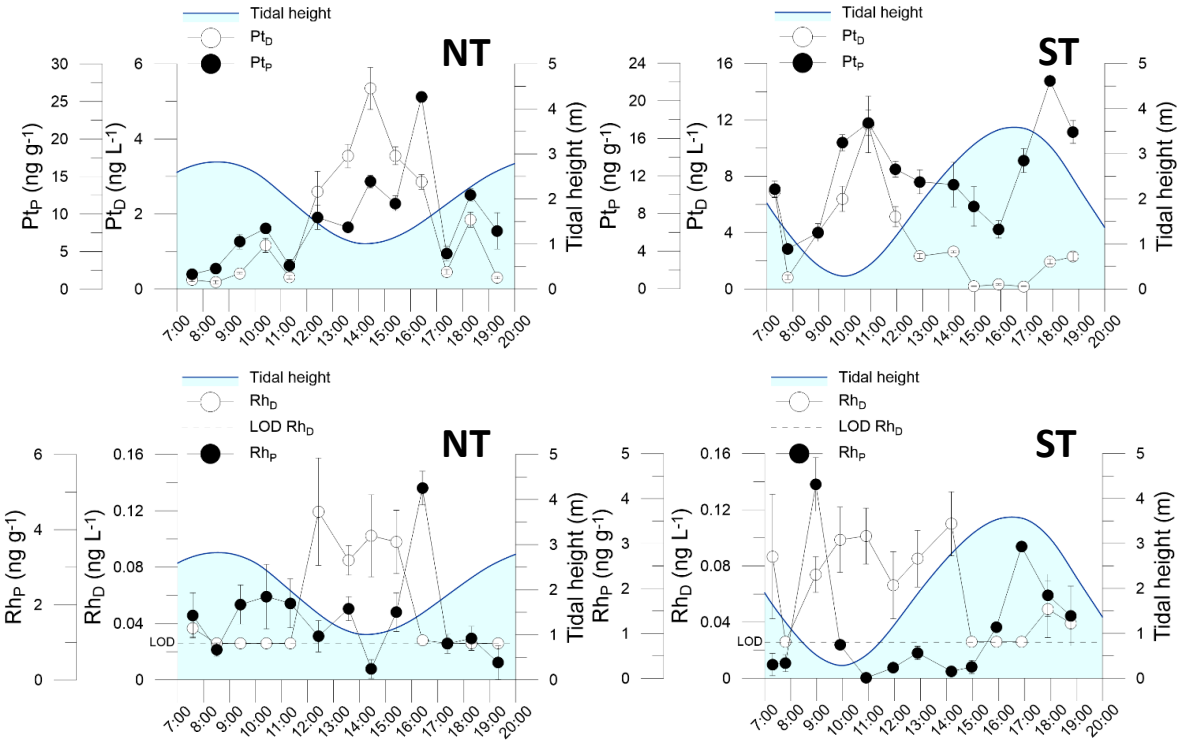

Figure VII-8 – Mean±SD concentrations of particulate (black circles) and dissolved (white circles) platinum (Pt_P and Pt_D, respectively) and rhodium (Rh_P and Rh_D, respectively) in the water column at ALC station during neap tide (NT) and spring tide (ST) surveys. Tidal height – blue line.

stated along with R_S, all samples from this station were considered (n=13).

In the NT survey, Pt_P presented significant negative correlations with conductivity (R_S=-0.885; p<0.0001; Figure VII-9a), pH (R_S=-0.707; p<0.01) and DO (R_S=-0.698; p<0.01). A positive correlation was found for Pt_P with temperature (R_S=0.835; p<0.0001; Figure VII-9b) and with SPM (R_S=0.571; p<0.05; Figure VII-9c). In ST, it was found a negative correlation between Pt_P and SPM (R_S=-0.560; p<0.05; Figure VII-9c) as opposed to NT. As to Pt_D, significant correlations (p<0.05) with temperature, pH, conductivity and DO were found in both tidal cycles following the same trends, except with SPM. A significant positive correlation (R_S=0.758; p<0.0001; Figure VII-9d) was also found between Pt_D and SPM in the NT survey, whereas in ST no correlation was found (p>0.05).

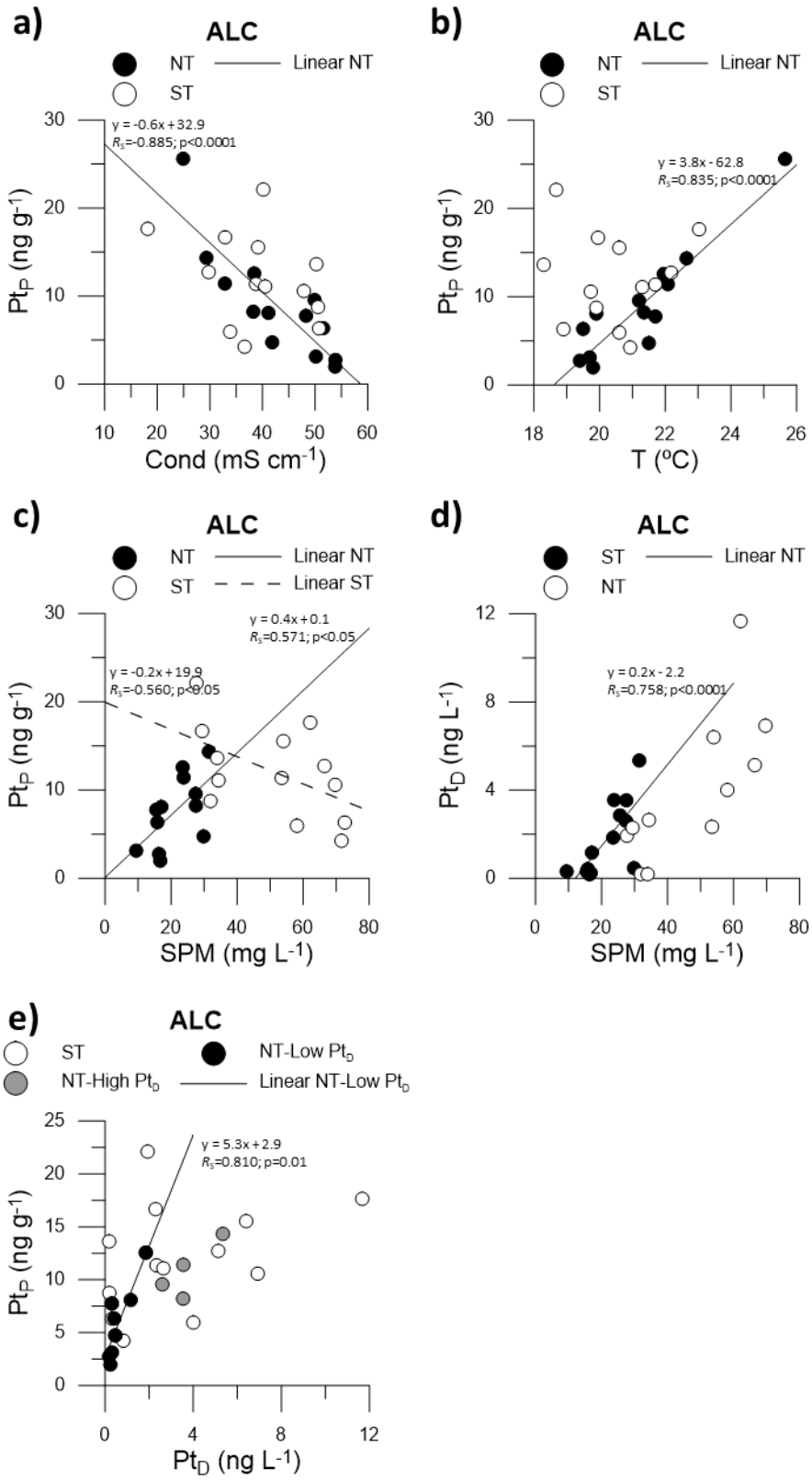

Figure VII-9 – Biplots of **a)** particulate platinum – Pt_P vs. temperature – T; **b)** Pt_P vs. conductivity – Cond; **c)** Pt_P vs. suspended particulate matter – SPM; **d)** dissolved platinum – Pt_D vs. SPM; and **e)** Pt_P vs. Pt_D.

In NT, Pt_P and Pt_D showed a significantly positive correlation (R_S=0.868; p<0.0001), whereas in ST no correlation was found (p>0.05). By separating the lower concentrations (<2.0 ng Pt L^{-1}) from the higher (>2.0 ng Pt L^{-1}), one linear relation was displayed (Figure VII-9e). The best linear fit was given by the low Pt_D concentrations (R_S=0.810; p=0.01; n=8) against Pt_P.

As to Rh_P and Rh_D, no significant correlations (p>0.05) were found in both cycles.

7.3.2.3. PCA and Relationships Between Metals and WWTP Effluent / Estuarine Waters Mixture

In Figure VII-10 is shown the PCA for the data surveyed at ALC. The three principal components (PC) explained 81.8 % of the variance of the results. The first component (PC1) alone described 58.1 %, while PC2 and PC3 accounted for 14.6 and 9.1 %, respectively.

The first principal component, PC1, distinctly showed the tidal regime during both cycles. The parameters that best defined the high tides were described by the properties of estuarine water, namely conductivity, pH, DO and %DO, as opposed to the low tide scores that did not fully reflect the estuarine waters. In the low tides, the scattering of the scores reflected the mixture of estuarine water with the WWTP effluent discharge. The second principal component, PC2, underpinned the effluent discharge as the urban source of Pt and Rh to the estuary. This component was best defined in the low tides,

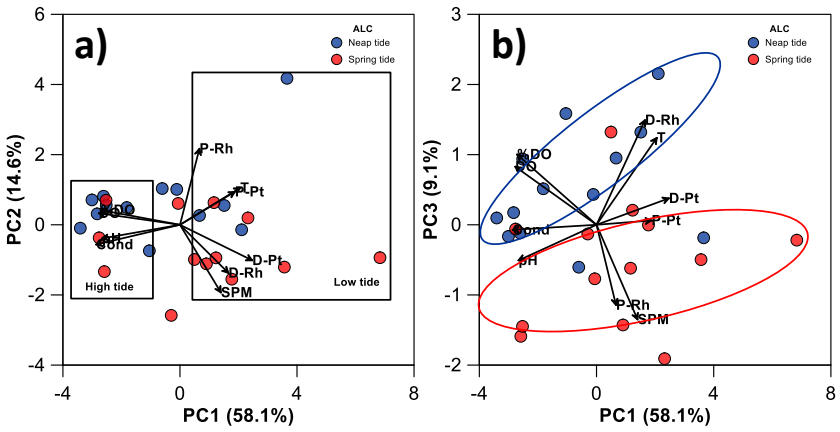

Figure VII-10 – Principal component analysis of ALC data (particulate Pt – P-Pt; dissolved Pt – D-Pt; particulate Rh – P-Rh; dissolved Rh – D-Rh; temperature – T; conductivity – Cond; pH, dissolved oxygen – DO and %DO; and suspended particulate matter – SPM) obtained during neap tide (NT) and spring tide (ST) surveys. **a)** PC1 vs. PC2; and **b)** PC1 vs. PC3.

evidenced by the relations of both particulate and dissolved fractions of Pt and Rh, as well as SPM and temperature. Despite causing minor variance, PC3 pointed out a minor effect of the fortnightly tidal cycling at ALC, by separating NT and ST yet considering some misunderstanding scores.

7.3.3. Geographical Inter-Comparison

7.3.3.1. Particle-Water Distribution Coefficients (K_D)

The distribution coefficients, defined as the ratio between the metals concentration in particulate phase (w/w) and aqueous phase (w/v), K_D (L g^{-1}) (e.g. Sung 1995; Tessier 2019), were evaluated. The distribution coefficients along the conductivity gradient of both surveys is presented in Figure VII-11a. Including both tidal cycles, the Log transformations of K_D (Figure VII-11b) for Pt ranged from 3.2 to 5.0 at ALC and from 3.4 to 4.6 at VFX. Similarly, Log K_D for Rh varied from 3.2 to 5.3 at ALC and from 3.0 to 4.7 at VFX. No significant differences differences ($p>0.05$) were found for both metals amongst sites.

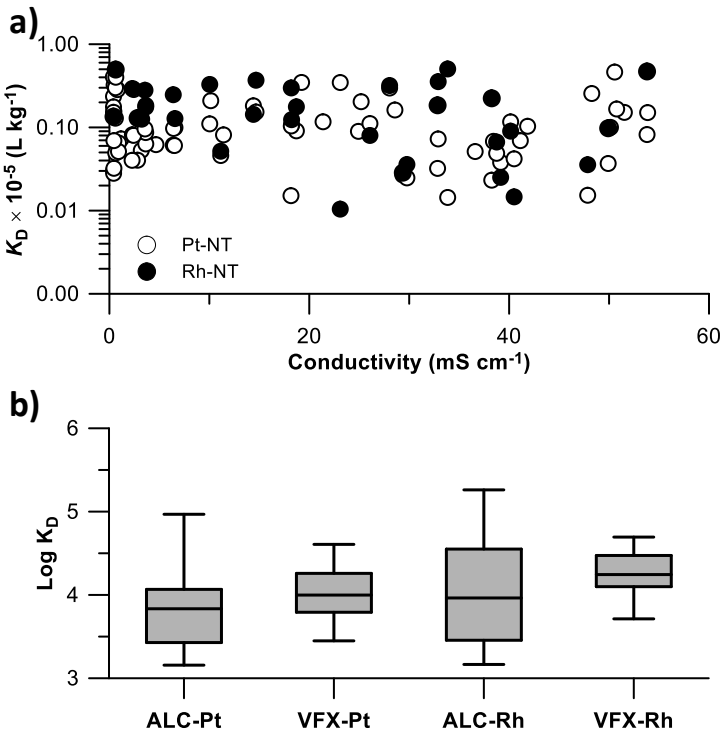

Figure VII-11 – a) Distribution coefficients (K_D) along the conductivity gradient including both tidal cycles; **b**) Boxplot of the Log transformation of K_D for Pt and Rh in both stations surveyed in Tagus estuary.

7.3.3.2. PCA

In Figure VII-12 it is presented the PCA for all data surveyed in Tagus estuary. Two principal components (PC) were extracted and together explained 64.9 % of the variance. The first component, PC1, described 40.9 %. It is noticeable that PC1 separated both locations surveyed in the estuary, most likely relating the salinity gradient. This is best described by the water characteristics that differ in downstream station ALC, near to the Atlantic Ocean, from the upstream station VFX. The main property attributed to this feature was conductivity, which was related to the more saline waters in the estuary. In opposition, near the riverine end-member at VFX station, with low saline water, the PCA exerted an opposite effect mainly controlled by temperature and SPM. The second component, PC2, accounted for 23.9 % of the explained variance. This component appeared to be associated with the semi-diurnal tidal regime. Noteworthy in the ALC station, the separation displayed between low and high tides evidenced this component' effect. The same was observed at VFX station during ST cycle, however with a fewer number of scores. In addition to the tidal regime, pH was exhibited as the main driver controlling PC2, associated to the semi-diurnal regime. Nevertheless, the variable' loadings had relevant distribution in the four quadrants of the PCA, evidencing their weight on both components. As such, both components reflected the major importance of the mixing features of Tagus estuary.

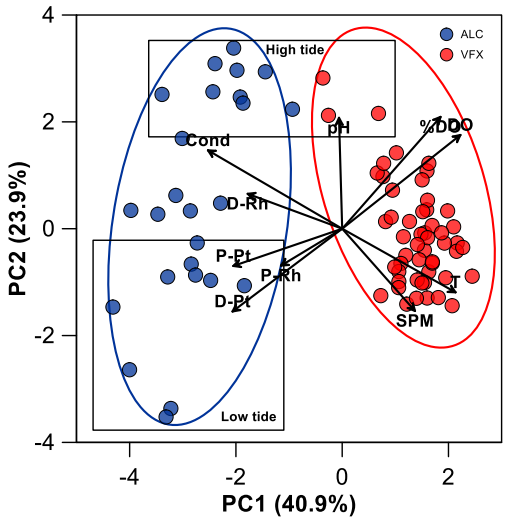

Figure VII-12 – Principal component analysis of data (particulate Pt – P-Pt; dissolved Pt – D-Pt; particulate Rh – P-Rh; dissolved Rh – D-Rh; temperature – T; conductivity – Cond; pH, dissolved oxygen – DO and %DO; and suspended particulate matter – SPM) obtained during neap tide (NT) and spring tide (ST) surveys for both ALC and VFX stations.

7.3.4. Estuarine and Coastal Exchanges of Pt and Rh

The potential exchanges of Pt and Rh between the Tagus estuary and the Atlantic Ocean were evaluated using the data from the downstream station ALC (Figure VII-1). Initially, the concentrations of metals were projected against the corresponding horizontal component (*u*) of the current velocity field obtained from the hydrodynamic model MOHID (Figure VII-13). Considering only current velocities higher than 0.75 m s^{-1}, differences were observed amongst the tides. Both fractions (dissolved and particulate) of Pt and Rh were particularly associated with the highest currents during the ebb tide, towards the Atlantic Ocean, as opposed to those during the flood. Towards the inner estuary, this was less pronounced, however, pointing out to recirculation in the inner bay. The exception was Rh_D, which presented similar range of concentrations in both ebb and flood tides during ST.

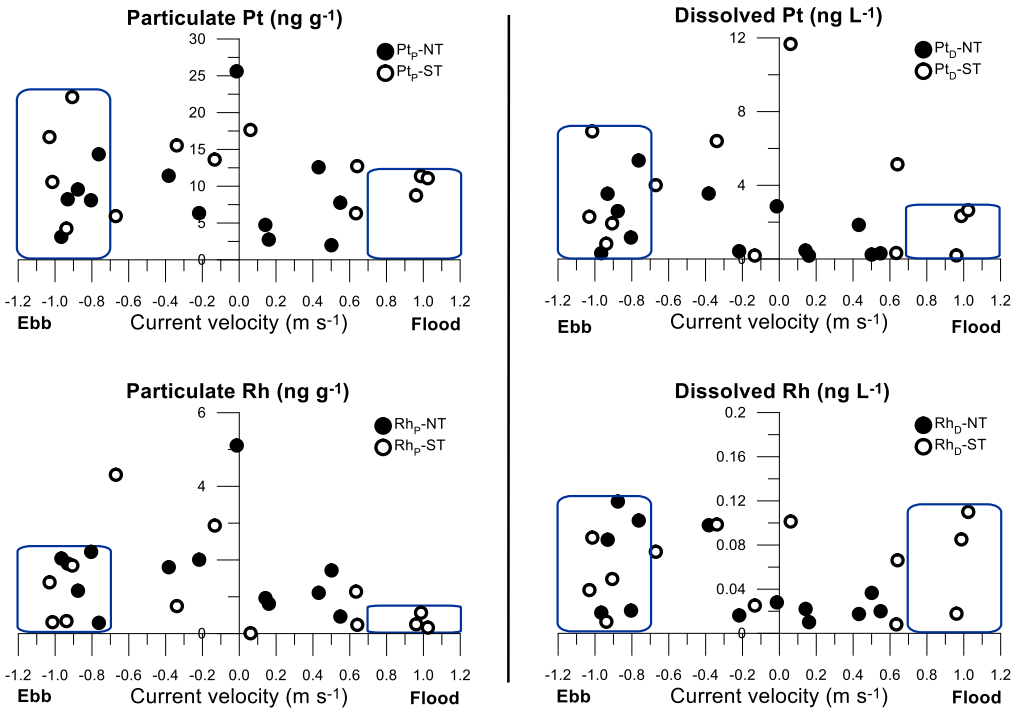

Figure VII-13 – Projection of particulate and dissolved Pt and Rh concentrations on the current velocity (u component) obtained for ALC station. Blue boxes indicate the magnitude of the concentrations found for current velocities between 0.75 and 1.2 m s^{-1}.

The Lagrangian method was also used by forcing the model for longer periods (over 21 days) that included NT and ST cycles. In these numerical simulations was considered the continuous release of 20 particles h^{-1} that acted as tracers of Pt and Rh only controlled by hydrodynamic conditions. Results for the ebb and flood periods of interest are presented in Figure VII-14, depicting approximately the cycles at the end of each day during turnover of the tide. Models were initiated in the ebb flow and the identification of the particles (ID) is indicated, being the latest particles released in red. This model only reflects the physical driving processes occurring and does not take into account any chemical interactions. Thus, results reproduce only the probability of dispersion of Pt and Rh. In addition to this, a dilution factor is not overviewed in the model results.

At day 1 it was observed that particles tend to remain in the inlet, either during the ebb or flood in NT conditions. In opposition, during ST, particles started to be transported to the inner estuary or towards the Atlantic Ocean. This reflects the stronger hydrodynamic conditions of ST in comparison to NT. At day 2 it was seen their transport out of the inlet, either towards the inner estuary during the flood and to the ocean during the ebb. The pattern was repeatedly observed in the following days of the simulation. At day 21 particles were found inside the estuary and in the adjacent coastal area independently of the tidal conditions, i.e. after a large number of particles released their dispersion was visible in both systems.

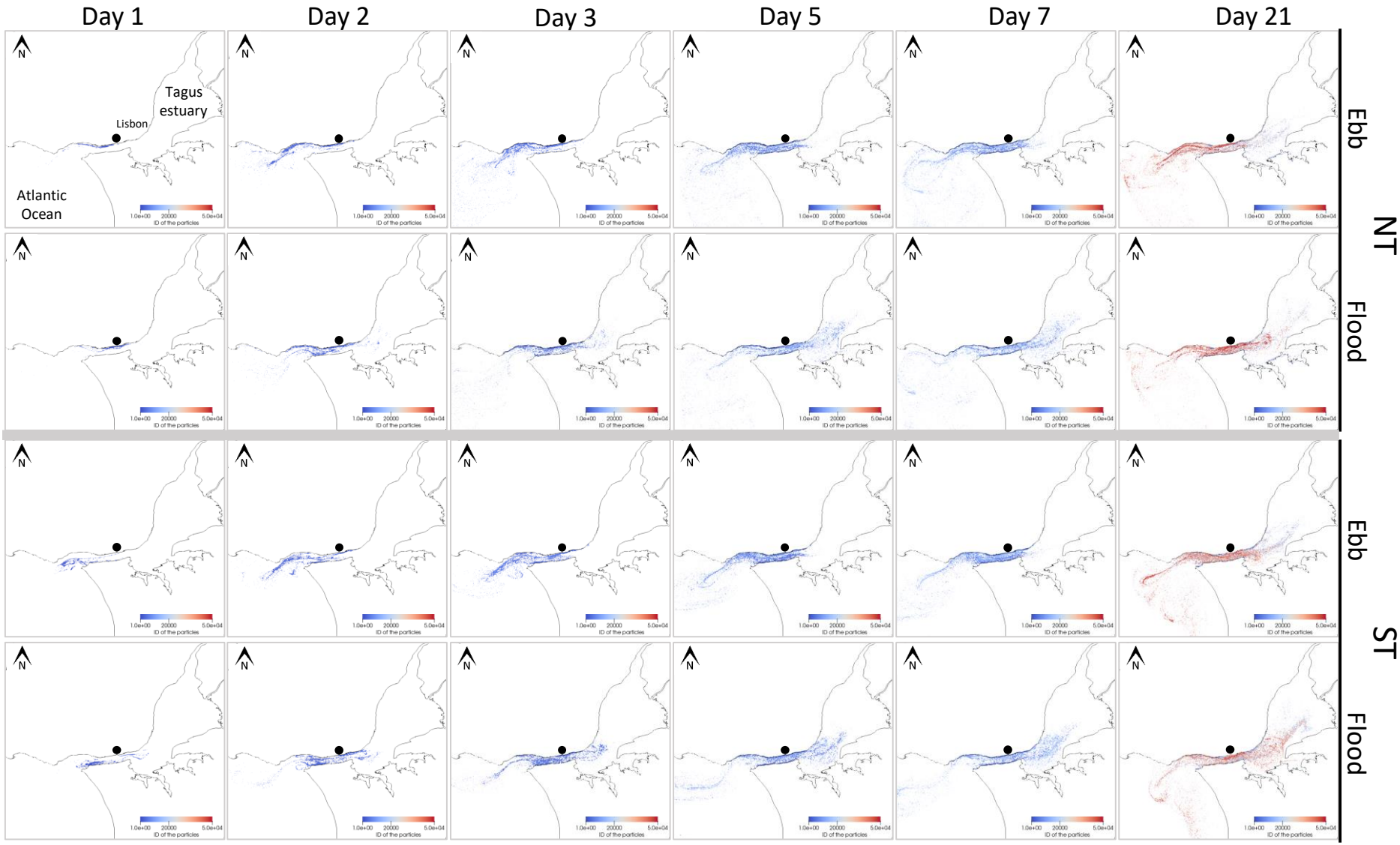
Day 1
Day 2
Day 3
Day 5
Day 7
Day 21
Tagus estuary
Lisbon
Atlantic Ocean
N
1.0e+00 20000 5.0e+04
ID of the particles
Ebb
Flood
NT
Ebb
Flood
ST

Figure VII-14 – Lagrangian distribution pattern of particles hourly released from the WWTP outfall (black circles) during 21 days of simulation using MOHID. Results are discriminated for ebb and flood tides for both neap tide (NT) and spring tide (ST) conditions.

7.4. Discussion

7.4.1. Environmental and Hydrographic Context

Variations of ancillary parameters at both sites followed the tidal regime, as well as the inputs of fresh- or wastewaters to the estuary from VFX and ALC, respectively. The water column at VFX station presented similar characteristics between the surface and bottom layers in both tidal cycles surveyed. This observation indicates that the water column was in general uniform and well mixed. Differences displayed between tidal cycles at VFX in some ancillary parameters indicated the extent of the tidal effect, as also evidenced by the PCA (Figure VII-6). Conductivity (Figure VII-2) was higher in ST than in NT, owing to the stronger upward movement of the tidal wave under this condition. The temperature of the waters showed an opposite trend to the tidal influence. Regardless the small variation in the temperature range, however, it could be seen that the entrance of freshwater to the estuary responded to the semi-diurnal oscillation. In ST, variations of pH closely followed the increase of conductivity and thus the tidal regime (Figure VII-2).

In the downstream station ALC, the tidal amplitude is larger than at VFX. Even so, the effect of the tidal regime in the water properties is less pronounced due to proximity to the Atlantic Ocean, as opposed to VFX. Thus, the physicochemical characteristics of the water at ALC did not vary considerably between tidal cycles but followed the semi-diurnal hydrodynamic, as also confirmed by the PCA (Figure VII-10). During low tides, the discharge of the WWTP' treated effluent to the estuary was more detectable, owing to the shallower water column. This was clear by the maximum values of temperature recorded in the low tide during both NT and ST surveys. Accordingly, a decrease in the conductivity and pH was found as opposed to those rises in temperature. Despite similar range on SPM levels found in both stations, relatively small increments were observed during low tides. Exceptionally, during ST survey at ALC station, a markedly increased of SPM concentration through the low tide was observed. Nonetheless, SPM concentrations found in Tagus estuary during these surveys indicated low turbidity in the water column in both sites as compared to other large estuaries (e.g. the Gironde, Cobelo-García et al. 2014).

The Tagus estuary is an ebb-dominated mesotidal system with fortnightly oscillations. The estuarine water at ALC usually presents characteristics close to the coastal waters while at VFX the characteristics mainly depend on the mixture of riverine and estuarine waters. Therefore, a salinity gradient was observed between both locations and tidal cycles, mainly at VFX during ST. Vertical stratification of riverine and estuarine waters did not occur due to bottom topography and tidal oscillation. The extent of the tidal wave can reach up to 50 km upstream (Guerreiro et al. 2015), passing upward VFX station, but the tidal amplitude is less pronounced at VFX than in ALC. In addition, it was observed particularly for VFX tidal cycles some gap between the physicochemical parameters data and the tidal height, which is given by the hydrodynamic model MOHID. This may be explained by the delay on the propagation of the tidal wave up to ~2 h from the mouth up to VFX.

7.4.2. Concentrations and Physicochemical Characterization of Pt and Rh in the Water Column

The particulate concentrations recorded during both tidal cycles ranged from 1.0 to 11.3 ng Pt g^{-1} at VFX and up to 25.6 ng Pt g^{-1} at ALC. These values are in line with the levels reported for other estuaries, such as the Lérez (2.1–8.0 ng Pt g^{-1}, Cobelo-García et al. 2013) and the Gironde (0.2–1.8 ng Pt g^{-1}, Cobelo-García et al. 2014). As to Rh_P, low concentrations were observed, ranging from 0.1 to 2.0 ng Rh g^{-1} at VFX and from 0.2 to 5.1 ng Rh g^{-1} at ALC. To our knowledge, data on Rh_P in water column of aquatic systems is not available. Consequently, comparison can only be done with matrices like sediments and road dusts, which may represent the closest approximation to SPM. Rhodium concentrations measured in SPM were relatively higher than those found in superficial sediments of Tagus estuary (0.02–1.5 ng Rh g^{-1}, Monteiro et al. 2019) and much lower than those reported by Monteiro et al. (2020) for an urban road dust (44 ng Rh g^{-1}).

As to the dissolved fraction, Pt_D ranged up to 0.73 ng Pt L^{-1} at the river end-member (VFX) and up to 11.7 ng Pt L^{-1} at the WWTP' effluent outfall (ALC). Cobelo-García et al. (2013) reported lower concentrations for the Lérez river estuary in Pontevedra Ria, Spain, with Pt_D ranging between 0.01 and 0.12 ng L^{-1}. Mashio et al. (2016) also reported in Arakawa, Kotsuchi and Otsuchi rivers, Japan, Pt_D ranging up to 1.3 ng L^{-1}. For the low to medium-salinity range in the waters sampled by those authors, the Pt_D levels found at

VFX are comparable to those findings. Moreover, Obata et al. (2006) found in Tama river, Japan, increased concentrations of Pt_D varying up to 6.9 ng Pt L^{-1} that, although higher, did not reach the values found at ALC station. Concentrations of Rh_D in the estuarine water column are described for the first time in this work. While in the river end-member Rh_D was often below 0.03 ng Rh L^{-1} (LOD), at the WWTP' effluent discharge site Rh_D reached 0.12 ng Rh L^{-1} in both tidal cycles. To date, the only data on Rh_D was reported for the open ocean by Bertine et al. (1993), whose concentrations were <0.1 ng Rh L^{-1}, and more recently by Monteiro et al. (2017) in wastewaters, whose average concentration was 0.23±0.06 ng Rh L^{-1}.

In general, Pt levels in both fractions were higher than Rh for the two sites sampled. At VFX station, the river end-member presented lower Pt_P and Rh_P compared to the downstream station ALC, which was influenced by the WWTP' discharge. As with the particulate fraction, Pt_D and Rh_D were also lower at VFX compared to ALC. These results point out spatial differences on the anthropogenic loadings of Pt and Rh to the Tagus estuary. Their direct point sources derived from ACC at VFX, whose main sources are a low-traffic influenced bridge and the drainage basin that covers largely rural areas. At ALC, the WWTP converges pluvial and sewage waste from a large drainage urban basin, which includes three municipalities from the most densely populated part of Lisbon region. During both surveys at ALC, increments of both Pt_P and Pt_D (Figure VII-8) were recorded in the morning (~10:00) and afternoon (~18:00) periods. This suggests added Pt levels in the WWTP' effluent (Laschka and Nachtwey 1997; Vyas et al. 2014), most likely deriving from Pt-based anticancer compounds (Vyas et al. 2014) and whose degradation in the environment could release Pt aqueous species (Curtis et al. 2010) presumably detectable by the voltammetric method used. Anticancer drugs are used in the treatment of 50–70 % of malignancies (Qi et al. 2019; Simpson et al. 2019). Hospital and domestic sewages that are drained to the WWTP may reflect the high doses administered to patients in chemotherapy (200–500 mg cisplatin L^{-1} or higher in the case of carboplatin, www.infarmed.pt). Since Pt-based drugs are mainly excreted in urine (Oun et al. 2018), those peaks can be related to earlier hygiene and personal care activities that usually induce higher fluxes at the WWTP at those times of the day. The Pt/Rh mass ratios (not shown) calculated for NT and ST cycles support the previous observations. At VFX, including both surveys, Pt/Rh was primarily within the range typically found for ACC emissions (4–16; Rauch and Peucker-Ehrenbrink 2015). At ALC, higher Pt/Rh mass

ratios (20–69) contrasted with those found at VFX, largely exceeding the reference interval for ACC, especially in ST. Furthermore, the elevated Pt/Rh mass ratios were observed during low tides of both cycles, which may be closely related with the lesser dilution of the effluent discharge in the estuary as opposed to the high tides. When using the dissolved fraction of the metals, the calculated mass ratios were slightly higher than in particulate fraction, yet following the same trend. Therefore, concentrations found in the water column of Tagus estuary reflected the different sources and contributions at both sites.

While irregular short-term variations of Pt_P and Rh_P were exhibited at VFX during NT, notwithstanding the tidal regime, the opposite was observed during ST at VFX and in both of ALC tidal cycles. The increase on Pt_P and Rh_P at VFX during ST (Figure VII-3) appeared to follow the semi-diurnal variation during the high tide (≈18:00). In surface, Pt_P increased with the conductivity and pH (Figure VII-2), as expressed by the significant correlations ($p<0.05$) found. Despite this signal was observed in a period of ~2 h concurrent to the high tide peak, this observation may be explained by the existence of a downstream bridge (within 20 km distance) largely impacted by vehicles traffic. In fact, Monteiro et al. (2019) observed in superficial sediments a signal of both Pt and Rh that pointed out large emissions from ACC. Those particles once in the surface of the water column may be transported during the flood tide up to VFX. As to ALC, Pt and Rh (Figure VII-8) closely followed the temperature short-term variation and showed an opposing trend to conductivity (Figure VII-7), reflecting the characteristics of the inputted sewage. The strong positive correlation found during NT for Pt with the temperature (R_S=0.835; $p<0.0001$; Figure VII-9b) as opposed to those found with the estuarine water characteristics (e.g. the conductivity, R_S=-0.885; $p<0.0001$; Figure VII-9a) support the WWTP as one of the main pathways of Pt entrance in the Tagus estuary. This distinct pattern may be easily explained by the water column shallowness, in addition to the impact of direct discharge of the WWTP' treated effluent. These results evidence a close relationship between the semi-diurnal tidal oscillations and the source inputs of both metals to the estuary, also evidenced in PCA of ALC data (Figure VII-10).

7.4.3. Particle-Water Interactions of Pt and Rh

In any geochemical study, the interaction of the solutes with solid phases is of great importance. Many processes can play a role in the interchange between solid and liquid phases such as dissolution, complexation, sorption/desorption, uptake or release by organisms, aggregation/disaggregation, flocculation and sedimentation. The calculation of the distribution coefficients, K_D (L kg^{-1}) can give some information about the relative affinity of Pt and Rh to be retained by a solid phase in a given aquatic matrix, and hence about their mobility.

Particle-water distribution coefficients described for Pt and Rh did not present significant differences ($p>0.05$) amongst tidal cycles and along the salinity gradient (Figure VII-11a). No significant differences ($p>0.05$) were also observed between sites and for both metals, as expressed by the Log transformation (Figure VII-11b). Thus, median values of Log K_D can be considered for Pt and Rh in Tagus estuary, 4.0±0.4 (n=75) and 4.1±0.5 (n=34), respectively. Data on K_D for Pt and Rh obtained from natural settings, such as rivers or estuaries, remain very limited in the literature (Cobelo-García et al., 2008, 2013, 2014). Comparison with published data must be careful due to varying cut-off membrane filters used to discriminate phases (<0.2 or <0.45 µm). Furthermore, the relatively large colloids included in the 'dissolved' phase may also rule Pt and Rh variability/partitioning. As discussed, similar levels of SPM were measured in VFX and ALC, with an average concentration of 50 mg L^{-1}, and consequently similar K_D values could be foreseen. The K_D values found for Pt in Tagus estuary are in between those previously reported for other estuaries with quite different concentrations of SPM. For the Lérez, a low turbidity estuary with SPM of a few mg L^{-1}, K_D in the range of 10^5 to 10^6 were determined (Cobelo-García et al. 2013) while in Gironde, with SPM in the 100–2000 mg L^{-1}, $K_D < 10^4$ were found (Cobelo-García et al. 2014). The larger values of SPM are many times associated with larger particles that are less prone to adsorb metal ions and then the inverse relationship between SPM and K_D. The negative significant correlations observed for Pt_P with SPM in all situations corroborates the previous observations, except for ALC in the NT survey. Here, the different behaviour was observed most probably due to the impact of the WWTP discharge. As to the observed K_D absence of variation with salinity (Figure VII-11a), it points out that the interaction with particulate matter is mostly likely due to neutral charge Pt and Rh, either in the metallic form or through neutral complexes. Constant K_D values along a salinity gradient

were also reported for the Gironde by Cobelo-García et al. (2014). Such invariant trend, as described here for the Tagus, may also reflect the higher anthropogenic input of both fractions of Pt and Rh to the system. Different local anthropogenic pressures may also affect soluble/insoluble species during estuarine mixing (Cobelo-García et al. 2014). Therefore, Pt, at least, appears to have non-conservative behaviour in the Tagus estuary.

7.4.4. Speciation Analysis of Pt and Rh in the Water Column

Recently, the speciation analysis of Pt and Rh in road dust leachates (<0.45 μm) was achieved through the determination of truly dissolved species by AdCSV (in this study just called dissolved) and total filter-passing species by ICP-MS. Truly dissolved forms of Pt and Rh in the leachates embodied part of total concentrations found in <0.45 μm pool (Monteiro et al. 2020). Following the same methodology, Pt_D and $Pt_{D\text{-}ICP\text{-}MS}$ were determined for the samples of VFX station NT cycle (Figure VII-5), with average conductivity of 1 mS cm^{-1}. The Pt_D and $Pt_{D\text{-}ICP\text{-}MS}$ concentrations were considerably different in all samples and no significant correlation ($p>0.05$) was found between them. Total Pt concentrations in the water column, ^{T}Pt (ng L^{-1}), were computed as the sum of Pt_P expressed in ng L^{-1} and $Pt_{D\text{-}ICP\text{-}MS}$ (Table VII.1).

Table VII.1 – Summary of concentrations found for Pt and Rh in particulate (Pt_P and Rh_P, respectively) and dissolved (Pt_D, $Pt_{D\text{-}ICP\text{-}MS}$ and Rh_D, respectively) fractions in ALC and VFX stations during neap tide (NT) and spring tide (ST).

	ALC - NT	***ALC - ST***	***VFX - NT***	***VFX - ST***
Pt_P (ng g^{-1})	2.0-25.6	4.2-22.1	1.0-11.3	2.7-11.3
Pt_P (ng L^{-1})	0.03-0.64	0.3-1.3	0.08-0.71	0.13-0.28
Pt_D (ng L^{-1})	0.2-5.3	0.2-11.7	0.18-0.43	0.12-0.73
$Pt_{D\text{-}ICP\text{-}MS}$ (ng L^{-1})	n.d.	n.d.	0.33-0.58	n.d.
Rh_P (ng g^{-1})	0.3-5.1	0.2-4.3	0.1-2.0	0.2-1.8
Rh_P (ng L^{-1})	0.01-0.13	0.01-0.43	0.01-0.15	0.01-0.09
Rh_D (ng L^{-1})	LOD*-0.12	LOD*-0.12	LOD*-0.05	LOD*-0.19

*n.d. – not determined; *LOD = 0.03 ng Rh L^{-1}*

Platinum speciation analysis in these samples showed that the truly dissolved forms represented 39±9 % of the total concentrations in the water column, $Pt_D/^TPt$. The percentage of total filter-passing (<0.45 μm) species, $Pt_{D\text{-}ICP\text{-}MS}/^TPt$, was 65±14 %. The differences observed are due to colloidal and/or nanoparticles forms, whether in the metallic state Pt^0 or strongly bounded both to inorganic and organic colloids. As it is known, DOC can play a role in colloids aggregation/disaggregation (Wilkinson et al. 2006), but comparable and low values were obtained in the water column, ranging 3–4 mg C L^{-1} (S.I. Figure S.VII 1). Thus, these results suggest that DOC does not rule the aggregation/disaggregation processes in the water column, at least when low concentrations of Pt were found such as in the case of VFX station.

As to Rh, no speciation analysis could be done in samples of VFX station NT cycle because Rh_D concentrations were in general below the LOD. Furthermore, due to operational difficulties of ICP-MS in dealing with more saline samples (conductivity >1 mS cm^{-1}, Wolf and Adams 2015), Pt and Rh speciation analysis in the water column at VFX at ST and ALC in both tidal cycles could not be done. However, some additional considerations can be made. In all samples, truly dissolved Rh concentrations were very low, usually below LOD, and they may result from the already oxidized forms present in the water column, as truly dissolved Pt as well. As to the particulate forms, the range of concentrations found, in ng L^{-1} (Table VII.1), were similar for both stations in NT conditions. In most of the samples, Rh_P could represent the total Rh found in the water column since no Rh_D concentrations were found. In some cases, Rh_P was more than 65 % of the Rh_D concentrations measured. Moreover, an increase in SPM may not represent an additional input of Pt and Rh, as observed for Pt at ALC station (Figure VII-9c). A contribution to the particulate pool could be the removal from the aqueous phase, by adsorption of cationic hydroxychlorides and precipitation of destabilized hydroxyl-complexes (Cobelo-García et al. 2008). However, higher concentrations were found for Pt_D in ALC as compared to VFX, suggesting that speciation in the water column is controlled by the dissolved forms even without taking into account the additional fraction that could be measured by ICP-MS. Other sources than the ACC are present, which are responsible by the increase of soluble forms of Pt into the estuary and those originate in medicinal uses of Pt-based compounds. As to Rh, these observations point out to ACC as the main source of Rh into the estuary. Contrarily to Pt, Rh_P may represent an important proportion of the bulk Rh in the water column.

7.4.5. Hydrodynamic Forcing on Pt and Rh Transport

The fate of metals such as Pt and Rh may vary in the estuary and coastal area depending on their sources and other factors, like the hydrodynamic regime that partly controls their distribution. As previously seen, the input of Pt and Rh to the Tagus estuary in the river end-member at VFX station is low and continuous. In opposition, at the downstream station ALC, higher and variable concentrations of Pt and Rh enter the estuary through the WWTP drainage, near the Atlantic Ocean. Here, solutes and particles discharged may be widely spread by advection through the strong tidal currents that reach velocities closer to 1.0 m s^{-1} and may dominate the transport. As confirmed in the PCA including all data obtained (Figure VII-12), it is noticeable the influence of the hydrodynamic regime on both locations surveyed. While the salinity gradient discriminated both locations dominated by the fortnightly oscillations, the semi-diurnal tidal oscillations had a stronger effect at ALC station, as expressed by the separation of low and high tides and the water characteristics. Moreover, Pt and Rh appeared to have non-conservative behaviour in Tagus estuary because of their different point sources. Non-conservative mixing was also observed in other estuaries (Cobelo-García et al. 2013, 2014).

Concerning the distribution of Pt and Rh in the water column and their fate, data from the downstream station ALC was evaluated because of the proximity to the Atlantic Ocean and the potential export to the adjacent coastal area. Depicting Pt and Rh concentrations against the corresponding current velocities (Figure VII-13), the export of the metals is pointed out towards the coastal area. Higher concentrations of both fractions of Pt and Rh were released mainly during the low tide. However, their association to the higher current velocities during the ebb was evidenced for Pt_P, Rh_P and Pt_D, whereas Rh_D presented similar levels during both tide periods in terms of the magnitude of the concentrations.

To confirm the previous observations and the spread of Pt and Rh under hydrodynamic conditions, the Lagrangian method provided better information by using particles as passive tracers released in the WWTP outfall. Monteiro et al. (2020) showed that for road dust leachates, relatively constant concentrations of truly dissolved Pt and Rh were observed up to 7 days. Indeed, the back and forth tidal movement in the model induced dispersion of particles towards both the estuary and the ocean. Thus, the

probability of recirculation and export of Pt and Rh to the adjacent coast is very high and perhaps within a couple of days. In Figure VII-14 is showed that after two days, particles (in blue) were spread out to the ocean. The latest emitted particles in the model (in red, Figure VII-14), near the end of the simulation (day 21), confirmed that the plume of tracers originated in the WWTP outfall was straightforwardly spread to the Atlantic Ocean and the inner estuary. It was also visible at day 21 that 'oldest' particles (in blue) remained inside the estuary during both NT and ST, which were released initially in the model. These results suggest that part of the Pt and Rh loadings kept in the water column during the tidal cycles can recirculate until, eventually, they settle in low hydrodynamic areas near the estuary margins. Moreover, the extent of the WWTP input reached the middle of the estuary and appeared to be independent of the tidal conditions, i.e. NT or ST. Nonetheless, other sources of Pt and Rh do exist in the Tagus estuary (Monteiro et al. 2019) and further research should aim to evaluate their extension and fate.

The importance of the hydrodynamic regime at the mouth of the Tagus estuary was previously investigated for other metals (e.g. Duarte and Caçador 2012; Vale 1986). Trace elements such as Pt and Rh can be largely introduced in the estuary through pluvial- and wastewaters and consequently increase the contamination in the inner estuary and the adjacent coastal area. Despite the Tagus estuary does not appear to be extensively contaminated by Pt and Rh to date (Monteiro et al. 2019), the estuary is a net source of both metals to the coastal environment. Records of Pt were previously reported by Cobelo-García et al. (2011) in sediments of the Tagus pro-delta. The authors described a Pt enrichment in sub-surface sediments at the adjacent coastal area, owing to the extensive industrial activities in Tagus estuary around 1960s/70s and mimicking the records found for Hg and Pb (Mil-Homens et al. 2009). However, a superficial enrichment of Pt was not fully observed in that core despite the relative increase of Pt concentration in the top layer of those sediments. This slight increment did not reflect the anthropogenic inputs at that time perhaps because the core was collected around in 2000, less than one decade after the introduction of European legislation regarding the control of pollutants emission using ACC (European Commission 1991). Thus, it is plausible that with the increase of Pt and Rh uses over the past two decades increased amounts of these metals could have been exported to the adjacent coastal area. Nevertheless, it was demonstrated that Pt and Rh are continuously released in the aquatic environment, at least evidenced through the Pt concentrations found at the downstream WWTP outfall in the Tagus estuary.

7.5. Conclusions

The concentrations of particulate and dissolved fractions (<0.45 µm) of Pt and Rh were evaluated in the water column of Tagus estuary. Data on dissolved Rh is reported for the first time in an estuary. Two stations presenting different characteristics were surveyed during semi-diurnal cycles over neap and spring tides. In the river end-member station, both particulate Pt and Rh, as well as Pt_D, were continuously introduced in the estuary although presenting low and relatively constant concentrations, whereas Rh_D was often below the limit of detection. Contrastingly, at the downstream station, a WWTP outfall close to the Atlantic Ocean, a markedly increase was registered in both fractions of Pt and Rh varying within a broad range of concentrations. Increments in Pt and Rh levels followed an inverse pattern in relation to the semi-diurnal tidal oscillation, with higher concentrations observed during the low tide. This was more pronounced at the WWTP outfall vicinity than in the river end-member, owing to their different loadings into the estuary. At the downstream station, one of the sources of Pt and Rh confirmed was that of ACC, expressed by the concomitant variation of both metals. An additional source of Pt in the wastewater derived from hospital and domestic sewages due to the use of Pt-based anticancer therapy, showing relative increments in periods that were associated with personal care activities. At the upstream station, the source of Pt and Rh is presumably mainly the ACC, though pointing to minor inputs to the estuary. The partition coefficients for Pt and Rh in Tagus estuary varied independently of the salinity, suggesting that the effects of Pt and Rh sources superimpose their chemical interactions with the estuarine water. The speciation analysis done in the riverine samples confirmed that different forms of Pt were released in the environment, whose dissolved fraction includes truly dissolved species and (nano)particles. Furthermore, it was also estimated that operationally defined forms of dissolved Pt represented the largest portion of total metal emitted as opposed to Rh, whose particulate forms dominated in the water column. Despite the chemical aspects associated, advection may largely control the distribution of Pt and Rh within the estuary and to the coastal area. These metals can be easily and rapidly dispersed through the water column owing to their low reactivity. Therefore, recirculation within the estuary and export towards the adjacent coastal environment are highly expected. Both chemical and physical drivers acting in the Tagus estuary will dictate the distribution, transport and fate of Pt and Rh. Ultimately, for coastal areas where the direct

sources of Pt and Rh are not relevant, the obtained results showed that estuaries are an important pathway to introduce PGE in the coastal region and transferring them towards the ocean.

References

Abdou, M., Gil-Díaz, T., Schäfer, J., Catrouillet, C., Bossy, C., Dutruch, L., et al. (2020). Short-term variations of platinum concentrations in contrasting coastal environments: The role of primary producers. *Marine Chemistry*, *222*, 103782. doi:10.1016/j.marchem.2020.103782

Almécija, C., Cobelo-García, A., & Santos-Echeandía, J. (2016). Improvement of the ultra-trace voltammetric determination of Rh in environmental samples using signal transformation. *Talanta*, *146*, 737–743. doi:10.1016/j.talanta.2015.06.032

Auffan, M., Rose, J., Bottero, J.-Y., Lowry, G. V, Jolivet, J.-P., & Wiesner, M. R. (2009). Towards a definition of inorganic nanoparticles from an environmental, health and safety perspective. *Nature Nanotechnology*, *4*(10), 634–641. doi:10.1038/nnano.2009.242

Bertine, K. K., Koide, M., & Goldberg, E. D. (1993). Aspects of rhodium marine chemistry. *Marine Chemistry*, *42*(3), 199–210. doi:https://doi.org/10.1016/0304-4203(93)90012-D

Bertine, K. K., Koide, M., & Goldberg, E. D. (1996). Comparative marine chemistries of some trivalent metals - bismuth, rhodium and rare earth elements. *Marine Chemistry*, *53*(1–2), 89–100. doi:10.1016/0304-4203(96)00015-1

Braunschweig, F., Martins, F., Chambel, P., & Neves, R. (2003). A methodology to estimate renewal time scales in estuaries: the Tagus Estuary case. *Ocean Dynamics*, *53*(3), 137–145. doi:10.1007/s10236-003-0040-0

Burden, F. R., Foerstner, U., McKelvie, I. D., & Guenther, A. (2002). *Environmental Monitoring Handbook*. New York: McGraw-Hill Education. doi:ISBN: 9780071351768

Cobelo-García, A., López-Sánchez, D. E., Almécija, C., & Santos-Echeandía, J. (2013). Behavior of platinum during estuarine mixing (Pontevedra Ria, NW Iberian Peninsula). *Marine Chemistry*, *150*, 11–18. doi:10.1016/j.marchem.2013.01.005

Cobelo-García, A., López-Sánchez, D. E., Schäfer, J., Petit, J. C. J., Blanc, G., & Turner, A. (2014). Behavior and fluxes of Pt in the macrotidal Gironde Estuary (SW France). *Marine Chemistry*, *167*, 93–101. doi:10.1016/j.marchem.2014.07.006

Cobelo-García, A., Neira, P., Mil-Homens, M., & Caetano, M. (2011). Evaluation of the contamination of platinum in estuarine and coastal sediments (Tagus Estuary and Prodelta, Portugal). *Marine Pollution Bulletin*, *62*(3), 646–650. doi:10.1016/j.marpolbul.2010.12.018

Cobelo-García, A., Turner, A., & Millward, G. E. (2008). Fractionation and reactivity of platinum group elements during estuarine mixing. *Environmental Science and*

Technology, *42*(4), 1096–1101. doi:10.1021/es0712118

Colodner, D. (1991). *The marine geochemistry of Rhenium, iridium and Platinum*. *Massachusetts Institute of Technology*.

Curtis, L., Turner, A., Vyas, N., & Sewell, G. (2010). Speciation and reactivity of cisplatin in river water and seawater. *Environmental Science and Technology*, *44*(9), 3345–3350. doi:10.1021/es903620z

de Pablo, H., Sobrinho, J., García, M., Campuzano, F., Juliano, M., & Neves, R. (2019). Validation of the 3D-MOHID hydrodynamic model for the Tagus coastal area. *Water (Switzerland)*, *11*(8). doi:10.3390/w11081713

Duarte, B., & Caçador, I. (2012). Particulate metal distribution in Tagus estuary (Portugal) during a flood episode. *Marine Pollution Bulletin*, *64*(10), 2109–2116. doi:10.1016/j.marpolbul.2012.07.016

Ek, K. H., Morrison, G. M., & Rauch, S. (2004). Environmental routes for platinum group elements to biological materials--a review. *The Science of the total environment*, *334–335*, 21–38. doi:10.1016/j.scitotenv.2004.04.027

Essumang, D. K., Dodoo, D. K., & Adokoh, C. K. (2008). The impact of vehicular fallout on the Pra estuary of Ghana (a case study of the impact of platinum group metals (PGMs) on the marine ecosystem). *Environmental Monitoring and Assessment*, *145*(1), 283–294. doi:10.1007/s10661-007-0037-0

European Commission. (1991). Council Directive 91/542/EEC of 1 October 1991 amending Directive 88/77/EEC on the approximation of the laws of the Member States relating to the measures to be taken against the emission of gaseous pollutants from diesel engines for use in vehicles. http://eur-lex.europa.eu/eli/dir/1991/542/oj. Accessed 22 January 2018

Folens, K., Van Acker, T., Bolea-Fernandez, E., Cornelis, G., Vanhaecke, F., Du Laing, G., & Rauch, S. (2018). Identification of platinum nanoparticles in road dust leachate by single particle inductively coupled plasma-mass spectrometry. *Science of The Total Environment*, *615*, 849–856. doi:https://doi.org/10.1016/j.scitotenv.2017.09.285

Fortunato, A., Baptista, A. M., & Luettich, R. A. (1997). A three-dimensional model of tidal currents in the mouth of the Tagus estuary. *Continental Shelf Research*, *17*(14), 1689–1714. doi:https://doi.org/10.1016/S0278-4343(97)00047-2

Fortunato, A., Oliveira, A., & Baptista, A. M. (1999). On the effect of tidal flats on the hydrodynamics of the Tagus estuary. *Oceanologica Acta*, *22*(1), 31–44. doi:https://doi.org/10.1016/S0399-1784(99)80030-9

Guerreiro, M., Fortunato, A. B., Freire, P., Rilo, A., Taborda, R., Freitas, M. C., et al. (2015). Evolution of the hydrodynamics of the Tagus estuary (Portugal) in the 21st century. *Journal of Integrated Coastal Zone Management*, *15*(1), 65–80. doi:10.5894/rgci515

Guo, L., & Santschi, P. H. (2006, December 15). Ultrafiltration and its Applications to Sampling and Characterisation of Aquatic Colloids. *Environmental Colloids and Particles*. doi:doi:10.1002/9780470024539.ch4

Hegarty, J., Draxler, R. R., Stein, A. F., Brioude, J., Mountain, M., Eluszkiewicz, J., et

al. (2013). Evaluation of lagrangian particle dispersion models with measurements from controlled tracer releases. *Journal of Applied Meteorology and Climatology*, *52*(12), 2623–2637. doi:10.1175/JAMC-D-13-0125.1

IMT. (2016). *Relatório de Tráfego na Rede Nacional de Autoestradas - 4º Trimestre*. Lisboa, Portugal.

Laschka, D., & Nachtwey, M. (1997). Platinum in municipal sewage treatment plants. *Chemosphere*, *34*(8), 1803–1812. doi:http://dx.doi.org/10.1016/S0045-6535(97)00036-2

López-Sánchez, D. E., Cobelo-García, A., Rijkenberg, M. J. A., Gerringa, L. J. A., & de Baar, H. J. W. (2019). New insights on the dissolved platinum behavior in the Atlantic Ocean. *Chemical Geology*, *511*, 204–211. doi:https://doi.org/10.1016/j.chemgeo.2019.01.003

Luis, J. F. (2007). Mirone: A multi-purpose tool for exploring grid data. *Computers and Geosciences*, *33*(1), 31–41. doi:10.1016/j.cageo.2006.05.005

Marques da Costa, E. (2016). Sócio-Economia. In J. Rocha (Ed.), *Atlas Digital da Área Metropolitana de Lisboa*. Lisboa, Portugal: Centro de Estudos Geográficos.

Mashio, A. S., Obata, H., & Gamo, T. (2017). Dissolved Platinum Concentrations in Coastal Seawater: Boso to Sanriku Areas, Japan. *Archives of Environmental Contamination and Toxicology*, *73*(2), 240–246. doi:10.1007/s00244-017-0373-1

Mashio, A. S., Obata, H., Tazoe, H., Tsutsumi, M., Ferrer i Santos, A., & Gamo, T. (2016). Dissolved platinum in rainwater, river water and seawater around Tokyo Bay and Otsuchi Bay in Japan. *Estuarine, Coastal and Shelf Science*, *180*, 160–167. doi:10.1016/j.ecss.2016.07.002

Mil-Homens, M., Branco, V., Vale, C., Boer, W., Alt-Epping, U., Abrantes, F., & Vicente, M. (2009). Sedimentary record of anthropogenic metal inputs in the Tagus prodelta (Portugal). *Continental Shelf Research*, *29*(2), 381–392. doi:10.1016/j.csr.2008.10.002

Miller, J., & Miller, J. (2010). *Statistics and chemometrics for analytical chemistry* (6th ed.). Pearson Education Limited.

Monteiro, C. E., Cobelo-García, A., Caetano, M., & Correia dos Santos, M. M. (2017). Improved voltammetric method for simultaneous determination of Pt and Rh using second derivative signal transformation – application to environmental samples. *Talanta*, *175*, 1–8. doi:10.1016/j.talanta.2017.06.067

Monteiro, C. E., Cobelo-García, A., Caetano, M., & Correia dos Santos, M. (2020). Speciation analysis of Pt and Rh in urban road dust leachates. *Science of The Total Environment*, *722*, 137954. doi:https://doi.org/10.1016/j.scitotenv.2020.137954

Monteiro, C. E., Correia dos Santos, M., Cobelo-García, A., Brito, P., & Caetano, M. (2019). Platinum and rhodium in Tagus estuary, SW Europe: sources and spatial distribution. *Environmental Monitoring and Assessment*, *191*(9), 579. doi:10.1007/s10661-019-7738-z

Monti, P., & Leuzzi, G. (2010). Lagrangian models of dispersion in marine environment. *Environmental Fluid Mechanics*, *10*(6), 637–656. doi:10.1007/s10652-010-9184-x

Neves, F. J. (2010). *Dynamics and hydrology of the Tagus estuary: results from in situ observations.* PhD Thesis, University of Lisbon, Portugal.

Neves, R. (1983). Biodimensional model for residual circulation in coastal zones: application to the Sado estuary. *Annales geophysicae (1983)*, *3*(4), 465–471.

Nygren, O., Vaughan, G. T., Florence, T. M., Morrison, G. M., Warner, I. M., & Dale, L. S. (1990). Determination of platinum in blood by adsorptive voltammetry. *Analytical chemistry*, *62*(15), 1637–40. doi:10.1021/ac00214a020

Obata, H., Yoshida, T., & Ogawa, H. (2006). Determination of picomolar levels of platinum in estuarine waters: A comparison of cathodic stripping voltammetry and isotope dilution-inductively coupled plasma mass spectrometry. *Analytica Chimica Acta*, *580*(1), 32–38. doi:https://doi.org/10.1016/j.aca.2006.07.044

Oun, R., Moussa, Y. E., & Wheate, N. J. (2018). The side effects of platinum-based chemotherapy drugs: a review for chemists. *Dalton Transactions*, *47*(19), 6645–6653. doi:10.1039/C8DT00838H

Pawlak, J., Lodyga-Chruścińska, E., & Chrustowicz, J. (2014). Fate of platinum metals in the environment. *Journal of Trace Elements in Medicine and Biology*, *28*(3), 247–254. doi:10.1016/j.jtemb.2014.03.005

Peucker-Ehrenbrink, B., & Jahn, B. (2001). Rhenium-osmium isotope systematics and platinum group element concentrations: Loess and the upper continental crust. *Geochemistry, Geophysics, Geosystems*, *2*(10), n/a-n/a. doi:10.1029/2001GC000172

Qi, L., Luo, Q., Zhang, Y., Jia, F., Zhao, Y., & Wang, F. (2019). Advances in Toxicological Research of the Anticancer Drug Cisplatin. *Chemical Research in Toxicology*, *32*(8), 1469–1486. doi:10.1021/acs.chemrestox.9b00204

Rauch, S., & Peucker-Ehrenbrink, B. (2015). Sources of Platinum Group Elements in the Environment BT - Platinum Metals in the Environment. In F. Zereini & C. L. S. Wiseman (Eds.), (pp. 3–17). Berlin, Heidelberg: Springer Berlin Heidelberg. doi:10.1007/978-3-662-44559-4_1

Ravindra, K., Bencs, L., & Van Grieken, R. (2004). Platinum group elements in the environment and their health risk. *The Science of the total environment*, *318*(1–3), 1–43. doi:10.1016/S0048-9697(03)00372-3

Simpson, P. V, Desai, N. M., Casari, I., Massi, M., & Falasca, M. (2019). Metal-based antitumor compounds: beyond cisplatin. *Future Medicinal Chemistry*, *11*(2), 119–135. doi:10.4155/fmc-2018-0248

Suh, S. W. (2006). A hybrid approach to particle tracking and Eulerian-Lagrangian models in the simulation of coastal dispersion. *Environmental Modelling and Software*, *21*(2), 234–242. doi:10.1016/j.envsoft.2004.04.015

Sung, W. (1995). Some Obsenmtions on Surface Partitioning of Cd, Cu, and Zn in Estuaries. *Environmental Science and Technology*, *29*(5), 1303–1312. doi:10.1021/es00005a024

Suzuki, A., Obata, H., Okubo, A., & Gamo, T. (2014). Precise determination of dissolved platinum in seawater of the Japan Sea, Sea of Okhotsk and western North Pacific Ocean. *Marine Chemistry*, *166*, 114–121.

doi:http://dx.doi.org/10.1016/j.marchem.2014.10.003

Taylor, S. R., & McLennan, S. M. (1995). The geochemical evolution of the continental crust. *Reviews of Geophysics*, *33*(2), 241–265. doi:10.1029/95RG00262

Tessier, A. (2019). Sorption of Trace Elements on Natural Particles in Oxic Environments. In J. Buffle & H. P. van Leeuwen (Eds.), *Environmental Particles* (p. 576). CRC Press. doi:10.1201/9780429286223

Turner, A., Crussell, M., Millward, G. E., Cobelo-García, A., & Fisher, A. S. (2006). Adsorption kinetics of platinum group elements in river water. *Environmental Science and Technology*, *40*(5), 1524–1531. doi:10.1021/es0518124

Vale, C. (1986). Transport of particulate metals at different fluvial and tidal energies in the Tagus River estuary. *Rapports (Process Verbal) des Réunions du Conseil international pour l'Exploration de la Mer Méditerranée*, *186*, 306–312.

Vale, C., & Sundby, B. (1987). Suspended sediment fluctuations in the Tagus estuary on semi-diurnal and fortnightly time scales. *Estuarine, Coastal and Shelf Science*, *25*(5), 495–508. doi:http://dx.doi.org/10.1016/0272-7714(87)90110-7

Vaz, N., & Dias, J. M. (2014). Residual currents and transport pathways in the Tagus estuary, Portugal: the role of freshwater discharge and wind. *Journal of Coastal Research*, 610–615. doi:10.2112/SI70-103.1

Vyas, N., Turner, A., & Sewell, G. (2014). Platinum-based anticancer drugs in waste waters of a major UK hospital and predicted concentrations in recipient surface waters. *Science of The Total Environment*, *493*, 324–329. doi:https://doi.org/10.1016/j.scitotenv.2014.05.127

Wilkinson, K. J., Lead, J. R., & Eds. (2006). *Environmental Colloids and Particles: Behaviour, Separation and Characterisation, Volume 10*. *Environmental Colloids and Particles: Behaviour, Separation and Characterisation* (1st ed.). Chichester, UK: John Wiley & Sons, Ltd. doi:ISBN: 9780470024539

Wolf, R. E., & Adams, M. (2015). *Multi-Elemental Analysis of Aqueous Geochemical Samples by ICP-MS*. doi:https://dx.doi.org/10.3133/ofr20151010

Zhong, L., Yan, W., Li, J., Tu, X., Liu, B., & Xia, Z. (2012). Pt and Pd in sediments from the Pearl River Estuary, South China: background levels, distribution, and source. *Environmental Science and Pollution Research*, *19*(4), 1305–1314. doi:10.1007/s11356-011-0653-7

VIII. GENERAL DISCUSSION

Platinum-group elements (PGE) are a group of rare and noble transitional elements that include platinum (Pt) and rhodium (Rh), which were particularly addressed in this work. Physical and chemical properties of Pt and Rh are remarkable and attractive to several sector-based industries of economic interest, having a large variety of applications. These are transverse from electronic to aeronautical industries as well as in the health sector and science (Johnson Matthey 2016). In the large industrial processes of manufacturing chemical compounds such as nitric and sulphuric acids, cortisone, hydrogen peroxide, ammonia and fertilizers, Pt and Rh supported catalysts are used (Hatfield et al. 1987; Lemaire et al. 2014; Paparatto et al. 2010). Drugs based on Pt, such as cisplatin, carboplatin and oxaliplatin, are efficient and thus administered to treat several malignancies (Falzone et al. 2018). Moreover, automotive catalytic converters (ACC) are equipped in cars throughout the world, imposed by regulatory authorities (e.g. European Commission 1991) to reduce toxic gases emission. The automotive sector *per se* has around 50 % of worldwide Pt and Rh demand (Johnson Matthey 2016). As a consequence of all necessities and the large diversity of usages, anthropogenic emissions of Pt and Rh into the environment will continue to raise and, therefore, responsible for an emerging environmental concern in spite of being critical elements. The abundance of both elements in the earth's upper continental crust (UCC) is very low, having in average global concentrations of 0.4 ng Pt g^{-1} and 0.06 ng Rh g^{-1} (Peucker-Ehrenbrink and Jahn 2001; Ravindra et al. 2004). In environmental matrices, Pt and Rh are usually found at concentrations of a few ng g^{-1} or L^{-1} (e.g. Zereini and Wiseman 2015). Therefore, to have suitable methods for the determination of Pt and Rh at the ultra-trace level is of major importance. Most of the commonly used techniques quantify the total concentration of elements after the proper pre-treatment of the sample. However, it is recognized that total concentrations *per se* do not reflect the potential toxicity of an element. Thus, sensitive and selective methods are still needed, in particular regarding speciation studies under relevant environmental conditions that demand sufficient selectivity and low limits of detection. The individual and simultaneous determination of Pt and Rh in different environmental matrices have resulted from the achieved improvements of the analytical techniques over the past few decades. This has been the case of ICP-MS and AdCSV (e.g. Zereini and Wiseman 2015). Despite the high sensitivity on Pt and Rh analysis, ICP-MS still presents some disadvantages, such as the need of matrix separation due to interferences of other elements (Labarraque et al. 2015). A simple and sensitive alternative is the use of voltammetric techniques, such as AdCSV, with the advantage of

direct Pt and Rh determination at ultra-trace levels. It is a less expensive method than ICP-MS and is also adequate for characterization and routine analysis of several environmental compartments (Zereini and Wiseman 2015; Locatelli 2007).

Information about Pt remains scarce in aquatic environments, despite all the efforts to understand its biogeochemical cycle. Research on Pt and Rh anthropogenic emissions has focused mainly on Pt and particularly on its distribution in rural, urban and industrial areas (e.g. Zereini and Wiseman 2015). In aquatic systems is noteworthy the limited number of studies dealing with a spatially-resolved distribution of Pt (Cobelo-García et al. 2011, 2013; Monteiro et al. 2019; Terashima et al. 1993; Wei and Morrison 1994; Zhong et al. 2012). This is even more restricted for Rh in particular, being such studies rarer (Essumang et al. 2008; Monteiro et al. 2019) and data still lacking in estuarine waters and organisms. Concentrations of Pt and Rh in sediments are usually close to background levels (<0.5 ng g^{-1}) or of a few ng g^{-1} (Cobelo-García et al. 2013; Monteiro et al. 2019; Zhong et al. 2012). Yet, other point sources may increase their levels, such as industries that use Pt and Rh catalysts in manufacturing processes. Another source of Pt to aquatic systems is the Pt-based compounds excreted by patients that enter hospital and domestic sewage during cancer treatments. Moreover, road dust also presents much higher concentrations of Pt and Rh, being a major anthropogenic reservoir of both elements (Zereini and Wiseman 2015) resulting from ACC, whose exhaust fumes contain Pt and Rh fine particulate material usually in the form of micro- or nanoparticles (Palacios et al. 2000). Deposited particles on the roadside are eventually washed by heavy rain events, entering the urban drainage. Thus, waste- and pluvial waters runoff are a pathway for urban Pt and Rh input to nearby aquatic systems (Monteiro et al. 2017; Vyas et al. 2014). Other dissemination mechanisms to aquatic systems may occur through the atmosphere, where Pt and Rh are dispersed in airborne particles by the wind action. This mechanism of spread has been essentially attributed to ACC, whose particles return to the earth's surface by wet or dry atmospheric deposition on either land or water.

Information about how and which forms of Pt and Rh are released to the aquatic systems nor their chemical behaviour under environmentally relevant conditions are clear. Some studies point to the emission of Pt and Rh from ACC mainly as particulate material (Ek et al. 2004; Ely et al. 2001; Prichard and Fisher 2012; Rauch et al. 2002), yet a soluble fraction has also been measured (Moldovan et al. 2002). Speciation analysis schemes in aquatic environments are used to discriminate between particulate and

dissolved fractions, i.e. the latter usually filtered through a 0.45 µm porous membrane (Burden et al. 2002). Yet, colloids (<1000 nm; Wilkinson et al. 2006) and nanoparticles (<100 nm; Auffan et al., 2009) are also included in the operationally defined 'dissolved' forms and whose mobility and bioavailability may be different from truly dissolved species (Guo and Santschi 2006). Furthermore, the solubility of Pt and Rh can vary depending on engine type and the age of the catalyst, as well as on the individual element chemistry (Ash et al. 2014). So, a combination of several methods can be a useful strategy in providing new insights into the speciation analysis of Pt and Rh. This could help to understand their chemical behaviour in aquatic systems, such as estuaries, as well as the metals fractionation.

Besides the essential chemical characterization of environmental and aquatic samples, Pt and Rh remain scarcely understood in the water column of estuaries (e.g. Cobelo-García et al. 2013; Cobelo-García et al. 2014). The levels of particulate Pt and Rh in waters are usually associated with suspended particulate matter (SPM), having concentrations of a few ng g^{-1} and often close to sediment levels (Cobelo-García et al. 2013; Cobelo-García et al. 2014). More recently, Abdou et al. (2020) also reported that phytoplankton played a role on the Pt levels observed in contrasting locations from the Atlantic and Mediterranean sea. As to their dissolved concentrations in the water column, Pt in general ranges up to 15 ng L^{-1} (Cobelo-García et al. 2013; Cobelo-García et al. 2014; Soyol-Erdene and Huh 2012). Dissolved Rh concentrations have only been reported in the ocean, between 0.04 and 0.1 ng L^{-1} (Bertine et al. 1993). Furthermore, there is a lack of knowledge on Pt and Rh chemical behaviour under hydrodynamic conditions, such as those in tidally driven estuaries, as well as the mass exchanges occur with adjacent coastal areas.

The Tagus estuary is one of the largest estuaries in Europe that possesses unique environmental features and considerable anthropogenic pressures, making it a natural laboratory to the study of Pt and Rh. The wide inner bay is shallow (<7 m) with a complex bathymetry that shapes towards a downstream deeper and narrow inlet, connecting to the Atlantic Ocean (e.g. Vale and Sundby 1987). The tidal regime of the Tagus estuary is mainly semi-diurnal and tidally driven, dominated by shorter ebbs but with stronger current velocities than in the floods (Fortunato et al. 1999; Guerreiro et al. 2015; Vaz and Dias 2014). The margins are densely populated and the urban area is linked to the estuary through several WWTP and pluvial water drainage channels. Several industries are also

settled around the estuary, with historical records of manufacturing chemicals, fertilizers, food, steel and ore processing. Moreover, two high traffic motorway bridges cross the estuary. All these characteristics made the Tagus estuary vulnerable to contamination over decades (Brito et al. 2018; Cesário et al. 2016, 2017; Mil-Homens et al. 2009; Vale et al. 2008). Platinum and Rh in sediments of the Tagus estuary unveiled an increasing concern on the extent of their contamination, addressed in a limited number of studies focusing mainly on Pt (Almécija et al. 2015, 2016a, 2016b; Cobelo-García et al. 2011). Therefore, this thesis intended to improve the current knowledge of this element and to add new information about Rh by addressing topics that were not clarified yet in Tagus estuary. Summarizing, the sources and extent of Pt and Rh contamination were evaluated through sediment, road dust and water samples, providing new insights on the occurrence and fate, as well as their biogeochemical behaviour in a hydrodynamic estuary such as the Tagus.

The optimization procedure for the simultaneous determination of Pt and Rh using AdCSV and its application to complex environmental matrices was carried out (Monteiro et al. 2017). The main goal of the work was to take advantage of using the second derivative signal transformation in the simultaneous analysis of Pt and Rh to reduce the intense background current and/or interfering peaks. These commonly cause ill-defined peaks that affect the target signal, influencing the accuracy of measurements (Almécija et al. 2016; Cobelo-García et al. 2014). The optimized procedure maintained the use of Pt surface-active complex with formazone, which is produced *in situ* from the reaction of formaldehyde (FA) and hydrazine (HZ) (Locatelli 2007; van den Berg and Jacinto 1988; León et al. 1997; Cobelo-García et al. 2014). The Pt-complex is adsorbed on the mercury electrode and the catalytic-promoted hydrogen reduction occurs in acidic conditions (e.g. H_2SO_4) due to the formation of Pt(0). Furthermore, the catalytic behaviour of Pt(IV) is similar to Pt(II), since hydrazine can quantitatively reduce Pt(IV) to Pt(II) (Zhao and Freiser 1986). In the case of Rh, catalytic waves in formaldehyde–HCl media have been reported (Cobelo-García 2013; Hong et al. 1994; Almécija et al. 2016), however, the nature of Rh surface-active formaldehyde complexes was confirmed. The investigated and optimized experimental conditions included the suitable electrolyte solution for the analysis of both elements, with reduced reagents consumption (0.25 M H_2SO_4, 0.05 M HCl, 0.01 M FA and 0.5 mM HZ). The deposition time (t_d) and deposition potential (E_d) were also surveyed for the optimal operating conditions. For t_d = 120 s and E_d = –0.75 V,

linearity presented r > 0.999, obtained for concentrations ranging up to 5.8 ng L^{-1} (27 pM) for Pt and up to 3.4 ng L^{-1} (34 pM) for Rh. The attained LODs were 0.2 ng Pt L^{-1} and 0.08 ng Rh L^{-1}. In addition, lower LOD were achieved by increasing t_d. Possible interferences were also evaluated and only the sensitivity of Pt during analysis was affected by elevated Zn concentrations (>2 mg L^{-1}), whereas for Rh a minor effect was observed. Intermediate precision expressed as relative standard deviation, based on spiked samples and digested road dust CRM BCR-723 using Pt and Rh standard solutions, was 17 % and 20 % for Pt and Rh, respectively. Recoveries of CRM were around 90 % for both elements. The optimized method for simultaneous determination of Pt and Rh was successfully applied in sediments from Tagus estuary and for the first time dissolved Rh was determined in water samples of a WWTP (Monteiro et al. 2017). From all the reasons abovementioned, the adequacy of the optimized procedure was proven to be suitable for several environmental matrices, even the most complex, such as road dust and wastewaters. Therefore, the subsequent thesis work was performed mainly using the AdCSV optimized procedure.

The spatial distribution of Pt and Rh in superficial sediment samples (n = 72) of Tagus estuary was assessed and their sources discussed (Monteiro et al. 2019). The concentrations found in the sediments varied within 0.18–5.1 ng Pt g^{-1} and 0.02–1.5 ng Rh g^{-1}. Four distinct areas were established for the Tagus: “reference”; waste- and pluvial water discharge; motorway bridges and industrialised areas. The median concentrations calculated for the reference samples, distant from potential point sources of Pt and Rh, were 0.55 ng Pt g^{-1} and 0.27 ng Rh g^{-1}. However, the reference level for Rh in the estuary was five times higher than the background estimated for the UCC, suggesting the steady increase of anthropogenic emissions. The highest concentrations of Pt and Rh were found nearby industrialised areas and a motorway bridge, corresponding to enrichments of 10 and 6 times the estuary reference levels of Pt and Rh, respectively. The main sources of contamination to the Tagus estuary derived from historical and present industrial activities as well as automotive catalytic converters. The large variations of Pt/Rh found (0.48–39) point to those different sources, with the highest ratio observed in industrial areas. This indicates that Pt and Rh loading from industrial activities to the estuary cannot be disregarded. Past and present industrial activities showed to have clear signatures of Pt and Rh, as documented by Monteiro et al. (2019). The authors estimated that a historical hotspot for metals contamination (BRR) has added to the estuary increased

levels of Pt in comparison to Rh. Furthermore, other sources of Pt and Rh to the aquatic environment exist (Rauch and Peucker-Ehrenbrink 2015) and data from spatial distribution in sediments are important to effectively assess them (Monteiro et al. 2019; Zhong et al. 2012). The medicinal uses of Pt and consequentially its emission remain poorly understood in the Tagus and further investigation is still needed to assess the extent of the contamination.

Even so, catalytic converters from vehicles may be considered, perhaps, the most widespread source of anthropogenic Pt and Rh to the Tagus estuary. Several pathways from urban areas towards the estuary exist, such as the waste- and pluvial runoff as well as the bridges crossing the estuary. While in the sediments of the wastewater outfalls there was a Pt and Rh signal imprinted, Monteiro et al. (2019) observed along the *Vasco da Gama* (VG) bridge a clear signature that could only result from ACC emissions. Moreover, the structural features of the bridge and its extension (~17 km) contributed largely to the observed pattern of distribution. The road dust material accumulated and concentrated along the bridge roadsides during dry periods is then washed directly to the estuary during rain periods. The road dust enters directly into the estuary through a system of gully pots located along the bridge and is spread according to the tidal and hydrodynamic regime. In opposition, the downstream *25 de Abril* (25A) bridge is shorter (~2 km) yet located higher than VG bridge, and has a gridded metallic deck that allows rainwater and road dust particles to pass through. Therefore, being more exposed to environmental conditions, such as wind, it easily allows the dispersion of road dust to either inland or the water regardless the higher traffic density (≈150 000 cars d^{-1}) than in VG bridge (≈50 000 cars d^{-1}). As such, the estimated emissions for both bridges confirm these observations. The computed total emissions since the opening of VG bridge in 1998 ranged from 542 – 937 g of Pt and 130 – 262 g of Rh. For the 25A bridge, lower intervals were found, 171 – 312 g of Pt and 41 – 87 g of Rh. Even with higher vehicle traffic on 25A bridge than in VG bridge, it is clear that their extension and structural characteristics play a crucial role in the distribution of Pt and Rh emissions from ACC.

As mentioned previously, physical drivers such as wind and rain events may force the transfer of Pt and Rh between compartments, affecting their distribution and ultimately transferring them from urban areas to the nearby aquatic systems. Along their path, Pt and Rh speciation may be affected by chemical changes in the media. A speciation analysis scheme for Pt and Rh in aquatic media was developed by Monteiro et

al. (2020) using a combination of several methods. A composite sample of road dust (<63 µm) was collected and thoroughly characterized. Some of its characteristics were similar to the certified reference material BCR-723 and other road dusts collected worldwide (Gunawardana et al. 2012). Yet, the differences found reflected local or regional circumstances, such as climacteric and moisture conditions, and the type of soil and surface properties of the pavements that affect the road dust mineralogical composition. Nevertheless, road dust is a major anthropogenic reservoir of Pt and Rh, as confirmed by the total concentrations found, 294 ng Pt g^{-1} and 44 ng Rh g^{-1}.

Monteiro et al. (2020) performed leaching experiments and analysed the filtered solutions (<0.45 µm) for Pt and Rh after incubation up to 7 days in synthetic rainwater and seawater. The leachates were measured for truly dissolved Pt and Rh concentrations using AdCSV (Monteiro et al. 2017), while total concentrations in the leachates were determined by ICP-MS. Truly dissolved species corresponded to a small fraction of total Pt and Rh in the road dust. Accordingly, Pt and Rh values in both media were 0.01 % and 0.1 %, respectively, of the total concentrations found in road dust and remained relatively constant over time. Contrarily, Folens et al. (2018) could only measure Pt nanoparticles. Furthermore, pH was found to have an impact on Pt dissolution (Jarvis et al. 2001), whereas in these experiments pH measured in all leachates was fairly constant and close to 8.

The concentration of total filter-passing species was higher than truly dissolved forms in the leachates and predominated by a factor of 10 for Pt and 2 to 3 for Rh. Particulate species coexist with truly dissolved forms in the operationally ‘dissolved’ fraction. Despite the uncertainties regarding the nature of the (nano)particles bearing Pt and Rh and/or Pt and Rh nanoparticles in the leachates, Monteiro et al. (2020) demonstrated that (nano)particles do exist in solution, with a higher concentration in seawater extracts. Nanoparticle tracking analysis (NTA) was used to investigate the presence of nanoparticles in the leachates, being an additional and independent evidence of their presence. Despite the limitations about the nature of Pt and Rh nanoparticles, the results confirmed their presence in the leachates and fully supported the conclusions drawn from AdCSV and ICP-MS data.

The simultaneous presence of (nano)particles and truly dissolved species was recently observed for Pt in real riverine samples of the Tagus estuary by Monteiro et al. (*in prep*). By using the same multi-method approach, differences between truly dissolved

forms and total filter-passing Pt species could be measured by AdCSV and ICP-MS, respectively. Moreover, the speciation analysis showed that total filter-passing forms of Pt were superimposed to those in the particulate fraction, with truly dissolved species representing nearly half of total Pt concentration in the water column. Contrarily, truly dissolved species of Rh were an important fraction of the total content released by ACC. Thus, dissolved species controlled Pt behaviour in the water column, whereas Rh appeared to be dominated by the particulate fraction (Monteiro et al. *in prep*). Moreover, particulate and dissolved Rh concentrations were never reported simultaneously in an estuary.

Although these are not listed as priority pollutants to be monitored in water quality programs, e.g. from the European Union, their rising concentrations in the aquatic environment bring interest about their chemical behaviour and distribution in waters. Monteiro et al. (*in prep*) described Pt and Rh occurrence in the water column of Tagus estuary in two distinct stations. The upstream station was the riverine end-member (VFX) of the Tagus and the downstream station was an outfall of a WWTP (ALC) near the Atlantic Ocean. Semi-diurnal tidal cycles, in neap (NT) and spring tides (ST), were evaluated for both particulate and dissolved (<0.45 m) fractions of Pt and Rh using AdCSV. Additional parameters such as temperature, conductivity, pH, dissolved oxygen and SPM were also measured. Concentrations in the particulate fraction ranged up to 25.6 ng Pt g^{-1} and 5.1 ng Rh g^{-1}, while in dissolved fraction concentrations ranged up to 11.7 ng Pt L^{-1} and 0.19 ng Rh L^{-1}. At the WWTP outfall, concentrations were higher than in the riverine end-member and Pt presented also higher concentrations than Rh. Moreover, dissolved Rh concentrations were below the LOD during NT at VFX. In the other tidal cycles surveyed, ST at VFX and both NT and ST at ALC, both particulate and dissolved Pt and Rh followed the hydrodynamic regime, in general presenting the highest concentrations during low tide. These results reflected the different anthropogenic inputs to the Tagus estuary. One was attributed to the ACC, whose road dust enters the urban drainage or is directly released to the estuary, as previously seen for the VG bridge (Monteiro et al. 2019). An additional source of Pt was pointed out at ALC station, where the input of Pt-based compounds could be confirmed. In addition to the Pt variation along with the tidal cycles, relative increments could be observed in the morning and afternoon periods, most likely related with personal care activities. This was also evidenced in the elevated mass Pt/Rh ratios, pointing to the presence of an additional source of Pt since

Rh levels were in the same order of magnitude of those found at VFX. Furthermore, the distribution coefficients of Pt and Rh did not vary along the salinity gradient observed in the estuary, as well as amongst tidal cycles and locations. However, Pt appeared to have non-conservative behaviour due to the larger inputs to the estuary than those estimated for Rh.

Additionally, there is also a need to understand the physical mechanisms that can act as driving forces on local and regional transport of Pt and Rh. The potential exchanges of both elements were also evaluated at the downstream station near the Atlantic Ocean, as it has shown the highest inputs to the estuary Monteiro et al. (*in prep*). It was noticed that higher metal concentrations were associated with the ebb opposing to the flood. By taking advantage of a hydrodynamic model implemented in the Tagus estuary and using a Lagrangian method to improve the understanding of only the physical drivers, the spread of the particles pointed out recirculation within the estuary and the export towards the Atlantic Ocean. The probability of particles' export from the inlet was very high and occurred fast, within 2 days. While the recirculation in the inner estuary may lead to the retention of some Pt and Rh, the export to the adjacent coastal area appears to be high, considering the concentrations found in the superficial sediments of the estuary (Monteiro et al. 2019). Therefore, the estuary is a net source of both Pt and Rh to the coastal environment.

Previously, Cobelo-García et al. (2011) reported a sub-surface Pt enrichment in a sediment core of the Tagus pro-delta. This was related to the extensive industrial activities in Tagus estuary around 1960s/70s that mimics the records found for Hg and Pb (Mil-Homens et al. 2009). Because the sampling of the core was in early 2000, less than one decade after the introduction of European legislation regarding the control of pollutants emission using ACC (European Commission 1991), a superficial enrichment of Pt was not fully observed. However, considering the increase of Pt and Rh uses for more than two decades, increased amounts of these metals could have been already exported to the adjacent coastal area. Once in the coastal environment, it is likely that regional-scale drivers, such as northerly winds and upwelling events, will affect the dispersion of Pt and Rh.

References

Abdou, M., Gil-Díaz, T., Schäfer, J., Catrouillet, C., Bossy, C., Dutruch, L., et al. (2020). Short-term variations of platinum concentrations in contrasting coastal environments: The role of primary producers. *Marine Chemistry*, *222*, 103782. doi:10.1016/j.marchem.2020.103782

Abdou, M., Schäfer, J., Hu, R., Gil-Díaz, T., Garnier, C., Brach-Papa, C., et al. (2019). Platinum in sediments and mussels from the northwestern Mediterranean coast: Temporal and spatial aspects. *Chemosphere*, *215*, 783–792. doi:https://doi.org/10.1016/j.chemosphere.2018.10.011

Almécija, C., Cobelo-García, A., & Santos-Echeandía, J. (2016). Improvement of the ultra-trace voltammetric determination of Rh in environmental samples using signal transformation. *Talanta*, *146*, 737–743. doi:10.1016/j.talanta.2015.06.032

Almécija, C., Cobelo-García, A., Santos-Echeandía, J., & Caetano, M. (2016). Platinum in salt marsh sediments: Behavior and plant uptake. *Marine Chemistry*, *185*, 91–103. doi:10.1016/j.marchem.2016.05.009

Almécija, C., Sharma, M., Cobelo-García, A., Santos-Echeandía, J., & Caetano, M. (2015). Osmium and platinum decoupling in the environment: Evidences in intertidal sediments (Tagus Estuary, SW Europe). *Environmental Science and Technology*, *49*(11), 6545–6553. doi:10.1021/acs.est.5b00591

Ash, P. W., Boyd, D. A., Hyde, T. I., Keating, J. L., Randlshofer, G., Rothenbacher, K., et al. (2014). Local Structure and Speciation of Platinum in Fresh and Road-Aged North American Sourced Vehicle Emissions Catalysts: An X-ray Absorption Spectroscopic Study. *Environmental Science & Technology*, *48*(7), 3658–3665. doi:10.1021/es404974e

Auffan, M., Rose, J., Bottero, J.-Y., Lowry, G. V, Jolivet, J.-P., & Wiesner, M. R. (2009). Towards a definition of inorganic nanoparticles from an environmental, health and safety perspective. *Nature Nanotechnology*, *4*(10), 634–641. doi:10.1038/nnano.2009.242

Bertine, K. K., Koide, M., & Goldberg, E. D. (1993). Aspects of rhodium marine chemistry. *Marine Chemistry*, *42*(3), 199–210. doi:https://doi.org/10.1016/0304-4203(93)90012-D

Brito, P., Prego, R., Mil-Homens, M., Caçador, I., & Caetano, M. (2018). Sources and distribution of yttrium and rare earth elements in surface sediments from Tagus estuary, Portugal. *Science of The Total Environment*, *621*, 317–325. doi:https://doi.org/10.1016/j.scitotenv.2017.11.245

Burden, F. R., Foerstner, U., McKelvie, I. D., & Guenther, A. (2002). *Environmental Monitoring Handbook*. New York: McGraw-Hill Education. doi:ISBN: 9780071351768

Cesário, R, Monteiro, C. E., Nogueira, M., O'Driscoll, N. J., Caetano, M., Hintelmann, H., et al. (2016). Mercury and Methylmercury Dynamics in Sediments on a Protected Area of Tagus Estuary (Portugal). *Water, Air, and Soil Pollution*. doi:10.1007/s11270-016-3179-2

Cesário, Rute, Hintelmann, H., O'Driscoll, N. J., Monteiro, C. E., Caetano, M., Nogueira,

M., et al. (2017). Biogeochemical Cycle of Mercury and Methylmercury in Two Highly Contaminated Areas of Tagus Estuary (Portugal). *Water, Air, & Soil Pollution*, *228*(7), 257. doi:10.1007/s11270-017-3442-1

Cobelo-García, A. (2013). Kinetic effects on the interactions of Rh(III) with humic acids as determined using size-exclusion chromatography (SEC). *Environmental Science and Pollution Research*, *20*(4), 2330–2339. doi:10.1007/s11356-012-1113-8

Cobelo-García, A., López-Sánchez, D. E., Almécija, C., & Santos-Echeandía, J. (2013). Behavior of platinum during estuarine mixing (Pontevedra Ria, NW Iberian Peninsula). *Marine Chemistry*, *150*, 11–18. doi:10.1016/j.marchem.2013.01.005

Cobelo-García, A., López-Sánchez, D. E., Schäfer, J., Petit, J. C. J., Blanc, G., & Turner, A. (2014). Behavior and fluxes of Pt in the macrotidal Gironde Estuary (SW France). *Marine Chemistry*, *167*, 93–101. doi:10.1016/j.marchem.2014.07.006

Cobelo-García, A., Neira, P., Mil-Homens, M., & Caetano, M. (2011). Evaluation of the contamination of platinum in estuarine and coastal sediments (Tagus Estuary and Prodelta, Portugal). *Marine Pollution Bulletin*, *62*(3), 646–650. doi:10.1016/j.marpolbul.2010.12.018

Cobelo-García, A., Santos-Echeandía, J., López-Sánchez, D. E., Almécija, C., & Omanović, D. (2014). Improving the Voltammetric Quantification of Ill-Defined Peaks Using Second Derivative Signal Transformation: Example of the Determination of Platinum in Water and Sediments. *Analytical Chemistry*, *86*(5), 2308–2313. doi:10.1021/ac403558y

Ek, K. H., Morrison, G. M., & Rauch, S. (2004). Environmental routes for platinum group elements to biological materials--a review. *The Science of the total environment*, *334–335*, 21–38. doi:10.1016/j.scitotenv.2004.04.027

Ely, J. C., Neal, C. R., Kulpa, C. F., Schneegurt, M. A., Seidler, J. A., & Jain, J. C. (2001). Implications of Platinum-Group Element Accumulation along U.S. Roads from Catalytic-Converter Attrition. *Environmental Science & Technology*, *35*(19), 3816–3822. doi:10.1021/es001989s

Essumang, D. K., Dodoo, D. K., & Adokoh, C. K. (2008). The impact of vehicular fallout on the Pra estuary of Ghana (a case study of the impact of platinum group metals (PGMs) on the marine ecosystem). *Environmental Monitoring and Assessment*, *145*(1), 283–294. doi:10.1007/s10661-007-0037-0

European Commission. (1991). Council Directive 91/542/EEC of 1 October 1991 amending Directive 88/77/EEC on the approximation of the laws of the Member States relating to the measures to be taken against the emission of gaseous pollutants from diesel engines for use in vehicles. http://eur-lex.europa.eu/eli/dir/1991/542/oj. Accessed 22 January 2018

Falzone, L., Salomone, S., & Libra, M. (2018). Evolution of cancer pharmacological treatments at the turn of the third millennium. *Frontiers in Pharmacology*. doi:10.3389/fphar.2018.01300

Folens, K., Van Acker, T., Bolea-Fernandez, E., Cornelis, G., Vanhaecke, F., Du Laing, G., & Rauch, S. (2018). Identification of platinum nanoparticles in road dust leachate by single particle inductively coupled plasma-mass spectrometry. *Science of The Total Environment*, *615*, 849–856.

doi:https://doi.org/10.1016/j.scitotenv.2017.09.285

Fortunato, A., Oliveira, A., & Baptista, A. M. (1999). On the effect of tidal flats on the hydrodynamics of the Tagus estuary. *Oceanologica Acta*, *22*(1), 31–44. doi:https://doi.org/10.1016/S0399-1784(99)80030-9

Guerreiro, M., Fortunato, A. B., Freire, P., Rilo, A., Taborda, R., Freitas, M. C., et al. (2015). Evolution of the hydrodynamics of the Tagus estuary (Portugal) in the 21st century. *Journal of Integrated Coastal Zone Management*, *15*(1), 65–80. doi:10.5894/rgci515

Gunawardana, C., Goonetilleke, A., Egodawatta, P., Dawes, L., & Kokot, S. (2012). Source characterisation of road dust based on chemical and mineralogical composition. *Chemosphere*, *87*(2), 163–170. doi:https://doi.org/10.1016/j.chemosphere.2011.12.012

Guo, L., & Santschi, P. H. (2006, December 15). Ultrafiltration and its Applications to Sampling and Characterisation of Aquatic Colloids. *Environmental Colloids and Particles*. doi:doi:10.1002/9780470024539.ch4

Hatfield, W. R., Beshty, B. S., Lee, H. C., Heck, R. M., & Hsiung, T. M. (1987, November 11). Method for recovering platinum in a nitric acid plant. Google Patents.

Hong, T.-K., Czae, M.-Z., Lee, C., Kwon, Y.-S., & Hong, M.-J. (1994). Determination of Ultratraces of Rhodium by Adsorptive Stripping Voltammetry of Formaldehyde Complex. *Bulletin of the Korean Chemical Society*, *15*(12), 1035–1037.

Jarvis, K. E., Parry, S. J., & Piper, J. M. (2001). Temporal and Spatial Studies of Autocatalyst-Derived Platinum, Rhodium, and Palladium and Selected Vehicle-Derived Trace Elements in the Environment. *Environmental Science & Technology*, *35*(6), 1031–1036. doi:10.1021/es0001512

Johnson Matthey. (2016). *Platinum Group Metals Market Report - November*.

Labarraque, G., Oster, C., Fisicaro, P., Meyer, C., Vogl, J., Noordmann, J., et al. (2015). Reference measurement procedures for the quantification of platinum-group elements (PGEs) from automotive exhaust emissions. *International Journal of Environmental Analytical Chemistry*, *95*(9), 777–789. doi:10.1080/03067319.2015.1058931

Lemaire, A., Dournel, P., & Deschrijver, P. (2014, March 13). Process for the manufacture of hydrogen peroxide. Google Patents.

León, C., Emons, H., Ostapczuk, P., & Hoppstock, K. (1997). Simultaneous ultratrace determination of platinum and rhodium by cathodic stripping voltammetry. *Analytica Chimica Acta*, *356*(1), 99–104. doi:http://dx.doi.org/10.1016/S0003-2670(97)00520-5

Locatelli, C. (2007). Voltammetric Analysis of Trace Levels of Platinum Group Metals – Principles and Applications. *Electroanalysis*, *19*(21), 2167–2175. doi:10.1002/elan.200704026

Mil-Homens, M., Branco, V., Vale, C., Boer, W., Alt-Epping, U., Abrantes, F., & Vicente, M. (2009). Sedimentary record of anthropogenic metal inputs in the Tagus prodelta (Portugal). *Continental Shelf Research*, *29*(2), 381–392. doi:10.1016/j.csr.2008.10.002

Moldovan, M., Palacios, M. A., Gómez, M. M., Morrison, G., Rauch, S., McLeod, C., et al. (2002). Environmental risk of particulate and soluble platinum group elements released from gasoline and diesel engine catalytic converters. *Science of The Total Environment*, *296*(1), 199–208. doi:https://doi.org/10.1016/S0048-9697(02)00087-6

Monteiro, C. E., Cobelo, A., Correia dos Santos, M., & Caetano, M. (n.d.). Drivers of Pt and Rh variability in the water column of a hydrodynamic estuary: effects of contrasting environments. *in prep*, prep.

Monteiro, C. E., Cobelo-García, A., Caetano, M., & Correia dos Santos, M. (2020). Speciation analysis of Pt and Rh in urban road dust leachates. *Science of The Total Environment*, *722*, 137954. doi:https://doi.org/10.1016/j.scitotenv.2020.137954

Monteiro, C. E., Cobelo-García, A., Caetano, M., & Santos, M. M. C. dos. (2017). Improved voltammetric method for simultaneous determination of Pt and Rh using second derivative signal transformation – application to environmental samples. *Talanta*. doi:10.1016/j.talanta.2017.06.067

Monteiro, C. E., Correia dos Santos, M., Cobelo-García, A., Brito, P., & Caetano, M. (2019). Platinum and rhodium in Tagus estuary, SW Europe: sources and spatial distribution. *Environmental Monitoring and Assessment*, *191*(9), 579. doi:10.1007/s10661-019-7738-z

Mulholland, R., & Turner, A. (2011). Accumulation of platinum group elements by the marine gastropod Littorina littorea. *Environmental Pollution*, *159*(4), 977–982. doi:https://doi.org/10.1016/j.envpol.2010.12.009

Neira, P., Cobelo-García, A., Besada, V., Santos-Echeandía, J., & Bellas, J. (2015). Evidence of increased anthropogenic emissions of platinum: Time-series analysis of mussels (1991–2011) of an urban beach. *Science of The Total Environment*, *514*, 366–370. doi:https://doi.org/10.1016/j.scitotenv.2015.02.016

Palacios, M. A., Gómez, M. M., Moldovan, M., Morrison, G., Rauch, S., McLeod, C., et al. (2000). Platinum-group elements: quantification in collected exhaust fumes and studies of catalyst surfaces. *Science of The Total Environment*, *257*(1), 1–15. doi:https://doi.org/10.1016/S0048-9697(00)00464-2

Paparatto, G., De, A. G., D'aloisio, R., & Buzzoni, R. (2010, September 28). Catalyst and its use in the synthesis of hydrogen peroxide. Google Patents.

Peucker-Ehrenbrink, B., & Jahn, B. (2001). Rhenium-osmium isotope systematics and platinum group element concentrations: Loess and the upper continental crust. *Geochemistry, Geophysics, Geosystems*, *2*(10), n/a-n/a. doi:10.1029/2001GC000172

Prichard, H. M., & Fisher, P. C. (2012). Identification of Platinum and Palladium Particles Emitted from Vehicles and Dispersed into the Surface Environment. *Environmental Science & Technology*, *46*(6), 3149–3154. doi:10.1021/es203666h

Rauch, S., Morrison, G. M., & Moldovan, M. (2002). Scanning laser ablation-ICP-MS tracking of platinum group elements in urban particles. *Science of The Total Environment*, *286*(1), 243–251. doi:https://doi.org/10.1016/S0048-9697(01)00988-3

Rauch, S., & Peucker-Ehrenbrink, B. (2015). Sources of platinum group elements in the environment. In *Platinum metals in the environment* (pp. 3–17). Springer.

Ravindra, K., Bencs, L., & Van Grieken, R. (2004). Platinum group elements in the environment and their health risk. *The Science of the total environment*, *318*(1–3), 1–43. doi:10.1016/S0048-9697(03)00372-3

Ruchter, N., & Sures, B. (2015). Distribution of platinum and other traffic related metals in sediments and clams (Corbicula sp.). *Water Research*, *70*, 313–324. doi:http://dx.doi.org/10.1016/j.watres.2014.12.011

Soyol-Erdene, T.-O., & Huh, Y. (2012). Dissolved platinum in major rivers of East Asia: Implications for the oceanic budget. *Geochemistry, Geophysics, Geosystems*, *13*(6), n/a-n/a. doi:10.1029/2012GC004102

Terashima, S., Katayama, H., & Itoh, S. (1993). Geochemical behavior of Pt and Pd in coastal marine sediments, southeastern margin of the Japan Sea. *Applied Geochemistry*, *8*(3), 265–271. doi:https://doi.org/10.1016/0883-2927(93)90041-E

Vale, C., Canário, J., Caetano, M., Lavrado, J., & Brito, P. (2008). Estimation of the anthropogenic fraction of elements in surface sediments of the Tagus Estuary (Portugal). *Marine Pollution Bulletin*, *56*(7), 1364–1367. doi:https://doi.org/10.1016/j.marpolbul.2008.04.006

Vale, C., & Sundby, B. (1987). Suspended sediment fluctuations in the Tagus estuary on semi-diurnal and fortnightly time scales. *Estuarine, Coastal and Shelf Science*, *25*(5), 495–508. doi:http://dx.doi.org/10.1016/0272-7714(87)90110-7

van den Berg, C. M. G., & Jacinto, G. S. (1988). The determination of platinum in sea water by adsorptive cathodic stripping voltammetry. *Analytica Chimica Acta*, *211*, 129–139. doi:http://dx.doi.org/10.1016/S0003-2670(00)83675-2

Vaz, N., & Dias, J. M. (2014). Residual currents and transport pathways in the Tagus estuary, Portugal: the role of freshwater discharge and wind. *Journal of Coastal Research*, 610–615. doi:10.2112/SI70-103.1

Vyas, N., Turner, A., & Sewell, G. (2014). Platinum-based anticancer drugs in waste waters of a major UK hospital and predicted concentrations in recipient surface waters. *Science of The Total Environment*, *493*, 324–329. doi:https://doi.org/10.1016/j.scitotenv.2014.05.127

Wei, C., & Morrison, G. M. (1994). Platinum in road dusts and urban river sediments. *Science of The Total Environment*, *146–147*(Supplement C), 169–174. doi:https://doi.org/10.1016/0048-9697(94)90234-8

Wilkinson, K. J., Lead, J. R., & Eds. (2006). *Environmental Colloids and Particles: Behaviour, Separation and Characterisation, Volume 10*. *Environmental Colloids and Particles: Behaviour, Separation and Characterisation* (1st ed.). Chichester, UK: John Wiley & Sons, Ltd. doi:ISBN: 9780470024539

Zereini, F., & Wiseman, C. L. S. (2015). *Platinum Metals in the Environment*. (F. Zereini & C. L. S. Wiseman, Eds.). Berlin, Heidelberg: Springer Berlin Heidelberg. doi:10.1007/978-3-662-44559-4

Zhao, Z., & Freiser, H. (1986). Differential pulse polarographic determination of trace levels of platinum. *Analytical Chemistry*, *58*(7), 1498–1501.

doi:10.1021/ac00298a050

Zhong, L., Yan, W., Li, J., Tu, X., Liu, B., & Xia, Z. (2012). Pt and Pd in sediments from the Pearl River Estuary, South China: background levels, distribution, and source. *Environmental Science and Pollution Research*, *19*(4), 1305–1314. doi:10.1007/s11356-011-0653-7

Zimmermann, S., Sures, B., & Ruchter, N. (2015). Laboratory Studies on the Uptake and Bioaccumulation of PGE by Aquatic Plants and Animals BT - Platinum Metals in the Environment. In F. Zereini & C. L. S. Wiseman (Eds.), (pp. 361–381). Berlin, Heidelberg: Springer Berlin Heidelberg. doi:10.1007/978-3-662-44559-4_23

IX. CONCLUSIONS AND FUTURE PERSPECTIVES

9.1. Conclusions

This work has provided new insights on Pt and Rh in the aquatic system of Tagus estuary, SW Europe. The increasing levels of Pt and Rh and their sources are visible in several matrices of the estuary, particularly owing to continuous and recent anthropogenic inputs. The current understanding of Pt and Rh occurrence and distribution in a highly hydrodynamic system such as the Tagus estuary has considerably improved with the contribution of this work. Moreover, some of the current knowledge gaps regarding Pt and Rh speciation analysis in aquatic systems were also addressed.

Several objectives were proposed in section II, upon questions for which answers were still poorly documented, in particular regarding Rh. Therefore, the main conclusions of this thesis respond to those goals and can be summarized as follows:

- The simultaneous determination of Pt and Rh by Adsorptive Cathodic Stripping Voltammetry (AdCSV) using the second derivative of the voltammograms was optimized and successfully applied to relevant environmental samples. (objective 1)
- The optimized and validated method offers the high sensitivity necessary to measure the low signals frequently observed in low contaminated environmental samples, therefore being suitable for the analytical quantification of Pt and Rh. (objective 1)
- Reagents consumption and time of analysis were also optimized in the analytical procedure, reducing the costs and time of analysis and turning the method attractive for routine analysis. (objective 1)
- At ultra-trace concentrations in water samples, the simultaneous determination of Pt and Rh using AdCSV was improved by the use of second derivative transformation of the signals. (objective 2)
- Dissolved and particulate Rh concentrations in the water column from an estuary and water samples from a wastewater treatment plant (WWTP) were reported for the first time. (objective 3)
- The high-resolution spatial distributions of Pt and Rh in superficial sediments of the Tagus estuary were assessed and reference levels are reported. (objective 3)

- Reference levels for Pt are close to the background but Rh was ca. 5 times higher than the estimated crustal abundance. (objective 4)
- The Pt/Rh mass ratios found in sediments did not reflect typical values for automotive catalytic converters (ACC), pointing out additional sources to the estuary. (objective 4)
- Motorway bridges are relevant pathways for the entrance of Pt and Rh into the estuary. (objective 4)
- The magnitude of Pt and Rh contamination deriving from industrial activities towards the estuary may have been larger and dominant in the past. (objective 4)
- An additional source of Pt found in the WWTP outfall could derive from the hospital and domestic sewage due to the use of Pt-based anticancer therapy, as shown by the relative increments in periods that were associated to personal care activities. (objective 4)
- The main sources of Pt and Rh in Tagus estuary were confirmed, in particular those from cars and industries through their use as catalysts. (objectives 4 and 5)
- The concentrations of particulate and dissolved fractions (<0.45 µm) of Pt and Rh were evaluated in the water column of Tagus estuary with distinct master characteristics. (objective 5)
- In the river end-member, both particulate Pt and Rh and dissolved Pt, were continuously introduced in the estuary, presenting low and relatively constant concentrations, whereas dissolved Rh was often below the limit of detection. (objective 6)
- At the WWTP outfall close to the Atlantic Ocean, both fractions of Pt and Rh showed a markedly increase and presented varying concentrations. (objective 6)
- Increments in Pt and Rh levels followed an inverse pattern in relation to the semi-diurnal tidal oscillation, with the highest concentrations observed during the low tides. (objective 6)

- Speciation analysis of Pt and Rh, and their potential mobility in aquatic systems, may be done using a combination of complementary analytical strategies. (objectives 6, 7 and 9)
- Different forms of Pt and Rh in urban road dust leachates (filtered <0.45 µm solutions) were discriminated. (objectives 7, 8 and 9)
- Non-dissolved species of Pt predominated over the dissolved forms, whereas for Rh truly dissolved species were an important fraction of the total content released by ACC. (objectives 7, 8 and 9)
- Truly dissolved Pt and Rh remained constant during the experimental period, while the (nano)particulate fraction in the leachates varied depending on the medium. (objective 7)
- In the leachates, (nano)particulate Pt longer exposure times in seawater led to an increase of total Pt concentration as opposed to the lower concentrations observed in rainwater. (objectives 7 and 8)
- Such variations are most likely to reflect the behaviour of (nano)particles rather than the effects of pH or ionic strength *per se*. (objective 8)
- The use of NTA confirmed for the first time the existence of (nano)particles in the leachates, in agreement with ICP-MS results that showed a higher proportion of Pt (nano)particles in seawater leachates. (objective 9)
- Truly dissolved species measured together with (nano)particles using ICP-MS can be discriminated employing AdCSV, which only determines the truly dissolved fraction. (objective 9)
- The partition coefficients for Pt and Rh in Tagus estuary varied within the same range of salinity; however, they remained unchanged along the salinity gradient. (objective 10)
- The pattern observed may indicate the influence of Pt and Rh sources rather than their chemical interactions with the estuarine water. (objective 10)

- Operationally defined forms of dissolved Pt represented the largest portion of total metal emitted as opposed to Rh, whose particulate forms dominated in the water column. (objective 10)
- Advection may largely control the distribution of Pt and Rh, being easily and rapidly dispersed in the water column owing to their low reactivity. (objective 11)
- Recirculation within the estuary and export of Pt and Rh towards the adjacent coastal region were predicted through modelling. (objectives 11 and 12)

9.2. Future Work and Perspectives

The developed research has provided comprehensive and reference information about Pt and Rh in Tagus estuary, highlighting the importance of understanding their occurrence and biogeochemistry in estuaries. Although for Pt and Rh this work has unveiled many aspects about its occurrence, sources and estuarine behaviour, their speciation still needs further investigation, as an example, including Pt analogues cisplatin, carboplatin and oxaliplatin. Despite the advances over the past decades regarding the knowledge of PGE in aquatic ecosystems, mainly for Pt, gaps still exist about the other PGE, e.g. Pd and Ru, and many questions continue to be posed. These sustain the need to better understand their occurrence, transport, speciation and potential toxicity in the aquatic environment. In addition, Pd and Ru are also two elements of great interest for future research. Palladium is also an important active component in ACC, presenting higher reactivity and potentially posing a greater environmental risk than Pt and Rh due to its larger solubility. As to Ru, its properties point it out also as a suitable element for medicinal applications. Therefore, anthropogenic uses and increasing emissions of these elements may be foreseen.

Current analytical techniques are not able to distinguish different redox states of Pt and Rh or the other PGE. The improvement of the available analytical techniques, or their combination, is thus necessary to assess accurate information in environmental compartments. Lowering the LOD for Pd and Ru determination in aquatic systems is a key issue to investigate their degree of contamination. The lack of a suitable voltammetric analytical method for Pd determination at this stage has hindered so far its speciation analysis in aquatic media. Moreover, although voltammetric techniques for the

determination of Pt-based compounds (e.g. cisplatin) exist, they need optimization for environmental analysis.

Industrial emissions of classical contaminants have been assessed in Tagus estuary over the past decades. Yet, PGE remains poorly documented in these areas. The historical record of Pt and Rh released by the industries settled in the Tagus estuary margins can be surveyed through the analysis of sediment cores. With the improved voltammetric method, Pt and Rh can be determined in the solids and interstitial waters of sediment cores of any aquatic system. Furthermore, an estimation of the transport of both metals across the sediment-water interface (diffusive and advective) can be made. This approach is relevant to understand the importance of the role of sediments as a sink and/or source of PGE to the water column and consequently to biota. Moreover, the information concerning the driven processes that influence the sediment-water fluxes on a time scale that may range from minutes associated with tides or years ruled by diagenetic processes in deeper sediment layers is vital to understanding the extension of PGE environmental contamination.

Because PGE will most likely increase in the aquatic environment, the estimation of regional and/or global PGE fluxes needs to be re-evaluated. Reliable speciation data and mechanisms acting in the mobility of PGE are needed. Furthermore, these should be included in the development of new and integrative modelling tools, whose barriers still need to be overcome. This will allow computing regional and global distribution and fluxes, as well as to predict "worst-case" scenarios and regions vulnerable to the impacts of anthropogenic activities. Ideally, models should include all environmental compartments, i.e. the atmosphere, land, aquatic (water and sediments) and biota.

The European Commission predicts a significant increase in demand and supply of these elements that are essential for producing technology-materials in the upcoming years. However, an accurate environmental risk assessment of PGE concerning the Water Framework Directive (WFD; 2000/60/EC) and Marine Strategy Framework Directive is missing. Thus, novel information should be provided on the effect of PGE on biota and potentially included in the revision of these directives with the scope to achieve a good status of all waters in Europe. Moreover, since estuaries and coastal areas subjected to continuous inputs of PGE they should be monitored and their fate evaluated.

X. ANNEXES

Supporting Information from Chapter IV

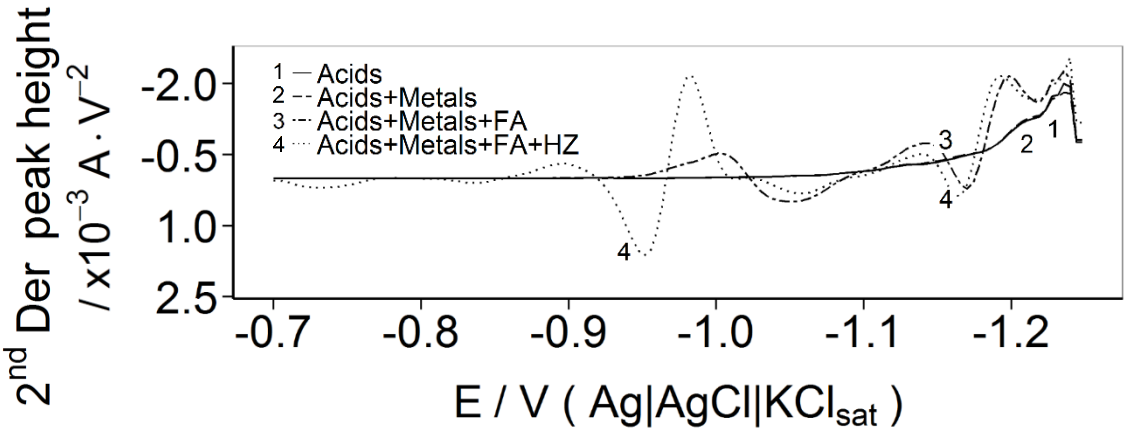

Figure S.IV 1 – Effect of medium composition in the Pt– and Rh–complexes detected by AdCSV using the second derivative (2^{nd} Der) transformation in the original voltammograms. Conditions: **1 –** baseline scan in 0.25 M H_2SO_4 and 0.05 M HCl; **2 –** addition of 2.0 ng L^{-1} Pt and 0.67 ng L^{-1} Rh; **3 –** addition of formaldehyde 0.01 M (FA); and **4 –** addition of hydrazine 0.5 mM (HZ) with formazone produced in situ; t_d =120 s and E_d = –0.75 V.

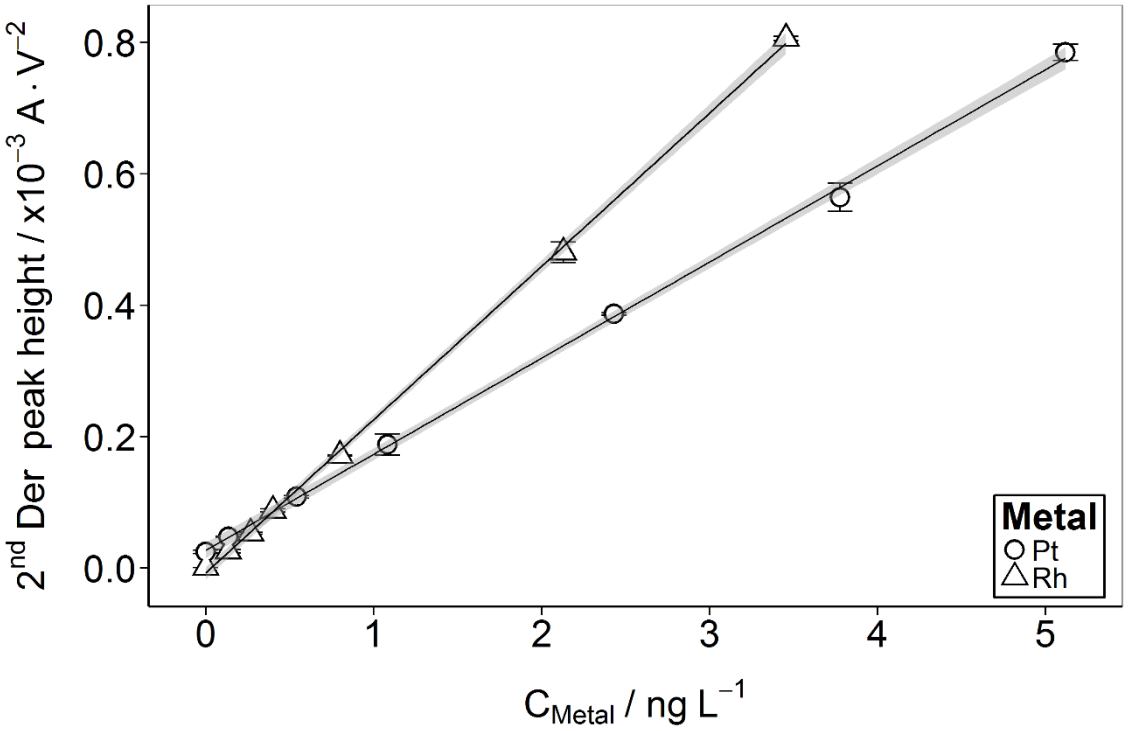

Figure S.IV 2 – Calibration plots of Pt, 2nd Der peak height = $2.7x10^{-5} + 1.5x10^{-4}\,C_{Pt}$ (circles) and of Rh, 2nd Der peak height = $-7.3x10^{-6} + 2.3x10^{-4}\,C_{Rh}$ (triangles), in simultaneous determination with the optimised experimental conditions: electrolyte 0.25 M H_2SO_4, 0.05 M HCl, 0.01 M FA and 0.5 mM HZ; t_d =120 s and E_d = –0.75 V. The grey shaded area represents the 95 % confidence interval of the calibration curve.

Supporting Information from Chapter V

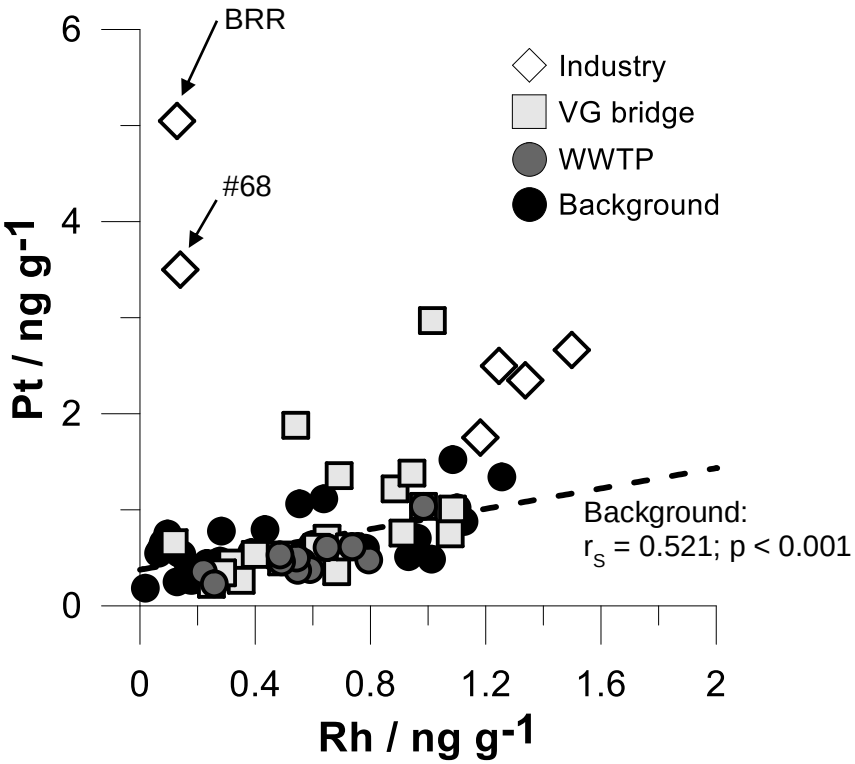

Figure S.V 1 – Bivariate plot of Pt and Rh in superficial sediments of Tagus estuary, depicted by section; trend on the background data and the respective Spearman correlation (r_S) are represented by the dashed line.

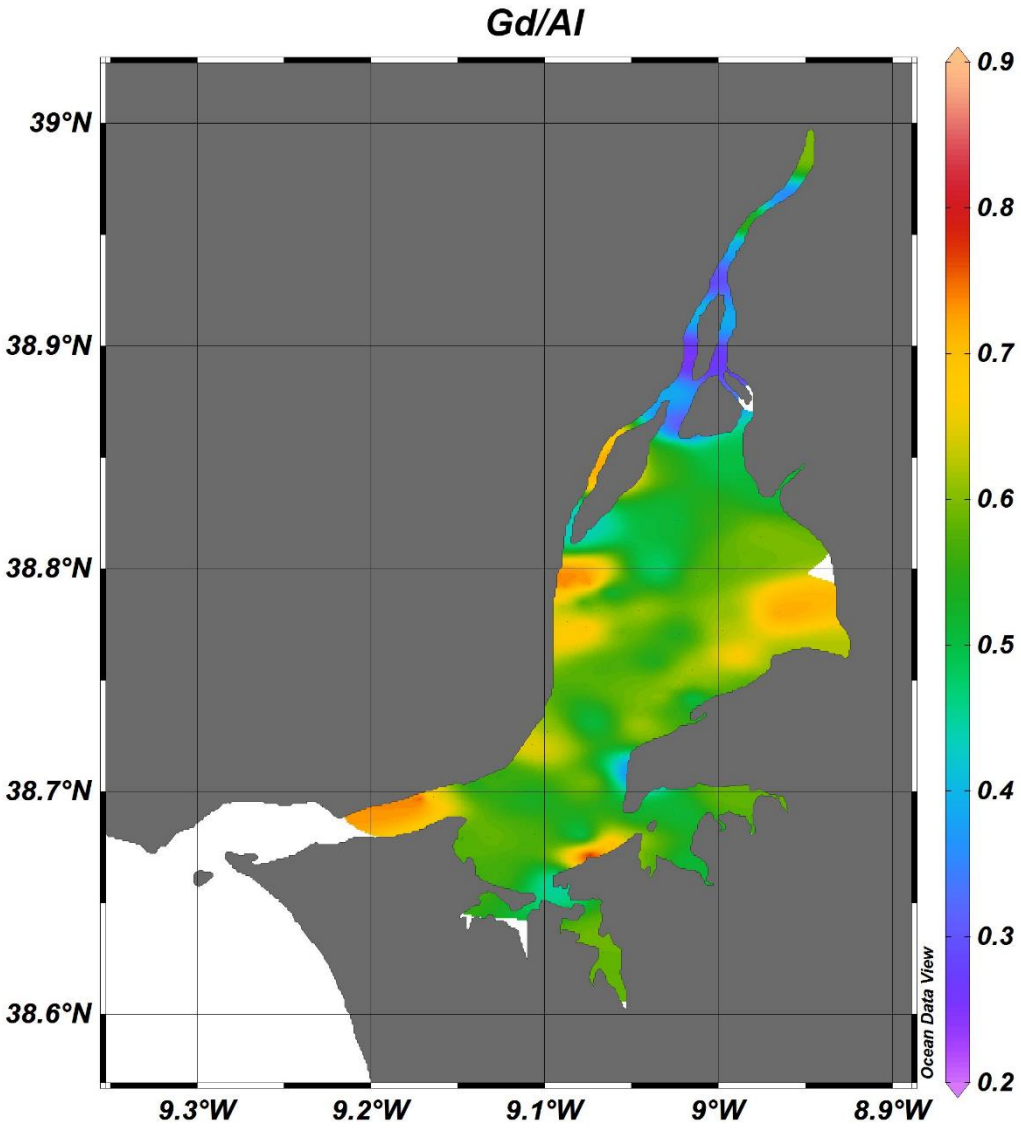

Figure S.V 2 – Spatial distribution of Gd concentrations normalised to Al in superficial sediments of Tagus estuary.

Estimation of Pt and Rh emissions

Using the same approach as in Almécija et al. (2015), we estimated the range of Pt and Rh emissions from ACC in VG and 25A bridges. Table S.V 1 summarises the calculations based on: (i) minimum and maximum number of vehicles per day crossing the bridges in one year period (2015/2016) before the sampling (IMT 2016); (ii) the deck lengths: 17.2 km long for VG bridge and 2.3 km for 25A bridge (www.lusoponte.pt); (iii) the proportion of gasoline engine vehicles to diesel engine that is approximately 4:6 (ACEA 2017); (iv) the range of estimated release of Pt and Rh from ACC at a rate of ng km^{-1} (Palacios et al. 2000); and (v) the number of days calculated since the opening of VG bridge until the sampling campaign (6631 days), as well as for 25A bridge for comparison purposes. Almécija et al. (2015) has estimated that nearly 450 and 1140 g of Pt has been released over 13 years since the opening of VG bridge, using two different approaches. Our estimation of total emissions ranged from 542 – 937 g of Pt and 130 – 262 g of Rh in VG bridge, while for 25A bridge were 171 – 312 g of Pt and 41 – 87 g of Rh, since the opening of VG bridge in 1998.

Table S.V 1 – Estimation of Pt and Rh range of emissions in Vasco da Gama (VG) bridge and in 25 de Abril (25A) bridge since the opening of VG bridge.

***Vasco da Gama* (VG) bridge**			
Beginning of activity	April 1998		
Sampling for this work	June 2016		
Estimated number of days		6631	
Vehicles traffic / day - 1 year previous to sampling			
	min	53264	
	max	61353	
Extension of the bridge		17.2	km
***25 de Abril* (25A) bridge**			

Beginning of activity		previous to 1990		
Sampling for this work		June 2016		
Estimated number of days		9125		
Vehicles traffic / day - 1 year previous to sampling				
	min	125649		
	max	152957		
Extension of the bridge		2.3	km	
For comparison purposes, nº days in calculations: 6631				
Diesel vehicles[a]	65	%		
Petrol vehicles[a]	35	%		
New vehicles[a]	7	%		
Old vehicles[a]	93	%		

Estimated range of Pt emissions[b]		**min**		**max**
Petrol				
New vehicles	ng M /km	102		
Old vehicles	ng M /km	6.3	-	8.2
Diesel				
New vehicles	ng M /km	404	-	812
Old vehicles	ng M /km	110	-	152
VG bridge TOTAL	**g Pt**	**542**	-	**937**
25A bridge TOTAL	**g Pt**	**171**	-	**312**

Estimated range of Rh emissions[b]		**min**		**max**
Petrol				
New vehicles	ng M /km	38	-	66
Old vehicles	ng M /km	3.7	-	12
Diesel				
New vehicles	ng M /km	82	-	184
Old vehicles	ng M /km	26	-	39
VG bridge TOTAL	**g Rh**	**130**	-	**262**

25A bridge TOTAL	**g Rh**	**41**	**- 87**

[a] Estimated from Instituto Nacional de Estatística and http://www.acea.be/statistics/
[b] Estimated emissions of Pt and Rh according to Palacios et al. (2000) and Almécija et al. (2015).

References

ACEA. (2017). *Vehicles in use - Europe 2017*. Brussels, Belgium.

Almécija, C., Sharma, M., Cobelo-García, A., Santos-Echeandía, J., & Caetano, M. (2015). Osmium and platinum decoupling in the environment: Evidences in intertidal sediments (Tagus Estuary, SW Europe). *Environmental Science and Technology*, *49*(11), 6545–6553. doi:10.1021/acs.est.5b00591

IMT. (2016). *Relatório de Tráfego na Rede Nacional de Autoestradas - 4º Trimestre*. Lisboa, Portugal.

Palacios, M. A., Gómez, M. M., Moldovan, M., Morrison, G., Rauch, S., McLeod, C., et al. (2000). Platinum-group elements: quantification in collected exhaust fumes and studies of catalyst surfaces. *Science of The Total Environment*, *257*(1), 1–15. doi:https://doi.org/10.1016/S0048-9697(00)00464-2

Supporting Information from Chapter VI

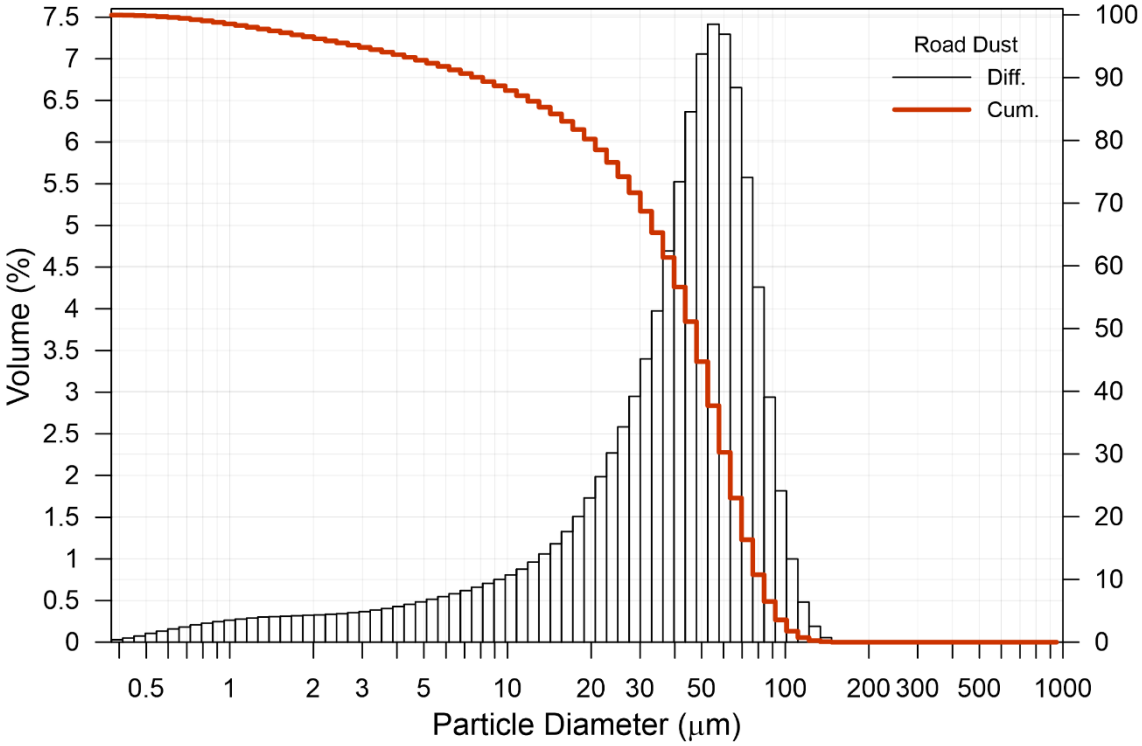

Figure S.VI 1 – Particle-size distribution of the road dust sample obtained by laser diffraction.

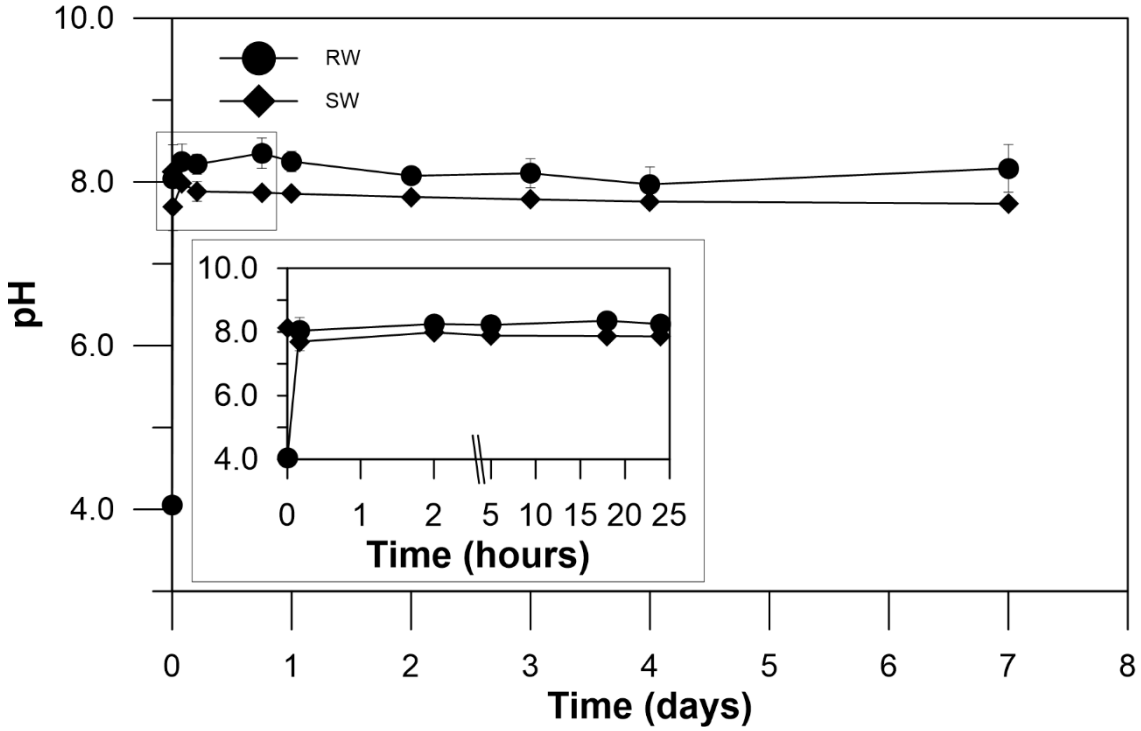

Figure S.VI 2 – Variation of pH during the road dust incubation period of 7 days; the inbox depicts pH variation within the first 24 hours of incubation.

Table S.VI 1 – Composition of synthetic rainwater and seawater.

Synthetic rainwater[1]		**Synthetic seawater**[2]	
Salt	**g L^{-1}**	**Salt**	**g L^{-1}**
$CaSO_4$	0.0051	NaCl	23.5
$MgCl_2$	0.002	Na_2SO_4	4.98
KCl	0.0019	$CaCl_2$	3.92
$NaNO_3$	0.0019	KCl	0.66
$NaHCO_3$	0.0056	$NaHCO_3$	0.19

References:

(1) Bielmyer, G. K.; Arnold, W. R.; Tomasso, J. R.; Isely, J. J.; Klaine, S. J. Effects of Roof and Rainwater Characteristics on Copper Concentrations in Roof Runoff. *Environ. Monit. Assess.* **2012**, *184* (5), 2797–2804. https://doi.org/10.1007/s10661-011-2152-1.

(2) Kester, D. R.; Duedall, I. W.; Connors, D. N.; Pytkowicz, R. M. Preparation of Artificial Seawater. *Limnol. Oceanogr.* **1967**, *12* (1), 176–179. https://doi.org/10.4319/lo.1967.12.1.0176.

Supporting Information from Chapter VII

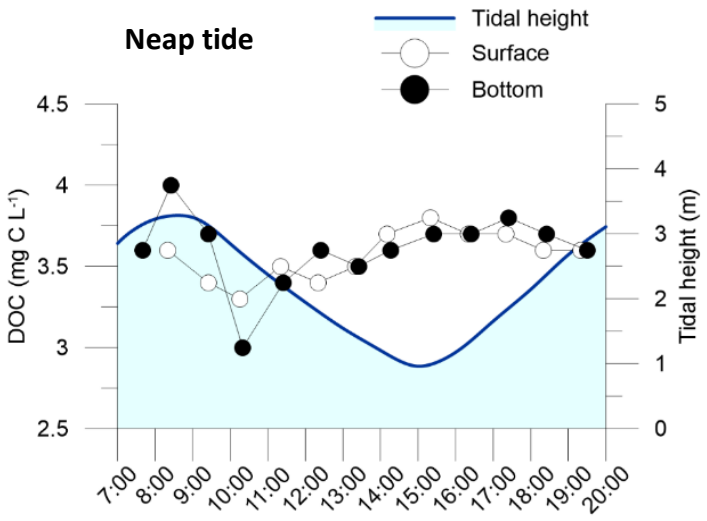

Figure S.VII 1 – Dissolved organic carbon (DOC) in the water column at VFX station during neap tide survey. Tidal height – blue line; surface – white circles; bottom – black circles.

Table S.VII 1 – Metals and water parameters correlation matrix in the water column at VFX during neap tide. Significant correlations ($p<0.05$) are highlighted in red.

	T	pH	Cond	%DO	DO	SPM	$Pt_{D\text{-}AdCSV}$	Pt_P	Rh_P	DOC	$Pt_{D\text{-}ICP\text{-}MS}$
T	1.000	0.223	-0.666	-0.196	-0.285	-0.241	-0.037	0.246	-0.188	0.232	0.156
pH	0.223	1.000	-0.234	-0.145	-0.192	-0.524	0.160	0.518	-0.201	-0.209	0.047
Cond	-0.666	-0.234	1.000	-0.216	-0.124	0.318	-0.240	-0.358	0.141	-0.618	-0.139
%DO	-0.196	-0.145	-0.216	1.000	0.984	0.194	0.133	0.079	-0.051	0.259	0.297
DO	-0.285	-0.192	-0.124	0.984	1.000	0.225	0.129	0.060	-0.020	0.256	0.222
SPM	-0.241	-0.524	0.318	0.194	0.225	1.000	-0.355	-0.544	0.248	-0.123	0.067
$Pt_{D\text{-}AdCSV}$	-0.037	0.160	-0.240	0.133	0.129	-0.355	1.000	0.092	-0.367	0.315	0.219
Pt_P	0.246	0.518	-0.358	0.079	0.060	-0.544	0.092	1.000	-0.274	0.233	-0.442
Rh_P	-0.188	-0.201	0.141	-0.051	-0.020	0.248	-0.367	-0.274	1.000	-0.034	0.017
DOC	0.232	-0.209	-0.618	0.259	0.256	-0.123	0.315	0.233	-0.034	1.000	-0.070
$Pt_{D\text{-}ICP\text{-}MS}$	0.156	0.047	-0.139	0.297	0.222	0.067	0.219	-0.442	0.017	-0.070	1.000

Table S.VII 2 – Metals and water parameters correlation matrix in the water column at VFX during spring tide. Significant correlations ($p<0.05$) are highlighted in red.

	T	pH	Cond	%DO	DO	SPM	Pt_D	Rh_D	Pt_P	Rh_P
T	1.000	-0.271	-0.446	0.004	-0.011	0.237	0.437	0.035	-0.298	0.236
pH	-0.271	1.000	0.688	0.694	0.514	-0.418	-0.404	-0.034	0.448	-0.229
Cond	-0.446	0.688	1.000	0.833	0.698	-0.324	-0.510	-0.028	0.417	-0.206
%DO	0.004	0.694	0.833	1.000	0.904	-0.227	-0.343	0.016	0.253	-0.085
DO	-0.011	0.514	0.698	0.904	1.000	-0.024	-0.306	-0.019	0.033	-0.177
SPM	0.237	-0.418	-0.324	-0.227	-0.024	1.000	0.028	-0.334	-0.614	0.060
Pt_D	0.437	-0.404	-0.510	-0.343	-0.306	0.028	1.000	0.266	-0.105	0.062
Rh_D	0.035	-0.034	-0.028	0.016	-0.019	-0.334	0.266	1.000	0.163	-0.081
Pt_P	-0.298	0.448	0.417	0.253	0.033	-0.614	-0.105	0.163	1.000	0.219
Rh_P	0.236	-0.229	-0.206	-0.085	-0.177	0.060	0.062	-0.081	0.219	1.000

Table S.VII 3 – Metals and water parameters correlation matrix for ALC in neap tide. Significant correlations ($p<0.05$) are highlighted in red.

	T	pH	Cond	%DO	DO	SPM	Pt_D	Rh_D	Pt_P	Rh_P
T	1.000	-0.646	-0.901	-0.473	-0.505	0.593	0.731	-0.200	0.835	-0.137
pH	-0.646	1.000	0.812	0.886	0.845	-0.652	-0.809	0.257	-0.707	-0.231
Cond	-0.901	0.812	1.000	0.720	0.714	-0.648	-0.879	0.200	-0.885	-0.132
%DO	-0.473	0.886	0.720	1.000	0.978	-0.412	-0.720	0.371	-0.687	-0.538
DO	-0.505	0.845	0.714	0.978	1.000	-0.319	-0.665	0.371	-0.698	-0.505
SPM	0.593	-0.652	-0.648	-0.412	-0.319	1.000	0.758	0.486	0.571	-0.203
Pt_D	0.731	-0.809	-0.879	-0.720	-0.665	0.758	1.000	0.314	0.868	0.110
Rh_D	-0.200	0.257	0.200	0.371	0.371	0.486	0.314	1.000	-0.029	-0.771
Pt_P	0.835	-0.707	-0.885	-0.687	-0.698	0.571	0.868	-0.029	1.000	0.071
Rh_P	-0.137	-0.231	-0.132	-0.538	-0.505	-0.203	0.110	-0.771	0.071	1.000

Table S.VII 4 – Metals and water parameters correlation matrix for ALC in spring tide. Significant correlations ($p<0.05$) are highlighted in red.

	T	pH	Cond	%DO	DO	SPM	Pt_D	Rh_D	Pt_P	Rh_P
T	1.000	-0.868	-0.729	-0.732	-0.800	0.289	0.600	0.444	0.006	-0.557
pH	-0.868	1.000	0.941	0.933	0.939	-0.212	-0.600	-0.017	-0.083	0.158
Cond	-0.729	0.941	1.000	0.951	0.924	-0.071	-0.577	0.250	-0.313	-0.042
%DO	-0.732	0.933	0.951	1.000	0.988	-0.247	-0.637	0.067	-0.214	-0.063
DO	-0.800	0.939	0.924	0.988	1.000	-0.278	-0.680	-0.117	-0.179	0.014
SPM	0.289	-0.212	-0.071	-0.247	-0.278	1.000	0.313	0.317	-0.560	-0.217
Pt_D	0.600	-0.600	-0.577	-0.637	-0.680	0.313	1.000	0.617	0.247	-0.273
Rh_D	0.444	-0.017	0.250	0.067	-0.117	0.317	0.617	1.000	-0.267	-0.548
Pt_P	0.006	-0.083	-0.313	-0.214	-0.179	-0.560	0.247	-0.267	1.000	0.210
Rh_P	-0.557	0.158	-0.042	-0.063	0.014	-0.217	-0.273	-0.548	0.210	1.000